DYNAMICS OF HELICAL WORMLIKE POLYMER CHAINS

TAKENAO YOSHIZAKI

1989

DYNAMICS OF HELICAL WORMLIKE POLYMER CHAINS

TAKENAO YOSHIZAKI

1989

CONTENTS

CHAPTER	1.	INTRODUCTION	1
	1–1.	Background	1
	1–2.	Outline	6
		References	8
CHAPTER	2.	DYNAMIC MODEL AND DIFFUSION EQUATION	12
	2–1.	Introduction	12
	2–2.	Dynamic Model	13
	2–3.	Diffusion Equation	25
	a.	Space of bond and infinitesimal rotation vectors	27
	b.	Space of Euler angles	34
	c.	Approximations	44
	2–4.	Conclusion	45
		References	47
CHAPTER	3.	EIGENVALUE PROBLEMS	49
	3–1.	Introduction	49
	3–2.	Transformation of the Basis Set	54
	a.	Standard basis set	54
	b.	Matrices E and L	59
		(i). (1, 1)–body elements	61
		(ii). (2, 2)–body elements	62
	c.	Time–correlation functions	64
	3–3.	Subspace Approximation	67
	3–4.	Block–Diagonal Approximation	73
	3–5.	Conditions on the Model Parameters	80
	a.	The diffusion matrix B	80
	b.	The lowest branch	85
		(i). Flexible chains	89

(ii). Stiff chains 92
3-6. Discussion and Concluding Remarks 94
a. The preaveraging approximation 94
b. Flexible constraints 96
c. Periodic vs nonperiodic boundary conditions 97
d. Conclusion 98
Appendix 3-A. The Three-Dimensional Eigenvalue Problem 98
Appendix 3-B. The Mean Reciprocal Distance 100
References 106
CHAPTER 4. DIELECTRIC RELAXATION 109
4-1. Introduction 109
4-2. Formulation 112
4-3. Eigenvalue Spectra 121
a. Flexible chains 123
b. Stiff chains 128
4-4. Correlation Functions 131
a. Flexible chains 131
b. Stiff chains 137
4-5. Comparison with Experiment 139
a. Flexible chains 140
b. Stiff chains 149
4-6. Discussion 157
Appendix 4-A. Eigenfunctions 159
References 162
CHAPTER 5. DYNAMIC INTRINSIC VISCOSITY 165
5-1. Introduction 165
5-2. Formulation 167
a. Time-dependent distribution function 169
b. Correlation function formalism of the excess stress tensor 171

c. Correlation function $<\Gamma(0)\Gamma(t)>_{eq}$ 177
d. Final expression for $[\eta]$ 182
5-3. Eigenvalue Spectra 184
5-4. High-Frequency Viscosity 187
5-5. Comparison with Experiment 193
5-6. Concluding Remarks 196
Appendix 5-A. Excess Stress Tensor 197
Appendix 5-B. Evaluation of the Function X 200
Appendix 5-C. Intrinsic Viscosity of the Einstein Sphere 202
Appendix 5-D. Matrix Elements 204
Appendix 5-E. The Six-Dimensional Eigenvalue Problem 206
References 209
LIST OF PUBLICATIONS 211
ACKNOWLEDGMENT 214

CHAPTER 1

INTRODUCTION

1–1. Background

During the last decade, a series of theoretical studies on static properties of polymer chains in dilute solution has been made on the basis of a new general continuous model, called the helical wormlike (HW) chain, by Yamakawa and his co–workers.[1–18] They have shown that the model can mimic the equilibrium conformational behavior of real polymer chains as well as the rotational isomeric state model,[19] and that various properties of both flexible and stiff chains may be evaluated very efficiently on the basis of the former. On the other hand, in the field of the dynamics of (flexible and stiff) polymer chains in dilute solution,[20–30] there still remain many problems, not completely solved as yet, such as dielectric relaxation and dynamic intrinsic viscosity. Thus, in this thesis, we shall study them on the basis of the HW chain.

The HW chain is a continuous elastic wire model with bending and torsional energies such that its total configurational energy becomes the minimum zero when it takes a regular helical form, which is called the characteristic helix. Necessarily, it is adequate for a description of equilibrium conformational and/or

steady-state transport properties of real chains on the bond length or somewhat longer scales, as shown by Yamakawa and his co-workers, but not, as it stands, for a description of local motions or conformational transitions, which we are interested in, apart from its mathematical difficulty. However, this will be achieved by replacing the continuous HW chain by its discrete analog. It has been proved by Yamakawa and Shimada[9,10] that the continuous HW chain may also be obtained by taking the continuous limit of a discrete chain of rigid subbodies, instead of bonds, under certain conditions, and also that local vectorial and tensorial properties of the continuous HW chain may be expressed in localized coordinate systems affixed to it, one corresponding to two successive skeletal bonds in the real chain. Considering these facts and also the length scales inherent in the continuous HW chain, it is appropriate to replace it by a discrete chain of identical rigid subbodies, each corresponding to two bonds or so. Its size may be determined in such a way that the equilibrium conformational behavior of the discrete chain is almost identical with that of the original continuous chain. This is our dynamic model to be used, and it is referred to as the discrete HW chain when necessary to distinguish it from the continuous HW chain. It is clear that our model corresponds to the real chain somewhat coarse-grained.

Now, we survey theoretical studies presented so far in the

field of the dynamics of polymer chains in dilute solution. It is useful for clarifying characteristic features of the dynamic model we have adopted and also for searching for theoretical approaches to the problems. There have been made three types of studies in this field, i. e., analytical investigations based on the diffusion equation for the time-dependent distribution function for proper chain models,[21,26-28,31-33] those based on the master equation for lattice chains,[34-36] and Brownian dynamics simulation studies by the use of realistic models.[29,37,38] In the second-type theories, one must make ad hoc assumptions on the transition rates of elementary motions artificially chosen, and therefore, no molecular information can be obtained from the values of the transition rate themselves. Moreover, the results of these theories exhibit extremely slow relaxation at long times which is inconsistent with experiments. In the third-type studies, there is little hope of getting an insight into the mechanism of the relaxation processes of polymer chains, especially of the interactions of local and global chain motions.

Our study in this thesis is categorized into the first type, and thus we review it rather in detail. A most general theoretical framework was given by Kirkwood[31] for the bond chain composed of frictional elements, each having three translational degrees of freedom. In this model, each bead corresponds to one of the atoms constituting the backbone of a given real polymer chain, and thus necessarily the constraints on the bond lengths and angles and also

the complicated potential energies as functions of rotation angles are taken into account. These constraints and potential energies make it difficult to perform analytical evaluation, and only formal results were obtained. Rouse[32] and Zimm[33] removed these difficulties by introducing the spring-bead model. It is composed of statistical segments or beads having translational friction, each of which corresponds to a group of several successive atoms of the chain backbone, and successive two beads are connected by the Gaussian spring. Although they achieved a remarkable success in a description of rather long-wavelength motions of polymer chains, they abandoned drawing information about local chain motions. A reconsideration of the bond chain was made by Fixman and his co-workers,[26-28] who rewrote the diffusion equation into a more transparent form by introducing the constraining matrix. However, the preaveraging approximation made in this matrix, which is inevitable for analytical developments, caused a serious error in the evaluation of the relaxation rates of the local motions. It may be said that Fixman's "model" or diffusion equation is a modified spring-bead model in which the effect of the constraints is taken into account by the preaveraged constraining matrix, and thus the results of Rouse and Zimm may be recovered if the constraining matrix is ignored. In short, there is not any theory based on the diffusion equation which provides a satisfactory description of the local chain motions.

In contrast to the bond chain, our model consists of rigid subbodies, each of which has three rotational degrees of freedom besides the translational ones and has a rotational relaxation rate associated with a motional (monomer) unit. It seems rather natural to replace repeating units of a given real polymer chain by the subbodies instead of frictional beads only with the translational degrees of freedom. In our model, the constraints, of course, exist on the distance between the centers of two successive subbodies and on the relative orientations between them, and therefore a proper preaveraging approximation must also be introduced into our constraining matrix. However, the approximation seems to make no serious effect on the description of the local chain motions because of the characteristic features of our model.

We have undertaken this work in the hope that local motions could be treated more effectively than on the basis of the bond chain for two reasons. First, a basis set corresponding to some local modes can be included through the rotational degrees of freedom of the subbodies even in a crude approximation. Second, we can avoid the serious errors in the evaluation of the relaxation rates of the local chain motions caused by the preaveraging of the constraining matrix.

1–2. Outline

The plan of this thesis is as follows.

In Chap. 2, we construct the discrete HW chain to be suitable for the study of the dynamics of polymer chains, both flexible and stiff. It is a chain of N identical rigid subbodies such that, apart from its location, its configuration may be specified by N sets of Euler angles, each associated with one subbody, and that its equilibrium behavior is almost identical with that of the continuous HW chain. Then, we formulate the configurational diffusion equation and give an explicit expression for the diffusion operator $\mathscr{L}$ associated with it. Following the procedure of Fixman,[26] the constraints are handled by setting the components of the flux associated with the constrained coordinates equal to zero through constraining forces, so that the diffusion equation and all configuration-dependent properties may be written in terms of only the unconstrained coordinates, i. e., the Euler angles.

Finding the solution of the diffusion equation is equivalent to solving the eigenvalue problem for the diffusion operator $\mathscr{L}$. Thus, in Chap. 3, we present a general solution of this eigenvalue problem by the use of the representation theory in the quantum mechanics. The problem is, to a great extent, decoupled by introducing a standard representation which is formed by the eigenfunctions of the total angular momentum operator for the

entire chain. In order to find the analytical solutions, the size of the problem thus reduced is further reduced by making two approximations: subspace approximation and block-diagonal approximation. The former is equivalent to neglecting the memory term in the projection operator method, and the latter consists of introducing Fourier modes as in the conventional chain. It is shown that the theory predicts a number of branches of eigenvalue spectra. We also examine the conditions that should be imposed on the parameters such as the translational and rotatory friction coefficients of the subbody.

By the use of the general solution given in Chap. 3, we readily evaluate various dynamical properties of polymer chains in dilute solution. Two typical examples are shown in the following two chapters.

In Chap. 4, dielectric relaxation of both flexible and stiff polymers in dilute solution is studied on the basis of the discrete HW chain such that an electric dipole moment is attached rigidly or with a rotational degree of freedom to each of the subbodies composing the chain. The complex dielectric constant is formulated with the dipole correlation function. Then, dielectrically active branches of the eigenvalue spectrum are identified for a given type of dipoles, and a mode analysis of them is made in order to inquire into the interaction between global and local modes. The decay behavior of the dipole correlation function is also examined

numerically for various chains. A comparison of theory with experiment is made with respect to the dispersion and loss, and also the dielectric correlation time τ_D as determined from the loss peak.

In Chap. 5, we study the dynamic intrinsic viscosity of flexible chain polymers in dilute solution. The correlation function formalism of the complex intrinsic viscosity $[\eta]$ is given, taking account of the effect of the finite hydrodynamic volumes of the subbodies of the chain. In this case, it is convenient to introduce a new basis set, which is a hybrid of the basis functions defined in Chap. 3. Then the eigenvalue problem for the representation of the diffusion operator $\mathscr{L}$ may be reduced to N six-dimensional eigenvalue problems. Among the six branches of the eigenvalue spectrum, one global and two local branches can be shown to make contribution to the dynamic intrinsic viscosity. It is shown that the theory predicts the existence of the high-frequency plateau which is distinguished from the infinitely high-frequency viscosity.

References

[1]H. Yamakawa, Annu. Rev. Phys. Chem., **35**, 23 (1984).

[2]H. Yamakawa, Macromolecules, **10**, 692 (1977).

[3]H. Yamakawa and M. Fujii, J. Chem. Phys., **64**, 5222 (1976).

[4]H. Yamakawa, M. Fujii, and J. Shimada, J. Chem. Phys., **65**, 2371

(1976).

[5]M. Fujii and H. Yamakawa, J. Chem. Phys., **66**, 2578 (1977).

[6]H. Yamakawa and M. Fujii, J. Chem. Phys., **66**, 2584 (1977).

[7]J. Shimada and H. Yamakawa, J. Chem. Phys., **67**, 344 (1977).

[8]H. Yamakawa, J. Shimada, and M. Fujii, J. Chem. Phys., **68**, 2140 (1978).

[9]H. Yamakawa and J. Shimada, J. Chem. Phys., **68**, 4722 (1978).

[10]H. Yamakawa and J. Shimada, J. Chem. Phys., **70**, 609 (1979).

[11]H. Yamakawa, M. Fujii, and J. Shimada, J. Chem. Phys., **71**, 1611 (1979).

[12]H. Yamakawa, J. Shimada, and K. Nagasaka, J. Chem. Phys., **71**, 3573 (1979).

[13]M. Fujii and H. Yamakawa, J. Chem. Phys., **72**, 6005 (1980).

[14]J. Shimada and H. Yamakawa, J. Chem. Phys., **73**, 4037 (1980).

[15]J. Shimada, K. Nagasaka, and H. Yamakawa, J. Chem. Phys., **75**, 469 (1981).

[16]M. Fujii, K. Nagasaka, J. Shimada, and H. Yamakawa, J. Chem. Phys., **77**, 986 (1982).

[17]M. Fujii, K. Nagasaka, J. Shimada, and H. Yamakawa, Macromolecules, **16**, 1613 (1983).

[18]J. Shimada and H. Yamakawa, J. Chem. Phys., **85**, 591 (1986).

[19]P. J. Flory, *Statistical Mechanics of Chain Molecules* (Interscience, New York, 1969).

[20]M. Fixman and W. H. Stockmayer, Annu. Rev. Phys. Chem., **21**, 407

(1970).

[21]H. Yamakawa, *Modern Theory of Polymer Solutions* (Harper & Row, New York, 1971).

[22]W. H. Stockmayer, Pure Appl. Chem., Macromol. Chem., **8**, 379 (1973).

[23]W. H. Stockmayer, Les Houches Lectures (1973) in *Molecular Fluids——Fluides Moleculaires*, edited by R. Balian and G. Weill (Gordon and Breach, New York, 1976), p. 107.

[24]J. D. Ferry, Les Houches Lectures (1973) in *Molecular Fluids——Fluides Moleculaires*, edited by R. Balian and G. Weill (Gordon and Breach, New York, 1976), p. 23.

[25]H. Yamakawa, Annu. Rev. Phys. Chem., **25**, 179 (1974).

[26]M. Fixman and J. Kovac, J. Chem. Phys., **61**, 4939, 4950 (1974).

[27]J. Kovac and M. Fixman, J. Chem. Phys., **63**, 935 (1975).

[28]M. Fixman and G. T. Evans, J. Chem. Phys., **64**, 3474 (1976); **68**, 195 (1978).

[29]M. Fixman, J. Chem. Phys., **69**, 1527 (1978).

[30]J. D. Ferry, Pure Appl. Chem., **50**, 299 (1978).

[31]J. G. Kirkwood, Rec. Trav. Chim., **68**, 649 (1949); J. Polym. Sci., **12**, 1 (1954).

[32]P. E. Rouse, Jr., J. Chem. Phys., **21**, 1272 (1953).

[33]B. H. Zimm, J. Chem. Phys., **24**, 269 (1956).

[34]E. Dubois-Violette, F. Geny, L. Monnerie, and O. Parodi, J. Chim. Phys., **66**, 1865 (1969).

[35]B. Valeur and L. Monnerie, J. Polym. Sci., Polym. Phys. Ed., **14**, 11

(1976).

[36]A. A. Jones and W. H. Stockmayer, J. Polym. Sci., Polym. Phys. Ed., **15**, 847 (1977).

[37]E. Helfand, Z. R. Wasserman, and T. A. Weber, J. Chem. Phys., **70**, 2016 (1979); Macromolecules, **13**, 526 (1980).

[38]J. Skolnick and E. Helfand, J. Chem. Phys., **72**, 5489 (1980).

CHAPTER 2

DYNAMIC MODEL AND DIFFUSION EQUATION

2–1. Introduction

Although the continuous helical wormlike (HW) chain[1–3] may provide a satisfactory description of equilibrium properties of real chains on the bond length or somewhat longer scales, it is difficult to apply this model to dynamical problems as it stands, since, in general, continuous models have an infinite number of degrees of freedom and therefore contain unphysical motions of wavelengths shorter than real bond lengths. Thus, in this chapter, we first replace the continuous HW chain by its discrete analog, i. e., the discrete HW chain composed of N identical subbodies, as mentioned in Chap. 1, and then derive the configurational diffusion equation.

The discrete HW chain has constraints on the distance between the centers of two successive subbodies and on the relative orientations between them. As has very often been discussed, such constraints may be handled in two fundamentally different methods[4,5]: the Kramers type[6,7] and the revised Kirkwood type.[8,9] The difference between the results from them is small for long enough chains. The latter may be further divided into two classes. One consists of taking the rigid limits of the "flexible" constraints,

as expressed by overdamped harmonically bound oscillators of small equilibrium root-mean-square amplitudes, at the final stage of calculation by letting the amplitudes approach zero. It is known that this method leads to correct results in some cases,[10,11] but not in others.[12] We therefore adopt the other, i. e., the procedure of Fixman and Kovac,[4,13] in which the constraints are introduced at an early stage of calculation, and which is more convenient for our model. The diffusion equation and all configuration-dependent properties may then be written in terms of only the unconstrained coordinates, i. e., N sets of Euler angles specifying the orientations of the N subbodies.

The plan of this chapter is as follows. In Sec. 2-2, we give a detailed description of the discrete HW chain with an explicit expression for its potential energy as a function of the Euler angles. A criterion for the determination of the number of subbodies in it is established from a comparison with the continuous HW chain with respect to the equilibrium mean-square end-to-end distance. In Sec. 2-3, we derive a diffusion equation satisfied by the time-dependent configurational distribution function.

2-2. Dynamic Model

Consider the continuous HW chain such that its total contour length is L, its stiffness is λ^{-1}, and the constant curvature and

torsion of its characteristic helix are κ_0 and τ_0, respectively, assuming that its Poisson's ratio σ is zero, for simplicity.[1,2] We first replace it by a discrete chain of N identical rigid subbodies of length a, which are numbered 1, 2, $\cdots$, N, as depicted in Figs. 2.1(a) and (b). The junctions between the $(p-1)$th and pth subbodies and between the pth and $(p+1)$th subbodies correspond to the contour points s and $s+\Delta s$ of the continuous HW chain (a), respectively, so that its part from s to $s+\Delta s$ corresponds to the pth subbody. We note that a is not equal to Δs, and therefore that the total contour length Na of the chain (b) is not equal to L. A relation between a and Δs is determined later. However, this discrete model is not amenable to mathematical treatment as yet. Therefore, we further replace it by the chain (c) composed of $N+1$ identical beads, in which the center of the pth bead ($p = 2, 3, \cdots, N$) corresponding to the pth subbody is located at the junction between the $(p-1)$th and pth subbodies, the centers of the first and $(N+1)$th beads are located at the chain ends, and the pth bond vector $\mathbf{a}_p$ ($p = 1, 2, \cdots, N$) of (fixed) length a, which joins the pth and $(p+1)$th beads, is affixed to the pth bead [not to the $(p+1)$th]. Thus, the total contour length of this chain is still equal to Na. Suppose then that all beads except the $(N+1)$th have translational and rotatory friction coefficients ζ_t and ζ_r and the $(N+1)$th bead has the same translational friction coefficient (ζ_t) but vanishing rotatory friction coefficient ($\zeta_r = 0$).

The addition of the $(N + 1)$th bead of this nature serves to remove certain annoying asymmetry in the diffusion equation. There is no difference between the potential energies of the chains (b) and (c) (see also below) while their dynamic properties differ, but this difference will be small for large N. The chain (c) is the discrete HW chain to be adopted. In what follows, all lengths are measured

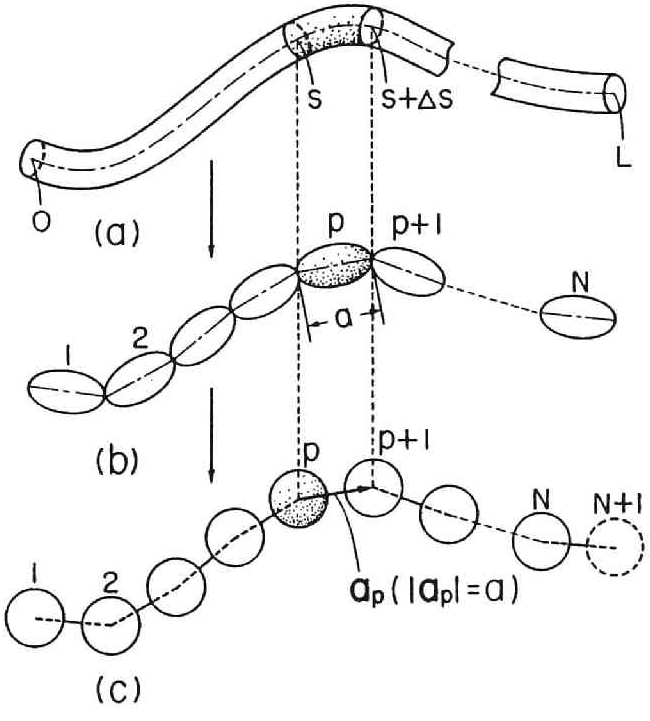

Fig. 2.1. Replacement of the continuous HW chain by the discrete HW chain (see text).

in units of the stiffness parameter λ^{-1}, and k_BT (with k_B the Boltzmann constant and T the absolute temperature) is chosen to be unity, for convenience.

Now we introduce N localized Cartesian coordinate systems $(\mathbf{e}_{\xi_p}, \mathbf{e}_{\eta_p}, \mathbf{e}_{\zeta_p})$ $(p = 1, 2, \cdots, N)$, the pth one being affixed to the pth bead with the origin at its center and with $\mathbf{e}_{\zeta_p}$ in the direction of $\mathbf{a}_p$ (from p to $p + 1$). Let $\Omega_p = (\theta_p, \varphi_p, \psi_p)$ $(p = 1, 2, \cdots, N)$ be the Euler angles defining the orientation of the pth localized system with respect to an external (lab) coordinate system. Apart from its location, the configuration of the chain can be specified by $3N$ variables (angles), $(\Omega_1, \Omega_2, \cdots, \Omega_N) \equiv \{\Omega_N\}$. Note that the orientation or the rotational degrees of freedom of the $(N + 1)$th bead are not considered, corresponding to the fact that its rotatory friction coefficient is taken as zero.

The total potential energy $U_0(\{\Omega_N\})$ of the chain may then be expressed as a sum of "pair" potentials $u(\Omega_p, \Omega_{p+1})$,

$$U_0 = \sum_{p=1}^{N-1} u(\Omega_p, \Omega_{p+1}) , \tag{2.1}$$

ignoring excluded volume potentials. We determine the form of u as follows. It is related to the equilibrium conditional distribution function $\Psi_{eq}(\Omega_{p+1} | \Omega_p)$ of Ω_{p+1} with Ω_p fixed, by the equation,

$$\Psi_{eq}(\Omega_{p+1} | \Omega_p) = \exp[- u(\Omega_p, \Omega_{p+1})] / \int \exp[- u(\Omega_p, \Omega_{p+1})] d\Omega_{p+1} , \tag{2.2}$$

where $d\Omega_p = \sin\theta_p d\varphi_p d\psi_p$. It is reasonable to assume that this Ψ_{eq} is identical with the corresponding conditional distribution function, i. e., the equilibrium Green's function $G(\Omega_{p+1} | \Omega_p; \Delta s)$ between the contour points s and $s + \Delta s$ of the continuous HW chain, where the arguments of Ψ_{eq} and G take the same values;

$$\Psi_{eq}(\Omega_{p+1} | \Omega_p) = G(\Omega_{p+1} | \Omega_p; \Delta s) . \tag{2.3}$$

Yamakawa et al[14] have shown that $G(\Omega | \Omega_0; s)$ may be expanded in terms of the normalized Wigner $\mathcal{D}$ functions $\mathcal{D}_l^{mj}$ as

$$G(\Omega | \Omega_0; s) = \sum_{l,m,j,j'} g_l^{jj'}(s)\mathcal{D}_l^{mj}(\Omega)\mathcal{D}_l^{mj'*}(\Omega_0) , \tag{2.4}$$

where the sums over $\mathcal{D}_l^{mj}$ are taken over $l \geq 0$, $|m| \leq l$, $|j| \leq l$, and the asterisk indicates the complex conjugate. $\mathcal{D}_l^{mj}$ is defined by

$$\mathcal{D}_l^{mj}(\Omega) = \mathcal{D}_l^{mj}(\theta, \varphi, \psi) = c_l e^{im\varphi} d_l^{mj}(\theta) e^{ij\psi} , \tag{2.5}$$

where

$$c_l = [(2l + 1)/8\pi^2]^{1/2}, \tag{2.6}$$

i is the imaginary unit, and

$$d_l^{mj}(\theta) = \left[\frac{(l + j)!(l - j)!}{(l + m)!(l - m)!} \right]^{1/2} (\cos\tfrac{1}{2}\theta)^{j+m} (\sin\tfrac{1}{2}\theta)^{j-m} \times P_{l-j}^{(j-m, j+m)}(\cos\theta) \tag{2.7}$$

with $P_n^{(\alpha,\beta)}(x)$ the Jacobi polynomial.[15] From Eqs. (2.2) and (2.3), we have

$$u(\Omega_p, \Omega_{p+1}) = - \ln G(\Omega_{p+1} | \Omega_p; \Delta s) , \tag{2.8}$$

where we have omitted a constant term. Strictly, the u thus obtained is not the potential energy of the continuous HW chain (as an elastic wire) of contour length Δs but rather the free energy. In the limit $\Delta s \longrightarrow 0$ ($a \longrightarrow 0$), the discrete HW chain becomes exactly identical with the continuous one with the potential energy u.

In the present case of σ (Poisson's ratio) = 0, G may also be expanded, by the use of the relations derived by Shimada and Yamakawa [Eqs. (25) and (26) with Eqs. (A6) and (A7) of Ref. 16], as follows,

$$G(\Omega \mid \Omega_0; s) = \sum_{l,m,k} h_l^k(s) \sum_j \mathscr{D}_l^{mj}(\Omega)\overline{\mathscr{D}}_l^{jk}(\Omega_a) \times \sum_{j'} \mathscr{D}_l^{mj'*}(\Omega_0)\overline{\mathscr{D}}_l^{j'k*}(\Omega_a), \tag{2.9}$$

where

$$h_l^j(s) = \exp\{-[l(l+1) + ij(\kappa_0^2 + \tau_0^2)^{1/2}]s\}, \tag{2.10}$$

$\overline{\mathscr{D}}_l^{mj}$ is the unnormalized Wigner function defined by

$$\overline{\mathscr{D}}_l^{mj}(\Omega) = c_l^{-1}\mathscr{D}_l^{mj}(\Omega), \tag{2.11}$$

and

$$\Omega_a = (\alpha, -\pi/2, \pi/2) \tag{2.12}$$

with

$$\alpha = -\tan^{-1}(\kappa_0/\tau_0), \quad (-\pi \leq \alpha \leq 0). \tag{2.13}$$

Comparing Eq. (2.4) with Eq. (2.9), we find

$$g_l^{l'}(s) = \sum_k h_l^k(s)\overline{\mathscr{D}}_l^{jk}(\Omega_a)\overline{\mathscr{D}}_l^{j'k*}(\Omega_a) \ . \tag{2.14}$$

Equation (2.1) with Eqs. (2.4), (2.8), and (2.14) gives the desired expression for U_0.

We then have for the equilibrium distribution function $\Psi_{eq}(\{\Omega_N\})$ of $\{\Omega_N\}$:

$$\Psi_{eq}(\{\Omega_N\}) = e^{-U_0} \Big/ \int e^{-U_0} d\{\Omega_n\}$$

$$= (8\pi^2)^{-1} \prod_{p=1}^{N-1} G(\Omega_{p+1} \mid \Omega_p \ ; \ \Delta s) \tag{2.15}$$

with $d\{\Omega_N\} = \prod_{p=1}^{N} d\Omega_p$. In what follows, Ψ_{eq} stands for $\Psi_{eq}(\{\Omega_N\})$ and $<\cdots>_{eq}$ denotes an equilibrium average evaluated with Ψ_{eq}.

Now the problem is to find the relation between a and Δs. This can be done by comparing the equilibrium moments of the discrete and continuous HW chains. It is then noted that vector moments such as the persistence vector[17,18] do not appear in dynamic properties: these may be written in terms of scalar moments, especially equilibrium ones, such as the mean-square radius of gyration and mean reciprocal distance between two contour points, in the regime of linear response. Therefore, the consideration of the equilibrium mean-square end-to-end distance $<R^2>_{eq}$ suffices for the present purpose.

For the discrete HW chain, $<R^2>_{eq} \equiv <R^2(N)>_{eq}$ may be expressed as

$$<R^2(N)>_{eq} = Na^2 + 2\sum_{p<q} <\mathbf{a}_p \cdot \mathbf{a}_q>_{eq}$$

$$= Na^2 + 2a^2 \sum_{n=1}^{N-1} (N - n) g_1^{00}(n\Delta s) , \tag{2.16}$$

where we have used the relation,

$$\int \Psi_{eq} d\{\Omega_N\} / d\Omega_p d\Omega_q = (8\pi^2)^{-1} G(\Omega_q \mid \Omega_p; n\Delta s) \tag{2.17}$$

with $q = p + n$. Substitution of Eq. (2.14) into the second line of Eqs. (2.16) leads to

$$<R^2(N)>_{eq} = \tilde{c}_\infty N\Delta s + \tilde{c}_0$$

$$+ [\tilde{c}_1 + \tilde{c}_2 \sin(\nu N\Delta s) + \tilde{c}_3 \cos(\nu N\Delta s)] e^{-2N\Delta s}, \tag{2.18}$$

where

$$\nu = (\kappa_0^2 + \tau_0^2)^{1/2}, \tag{2.19}$$

and

$$\tilde{c}_\infty = \frac{a^2}{\Delta s}\{1 + 2\tau_0^2 \nu^{-2} \tilde{c}_4 e^{-2\Delta s}$$

$$+ 2\kappa_0^2 \nu^{-2} \tilde{c}_5 e^{-2\Delta s}[\cos(\nu\Delta s) - e^{-2\Delta s}]\},$$

$$\tilde{c}_0 = -2a^2 e^{-2\Delta s}\{\tau_0^2 \nu^{-2} \tilde{c}_4^2$$

$$+ \kappa_0^2 \nu^{-2} \tilde{c}_6[(1 + e^{-4\Delta s})\cos(\nu\Delta s) - 2e^{-2\Delta s}]\},$$

$$\tilde{c}_1 = 2a^2 \tau_0^2 \nu^{-2} \tilde{c}_4(\tilde{c}_4 - 1) ,$$

$$\tilde{c}_2 = 2a^2 \kappa_0^2 \nu^{-2}\{\tilde{c}_5 e^{-2\Delta s} \sin(\nu\Delta s)$$

$$+ \tilde{c}_6[-2e^{-2\Delta s} \sin(\nu\Delta s) + e^{-4\Delta s} \sin(2\nu\Delta s)]\},$$

$$\tilde{c}_3 = 2a^2\kappa_0{}^2\nu^{-2}\{ - \tilde{c}_5[1 - e^{-2\Delta s}\cos(\nu\Delta s)]$$

$$+ \tilde{c}_6[1 - 2e^{-2\Delta s}\cos(\nu\Delta s) + e^{-4\Delta s}\cos(2\nu\Delta s)]\}, \tag{2.20}$$

with

$$\tilde{c}_4 = (1 - e^{-2\Delta s})^{-1},$$

$$\tilde{c}_5 = [1 - 2e^{-2\Delta s}\cos(\nu\Delta s) + e^{-4\Delta s}]^{-1},$$

$$\tilde{c}_6 = \{1 - 4e^{-2\Delta s}\cos(\nu\Delta s) + 2e^{-4\Delta s}[2 + \cos(2\nu\Delta s)]$$

$$- 4e^{-6\Delta s}\cos(\nu\Delta s) + e^{-8\Delta s}\}^{-1}. \tag{2.21}$$

For the continuous HW chain, $<R^2>_{eq} \equiv <R^2(L)>_{eq}$ has been given by Yamakawa and Fujii [Eq. (54) of Ref. 3 (with $t = L$ and $\sigma = 0$)]; that is,

$$<R^2(L)>_{eq} = c_\infty L - \tfrac{1}{2}\tau_0{}^2\nu^{-2} - 2\kappa_0{}^2\nu^{-2}(4 - \nu^2)(4 + \nu^2)^{-2} + e^{-2L}\{\tfrac{1}{2}\tau_0{}^2\nu^{-2}$$

$$+ 2\kappa_0{}^2\nu^{-2}(4 + \nu^2)^{-2}[(4 - \nu^2)\cos(\nu L) - 4\nu\sin(\nu L)]\}, \tag{2.22}$$

where c_∞ is its Kuhn segment length and is given by

$$c_\infty = \lim_{L\to\infty}(<R^2(L)>_{eq}/L) = (4 + \tau_0{}^2)/(4 + \kappa_0{}^2 + \tau_0{}^2)\ . \tag{2.23}$$

It is clear that in Eq. (2.18), we may put

$$N\Delta s = L\ . \tag{2.24}$$

We then impose the condition that

$$\tilde{c}_\infty = c_\infty \tag{2.25}$$

in order that $<R^2(N)>_{eq}$ becomes equal to $<R^2(L)>_{eq}$ in the limit $N \longrightarrow \infty$. From the first of Eq. (2.20) and Eq. (2.25), we have the

desired relation between a and Δs,

$$a = (c_\infty \Delta s)^{1/2}\{1 + 2\tau_0^2\nu^{-2}\tilde{c}_4 e^{-2\Delta s} + 2\kappa_0^2\nu^{-2}\tilde{c}_5 e^{-2\Delta s} \times [\cos(\nu\Delta s) - e^{-2\Delta s}]\}^{-1/2}. \quad (2.26)$$

Note that a can be uniquely determined if κ_0, τ_0, and Δs are given.

Our final problem regarding the model is to establish a criterion for the determination of Δs. The difference between the discrete and continuous chains becomes negligibly small as Δs is decreased to zero, while as remarked in Sec. 1–1, Δs must be equal to or greater than the contour length corresponding to two successive skeletal bonds in the real chain when it is flexible. This is also reasonable if we notice that the smallest motional unit in the real flexible chain to be probed must be composed of two or three skeletal bonds. On the other hand, Δs is not permitted to exceed some value, since then the difference between the discrete and continuous chains becomes appreciably large. This is clearly seen if we compare the dependence of $<R^2(N)>_{eq}$ and $<R^2(L)>_{eq}$ on N or L. We take as examples two cases: $\kappa_0 = 10$ and $\tau_0 = 15$ [isotactic polystyrene (i–PS)] and $\kappa_0 = 5$ and $\tau_0 = 1$ [syndiotactic poly(methyl methacrylate) (s–PMMA)].[19] Their values of $<R^2>_{eq}/c_\infty L$ are plotted against the logarithm of L in Figs. 2.2 and 2.3, respectively, where the full curves represent the values calculated from Eq. (2.22) for the continuous chains, and the points represent the values calculated from Eq. (2.18) with Eqs. (2.24)–(2.26) for the

discrete chains with Δs = 0.05 (open circles), 0.1 (filled circles), 0.2 (squares), and 0.4 (triangles), each for N = 1, 2, 3, 4, 5, 6, 8, 10, 30, and 100. In both cases, the deviation of the discrete chain with Δs = 0.4 (triangles) from the continuous chain is appreciably large for $L \lesssim 5$, so that Δs must be smaller than $\sim$ 0.4. More important is the fact that for large Δs, the local chain motions are over coarse-grained. (As Δs is increased, U_0 becomes asymptotically

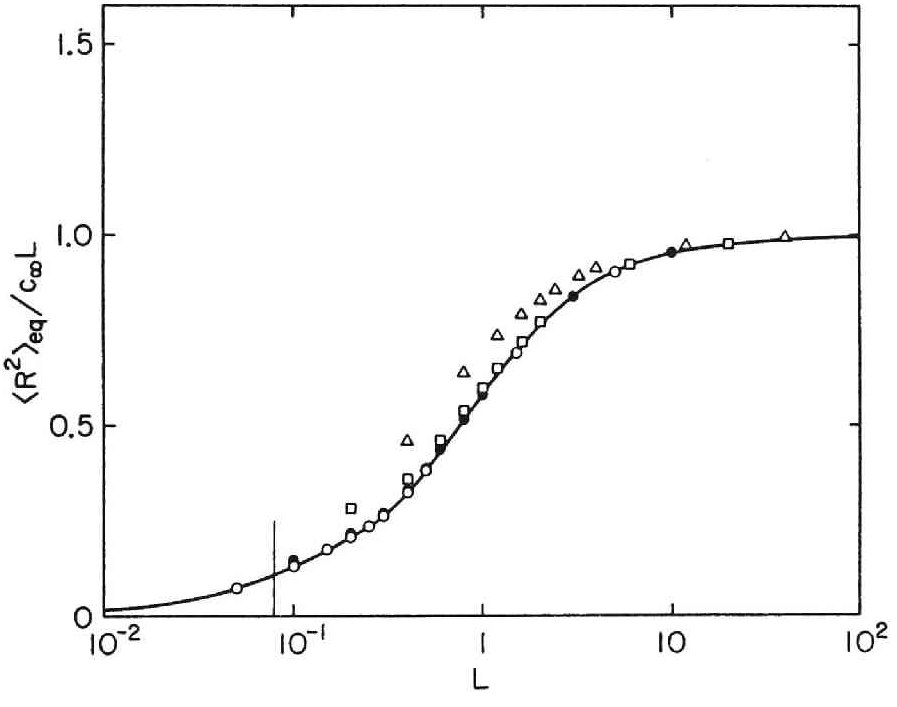

Fig. 2.2. Comparison between $\langle R^2 \rangle_{eq}/c_\infty L$ as functions of L for the continuous and discrete HW chains in the case of κ_0 = 10 and τ_0 = 15 (isotactic polystyrene). The full curve represents the values for the continuous chain, and the points represent the values for the discrete chains with Δs = 0.05 (open circles), 0.1 (filled circles), 0.2 (squares), and 0.4 (triangles), each for N = 1, 2, 3, 4, 5, 6, 8, 10, 30, and 100. The vertical line segment indicates the lower bound of L, which is equal to the length corresponding to two skeletal bonds.

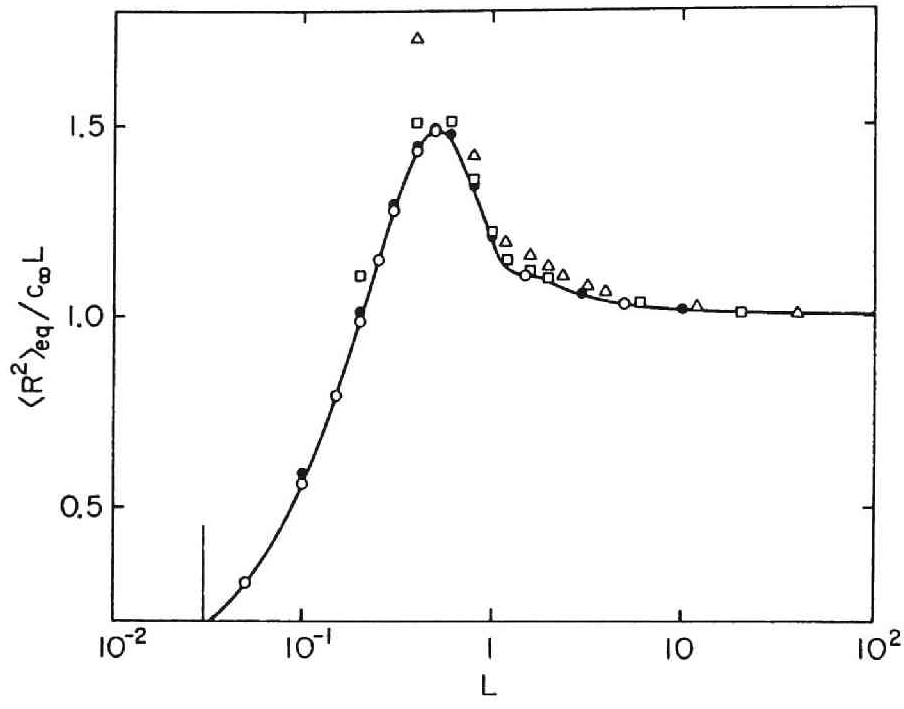

Fig. 2.3. Comparison between $<R^2>_{eq}/c_\infty L$ as functions of L for the continuous and discrete HW chains in the case of $\kappa_0 = 5$ and $\tau_0 = 1$ [syndiotactic poly(methyl methacrylate)]; see legend to Fig. 2.2.

independent of $\{\Omega_N\}$.) It is also helpful to note that the contour length Δs corresponding to two bonds is equal to ~ 0.08 for i-PS ($\lambda^{-1} = 25$ Å) and 0.03 for s-PMMA ($\lambda^{-1} = 65$ Å). The vertical line segments in Figs. 2.2 and 2.3 indicate these values as the lower bounds of L.

Thus, in the case of flexible chains, it is best to choose Δs to be equal to the contour length corresponding to two or three bonds, since it corresponds to the smallest motional unit and since

the deviation of the equilibrium conformational behavior of such a discrete chain from that of the continuous chain (real chain) is negligibly small. In the case of stiff chains, the important range of L is smaller, so that Δs must be much smaller; for DNA, for example, Δs will be equal to the distance between base pairs or so.

In sum, the discrete HW chain, i. e., our dynamic model may be described completely in terms of six parameters N, Δs (or a), κ_0, τ_0, ζ_t, and ζ_r, as far as all length are reduced by λ^{-1}. As shown above, if Δs is properly chosen, all equilibrium moments appearing in dynamic properties may be replaced in a very good approximation by those for the corresponding continuous HW chain. In anticipation of the results, we further note that in the study of dielectric relaxation, permanent electric dipole moments may be attached to the beads rigidly or with some rotational degrees of freedom.

2–3. Diffusion Equation

In this section, we derive the configurational diffusion equation for the discrete HW chain having $3(N + 1)$ degrees of freedom, i. e., three coordinates specifying its location and the N sets of Euler angles defining the orientations of the beads except the $(N + 1)$th. For this purpose, we first consider the chain without

(rigid) constraints such that each of the first N beads has six, translational and rotational, degrees of freedom and the $(N+1)$th has only three translational degrees, so that the magnitude of the bond vector $\mathbf{a}_p$ is not always equal to a, nor does its direction always coincide with the ζ_p axis of the localized coordinate system affixed to the pth bead, as depicted in Fig. 2.4. We then impose $3N$ rigid constraints on this chain through constraining forces in

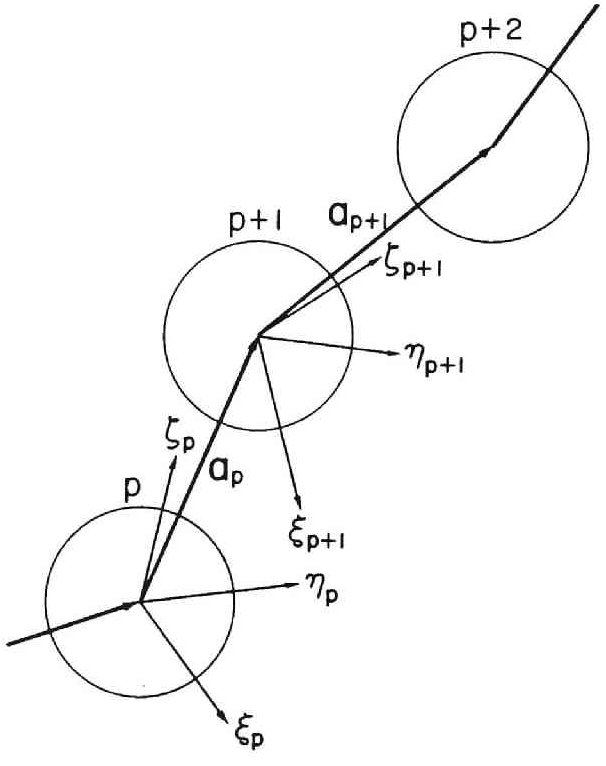

Fig. 2.4. Localized coordinate systems affixed to the beads in the chain having $6N+3$ degrees of freedom without rigid constraints.

such a way that the magnitude of $\mathbf{a}_p$ becomes equal to a and its direction becomes coincident with the ζ_p axis. This can be actually done by setting the components of the flux associated with the constrained coordinates equal to zero. For convenience, the derivation is made in two steps.

a. Space of bond and infinitesimal rotation vectors

We consider the chain having $6N + 3$ degrees of freedom (without rigid constraints) as defined above. Let $\mathbf{R}_p = (R_{px}, R_{py}, R_{pz})$ be the position vector of the center of the pth bead in an external Cartesian coordinate system ($\mathbf{e}_x$, $\mathbf{e}_y$, $\mathbf{e}_z$), and let $d\boldsymbol{\chi}_p = (d\chi_{p\xi}, d\chi_{p\eta}, d\chi_{p\zeta})$ be its infinitesimal rotation in the pth localized coordinate system having the orientation Ω_p with respect to the former. The metric form in $(d\{\mathbf{R}_{N+1}\}, d\{\chi_N\})$ space is

$$(dl)^2 = \sum_{p=1}^{N+1} (d\mathbf{R}_p)^2 + \sum_{p=1}^{N} (d\chi_p)^2. \tag{2.27}$$

The time-dependent distribution function $\Psi(\{\mathbf{R}_{N+1}\}, \{\Omega_N\}; t)$ for the chain satisfies the conservation equation in this space,

$$\frac{\partial \Psi}{\partial t} = -\sum_{p=1}^{N+1} \nabla_p^R \cdot \mathbf{J}_p^R - \sum_{p=1}^{N} \nabla_p^\chi \cdot \mathbf{J}_p^\chi , \tag{2.28}$$

where $\nabla_p^R = (\partial/\partial R_{px}, \partial/\partial R_{py}, \partial/\partial R_{pz})$, $\nabla_p^\chi = (\partial/\partial \chi_{p\xi}, \partial/\partial \chi_{p\eta}, \partial/\partial \chi_{p\zeta})$, and $\mathbf{J}_p^R$ and $\mathbf{J}_p^\chi$ are the fluxes associated with $d\mathbf{R}_p$ and $d\boldsymbol{\chi}_p$, respectively. Note that the second term on the right-hand side

of Eq. (2.28) does not appear for the ordinary model. If $\mathbf{V}_p$ and $\mathbf{W}_p$ are the translational and angular velocities of the pth bead in the external system, respectively, $\mathbf{J}_p^R$ and $\mathbf{J}_p^\chi$ may be expressed as

$$\mathbf{J}_p^R = \Psi \mathbf{V}_p , \quad (p = 1, 2, \cdots, N + 1) , \tag{2.29}$$

$$\mathbf{J}_p^\chi = \Psi \mathbf{A}_p \cdot \mathbf{W}_p , \quad (p = 1, 2, \cdots, N) , \tag{2.30}$$

where $\mathbf{A}_p = \mathbf{A}(\Omega_p)$ is the matrix for transformation from the external system to the pth localized system, and is given by

$$\mathbf{A}_p = \begin{pmatrix} c_{\theta_p}c_{\varphi_p}c_{\psi_p} - s_{\varphi_p}s_{\psi_p} & c_{\theta_p}s_{\varphi_p}c_{\psi_p} + c_{\varphi_p}s_{\psi_p} & -s_{\theta_p}c_{\psi_p} \\ -c_{\theta_p}c_{\varphi_p}s_{\psi_p} - s_{\varphi_p}c_{\psi_p} & -c_{\theta_p}s_{\varphi_p}s_{\psi_p} + c_{\varphi_p}c_{\psi_p} & s_{\theta_p}s_{\psi_p} \\ s_{\theta_p}c_{\varphi_p} & s_{\theta_p}s_{\varphi_p} & c_{\theta_p} \end{pmatrix} \tag{2.31}$$

with $s_{\theta_p} = \sin\theta_p$, $c_{\theta_p} = \cos\theta_p$, and so on.

Let $\mathbf{F}_p$ and $\mathbf{T}_p$ be the frictional force and torque, respectively, exerted by the pth bead on the solvent, and the force balance equations are

$$\mathbf{F}_p = -\nabla_p^R(U + \ln\Psi) + \mathbf{P}_p^R , \quad (p = 1, 2, \cdots, N + 1) , \tag{2.32}$$

$$\mathbf{A}_p \cdot \mathbf{T}_p = -\nabla_p^\chi(U + \ln\Psi) + \mathbf{P}_p^\chi , \quad (p = 1, 2, \cdots, N) , \tag{2.33}$$

where U is a "soft" potential,

$$U = U_0 + U_e \tag{2.34}$$

with $U_0(\{\Omega_N\})$ the configurational potential energy given by Eq. (2.1) (ignoring excluded volume potentials) and $U_e(\{\mathbf{R}_{N+1}\}, \{\Omega_N\})$ an external potential, and $\mathbf{P}_p^R$ and $\mathbf{P}_p^\chi$ are the constraining forces on

the pth bead associated with $d\mathbf{R}_p$ and $d\boldsymbol{\chi}_p$, respectively, which arises from "hard" potentials.

If $\mathbf{V}_p^0$ is the unperturbed solvent velocity at the location of the pth bead, $\mathbf{V}_p$ and $\mathbf{W}_p$ may be expressed in the form,

$$\mathbf{V}_p = \mathbf{V}_p^0 + \zeta_t^{-1}\mathbf{F}_p + \sum_{\substack{q=1 \\ \neq p}}^{N+1} \mathbf{T}_{pq}\cdot\mathbf{F}_q \ , \quad (p = 1, 2, \cdots, N+1) \ , \tag{2.35}$$

$$\mathbf{W}_p = \mathbf{W}_p^0 + \zeta_r^{-1}\mathbf{T}_p \ , \quad (p = 1, 2, \cdots, N) \ , \tag{2.36}$$

where

$$\mathbf{W}_p^0 = \tfrac{1}{2}\nabla_p^R \times \mathbf{V}_p^0 \ , \tag{2.37}$$

and $\mathbf{T}_{pq} = \mathrm{T}(\mathbf{R}_{pq})$ with $\mathbf{R}_{pq} = \mathbf{R}_q - \mathbf{R}_p$ is the Oseen hydrodynamic interaction tensor given by

$$\mathbf{T}(\mathbf{R}) = (8\pi\eta_0 R)^{-1}(\mathbf{I} + \mathbf{RR}/R^2) \tag{2.38}$$

with $\mathbf{I}$ the 3×3 unit tensor and η_0 the solvent viscosity. Equations (2.35) and (2.36) require some comments. They take into account correctly the hydrodynamic interaction between beads to terms of $\mathcal{O}(R^{-1})$. The effect of frictional force on angular velocity and that of frictional torque on translational velocity are at most of $\mathcal{O}(R^{-2})$, and the effect of frictional torque on angular velocity is at most of $\mathcal{O}(R^{-3})$.[20] Then the Oseen tensor cannot be modified so as to give correctly both translational and angular velocities to terms of $\mathcal{O}(R^{-3})$.[21] In what follows, we use, as usual, the configuration-independent preaveraged Oseen tensor,

$$<\mathbf{T}_{pq}> = (6\pi\eta_0)^{-1}<R_{pq}^{-1}>\mathbf{I} \ , \tag{2.39}$$

where $<\cdots>$ denotes an average taken with Ψ, and $<\mathbf{T}_{pq}>$ may be replaced by $<\mathbf{T}_{pq}>_{eq}$ in the regime of linear response.

Substitution of Eqs. (2.35) and (2.36) with Eqs. (2.32), (2.33), and (2.39) into Eqs. (2.29) and (2.30) leads to

$$\mathbf{J}_p^R = \sum_{q=1}^{N+1} D_{pq}(- \nabla_q^R \Psi - \Psi \nabla_q^R U + \Psi \mathbf{P}_p^R) + \Psi \mathbf{V}_p^0 , \tag{2.40}$$

$$\mathbf{J}_p^\chi = \zeta_r^{-1}(- \nabla_p^\chi \Psi - \Psi \nabla_p^\chi U + \Psi \mathbf{P}_p^\chi) + \Psi \mathbf{A}_p \cdot \mathbf{W}_p^0 \tag{2.41}$$

with

$$D_{pq} = \delta_{pq}\zeta_t^{-1} + (1 - \delta_{pq})(6\pi\eta_0)^{-1}<R_{pq}^{-1}> . \tag{2.42}$$

Equation (2.28) with Eqs. (2.40)–(2.42) gives the diffusion equation in $(d\{\mathbf{R}_{N+1}\}, d\{\boldsymbol{\chi}_N\})$ space.

Now we transform $\{\mathbf{R}_{N+1}\}$ to bond coordinates. Since $d\{\mathbf{R}_{N+1}\}$ is separable from $d\{\boldsymbol{\chi}_N\}$ in the above diffusion equation, we may consider only the former part. We put[22]

$$\mathbf{a}_p = \mathbf{R}_{p+1} - \mathbf{R}_p , \quad (p = 1, 2, \cdots, N) , \tag{2.43}$$

$$\mathbf{R}_C = \sum_{p=1}^{N+1} \omega_p \mathbf{R}_p , \tag{2.44}$$

where ω_p are constants independent of coordinates and satisfy

$$\sum_{p=1}^{N+1} \omega_p = 1 . \tag{2.45}$$

The differential operators may then be transformed to one another by

$$\nabla_p^R = \omega_p \nabla_C + (1 - \delta_{p1})\nabla_{p-1}^a - (1 - \delta_{p,N+1})\nabla_p^a ,$$

$$(p = 1, 2, \cdots, N + 1) , \tag{2.46}$$

where $\nabla_C = (\partial/\partial R_{Cx}, \partial/\partial R_{Cy}, \partial/\partial R_{Cz})$ and $\nabla_p^a = (\partial/\partial a_{px}, \partial/\partial a_{py}, \partial/\partial a_{pz})$. The transformation of the velocities $\mathbf{V}_p$ (and $\mathbf{V}_p^0$) to those, $\mathbf{V}_C$ and $\mathbf{v}_p$ (and $\mathbf{V}_C^0$ and $\mathbf{v}_p^0$) ($p = 1, 2, \cdots, N$), in $(\mathbf{R}_C, \{\mathbf{a}_N\})$ space of bond vectors obeys the same (contravariant) law as that of $\mathbf{R}_p$,

$$\mathbf{V}_C = \sum_{p=1}^{N+1} \omega_p \mathbf{V}_p , \tag{2.47}$$

$$\mathbf{v}_p = \mathbf{V}_{p+1} - \mathbf{V}_p , \quad (p = 1, 2, \cdots, N) , \tag{2.48}$$

while the transformation of the frictional forces $\mathbf{F}_p$ to those, $\mathbf{F}_C$ and $\mathbf{f}_p$ ($p = 1, 2, \cdots, N$), in $(\mathbf{R}_C, \{\mathbf{a}_N\})$ space obeys the same (covariant) law as that of ∇_p^R,

$$\mathbf{F}_p = \omega_p \mathbf{F}_C + (1 - \delta_{p1})\mathbf{f}_{p-1} - (1 - \delta_{p,N+1})\mathbf{f}_p ,$$

$$(p = 1, 2, \cdots, N + 1) . \tag{2.49}$$

Further, the transformation of the constraining forces $\mathbf{P}_p^R$ to those, $\mathbf{p}_p^a$ ($p = 1, 2, \cdots, N$), in $(\mathbf{R}_C, \{\mathbf{a}_N\})$ space is given by Eq. (2.49) with $\mathbf{F}_C = \mathbf{0}$ and with $\mathbf{P}_p^R$ and $\mathbf{p}_p^a$ in place of $\mathbf{F}_p$ and $\mathbf{f}_p$, respectively. (Note that there is not a constraining forces associated with $\mathbf{R}_C$.)

With these transformations, in $(\mathbf{R}_C, \{\mathbf{a}_N\})$ space, the translational part on the right-hand side of the conservation Eq. (2.28) may be written in the form,

$$\sum_{p=1}^{N+1} \nabla_p^R \cdot \mathbf{J}_p^R = \nabla_C \cdot \mathbf{J}_C + \sum_{p=1}^{N} \nabla_p^a \cdot \mathbf{J}_p^a , \tag{2.50}$$

where

$$\mathbf{J}_C = - D_C(\nabla_C \Psi + \Psi \nabla_C U_e)$$

$$+ \mathbf{V}_C^0 \Psi - \sum_{p=1}^{N} D_{C,p}(\nabla_p^a \Psi + \Psi \nabla_p^a U - \Psi \mathbf{p}_p^a) , \tag{2.51}$$

$$\mathbf{J}_p^a = - \sum_{q=1}^{N} B_{pq}(\nabla_p^a \Psi + \Psi \nabla_q^a U - \Psi \mathbf{p}_q^a)$$

$$+ \mathbf{v}_p^0 \Psi - D_{C,p}(\nabla_C \Psi + \Psi \nabla_C U_e) \tag{2.52}$$

with

$$D_C = \sum_{p,q=1}^{N+1} w_p w_q D_{pq} , \tag{2.53}$$

$$D_{C,p} = \sum_{q=1}^{N+1} w_q(- D_{qp} + D_{q,p+1}) , \tag{2.54}$$

$$B_{pq} = 2D_{pq} - D_{p,q+1} - D_{p+1,q} . \tag{2.55}$$

We note that we have used here the fact that U_0 is independent of $\mathbf{R}_C$.

If w_p is chosen to give

$$D_{C,p} = 0 \qquad \text{for all } p , \tag{2.56}$$

$\mathbf{J}_C$ and $\mathbf{J}_p^a$ are the fluxes associated with only $\mathbf{R}_C$ and $\mathbf{a}_p$, respectively, so that $\mathbf{R}_C$ and $\{\mathbf{a}_N\}$ may be decoupled. The w_p thus determined has the following meaning. From Eqs. (2.54) and (2.56), we have

$$\sum_{q=1}^{N+1} D_{pq} w_q = V , \quad (p = 1, 2, \cdots, N + 1) , \tag{2.57}$$

where V is a constant independent of p. It is seen from Eqs. (2.35), (2.39), (2.42), (2.45), and (2.57) that this ω_p is equal to the frictional force exerted by the pth bead when all beads are moved by the unit total force with the same translational velocity V, and from Eq. (2.53) that D_C is then equal to V and identical with the translational diffusion coefficient of the chain obtained from the exact solution of the Kirkwood–Riseman integral equation,[23] as given by $D_C = 0.192/\eta_0 <R^2>_{eq}^{1/2}$ in the nondraining coil limit.[24,25] We note that $\mathbf{R}_C$ is then Zimm's center of resistance.[26] In what follows, we use the ω_p thus chosen, so that the $D_{C,p}$ terms in $\mathbf{J}_C$ and $\mathbf{J}_p^a$ may be suppressed. It is also interesting to note that if ω_p is chosen to be equal to $(N+1)^{-1}$, so that $\mathbf{R}_C$ is the molecular center of mass, then Eq. (2.56) does not hold and the D_C given by Eq. (2.53) is identical with the translational diffusion coefficient in the Kirkwood general theory,[7] or the approximate solution of the Kirkwood–Riseman integral equation, as given by $D_C = 0.196/\eta_0 <R^2>_{eq}^{1/2}$ in the nondraining coil limit.[24,25] When the translational mode ($\mathbf{R}_C$) is not considered, the diffusion equation does not depend on the choice of ω_p, since then $\nabla_C \cdot \mathbf{J}_C$ in Eq. (2.50) and the $D_{C,p}$ term in $\mathbf{J}_p^a$ drop.

Thus, from Eqs. (2.28) and (2.50), we obtain for the diffusion equation for $\Psi(\mathbf{R}_C, \{\mathbf{a}_N\}, \{\Omega_N\}; t)$ in $(\mathbf{R}_C, \{\mathbf{a}_N\}, d\{\chi_N\})$ space

$$\frac{\partial \Psi}{\partial t} = -\nabla_C \cdot \mathbf{J}_C - \sum_{p=1}^{N} (\nabla_p^a \cdot \mathbf{J}_p^a + \nabla_p^\chi \mathbf{J}_p^\chi) , \tag{2.58}$$

where the fluxes $\mathbf{J}_C$, $\mathbf{J}_p^a$, and $\mathbf{J}_p^\chi$ are given by Eqs. (2.51) and (2.52) with Eq. (2.56) and Eq. (2.41), respectively. The force balance Eq. (2.32) is transformed, by the use of Eqs. (2.46) and (2.49), to those in this space,

$$\mathbf{F}_C = -\nabla_C(U_e + \ln \Psi) , \tag{2.59}$$

$$\mathbf{f}_p = -\nabla_p^a(U + \ln \Psi) + \mathbf{p}_p^a , \quad (p = 1, 2, \cdots, N) , \tag{2.60}$$

and Eq. (2.33) remains unaltered.

b. Space of Euler angles

Let $\tilde{\mathbf{a}}_p = (\tilde{a}_{p\xi}, \tilde{a}_{p\eta}, \tilde{a}_{p\zeta})$ be the pth bond vector expressed in the pth localized Cartesian system, with spherical polar coordinates $(\tilde{a}_p, \tilde{\theta}_p, \tilde{\varphi}_p)$ associated with it, so that

$$\tilde{\mathbf{a}}_p = \mathbf{A}_p \cdot \mathbf{a}_p , \tag{2.61}$$

with

$$\tilde{\mathbf{a}}_p = \tilde{a}_p \begin{pmatrix} \sin\tilde{\theta}_p \cos\tilde{\varphi}_p \\ \sin\tilde{\theta}_p \sin\tilde{\varphi}_p \\ \cos\tilde{\theta}_p \end{pmatrix} . \tag{2.62}$$

We transform the Cartesian coordinates $(d\mathbf{a}_p, d\boldsymbol{\chi}_p)$ to curvilinear coordinates (Θ_p, Ω_p) with $\Theta_p \equiv (\tilde{a}_p, \tilde{\theta}_p, \tilde{\varphi}_p)$ by

$$\begin{pmatrix} d\mathbf{a}_p \\ d\boldsymbol{\chi}_p \end{pmatrix} = \mathbf{U}_p \cdot \begin{pmatrix} d\Theta_p \\ d\Omega_p \end{pmatrix} \tag{2.63}$$

with

$$\mathbf{U}_p = \begin{pmatrix} \mathbf{U}_p^{a\Theta} & \mathbf{U}_p^{a\Omega} \\ \mathbf{0} & \mathbf{U}_p^{\chi\Omega} \end{pmatrix} , \tag{2.64}$$

where $\mathbf{0}$ is the 3×3 null matrix, and $\mathbf{U}_p^{a\Theta}$, $\mathbf{U}_p^{a\Omega}$, and $\mathbf{U}_p^{\chi\Omega}$ are the 3×3 matrices given by

$$U_{p.ij}^{a\Theta} = \sum_{k=1}^{3} A_{p,ki} \frac{\partial \tilde{a}_{p,k}}{\partial \Theta_{p,j}} , \quad (i, j = 1, 2, 3) , \tag{2.65}$$

$$U_{p.ij}^{a\Omega} = \sum_{k=1}^{3} \frac{\partial A_{p,ki}}{\partial \Omega_{p,j}} \tilde{a}_{p,k} , \quad (i, j = 1, 2, 3) , \tag{2.66}$$

$$\mathbf{U}_p^{\chi\Omega} = \begin{pmatrix} s_{\psi_p} & -s_{\theta_p} s_{\psi_p} & 0 \\ c_{\psi_p} & s_{\theta_p} s_{\psi_p} & 0 \\ 0 & c_{\theta_p} & 1 \end{pmatrix} \tag{2.67}$$

with $\Theta_p = (\Theta_{p.1}, \Theta_{p.2}, \Theta_{p.3}) = (\tilde{a}_p, \tilde{\theta}_p, \tilde{\varphi}_p)$, $\Omega_p = (\Omega_{p.1}, \Omega_{p.2}, \Omega_{p.3}) = (\theta_p, \varphi_p, \psi_p)$, and $\tilde{\mathbf{a}}_p = (\tilde{a}_{p.1}, \tilde{a}_{p.2}, \tilde{a}_{p.3}) = (\tilde{a}_{p\xi}, \tilde{a}_{p\eta}, \tilde{a}_{p\zeta})$, and with $U_{p.ij}^{a\Theta}$ and so on being the ij components of $\mathbf{U}_p^{a\Theta}$ and so on.

It is now convenient to use tensor algebra, although we have readily derived the diffusion Eq. (2.58) without its explicit use. Let $\mathbf{g}'$ and $\mathbf{g}$ be the $(6N + 3)\times(6N + 3)$ metric tensors in $(\mathbf{R}_C, \{\mathbf{a}_N\}, d\{\boldsymbol{\chi}_N\})$ and $(\mathbf{R}_C, \{\Theta_N\}, \{\Omega_N\})$ spaces, respectively, and let $\mathbf{U}'$ and $\mathbf{U}$ be the $(6N + 3)\times(6N + 3)$ transformation matrices between $(d\{\mathbf{R}_{N+1}\}, d\{\boldsymbol{\chi}_N\})$ and $(\mathbf{R}_C, \{\mathbf{a}_N\}, d\{\boldsymbol{\chi}_N\})$ and between $(\mathbf{R}_C, \{\mathbf{a}_N\}, d\{\boldsymbol{\chi}_N\})$ and $(\mathbf{R}_C, \{\Theta_N\}, \{\Omega_N\})$, respectively. We have $\mathbf{g}' = \mathbf{U}'^T \cdot \mathbf{U}'$ and $\mathbf{g} = \mathbf{U}^T \cdot \mathbf{g}' \cdot \mathbf{U}$, where the superscript T indicates the transpose. Noting the facts that the latter transformation is separable with respect to $\mathbf{R}_C$ and the bond (or bead) number p, and that $|\mathbf{g}'|$

= 1, we obtain for the determinant of $\mathbf{g}$:

$$|\mathbf{g}| = \prod_{p=1}^{N} g_p \tag{2.68}$$

with

$$g_p = |\mathbf{U}_p^T \cdot \mathbf{U}_p| = \tilde{a}_p^4 \sin^2\tilde{\theta}_p \sin^2\theta_p \,, \tag{2.69}$$

where we have used Eq. (2.63) for the transformation for the pth bond and bead. The diffusion Eq. (2.58) may then be transformed to that in ($\mathbf{R}_C$, $\{\Theta_N\}$, $\{\Omega_N\}$) space,

$$\frac{\partial \Psi}{\partial t} = -\nabla_C \cdot \mathbf{J}_C - \sum_{p=1}^{N} g_p^{-1/2} (\nabla_p^{\theta} g_p^{1/2} \cdot \mathbf{J}_p^{\theta} + \nabla_p^{\Omega} g_p^{1/2} \cdot \mathbf{J}_p^{\Omega}) \,, \tag{2.70}$$

where $\nabla_p^{\theta} = (\partial/\partial\tilde{a}_p,\ \partial/\partial\tilde{\theta}_p,\ \partial/\partial\tilde{\varphi}_p)$, $\nabla_p^{\Omega} = (\partial/\partial\theta_p,\ \partial/\partial\varphi_p\ \partial/\partial\psi_p)$, and $\mathbf{J}_p^{\theta}$ and $\mathbf{J}_p^{\Omega}$ are the fluxes associated with Θ_p and Ω_p, respectively.

These fluxes are obtained from $\mathbf{J}_p^{a}$ and $\mathbf{J}_p^{\chi}$ given by Eq. (2.52) with Eq. (2.56) and Eq. (2.41), respectively, by the contravariant transformation law,

$$\begin{pmatrix} \mathbf{J}_p^{\theta} \\ \mathbf{J}_p^{\Omega} \end{pmatrix} = \mathbf{U}_p^{-1} \begin{pmatrix} \mathbf{J}_p^{a} \\ \mathbf{J}_p^{\chi} \end{pmatrix} . \tag{2.71}$$

The gradient operators ∇_p^{a} and ∇_p^{χ} and the constraining forces $\mathbf{p}_p^{a}$ and $\mathbf{P}_p^{\chi}$ involved in $\mathbf{J}_p^{a}$ and $\mathbf{J}_p^{\chi}$ may be transformed to the gradient operators ∇_p^{θ} and ∇_p^{Ω} and the constraining forces $\mathbf{p}_p^{\theta}$ and $\mathbf{P}_p^{\Omega}$ on Θ_p and Ω_p, respectively, by the covariant law,

$$\begin{pmatrix} \nabla_p^{a} \\ \nabla_p^{\chi} \end{pmatrix} = \mathbf{U}_p^{-1T} \cdot \begin{pmatrix} \nabla_p^{\theta} \\ \nabla_p^{\Omega} \end{pmatrix} , \tag{2.72}$$

$$\begin{pmatrix} \mathbf{p}_p^{\alpha} \\ \mathbf{P}_p^{\chi} \end{pmatrix} = \mathbf{U}_p^{-1T} \cdot \begin{pmatrix} \mathbf{p}_p^{\theta} \\ \mathbf{P}_p^{\Omega} \end{pmatrix} . \tag{2.73}$$

The inverse $\mathbf{U}_p^{-1}$ in Eqs. (2.71)–(2.73) is found, from Eq. (2.64), to be

$$\mathbf{U}_p^{-1} = \begin{pmatrix} (\mathbf{U}_p^{\alpha\theta})^{-1} & -(\mathbf{U}_p^{\alpha\theta})^{-1} \cdot \mathbf{U}_p^{\alpha\Omega} \cdot (\mathbf{U}_p^{\chi\Omega})^{-1} \\ \mathbf{0} & (\mathbf{U}_p^{\chi\Omega})^{-1} \end{pmatrix} . \tag{2.74}$$

Thus, the results for $\mathbf{J}_p^{\theta}$ and $\mathbf{J}_p^{\Omega}$ are

$$\begin{aligned} \mathbf{J}_p^{\theta} = & -\zeta_r^{-1} \sum_{q=1}^{N} (\mathbf{U}_p^{\alpha\theta})^{-1} \cdot \mathbf{C}_{pq} \cdot (\mathbf{U}_q^{\alpha\theta})^{-1T} \cdot (\nabla_q^{\theta}\Psi + \Psi\nabla_q^{\theta}U_e - \Psi\mathbf{p}_q^{\theta}) \\ & + \zeta_r^{-1}(\mathbf{U}_p^{\alpha\theta})^{-1} \cdot \mathbf{E}_p \cdot (\mathbf{U}_p^{\chi\Omega})^{-1} \cdot (\nabla_p^{\Omega}\Psi + \Psi\nabla_p^{\Omega}U) \\ & + (\mathbf{U}_p^{\alpha\theta})^{-1} \cdot (\mathbf{v}_p^0 - \mathbf{E}_p \cdot \mathbf{A}_p \cdot \mathbf{W}_p^0)\Psi , \end{aligned} \tag{2.75}$$

$$\begin{aligned} \mathbf{J}_p^{\Omega} = & -\zeta_r^{-1}(\mathbf{U}_p^{\chi\Omega})^{-1} \cdot (\mathbf{U}_p^{\chi\Omega})^{-1T} \cdot (\nabla_p^{\Omega}\Psi + \Psi\nabla_p^{\Omega}U) \\ & + \zeta_r^{-1}(\mathbf{U}_p^{\chi\Omega})^{-1} \cdot \mathbf{E}_p^T \cdot (\mathbf{U}_p^{\alpha\theta})^{-1T} \cdot (\nabla_p^{\theta}\Psi + \Psi\nabla_p^{\theta}U_e - \Psi\mathbf{p}_p^{\theta}) \\ & + (\mathbf{U}_p^{\chi\Omega})^{-1} \cdot \mathbf{A}_p \cdot \mathbf{W}_p^0\Psi , \end{aligned} \tag{2.76}$$

with

$$\mathbf{C}_{pq} = \zeta_r B_{pq}\mathbf{I} + \delta_{pq}\mathbf{E}_p \cdot \mathbf{E}_p^T , \tag{2.77}$$

$$\mathbf{E}_p = \mathbf{U}_p^{\alpha\Omega} \cdot (\mathbf{U}_p^{\chi\Omega})^{-1} , \tag{2.78}$$

where in Eqs. (2.75) and (2.76), we have used the facts that U_0 is independent of $\{\Theta_N\}$, and that

$$\mathbf{p}_p^{\Omega} = \mathbf{0} , \quad (p = 1, 2, \cdots, N) . \tag{2.79}$$

Note that Eq. (2.79) does hold since the constraining forces must

be perpendicular to the unconstrained subspace.

Now, we consider the constraining forces $\mathbf{p}_p^{\Theta}$ ($p = 1, 2, \cdots, N$) to make the fluxes $\mathbf{J}_p^{\Theta}$ vanish,

$$\mathbf{J}_p^{\Theta} = \mathbf{0} , \quad (p = 1, 2, \cdots, N) . \tag{2.80}$$

The solution for $\mathbf{p}_p^{\Theta}$ is then found, from Eqs. (2.75) and (2.80), to be

$$\mathbf{p}_p^{\Theta} = \nabla_p^{\Theta}(\ln \Psi + U_e) - \sum_{q=1}^{N} (\mathbf{U}_p^{a\Theta})^T \cdot (\mathbf{C}^{-1})_{pq} \cdot [\mathbf{E}_q \cdot (\mathbf{U}_q^{\zeta\Omega})^{-1T}$$

$$\cdot (\nabla_q^{\Omega} \ln \Psi + \nabla_q^{\Omega} U) + \zeta_r(\mathbf{v}_q^0 - \mathbf{E}_q \cdot \mathbf{A}_q \cdot \mathbf{W}_q^0)] , \tag{2.81}$$

where $(\mathbf{C}^{-1})_{pq}$ is the pq element (3×3 matrix) of the inverse of the $3N \times 3N$ matrix $\mathbf{C}$ whose pq element is the 3×3 matrix $\mathbf{C}_{pq}$. As a result, Θ_p or $\tilde{\mathbf{a}}_p$ take *some* fixed values, and the corresponding fluxes $\mathbf{J}_p^{\Omega}$ are obtained from Eq. (2.76) with Eq. (2.81). For our purpose, we want to set $\Theta_p = (a, 0, \tilde{\varphi}_p)$ or $\tilde{\mathbf{a}}_p = (0, 0, a)$. However, the matrix $(\mathbf{U}_p^{a\Theta})^{-1T}$ in the second term on the right-hand side of Eq. (2.76) diverges at $\tilde{\theta}_p = 0$, and therefore these fixed values must be taken after substitution of Eq. (2.81) in to Eq. (2.76). Then this matrix does not appear in $\mathbf{J}_p^{\Omega}$. It can easily be shown that the $\mathbf{J}_p^{\Omega}$ thus obtained is exactly the same as that derived following the Ikeda-Erpenbeck-Kirkwood procedure.[8,9,24] However, we note that the present (Fixman-Kovac) procedure is more straightforward since in the course of the derivation of $\mathbf{J}_p^{\Omega}$, we also have $\mathbf{p}_p^{\Theta}$ as above that is required to complete Eq. (2.60) for $\mathbf{f}_p$.

Now that Θ_p takes the fixed values $(a,\ 0,\ \tilde{\varphi}_p)$, the distribution function $\Psi(\mathbf{R}_C,\ \{\Theta_N\},\ \{\Omega_N\};\ t)$ may be written in the form,

$$\Psi = \Psi_0(\{\Theta_N\})\overline{\Psi}(\mathbf{R}_C,\ \{\Omega_N\};\ t) \tag{2.82}$$

with

$$\Psi_0 = \prod_{p=1}^{N} [2\pi\tilde{a}_p^2 \sin\tilde{\theta}_p]^{-1}\delta(\tilde{a}_p - a)\delta(\tilde{\theta}_p)\ . \tag{2.83}$$

The average of any configuration-dependent quantity α may then be calculated from

$$\begin{aligned} <\alpha> &= \int \alpha\Psi\, |\,\mathrm{g}\,|^{1/2} d\mathbf{R}_C \prod_{p=1}^{N} d\tilde{a}_p d\tilde{\theta}_p d\tilde{\varphi}_p d\theta_p d\varphi_p d\psi_p \\ &= \int \alpha\overline{\Psi} d\mathbf{R}_C d\{\Omega_N\}\ , \end{aligned} \tag{2.84}$$

where we have used Eq. (2.68) with Eq. (2.69), and note that $\Theta_p = (a,\ 0,\ \tilde{\varphi}_p)$ or $\tilde{\mathbf{a}}_p = (0,\ 0,\ a)$ in $\overline{\Psi}$. It is also clear that Ψ_0 may be removed from the diffusion equation at the final stage. In what follows, therefore, we designate $\overline{\Psi}$ by Ψ.

Further, recall that the divergence and gradient operators with respect to $d\boldsymbol{\chi}_p$ and Ω_p may be written in terms of the angular momentum operator $\mathbf{L}_p = (L_{p\xi},\ L_{p\eta},\ L_{p\zeta})$,

$$\begin{aligned} &\nabla_p^{\chi}\cdot = (\sin\theta_p)^{-1}\nabla_p^{\Omega}\sin\theta_p \cdot (\mathbf{U}_p^{\chi\Omega})^{-1}\cdot = \mathbf{L}_p\cdot\ , \\ &\nabla_p^{\chi} = (\mathbf{U}_p^{\chi\Omega})^{-1T}\cdot\nabla_p^{\Omega} = \mathbf{L}_p \end{aligned} \tag{2.85}$$

with

$$L_{p\xi} = \sin\psi_p \frac{\partial}{\partial\theta_p} - \frac{\cos\psi_p}{\sin\theta_p}\frac{\partial}{\partial\varphi_p} + \cot\theta_p\cos\psi_p\frac{\partial}{\partial\psi_p} ,$$

$$L_{p\eta} = \cos\psi_p \frac{\partial}{\partial\theta_p} + \frac{\sin\psi_p}{\sin\theta_p}\frac{\partial}{\partial\varphi_p} - \cot\theta_p\sin\psi_p\frac{\partial}{\partial\psi_p} , \tag{2.86}$$

$$L_{p\zeta} = \frac{\partial}{\partial\psi_p} .$$

Thus, substituting Eqs. (2.76) and (2.80) with Eq. (2.81) into Eq. (2.70) and putting $\tilde{\mathbf{a}}_p = (0, 0, a)$ in $\mathbf{E}_p$ (and $\overline{\Psi}$), we obtain for the desired diffusion equation for $\overline{\Psi} \equiv \Psi(\mathbf{R}_C, \{\Omega_N\}; t)$ in $(\mathbf{R}_C, \{\Omega_N\})$ space

$$\frac{\partial\Psi}{\partial t} = -\nabla_C\cdot\mathbf{J}_C + \sum_{p,q=1}^{N}\mathbf{L}_p\cdot\{\mathbf{M}_{pq} \cdot[\zeta_r^{-1}(\mathbf{L}_q\Psi + \Psi\mathbf{L}_qU) - \mathbf{A}_q\cdot\mathbf{W}_q^0\Psi] - \mathbf{N}_{pq}\cdot\mathbf{v}_q^0\Psi\} , \tag{2.87}$$

where

$$\mathbf{M}_{pq} = \delta_{pq}\mathbf{I} - \mathbf{E}_p^T\cdot(\mathbf{C}^{-1})_{pq}\cdot\mathbf{E}_q , \tag{2.88}$$

$$\mathbf{N}_{pq} = \mathbf{E}_p^T\cdot(\mathbf{C}^{-1})_{pq} \tag{2.89}$$

with

$$\mathbf{E}_p = a\begin{pmatrix} c_{\theta_p}c_{\varphi_p}s_{\psi_p} + s_{\varphi_p}c_{\psi_p} & c_{\theta_p}c_{\varphi_p}c_{\psi_p} - s_{\varphi_p}s_{\psi_p} & 0 \\ c_{\theta_p}s_{\varphi_p}s_{\psi_p} - c_{\varphi_p}c_{\psi_p} & c_{\theta_p}s_{\varphi_p}c_{\psi_p} + c_{\varphi_p}s_{\psi_p} & 0 \\ -s_{\theta_p}s_{\psi_p} & -s_{\theta_p}c_{\psi_p} & 0 \end{pmatrix} . \tag{2.90}$$

The first term on the right-hand side of Eq. (2.87) will be necessary only in a few cases, such as in dynamic light scattering, for which

the translational mode must be considered, and therefore, in what follows, it is suppressed, so that $\Psi = \Psi(\{\Omega_N\};\ t)$.

It is then convenient to rewrite Eq. (2.87) in matrix notation as usual,

$$\frac{\partial \Psi}{\partial t} = \mathbf{L}\cdot\{\mathbf{M}\cdot[\zeta_r^{-1}(\mathbf{L}\Psi + \Psi\mathbf{L}U) - \mathbf{A}\cdot\mathbf{W}^0\Psi] - \mathbf{N}\cdot\mathbf{v}^0\Psi\} \tag{2.91}$$

with $\mathbf{v}^0 = (\mathbf{v}_1^0,\ \mathbf{v}_2^0,\ \cdots,\ \mathbf{v}_N^0)$, $\mathbf{W}^0 = (\mathbf{W}_1^0,\ \mathbf{W}_2^0,\ \cdots,\ \mathbf{W}_N^0)$, $\mathbf{L} = (\mathbf{L}_1,\ \mathbf{L}_2,\ \cdots,\ \mathbf{L}_N)$, and

$$\mathbf{M} = \mathbf{I}_N - \mathbf{E}^T\cdot\mathbf{C}^{-1}\cdot\mathbf{E}\ , \tag{2.92}$$

$$\mathbf{N} = \mathbf{E}^T\cdot\mathbf{C}^{-1}, \tag{2.93}$$

$$\mathbf{C} = \zeta_r\mathbf{B} + \mathbf{E}\cdot\mathbf{E}^T\ , \tag{2.94}$$

where $\mathbf{M}$, $\mathbf{N}$, $\mathbf{B}$, $\mathbf{A}$, $\mathbf{E}$, and $\mathbf{I}_N$ are the $3N\times3N$ matrices whose pq elements are the 3×3 matrices $\mathbf{M}_{pq}$, $\mathbf{N}_{pq}$, $\mathbf{B}_{pq}$, $\mathbf{A}_{pq}$, $\mathbf{E}_{pq}$, and $\mathbf{I}_{N,pq}$, respectively, with

$$\mathbf{B}_{pq} = B_{pq}\mathbf{I}\ , \tag{2.95}$$

and

$$\mathbf{A}_{pq} = \delta_{pq}\mathbf{A}_p\ ,\quad \mathbf{E}_{pq} = \delta_{pq}\mathbf{E}_p\ ,\quad \mathbf{I}_{N,pq} = \delta_{pq}\mathbf{I}\ . \tag{2.96}$$

It is also useful to introduce the self-adjoint formulation of the diffusion equation. We factor Ψ into the equilibrium distribution function Ψ_{eq} given by the first line of Eqs. (2.15) and Φ,

$$\Psi = \Psi_{eq}\Phi\ . \tag{2.97}$$

Equation (2.91) reduces to

$$(\partial/\partial t + \mathscr{L})\Phi = X\Phi \ , \tag{2.98}$$

where $\mathscr{L}$ and X are operators defined by

$$\mathscr{L} = -\zeta_r^{-1}\Psi_{eq}^{-1}\mathbf{L}\Psi_{eq}\cdot\mathbf{M}\cdot\mathbf{L} \ , \tag{2.99}$$

$$X = -\Psi_{eq}^{-1}\mathbf{L}\Psi_{eq}\cdot[\mathbf{M}\cdot\mathbf{A}\cdot\mathbf{W}^0 + \mathbf{N}\cdot\mathbf{v}^0 - \zeta_r^{-1}\mathbf{M}\cdot(\mathbf{L}U_e)] \ . \tag{2.100}$$

If the scalar product $<\alpha, \beta>$ of any two functions α and β of $\{\Omega_N\}$ is defined with the weighting function Ψ_{eq},

$$<\alpha, \beta> = \int \Psi_{eq}\alpha^*\beta d\{\Omega_N\} = <\alpha^*\beta>_{eq} \ , \tag{2.101}$$

then the operator $\mathscr{L}$ becomes self-adjoint,

$$<\alpha, \mathscr{L}\beta> = <\mathscr{L}\alpha, \beta>$$

$$= <(\mathbf{L}\alpha^*)\cdot\zeta_r^{-1}\mathbf{M}\cdot(\mathbf{L}\beta)>_{eq} \ . \tag{2.102}$$

For the later development, it is convenient to expand Ψ_{eq} in terms of the $\mathscr{D}$ functions as follows,

$$\Psi_{eq} = \sum_{l,m,j} g_l^{mj}(\Delta s)D_l^{mj}(\{\Omega_N\}) \ , \tag{2.103}$$

where

$$D_l^{mj}(\{\Omega_N\}) = \prod_{p=1}^{N} \mathscr{D}_{l_p}^{m_p j_p}(\Omega_p) \ , \tag{2.104}$$

with $\mathbf{l} = (l_1, l_2, \cdots, l_N)$, and so on. The coefficient g_l^{mj} may be obtained by multiplying the second line of Eqs. (2.15) by $D_l^{mj*}(\{\Omega_N\})$ and then integrating over $\{\Omega_N\}$. The result is

$$g_1^{\mathbf{mj}}(\Delta s) = (-1)^{m_1-j_1}(8\pi^2)^{N-3} \sum_{\mathbf{l}',\mathbf{m}'} \delta_{l_1'0}\delta_{j_1'0}\delta_{l_2'l_1}\delta_{l_N'l_N}\delta_{j_N'j_N}$$

$$\times\left[\prod_{p=2}^{N} g_{l_p'}^{j_p'(j_{p-1}'-j_{p-1})}(\Delta s)\right]\prod_{p=2}^{N-1} c_{l_p}c_{l_p'}c_{l_{p+1}'}(-1)^{c(p)+j_p'}$$

$$\times\begin{pmatrix} l_p' & l_{p+1}' & l_p \\ -c(p) & c(p+1) & -m_p \end{pmatrix}\begin{pmatrix} l_p' & l_{p+1}' & l_p \\ j_p' & -j_p'+j_p & -j_p \end{pmatrix}$$

$$\text{for } c(N+1) = 0 ,$$

$$= 0 \qquad \text{for } c(N+1) \neq 0 \tag{2.105}$$

with

$$c(p) = \sum_{q=1}^{p-1} m_q , \tag{2.106}$$

where c_l is given by Eq. (2.6), $g_l^{jj'}$ is given by Eq. (2.14), and (:::) is the Wigner $3-j$ symbol.[27] In deriving Eq. (2.105), we have used the properties of $\mathscr{D}_l^{mj}$,

$$\mathscr{D}_l^{mj*}(\Omega) = (-1)^{m-j}\mathscr{D}_l^{(-m)(-j)}(\Omega) , \tag{2.107}$$

$$\int \mathscr{D}_{l_1}^{m_1j_1}(\Omega)\mathscr{D}_{l_2}^{m_2j_2}(\Omega)\mathscr{D}_{l_3}^{m_3j_3}(\Omega)d\Omega$$

$$= 8\pi^2 c_{l_1}c_{l_2}c_{l_3}\begin{pmatrix} l_1 & l_2 & l_3 \\ m_1 & m_2 & m_3 \end{pmatrix}\begin{pmatrix} l_1 & l_2 & l_3 \\ j_1 & j_2 & j_3 \end{pmatrix} , \tag{2.108}$$

and the property of the $3-j$ symbol that it takes a nonzero value only when the following two relations hold at the same time:

$$m_1 + m_2 + m_3 = 0 ,$$

$$|l_1 - l_2| \leq l_3 \leq l_1 + l_2 . \tag{2.109}$$

c. Approximations

In order to obtain the solutions, we must make an approximation in the matrix $\mathbf{M}$ given by Eq. (2.92). It is then reasonable to preaverage the second term $\mathbf{E}\cdot\mathbf{E}^T$ on the right-hand side of Eq. (2.94) for the matrix $\mathbf{C}$, since the first term is already independent of the configuration through the preaveraged Oseen tensor. Thus, we have, from Eq. (2.90),

$$<\mathbf{E}_p\cdot\mathbf{E}_p^T>_{eq} = \tfrac{2}{3}a^2\mathbf{I}\ , \tag{2.110}$$

so that the pq element of $\mathbf{C}$ becomes a constant multiple of the unit matrix,

$$\mathbf{C}_{pq} = C_{pq}\mathbf{I} \tag{2.111}$$

with

$$C_{pq} = \zeta_r B_{pq} + \tfrac{2}{3}\delta_{pq}a^2\ . \tag{2.112}$$

The pq element of $\mathbf{M}$ then becomes

$$\mathbf{M}_{pq} = \delta_{pq}\mathbf{I} - (C^{-1})_{pq}\mathbf{E}_p^T\cdot\mathbf{E}_q\ , \tag{2.113}$$

where $\mathbf{E}_p^T\cdot\mathbf{E}_q$ may be expressed in terms of the $\mathscr{D}$ functions as follows;

$$\mathbf{E}_p^T\cdot\mathbf{E}_q = \tfrac{4}{3}\pi^2a^2\sum_{m,j,j'}(1-\delta_{j0})(1-\delta_{j'0})(\mathbf{n}_j\mathbf{n}_{j'}^*)$$

$$\times\mathscr{D}_1^{mj}(\Omega_p)\mathscr{D}_1^{mj'*}(\Omega_q) \tag{2.114}$$

with

$$\mathbf{n}_1 = \mathbf{n}_{-1}^{*} = (1,\ i,\ 0)\ . \tag{2.115}$$

The replacement of $\mathbf{E}_p \cdot \mathbf{E}_p^T$ by its average in $\mathbf{C}$ may be regarded as having no significant effects on the final results since it depends only on the orientation of a single bead. However, the further preaveraging on the $\mathbf{M}_{pq}$ given by Eq. (2.113) will destroy to a great extent the orientational correlations between beads and also the rigid constraints imposed, and therefore this must be avoided. Note that with the above approximation, $\mathscr{L}$ is still self-adjoint.

2-4. Conclusion

We have constructed a model suitable for the study of polymer chain dynamics, i. e., the discrete HW chain, in such a way that its equilibrium conformational behavior is almost identical with that of the continuous HW chain whose equilibrium properties have already been investigated in detail. The present model, on the one hand, may be expected to simulate rather well large- and small-scale motions of real chains, both flexible and stiff. On the other hand, it has an advantage in that the diffusion equation and all configuration-dependent properties may be expressed in terms of the $\mathscr{D}$ functions of Euler angles. In other words, the present model with the orientational degrees of freedom of beads will give more detailed information, especially about local

motions.

In this connection, three remarks should be made. First, there are constraints on bond lengths in the present model as well as in the bond chain, while the constrains on bond angles are replaced conveniently by those on orientations of beads (subbodies) in the former. Second, the present model does not require any preaveraging approximation other than that in matrix **C**, which is related to the hydrodynamic interaction between beads and the orientation of a single bead. Therefore, it scarcely breaks, to a great extent, the orientational correlations between beads and also the above constraints imposed. Third, for the present model with N sets of Euler angles as unconstrained (soft) coordinates, the correct diffusion equation can be derived straightforwardly following the rather old procedure of Ikeda, Erpenbeck, and Kirkwood,[8,9,24] as noted in Sec. 2–3*b*. Then, the determinant of the metric tensor (of the full coordinate space) can readily be evaluated, and the constraints can easily be imposed. (The latter has been actually done by the Fixman–Kovac procedure.[4,13]) Note that the usual bond chain with rigid constraints on bond lengths and angles is difficult to treat by this old (or the present FK) procedure if internal rotation (torsion) angles are used as soft coordinates, though the Fixman–Kovac procedure using bond coordinates is effective for it.

Finally, it should be mentioned that for the present model,

the procedure based on the Fixman general diffusion equation[13] including the metric potential is more laborious than the present one. The reason for this is that it requires the evaluation of the determinant of the metric tensor of the unconstrained subspace. At present, it is known to be useful for the short bond chain with internal rotation angles as soft coordinates,[28] and also for some small rigid molecules.[29]

References

[1]H. Yamakawa, Annu. Rev. Phys. Chem., **35**, 23 (1984).

[2]H. Yamakawa, Macromolecules, **10**, 692 (1977).

[3]H. Yamakawa and M. Fujii, J. Chem. Phys., **64**, 5222 (1976).

[4]M. Fixman and J. Kovac, J. Chem. Phys., **61**, 4939 (1974).

[5]M. Fixman, Proc. Natl. Acad. Sci. USA, **71**, 3050 (1974).

[6]H. A. Kramers, J. Chem. Phys., **14**, 415 (1946).

[7]J. G. Kirkwood, Rec. Trav. Chim., **68**, 649 (1949); J. Polym. Sci., **12**, 1 (1954).

[8]Y. Ikeda, Bull. Kobayashi Inst. Phys. Res., **6**, 44 (1956).

[9]J. J. Erpenbeck and J. G. Kirkwood, J. Chem. Phys., **29**, 909 (1958); **38**, 1023 (1963).

[10]G. Wilemski, J. Chem. Phys., **63**, 2540 (1975).

[11]U. M. Titulaer and J. M. Deutch, J. Chem. Phys., **63** 4505 (1975).

[12]W. H. Stockmayer and W. Burchard, J. Chem. Phys., **70**, 3138 (1979).

[13]M. Fixman, J. Chem. Phys., **69**, 1527 (1978).

[14]H. Yamakawa, M. Fujii, and J. Shimada, J. Chem. Phys., **65**, 2371 (1976).

[15]M. Abramowitz and I. A. Stegun, *Handbook of Mathematical Functions* (Dover, New York, 1965), p. 785.

[16]J. Shimada and H. Yamakawa, J. Chem. Phys., **73**, 4037 (1980).

[17]P. J. Flory, Proc. Natl. Acad. Sci. USA, **70**, 1819 (1973).

[18]H. Yamakawa and M. Fujii, J. Chem. Phys., **66**, 2584 (1977).

[19]H. Yamakawa and J. Shimada, J. Chem. Phys., **70**, 609 (1979).

[20]P. G. Wolynes and J. M. Deutch, J. Chem. Phys., **67**, 733 (1977).

[21]T. Yoshizaki and H. Yamakawa, J. Chem. Phys., **73**, 578 (1980).

[22]O. Hassager and R. B. Bird, J. Chem. Phys., **56**, 2498 (1972).

[23]J. G. Kirkwood and J. Riseman, J. Chem. Phys., **16**, 565 (1948).

[24]H. Yamakawa, *Modern Theory of Polymer Solutions* (Harper & Row, New York, 1971).

[25]B. H. Zimm, Macromolecules, **13**, 592 (1980).

[26]B. H. Zimm, J. Chem. Phys., **24**, 269 (1956).

[27]A. R. Edmonds, *Angular Momentum in Quantum Mechanics* (Princeton University, Princeton, N. J., 1974).

[28]D. C. Knauss and G. T. Evans, J. Chem. Phys., **72**, 1499 (1980).

[29]D. C. Knauss, G. T. Evans, and D. M. Grant, Chem. Phys. Lett., **71**, 158 (1980).

CHAPTER 3

EIGENVALUE PROBLEMS

3–1. Introduction

In Chap. 2, the diffusion equation has been derived for a new (dynamic) model, called the discrete helical wormlike (HW) chain. In this chapter, we inquire into a general method of solution of the eigenvalue problems associated with the diffusion operator $\mathscr{L}$.

Now, the derived diffusion equation, when linearized, is analogous to the Schrödinger equation. Because of this and the model itself, the solution may be formulated by analogy with the representation (or transformation) theory in quantum mechanics.[1] In fact, in Chap. 2, we have been able to choose as our basis set the products of the eigenfunctions of the angular momentum operators of subbodies, i. e., the Wigner $\mathscr{D}$ functions of Ω_p with Ω_p the Euler angles specifying the orientation of the pth subbody. (Note that for the conventional bond chain, it is difficult to prepare such a complete basis set.) Thus, the problem has been reduced to the eigenvalue problem for the matrix representation of the diffusion operator in this basis set. In this chapter, we transform it to a more convenient basis set, i. e., a *standard* representation[2]

which is formed by the eigenfunctions of total angular momentum operator[3,4] of the entire chain. With this new basis set, the problem may readily be, to a great extent, decoupled (diagonalized). As the result, it is reduced to an infinite number of eigenvalue problems of much smaller size, among which the number of the ones that are necessary to actually solve is very small. Moreover, this representation is very transparent since there is clear correspondence between the matrix elements and time-correlation functions relevant to a given observable; one (or some) observable corresponds to one reduced eigenvalue problem.

However, the size of every reduced eigenvalue problem, which is to be solved numerically, is still very large. Therefore, we treat a necessary reduced eigenvalue problem in a subspace (of full Hilbert space) containing those standard basis functions which are required for the formulation of time-correlation functions relevant to a given observable. This approximation is referred to as the subspace approximation. It is equivalent to neglecting the memory term in the projection operator method of Mori,[5] Zwanzig,[6] and Evans.[7] Mathematically, therefore, our approximation is on a level with that employed by Evans in his study of the dynamics of short bond chains.[7,8] However, the correctness of the results must depend on both the model adopted and the basis set chosen. Since our model is composed of subbodies having rotational degrees of freedom, it will give results that are quite different from earlier

ones for the conventional bond chain in some respects and that provide more detailed information, e. g., a number of branches of eigenvalue spectra (with unavoided and avoided crossings).

Even in the subspace approximation, the solution is actually impossible for large N. Therefore, we must introduce an additional approximation, i. e., a block-diagonal approximation with Fourier modes (or in standard Fourier representations), which becomes asymptotically correct in the limit $N \longrightarrow \infty$. With these approximations for $N \gg 1$, the problem may finally be reduced to N three- or several-dimensional problems as the case may be.

In order to carry out the numerical computations based on the general solution thus obtained, we must assign proper values to the six model parameters other than the number N of subbodies in the chain, i. e., the constant curvature κ_0 and torsion τ_0 of the characteristic helix of the (continuous) HW chain, the stiffness parameter λ^{-1}, the bond length a (or its equivalent Δs), and the translational and rotatory friction coefficients ζ_t and ζ_r of the subbody. The first three may be determined from equilibrium conformational properties, while the remaining three are characteristic of the dynamics of the present model. If Δs and N (or the total contour length L of the corresponding continuous HW chain) are given, L (or N) is determined from the relation $L = N\Delta s$. (Note that L may be converted to the molecular weight M by the relation $M = M_L L$ with M_L the so-called shift factor.)

For flexible chains, Δs should finally be chosen within its bounds set in Chap. 2 to give good agreement between calculated and observed values for, for instance, relaxation times, and thus it provides important information about the smallest motional unit in the chain backbone relevant to a given observable (or time scale). For stiff chains, Δs may be assigned, from the outset, a value corresponding to the smallest possible division that gives nearly a continuous model. The friction coefficients ζ_t and ζ_r need not necessarily be assigned Stokes law values precisely. However, it should be mentioned that their possible ranges are rather limited. The determination of them is also an important part of the study in this chapter.

Then, we consider conditions to be imposed on ζ_t and ζ_r. The parameter ζ_t determines the strength of hydrodynamic interaction, and it must lie in the range over which the Zwanzig singularities[9] never occur and the diffusion matrix B given by Eq. (2.55) with Eq. (2.42) is positive definite. Recall that they do for finite N whenever the Oseen hydrodynamic interaction tensor is used whether it is or is not preaveraged.[10] On the other hand, ζ_r does not appear in the theory of conventional bond chains. For the present model, the eigenvalues (or the relaxation rates) $\lambda^0_{L,k}$, which form the lowest of the $L = 1$ branches of the spectrum for the diffusion operator in the block-diagonal approximation (with L the "total angular momentum quantum number"), become

positive or negative at small wave number k depending on N and ζ_r (and also on ζ_t weakly), while the Fixman–Evans eigenvalues[11] for the constrained bond chain may possibly become negative at large wave numbers. Such breakdown of the positive definiteness of the diffusion operators arises from the preaveraging approximations adopted in Chap. 2, whose effects are different in ours and their cases. Fortunately, however, for flexible chains, it is possible to make our $\lambda^0_{1,0}$ small in magnitude and recover the Rouse–Zimm values[12,13] for $\lambda^0_{1,k}$ at small k in the *coil* limit of $N \gg 1$ in a very good approximation by choosing ζ_r properly. This determines its possible range. For typical stiff chains such as DNA, $\lambda^0_{1,0}$ is very small in magnitude independently of ζ_r, and then the possible range of ζ_r, or of the ratio $\zeta_r/a^2\zeta_t$, must be determined from a classical–hydrodynamic calculation, assuming a proper model for the subbody. Thus, in any case, we neglect the small $|\lambda^0_{1,0}|$ to make the lowest branch $\lambda^0_{1,k}$ start from zero (the translational mode) at $k = 0$, and remove completely the negative eigenvalues if any (for flexible chains). And ζ_t and ζ_r (along with Δs in the case of flexible chains) should finally be chosen in their allowed ranges to give good agreement between theory and experiment.

The plan of this chapter is as follows. In Sec. 3–2, we consider a unitary transformation to the standard basis set, and give expressions for the matrix elements of the identity and

diffusion operators and for time-correlation functions in this new basis set. In Sec. 3-3, we introduce the subspace approximation, and show its equivalence to the neglect of the memory term in the projection operator method. In Sec. 3-4, we decouple the problem into N problems of a small number of dimensions in the block-diagonal approximation (with the subspace approximation) for large N. In Sec. 3-5, we first examine the correctness of the diagonal approximation to the diffusion matrix B and its positive definiteness, and then make a detailed analysis of the lowest branch of the eigenvalue spectrum in order to determine the possible ranges of ζ_t and ζ_r. In Sec. 3-6, we discuss some general aspects of the theory developed in Chaps. 2 and 3. In the Appendices, we give the analytical solutions of the eigenvalue problems for dielectric relaxation. We also give an interpolation formula for the mean reciprocal distance between two subbodies, which is necessary for the evaluation of the approximate eigenvalues λ_k^B of the diffusion matrix B (strictly $\zeta_t B$).

3-2. Transformation of the Basis Set

a. Standard basis set

We want to construct from the set $\{D_\mu\}$ [$= \{D_l^{mj}\}$ defined by Eq. (2.104)] a new set of those basis functions which are

simultaneous eigenfunctions of the square $\mathbf{L}^2$ and the z component L_z of the total angular momentum operator $\mathbf{L} = \mathbf{L}_1 + \mathbf{L}_2 + \cdots + \mathbf{L}_N$. This can be done by an application of the theory for the coupling of angular momentum vectors.[3,4] For this purpose, it is convenient to first divide the set $\{D_\mu\}$ into subsets, each specified by the index n (= 0, 1, $\cdots$, N) and composed of functions,

$$D^{\{m_n\}\{j_n\}}_{\{l_n\}[p_n]}(\Omega_{p_1}, \Omega_{p_2}, \cdots, \Omega_{p_n}) \equiv (8\pi^2)^{-(N-n)/2} \sum_{k=1}^{n} \mathscr{D}^{m_k j_k}_{l_k}(\Omega_{p_k}) , \tag{3.1}$$

where $\{l_n\} = l_1, l_2, \cdots, l_n$ and so on, and $[p_n] = p_1, p_2, \cdots, p_n$ ($p_1 < p_2 < \cdots < p_n$). The function defined by Eq. (3.1) is just equal to the D_μ [given by Eq. (2.104)] with $l_p = 0$ for $p \neq p_1, p_2, \cdots, p_n$, implying that only n particular subbodies, the p_1th, the p_2th, $\cdots$, the p_nth, are "excited." For convenience, therefore, these functions specified by n (irrespective of $[p_n]$) are referred to as the n-body excitation basis functions. Then, for given $[p_n]$, those new n-body excitation basis functions which are simultaneous eigenfunctions of $\mathbf{L}^2$ and L_z may be constructed from linear combinations of the above n-body functions. In practice, we may construct those linear combinations which are simultaneous eigenfunctions of the square and the z component of $\mathbf{L}_{p_1} + \mathbf{L}_{p_2} + \cdots + \mathbf{L}_{p_n}$. The new basis functions thus constructed for all n and $[p_n]$ form the desired new complete basis set. The zero-body excitation is trivial, and therefore we consider the case of one-, two-, and n-body ($n \geq 3$) excitations in order.

In the case of $n = 1$, it is seen that the one-body functions given by Eq. (3.1) are just the simultaneous eigenfunctions of $\mathbf{L}^2$ and L_z, since $\mathscr{D}_l^{mj}(\Omega_p)$ are the simultaneous eigenfunctions of $\mathbf{L}_p^2$, L_{pz} $(= \partial/\partial\varphi_p)$, and $L_{p\zeta}$ $(= \partial/\partial\psi_p)$, i. e.,[14]

$$\begin{pmatrix} \mathbf{L}_p^2 \\ L_{pz} \\ L_{p\zeta} \end{pmatrix} \mathscr{D}_l^{mj}(\Omega_p) = \begin{pmatrix} -l(l+1) \\ im \\ ij \end{pmatrix} \mathscr{D}_l^{mj}(\Omega_p) \tag{3.2}$$

with i the imaginary unit. We designate these (new) one-body excitation basis functions by $\tilde{D}_{L,[p]}^{M,j}(\Omega_p)$, where we have used the (resultant) quantum numbers L and M to indicate that the eigenvalues of $\mathbf{L}^2$ and L_z are $-L(L+1)$ and iM, respectively. Thus, we have

$$\tilde{D}_{L,[p]}^{M,j}(\Omega_p) = D_{L[p]}^{Mj}(\Omega_p) = (8\pi^2)^{-(N-1)/2}\mathscr{D}_L^{Mj}(\Omega_p)\ . \tag{3.3}$$

In the case of $n = 2$, the new two-body excitation basis functions, which we designate by $\tilde{D}_{L,(l_1l_2)[p_1p_2]}^{M,(j_1j_2)}(\Omega_{p_1}, \Omega_{p_2})$, may be obtained from, for instance, Eq. (3.5.1) of Edmonds[3] as

$$\begin{aligned} &\tilde{D}_{L,(l_1l_2)[p_1p_2]}^{M,(j_1j_2)}(\Omega_{p_1}, \Omega_{p_2}) \\ &\quad = \sum_{m_1,m_2} <l_1m_1l_2m_2 \mid l_1l_2LM> D_{(l_1l_2)[p_1p_2]}^{(m_1m_2)(j_1j_2)}(\Omega_{p_1}, \Omega_{p_2}) \\ &\quad = (8\pi^2)^{-(N-2)/2} \sum_{m_1,m_2} <l_1m_1l_2m_2 \mid l_1l_2LM> \mathscr{D}_{l_1}^{m_1j_1}(\Omega_{p_1})\mathscr{D}_{l_2}^{m_2j_2}(\Omega_{p_2})\ , \end{aligned} \tag{3.4}$$

where $<\cdots \mid \cdots>$ is the vector-coupling (VC) coefficient.[3] These new functions are the simultaneous eigenfunctions of $\mathbf{L}_{p_1}^2$, $\mathbf{L}_{p_2}^2$, $(\mathbf{L}_{p_1} + \mathbf{L}_{p_2})^2$, $L_{p_1z} + L_{p_2z}$, $L_{p_1\zeta}$, and $L_{p_2\zeta}$ with the eigenvalues $-l_1(l_1+1)$, $-l_2(l_2+1)$, $-L(L+1)$, iM, ij_1, and ij_2, respectively. We note that the quantum numbers l_1, l_2, m_1, m_2, j_1, and j_2 are changed

to L, M, l_1, l_2, j_1, and j_2 in the transformation given by Eq. (3.4), which does not depend on the *additional* quantum numbers j_1 and j_2, and also that the above VC coefficient vanishes unless $|l_1 - l_2| \leq L \leq l_1 + l_2$ and $m_1 + m_2 = M$ $(= -L, -L+1, \cdots, L-1, L)$, so that L and M lie in these ranges and the sum in Eq (3.4) may be taken over m_1 and m_2 compatible with $m_1 + m_2 = M$.

In the case of $n \geq 3$, there exist two or more (in general many) different schemes of the coupling of angular momentum vectors. We here adopt the scheme in which n angular momenta $\mathbf{L}_{p_1}$, $\mathbf{L}_{p_2}$, $\cdots$, $\mathbf{L}_{p_n}$ are added step-by-step with $n-2$ intermediate angular momenta $\hat{\mathbf{L}}_k$ $(k = 2, 3, \cdots, n-1)$

$$\hat{\mathbf{L}}_k = \hat{\mathbf{L}}_{k-1} + \mathbf{L}_{p_k}, \quad (k = 2, 3, \cdots, n-1), \tag{3.5}$$

with $\hat{\mathbf{L}}_1 \equiv \mathbf{L}_{p_1}$ and $\hat{\mathbf{L}}_n \equiv \mathbf{L}_{p_1} + \mathbf{L}_{p_2} + \cdots + \mathbf{L}_{p_n}$. Then, those new n-body excitation basis functions which are simultaneous eigenfunctions of $\mathbf{L}_{p_k}^2$ $(k = 1, 2, \cdots, n)$, $\hat{\mathbf{L}}_k^2$ $(k = 2, 3, \cdots, n-1)$, $(\mathbf{L}_{p_1} + \mathbf{L}_{p_2} + \cdots + \mathbf{L}_{p_n})^2$, $L_{p_1 z} + L_{p_2 z} + \cdots + L_{p_n z}$, and $L_{p_k \zeta}$ $(k = 1, 2, \cdots, n)$ with the eigenvalues $-l_k(l_k+1)$ $(k = 1, 2, \cdots, n)$, $-\hat{l}_k(\hat{l}_k+1)$ $(k = 2, 3, \cdots, n-1)$, $-L(L+1)$, iM, and ij_k $(k = 1, 2, \cdots, n)$, respectively, are given by[4]

$$\tilde{D}^{M}_{L,\gamma} \equiv D^{M,\{j_n\}}_{L,\{\hat{l}_n\}\{l_{n-2}\}[p_n]}(\Omega_{p_1}, \Omega_{p_2}, \cdots, \Omega_{p_n})$$

$$= \sum_{\{m_n\}} \delta_{\hat{m}_n, M} \left[\prod_{k=2}^{n} \langle \hat{l}_{k-1} \hat{m}_{k-1} l_k m_k \,|\, \hat{l}_{k-1} l_k \hat{l}_k \hat{m}_k \rangle \right]$$

$$\times D^{\{m_n\}\{j_n\}}_{\{l_n\}\{p_n\}}(\Omega_{p_1}, \Omega_{p_2}, \cdots, \Omega_{p_n}) , \tag{3.6}$$

where $\gamma = \{l_n\}\{\hat{l}_{n-2}\}\{j_n\}[p_n]$, $\{\hat{l}_{n-2}\} = \hat{l}_2, \hat{l}_3, \cdots, \hat{l}_{n-1}$ with $\hat{l}_1 = l_1$ and $\hat{l}_n = L$, and $\hat{m}_k$ is given by

$$\hat{m}_k = \sum_{i=1}^{k} m_i , \quad (k = 1, 2, \cdots, n) . \tag{3.7}$$

In the transformation given by Eq. (3.6), the quantum numbers $\{l_n\}$, $\{m_n\}$, $\{j_n\}$, and the subbody numbers $[p_n]$ are changed to L, M, and γ (L, M, and $\{\hat{l}_{n-2}\}$ on the left-hand side instead of $\{m_n\}$ on the right-hand side), $\{j_n\}$ being the additional quantum numbers. We note that $\max[2\max(l_1, l_2, \cdots, l_n) - \sum_{k=1}^{n} l_k, 0] \leq L \leq \sum_{k=1}^{n} l_k$, and $M = \sum_{k=1}^{n} m_k = -L, -L+1, \cdots, L$. In what follows, we also designate the new one- and two-body excitation basis functions simply by $\tilde{D}^M_{L,\gamma}$ with $\gamma = j[p]$ for $n = 1$ and $\gamma = (l_1 l_2)(j_1 j_2)[p_1 p_2]$ for $n = 2$.

Now, from the orthonormality of the $\mathscr{D}$ functions, i. e.,

$$\int \mathscr{D}^{mj*}_{l}(\Omega)\mathscr{D}^{m'j'}_{l'}(\Omega)d\Omega = \delta_{ll'}\delta_{mm'}\delta_{jj'} \tag{3.8}$$

with the asterisk indicating the complex conjugate, and the unitarity of the VC coefficients, as given by Eq. (3.5.4) of Edmonds,[3] the new basis functions $\tilde{D}^M_{L,\gamma}$ thus obtained (for all n and $[p_n]$) are seen to have the orthonormality

$$\int \tilde{D}^{M*}_{L,\gamma}\tilde{D}^{M'}_{L',\gamma'}d\{\Omega_N\} = \delta_{LL'}\delta_{MM'}\delta_{\gamma\gamma'} . \tag{3.9}$$

Therefore, if in matrix notation, the above transformation from D_μ to $\tilde{D}^M_{L,\gamma}$ is written as

$$\tilde{D} = U^T D \ , \tag{3.10}$$

then the matrix U is unitary, and in fact orthogonal since the VC coefficient is real. As seen from Eqs. (3.3), (3.4), and (3.6) this transformation is decoupled into those between finite-dimensional subspaces of full Hilbert space with n, $\{l_n\}$, $\{j_n\}$, and $[p_n]$ fixed, so that U is diagonal in these indices. We also note that the new basis set $\{\tilde{D}^M_{L,\gamma}\}$ is complete since the inverse of U exists. Finally, from the fact that $\tilde{D}^M_{L,\gamma}$ are the simultaneous eigenfunctions of $\mathbf{L}^2$ and L_z and satisfy the orthonormality given by Eq. (3.9), we see that the set $\{\tilde{D}^M_{L,\gamma}\}$ is just a standard basis set in the full Hilbert space,[2] and thus the desired one.

b. Matrices E and L

Let $\tilde{E}$ and $\tilde{L}$ be the standard matrix representations of the identity operator and the diffusion operator $\mathscr{L}$ with weight $\Psi_{\rm eq}$, respectively, in the basis set $\{\tilde{D}^M_{L,\gamma}\}$. For convenience, the matrix elements constructed from the n- and n'-body excitation basis functions are referred to as the (n, n')-body elements. In what follows, the standard basis functions and standard representations are designated by the symbols without tilde unless noted otherwise. As in Chap. 2, all lengths are measured in units of the length λ^{-1}, and $k_{\rm B}T$ is chosen to be unity, where $k_{\rm B}$ is the Boltzmann constant and T is the absolute temperature.

Now, the scalar Ψ_{eq} and the scalar operator $\mathcal{L}$ are rotationally invariant, and commute with the components of the total angular momentum operator **L**. According to the theory of angular momentum,[2] therefore, the standard representation E and L are diagonal in the total angular momentum and magnetic quantum numbers L and M, and moreover their diagonal elements are independent of M (a special case of the Wigner–Eckart theorem). This leads to $(2L + 1)$–fold degeneracy with respect to M. The matrix elements may then be written in the form

$$<D^{M*}_{L,\gamma} D^{M'}_{L',\gamma'}>_{eq} = \delta_{LL'}\delta_{MM'}E_{L,\gamma\gamma'} , \tag{3.11}$$

$$<D^{M*}_{L,\gamma} \mathcal{L} D^{M'}_{L',\gamma'}>_{eq} = \delta_{LL'}\delta_{MM'}L_{L,\gamma\gamma'} . \tag{3.12}$$

(We note that in any nonstandard basis $|\gamma LM>$ such that $<\gamma LM|\gamma' L'M'> = \delta_{LL'}\delta_{MM'}C_{\gamma\gamma'}$ with $C_{\gamma\gamma'} \neq \delta_{\gamma\gamma'}$, the matrix representation of a scalar operator is diagonal in L and M, but then its diagonal elements are dependent on both L and M.) Thus, the elements $E_{L,\gamma\gamma'}$ and $L_{L,\gamma\gamma'}$ of the submatrices E_L and L_L may be evaluated simply at $M = M' = 0$. Note also that E_L and L_L are self–adjoint, i. e., $E_L = E_L^\dagger$ and $L_L = L_L^\dagger$, where the dagger indicates the adjoint.

In the following, we give explicit expressions only for the (1, 1)– and (2, 2)–body elements of E_L and L_L. The (1, 2)– and (2, 1)–body elements may readily be found from the (2, 2)–body elements. These will be sufficient for later practical use. In the

evaluation, we have used Eq. (3.7.3) of Edmonds[3] for the relationship between the VC coefficient and the $3-j$ symbol, Eq. (3.7.8) for the orthogonality of the $3-j$ symbols, and Eq. (6.2.8) for the replacement of the sum of products of three $3-j$ symbols by the product of a $3-j$ symbol and a $6-j$ symbol.

(i). (1, 1)–body elements

We have for the (1, 1)–body elements $E_{L,\gamma\gamma'}$ and $L_{L,\gamma\gamma'}$, with $\gamma = j[p]$ and $\gamma' = j'[p']$ for $p \leq p'$

$$E^{(j,j')}_{L,[p,p']} = (8\pi^2)^{-N} g^{jj'*}_L [(p' - p)\Delta s] , \tag{3.13}$$

$$L^{(j,j')}_{L,[p,p']} = (8\pi^2)^{-N} \zeta_r^{-1} \{ j^2 \delta_{jj'} \delta_{pp'} - [a^2 (C^{-1})_{pp'} - \delta_{pp'}]$$
$$\times \sum_{\Delta l=-1}^{1} (L + \Delta l + \tfrac{1}{2}) f(L, j; \Delta l) f(L, j'; \Delta l) g^{jj'*}_{L+\Delta l} [(p' - p)\Delta s] \} , \tag{3.14}$$

where $g^{jj'}_l$ is given by Eq. (2.14) and $f(l, j; \Delta l)$ is given by

$$f(l, j; \Delta l) \equiv \sum_{k=-1}^{1} (1 - \delta_{k0}) c^{kj}_l \begin{pmatrix} l & 1 & l + \Delta l \\ j + k & -k & -j \end{pmatrix}$$

$$= 2l(-1)^{l+j+1} \left[\frac{(l + j + 1)(l - j + 1)}{(2l + 1)(2l + 2)(2l + 3)} \right]^{1/2} \quad \text{for } \Delta l = 1$$

$$= 2j(-1)^{l+j} \left[\frac{1}{l(2l + 1)(2l + 2)} \right]^{1/2} \quad \text{for } \Delta l = 0$$

$$= 2(l + 1)(-1)^{l+j+1} \left[\frac{(l + j)(l - j)}{2l(2l - 1)(2l + 1)} \right]^{1/2} \quad \text{for } \Delta l = -1 \tag{3.15}$$

with (:::) being the $3-j$ symbol and with

$$c^j_l = [(l - j)(l + j + 1)]^{1/2} . \tag{3.16}$$

The elements for $p > p'$ may be obtained from Eqs. (3.13) and (3.14) with the self-adjointness of E_L and L_L, e. g., $E^{(j,j')}_{L,[p,p']} = E^{(j',j)*}_{L,[p',p]}$.

(ii). (2, 2)-body elements

We have for the (2, 2)-body elements $E_{L,\gamma\gamma'}$ with $\gamma = (l_1 l_2)(j_1 j_2)[p_1 p_2]$ and $\gamma' = (l_1' l_2')(j_1' j_2')[p_1' p_2']$ for $p_1 \leq p_1'$ (where $p_1 < p_2$ and $p_1' < p_2'$ by the assumption)

$$E^{(j_1 j_2, j_1' j_2')}_{L,(l_1 l_2, l_1' l_2')[p_1 p_2, p_1' p_2']} = (-1)^{L+l_1'+l_2'+j_1'+j_2'}(8\pi^2)^{-N}$$
$$\times \sum_{l} F_{Ll(l_1 l_2, l_1' l_2')[p_1 p_2, p_1' p_2']} \sum_{j_2'', j_3''} J^{w(j_1 j_2, -j_1', -j_2')j_2'' j_3''}_{lw(l_1 l_2 l_1' l_2')} [\bar{w}(p_1 p_2 p_1' p_2')] \ . \qquad (3.17)$$

Here, F . . . are numerical constants given by

$$F_{Ll(l_1 l_2, l_1' l_2')[p_1 p_2, p_1' p_2']}$$
$$= \delta_{Ll}(-1)^l(2l+1)^{-1/2} \qquad \text{for } p_1 < p_2 < p_1' < p_2'$$
$$= (-1)^{l+l_2+l_1'}(2l+1)^{1/2}\begin{Bmatrix} l_1' & l_2' & L \\ l_2 & l_1 & l \end{Bmatrix} \qquad \text{for } p_1 < p_1' < p_2 < p_2'$$
$$= (-1)^{l_1'+l_2'}(2l+1)^{1/2}\begin{Bmatrix} l_1' & l_2' & L \\ l_2 & l_1 & l \end{Bmatrix} \qquad \text{for } p_1 < p_1' < p_2' < p_2 \ , \qquad (3.18)$$

where $\{\cdots\}$ is the $6-j$ symbol,[3] and vanishes unless $|l_1 - l_1'| \leq l \leq l_1 + l_1'$. $\bar{w}$ is an operator that rearranges the subbody numbers p_1, p_2, p_1', p_2' in the increasing order, and w is an operator that rearranges the four indices l_1, l_2 l_1', l_2' or j_1, j_2, $-j_1'$, $-j_2'$ in the

order corresponding to that of the subbody numbers, e. g.,

$$\omega(l_1 l_2 l_1' l_2') = (l_1 l_2 l_1' l_2') \quad \text{for} \quad p_1 < p_2 < p_1' < p_2'$$

$$= (l_1 l_1' l_2 l_2') \quad \text{for} \quad p_1 < p_1' < p_2 < p_2'$$

$$= (l_1 l_1' l_2' l_2) \quad \text{for} \quad p_1 < p_1' < p_2' < p_2 \,. \tag{3.19}$$

Thus, $J^{:::}$ as a function of the subbody numbers depends on the order of them, and for $p_1 < p_2 < p_3 < p_4$, it is given by

$$J^{(j_1 j_2 j_3 j_4) j_2'' j_3''}_{((l_1 l_2 l_3 l_4)}(p_1 p_2 p_3 p_4)$$

$$= (-1)^l [(2l+1)(2l_1+1)(2l_2+1)(2l_3+1)(2l_4+1)]^{1/2}$$

$$\times (-1)^{j_1 + j_2'' + j_3''} \begin{pmatrix} l_4 & l & l_3 \\ j_3 - j_3'' & j_3'' & -j_3 \end{pmatrix} \begin{pmatrix} l_2 & l & l_1 \\ -j_2 & j_2 - j_2'' & j_2'' \end{pmatrix}$$

$$\times g_{l_4}^{j_4 (j_3'' - j_3)} [(p_4 - p_3)\Delta s]\, g_{l}^{j_3'' (j_2'' - j_2)} [(p_3 - p_2)\Delta s]$$

$$\times g_{l_1}^{j_2'' (-j_1)} [(p_2 - p_1)\Delta s] \,. \tag{3.20}$$

Next the (2, 2)-body elements $L_{L,\gamma\gamma'}$ for $p_1 \leq p_1'$ are given by

$$L^{(j_1 j_2, j_1' j_2')}_{L,((l_1 l_2, l_1' l_2')[p_1 p_2, p_1' p_2']} = \sum_{\alpha=1}^{2} \sum_{\beta=1}^{2} L_{L,\gamma\gamma', p_\alpha p_\beta'} \,, \tag{3.21}$$

where

$$L_{L,\gamma\gamma', p_\alpha p_\beta'} = \zeta_{\mathrm{r}}^{-1} \Big(j_\alpha j_\beta' \delta_{p_\alpha p_\beta'} E_{L,\gamma\gamma'}$$

$$- (-1)^{j_\alpha + j_\beta' + l_\alpha'' + l_\beta''} [(2l_\alpha + 1)(2l_\beta' + 1)]^{1/2} [\alpha^2 (C^{-1})_{p_\alpha p_\beta'} - \delta_{p_\alpha p_\beta'}]$$

$$\times \sum_{\Delta l, \Delta l' = -1}^{1} \sum_{L'} (-1)^{\delta_{1\alpha}(L + L' + \Delta l) + \delta_{1\beta}(L + L' + \Delta l')}$$

$$\times (2L' + 1) [(l_\alpha + \Delta l + \tfrac{1}{2})(l_\beta' + \Delta l' + \tfrac{1}{2})]^{1/2} f(l_\alpha, j_\alpha; \Delta l) f(l_\beta', j_\beta'; \Delta l')$$

$$\times \begin{Bmatrix} L' & 1 & L \\ l_\alpha & l''_\alpha & l_\alpha + \Delta l \end{Bmatrix} \begin{Bmatrix} L' & 1 & L \\ l'_\beta & l''_\beta & l'_\beta + \Delta l' \end{Bmatrix} E_{L',\gamma_{\alpha(\Delta l)}\gamma'_{\beta(\Delta l')}} \Big) \tag{3.22}$$

with $l''_\alpha = l_1 + l_2 - l_\alpha$ and $l''_\beta = l'_1 + l'_2 - l'_\beta$; $\gamma_{\alpha(\Delta l)} = (l_1 + \delta_{1\alpha}\Delta l, l_2 + \delta_{2\alpha}\Delta l)(j_1 j_2)[p_1 p_2]$; and $\gamma'_{\beta(\Delta l')} = (l'_1 + \delta_{1\beta}\Delta l', l'_2 + \delta_{2\beta}\Delta l')(j'_1 j'_2)[p'_1 p'_2]$, and in Eq. (3.22), $E_{L,\gamma\gamma'}$ are the (2, 2)-body elements.

The elements for $p_1 > p'_1$ may be obtained again by the use of the self-adjointness of E_L and L_L. Further, we note that the (1, 2)- or (2, 1)-body elements may be obtained from the (2, 2)-body elements by putting $l_2 = 0$ or $l'_2 = 0$, and also that they reduce to the (1, 1)-body elements if we put $l_2 = l'_2 = 0$.

c. Time-correlation functions

We introduce time-correlation functions of the standard basis functions or a standard correlation matrix C. It is just the standard representation of the (time-displacement) operator $e^{-\mathcal{L}t}$, and therefore also diagonal in L and M, i. e.,

$$\begin{aligned} <D^{M*}_{L,\gamma}(\{\Omega_N\}, 0) D^{M'}_{L',\gamma'}(\{\Omega_N\}, t)>_{\text{eq}} &= <D^{M*}_{L,\gamma}\, e^{-\mathcal{L}t}\, D^{M'}_{L',\gamma'}>_{\text{eq}} \\ &= \delta_{LL'}\delta_{MM'} C_{L,\gamma\gamma'}(t) , \end{aligned} \tag{3.23}$$

where the submatrix elements $C_{L,\gamma\gamma'}(t)$ are independent of M and may be evaluated simply at $M = M' = 0$. Further, since $\mathcal{L}$ is a self-adjoint operator, the matrices C and C_L are seen to be self-adjoint, i. e., $C_L = C_L^\dagger$, so that in particular, $C_{L,\gamma\gamma}(t)$ are real.

Now, we formulated the eigenvalue problem in the standard representation. Let Q_L be the simultaneous diagonalizing matrix for the two submatrices E_L and L_L of the full standard representations E and L, respectively, i. e.,

$$Q_L^{\dagger} E_L Q_L = 1_L \ , \tag{3.24}$$

$$Q_L^{\dagger} L_L Q_L = \Lambda_L \ , \tag{3.25}$$

where 1_L and Λ_L are diagonal matrices with diagonal elements 1 and λ_k, respectively. Note that Q_L is not unitary. It is then easy to show that the correlation submatrix $C_L(t)$ is written in terms of the solutions Q_L and Λ_L of the eigenvalue problem given by Eqs. (3.24) and (3.25) as

$$C_L(t) = Q_L^{-1\dagger} \exp(-\Lambda_L t) Q_L^{-1} \ . \tag{3.26}$$

It should be noted that the same relations as Eqs. (3.24)–(3.26) are held for the full standard representations E, L, and C, and that this full problem has been, to a great extent, decoupled by the properties of the standard set given by Eqs. (3.11), (3.12), and (3.23).

The full standard representations E, L, and C are shown schematically in Fig. 3.1, where E_L, L_L, or C_L ($L = 0, 1, 2, \cdots$) appear in the diagonal blocks (with $L = L'$), the submatrices in the off-diagonal blocks 0 (with $L \neq L'$) are null matrices, and the M degeneracy has not been shown. In what follows, $L(n)$ denotes the n-body excitation for a given value of the quantum

number L, or the corresponding subspace of the full Hilbert space. Note that $n = 0, 1, 2, \cdots, N$ for $L = 0$, and $n = 1, 2, \cdots, N$ for $L \neq 0$. As is evident from the above remarks, the dielectric susceptibility (D) is associated with the 1(1), 1(1) elements, i. e., the subblock D in the figure, the fluorescence depolarization (F) and

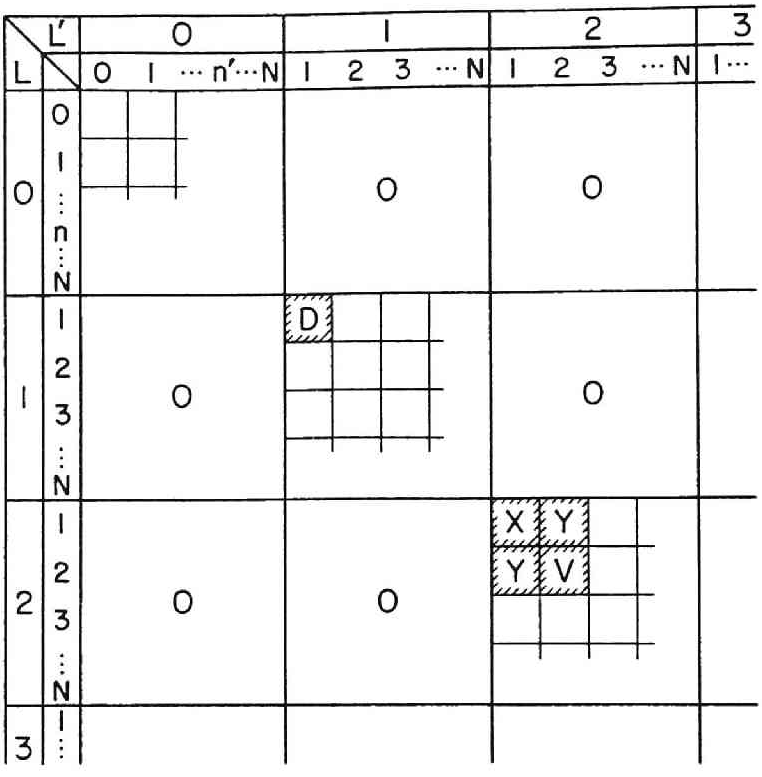

X = F, S, B_f, V ; Y = B_f, V

Fig. 3.1. The full standard representations E, L, and C of the identity operator, the diffusion operator $\mathscr{L}$, and the operator $\exp(-\mathscr{L}t)$, respectively (C is the standard correlation matrix). The submatrices E_L, L_L, or C_L appear in the diagonal blocks ($L=L'$), where the subscript L (= 0, 1, 2, $\cdots$) denotes the "total angular momentum quantum number." Dielectric relaxation (D) is associated with the subblock D with $L=L'=1$ and $n=n'=1$, where n is the number of "excited" subbodies. Fluorescence depolarization (F) and nuclear magnetic spin relaxation (S) are associated with the subblock X, flow birefringence (B_f) with X and Y, and viscosity (V) with X, Y, and V.

the nuclear magnetic spin relaxation (S) with the subblock X, the flow birefringence (B_f) with the subblocks X and Y, and the viscosity (V) with the subblocks X, Y, and V.

3-3. Subspace Approximation

Although we have thus reduced the size of the eigenvalue problem, and we have seen that the correlation submatrix elements relevant to a given observable are greatly localized, the size of the reduced problem is still very large (infinite). For example, in order to find the correlation matrix in the subblock D, we must solve the eigenvalue problem for the infinite matrices E_1 and L_1. Therefore, we introduce approximations to further reduce its size.

First, we introduce the subspace approximation, as mentioned in Sec. 3-1. That is, we approximately decouple the space (strictly the subspace of the full Hilbert space) specified by the quantum number L into a subspace relevant to a given observable and its complementary space; e. g., the subspace 1(1) and its complementary space $\{1(2), 1(3), \cdots, 1(N)\}$ in the case of dielectric relaxation, and the subspace $\{2(1), 2(2)\}$ and its complementary space $\{2(3), 2(4), \cdots, 2(N)\}$ in the case of viscosity. In this approximation, therefore, E_L, L_L, and Q_L become block diagonal with the null off-diagonal blocks between these two subspaces, so that the problem may be solved only in the subblock D, X, or X + Y + V.

Then the subspace $L(1)$ is $(2L+1)N$-dimensional except the M degeneracy [since $p = 1, 2, \cdots, N$ and $j = -L, -L+1, \cdots, L-1, L$ in Eqs. (3.13) and (3.14)], while the subspace $L(n)$ $(2 \leq n \leq N)$ is infinite dimensional. Therefore, the subspace approximation must be somewhat modified in the case of viscosity, and this problem will be considered separately in Chap. 5.

Thus, in order to obtain the correlation matrix $C_{L(1)}(t)$ appearing in the subblock D $(L = 1)$ or X $(L = 2)$, we may solve the eigenvalue problem for the $(2L+1)N \times (2L+1)N$ submatrices $E_{L(1)}$ and $L_{L(1)}$ in the subspace $L(1)$, whose elements are given by Eqs. (3.13) and (3.14), respectively, i. e.,

$$Q^{\dagger}_{L(1)} E_{L(1)} Q_{L(1)} = 1_{L(1)} , \tag{3.27}$$

$$Q^{\dagger}_{L(1)} L_{L(1)} Q_{L(1)} = \Lambda_{L(1)} , \tag{3.28}$$

$$C_{L(1)}(t) = Q^{-1\dagger}_{L(1)} \exp(-\Lambda_{L(1)} t) Q^{-1}_{L(1)} . \tag{3.29}$$

instead of Eqs. (3.24)–(3.26), respectively. Clearly, this is a crude approximation. Higher-order approximations may probably be obtained, though not systematically, if we solve the eigenvalue problem of somewhat larger size by augmenting the $L(1)$ subset with some basis functions suitably chosen from the complementary space $\{L(2), L(3), \cdots, L(N)\}$. Note that at $t = 0$, the $C_{L(1)}(0)$ given by Eq. (3.29) is exactly correct even in the crude subspace approximation.

Now, let us show that the above subspace approximation (with or without augmentation) is equivalent to neglecting the memory term appearing in the projection of the full space dynamics onto the subspace $L(1)$ (with or without augmentation) by the projection operator method.[5,6] Since the full Hilbert space is decoupled with respect to L and M, we may consider the space (strictly subspace) specified by L from the start. Let $A(t)$ be some dynamical variable, and consider in general a subspace spanned by ν_d basis functions D^M_{L,γ_i} $(i = 1, 2, \cdots, \nu_d)$. [Note that if $A(0)$ is confined in the space L, so is also $A(t)$.] We define the projection $\mathscr{P}A$ of $A(t)$ onto this subspace by

$$\mathscr{P}A = \sum_{i,j=1}^{\nu_d} D^M_{L,\gamma_i}(E_s^{-1})_{\gamma_i\gamma_j}<D^{M*}_{L,\gamma_j}A>_{eq} , \tag{3.30}$$

where the subscript s has been used to indicate the $\nu_d \times \nu_d$ submatrix in the subspace. If we take $A(t) = e^{-\mathfrak{L}t}D^M_{L,\gamma_k}$ $(k = 1, 2, \cdots, \nu_d)$ then following Mori[5] and Zwanzig,[6] we find the kinetic equation satisfied by the correlation submatrix $C_s(t)$

$$\frac{\partial}{\partial t}C_s(t) = - L_sE_s^{-1}C_s(t) + \int_0^t K(t - t')C_s(t')dt' , \tag{3.31}$$

with $C_s(0) = E_s$, where the $\nu_d \times \nu_d$ memory kernel matrix $K = [K_{\gamma_i\gamma_j}(t)]$ is given by

$$K_{\gamma_i\gamma_j}(t) = \sum_{k=1}^{\nu_d} <D^{M*}_{L,\gamma_i}\mathscr{L}$$

$$\times \exp[-(1 - \mathscr{P})\mathscr{L}t](1 - \mathscr{P})\mathscr{L}D^M_{L,\gamma_k}>_{eq}(E_s^{-1})_{\gamma_k\gamma_j} . \tag{3.32}$$

Note that $<D^M_{L,\gamma}>_{eq} = 0$ for the present case ($L \neq 0$). (If $<D^M_{L,\gamma}>_{eq} \neq 0$, such $D^M_{L,\gamma}$ must be replaced by $D^M_{L,\gamma} - <D^M_{L,\gamma}>_{eq}$.) If we neglect the memory term in Eq. (3.31), we obtain

$$\frac{\partial}{\partial t}C_s(t) = - L_s E_s^{-1} C_s(t) , \tag{3.33}$$

with $C_s(0) = E_s$. When s = $L(1)$, it is easy to show that the solution of Eq. (3.33) is identical with the $C_{L(1)}(t)$ approximated by Eq. (3.29). Thus, we have shown the equivalence. Note that if we take the present full space L as the space s, we have $\mathscr{P} = 1$ and therefore $K = 0$, so that $C_L(t)$ exactly obeys Eq. (3.33) with E_L and L_L in place of E_s and L_s, respectively. In fact, this is consistent with Eq. (3.26). Exact solution of Eq. (3.31) with the memory term is equivalent to finding the exact $C_s(t)$ by solving the full eigenvalue problem for E_L and L_L, and is also impossible. However, it is possible to take account of some interactions between the subspace and its complementary space by augmentation of the subspace with a small number of basis functions in the subspace approximation, as noted above, and this is equivalent to partly retaining the memory term after the projection onto the lowest subspace.

In this connection, we should mention the work of Evans. He has evaluated several kinds of time-correlation functions for short bond chains by the projection operator method.[7] Further, he has chosen 25 basis functions from a complete set of them for three-bond chains,[8] but his treatments for longer chains correspond

to the above crude subspace approximation without augmentation. Our actual evaluation will also be carried out in this approximation. However, because of the rotational degrees of freedom of the subbodies in the HW chain, our approximation may be regarded as being on a level with a somewhat augmented crude approximation in the (long) bond chain. Recall that there are at least $(2L + 1)N$ basis functions in the case of $C_{L(1)}(t)$. (For the three-bond chain, our evaluation is of course less complete than the above specific treatment of Evans.)

Thus, we return to the eigenvalue problem given by Eqs. (3.27) and (3.28). It may be solved by a standard method. We first diagonalize the self-adjoint matrix $E_{L(1)}$ with a unitary matrix $Q^E_{L(1)}$

$$Q^{E\dagger}_{L(1)} E_{L(1)} Q^E_{L(1)} = \Lambda^E_{L(1)} , \tag{3.34}$$

where $\Lambda^E_{L(1)}$ is a diagonal matrix with diagonal elements λ^E_k. Let $(\Lambda^E_{L(1)})^{-1/2}$ be the diagonal matrix with diagonal elements $(\lambda^E_k)^{-1/2}$. We then transform $L_{L(1)}$ to another self-adjoint matrix with $Q^E_{L(1)}(\Lambda^E_{L(1)})^{-1/2}$, and finally diagonalize it with a unitary matrix $Q^L_{L(1)}$

$$Q^{L\dagger}_{L(1)} [\, (\Lambda^E_{L(1)})^{-1/2} Q^{E\dagger}_{L(1)} L_{L(1)} Q^E_{L(1)} (\Lambda^E_{L(1)})^{-1/2} \,] Q^L_{L(1)} = \Lambda_{L(1)} \tag{3.35}$$

The diagonal matrix $\Lambda_{L(1)}$ must be identical with the one on the right-hand side of Eq. (3.28), and the diagonalizing matrix $Q_{L(1)}$ in Eqs. (3.27) and (3.28) (which is not unitary) is given by

$$Q_{L(1)} = Q^E_{L(1)} (\Lambda^E_{L(1)})^{-1/2} Q^L_{L(1)} . \tag{3.36}$$

Now the diagonalization in Eq. (3.34) may partly be performed analytically. By the use of Eq. (2.14) with Eqs. (2.10)–(2.13), Eq.(3.13) for the elements of $E_{L(1)}$ may be rewritten as

$$E^{(j,j')}_{L,[p,p']} = \sum_{m=-L}^{L} \sum_{q,q'=1}^{N} \hat{Q}^{jm}_{L,pq} \hat{Q}^{j'm*}_{L,p'q'} \hat{E}_{L,[q,q']} \tag{3.37}$$

with

$$\hat{E}_{L,[p,p']} = (8\pi^2)^{-N} \exp[\, -L(L+1)\,|\,p'-p\,|\,\Delta s\,]\ , \tag{3.38}$$

$$\hat{Q}^{jj'}_{L,pp'} = \delta_{pp'} \overline{\mathscr{D}}^{jj'}_{L}(\Omega_a) \exp(-ij'\nu p \Delta s)\ , \tag{3.39}$$

where ν is given by Eq. (2.19). From Eq. (3.39) with the unitarity of the unnormalized Wigner $\overline{\mathscr{D}}$ functions [Eq. (43.10) of Davydov[1]], the matrix $\hat{Q}_{L(1)} = (\hat{Q}^{jj'}_{L,pp'})$ is seen to be unitary, i. e.,

$$\sum_{m=-L}^{L} \sum_{q=1}^{N} \hat{Q}^{mj*}_{L,qp} \hat{Q}^{mj'}_{L,qp'} = \delta_{jj'} \delta_{pp'}\ . \tag{3.40}$$

We then solve Eq. (3.37) for $\hat{E}_{L,[p,p']}$ by the use of Eq. (3.40) to find

$$\sum_{m,m'=-L}^{L} \sum_{q,q'=1}^{N} \hat{Q}^{mj*}_{L,qp} E^{(m,m')}_{L,[q,q']} \hat{Q}^{m'j'}_{L,q'p'} = \delta_{jj'} \hat{E}_{L,[p,p']}\ . \tag{3.41}$$

Thus, the diagonalization of $E_{L(1)}$ in Eq. (3.34) is reduced to a diagonalization of the $N \times N$ real symmetric matrix $\hat{E}_{L,[p,p']}$. This diagonalization and also that of $L_{L(1)}$ in Eq. (3.35) must be performed numerically. Note that there is $(2L+1)$–fold degeneracy with respect to j in $E_{L(1)}$, as seen from Eq. (3.41) with Eq. (3.38), but this is not generally the case with $L_{L(1)}$.

However, for the Kratky–Porod (KP) wormlike chain[15] as a special case of the HW chain with $\kappa_0 = 0$, the problem is somewhat simplified. In this case, $g_L^{jj'}(s)$ has been given by Yamakawa and Shimada [Eq. (55) of Ref. 16 (with $\sigma = 0$)]

$$g_L^{jj'}(s) = \delta_{jj'}\exp\{-[L(L+1) + ij\tau_0]s\} \quad \text{(KP)}, \tag{3.42}$$

so that $E_{L(1)}$ and $L_{L(1)}$ given by Eqs. (3.13) and (3.14) become diagonal in j, and also we have $\bar{\mathscr{D}}_L^{jj'}(\Omega_a) = \delta_{jj'}$ in Eq. (3.39). Since we then have further $E_{L,[p,p']}^{(-j,-j)} = E_{L,[p,p']}^{(j,j)*}$ and $L_{L,[p,p']}^{(-j,-j)} = L_{L,[p,p']}^{(j,j)*}$ and from Eqs. (3.13), (3.14), and (3.42), we see that there are also L sets of twofold degeneracy with respect to j ($\neq 0$) between j and $-j$ in $L_{L(1)}$ in addition to the $(2L+1)$-fold j degeneracy in $E_{L(1)}$.

3–4. Block–Diagonal Approximation

We have seen that the problem is reduced to the $3N$– or $5N$–dimensional eigenvalue problem (for $L = 1$ or 2) in the $L(1)$ subspace approximation. This reduction suffices for a numerical solution for $N \lesssim 30$ (with use of a FACOM M–200 digital computer in this University), but it will actually be impossible for large N. We must, therefore, introduce an additional approximation, i. e., the block–diagonal approximation, as mentioned in Sec. 3–1. This is done by a further transformation to another standard basis set.

The useful transformation is then the one that approximately

diagonalizes the matrix B defined by Eq. (2.55) with Eq. (2.42), and therefore also the matrix C defined by Eq. (2.112). The matrix B, or its minor modification in the Zimm version,[13] always appears in the dynamics of polymer chains.[12,13,17] For conventional bond chains, both flexible and stiff, it is well known that B may be diagonalized in a good approximation with the orthogonal, symmetric matrix Q^0_{pk},[11]

$$Q^0_{pk} = [2/(N+1)]^{1/2}\sin[\pi pk/(N+1)]$$

$$(p, k = 1, 2, \cdots, N)\,, \tag{3.43}$$

which exactly diagonalizes the free-draining matrix $B^0 = B$ with neglect of the second term on the right-hand side of Eq. (2.42) (i. e., the Rouse matrix[12] except the factor ζ_t^{-1}). For the present model, we also adopt this approximation, i. e.,

$$(Q^0BQ^0)_{kk'} = \delta_{kk'}\zeta_t^{-1}\lambda_k^B\,, \tag{3.44}$$

$$(Q^0CQ^0)_{kk'} = \delta_{kk'}a^2\lambda_k^C\,, \tag{3.45}$$

where

$$\lambda_k^C = \tfrac{2}{3} + (\zeta_r/a^2\zeta_t)\lambda_k^B \tag{3.46}$$

with $\lambda_k^B = \zeta_t(Q^0BQ^0)_{kk}$. Note that in the coil limit, λ_k^B are just the Rouse-Zimm eigenvalues in the Hearst version.[18,19] The correctness of Eq. (3.44) will be examined numerically in Sec. 3-5a.

Now we transform the basis functions $D^{M,j}_{L,[p]}$ in the subspace $L(1)$ to new basis functions $F^{M,j}_{L,[k]}$ not only with Q^0 but also with the $\overline{\mathscr{D}}$ functions in Eq. (3.39) as follows:

$$F^{M,j}_{L,[k]}(\{\Omega_N\}) = \sum_{p=1}^{N} \sum_{j'=-L}^{L} Q^0_{pk} \overline{\mathscr{D}}^{j'j}_L(\Omega_a) D^{M,j'}_{L,[p]}(\Omega_p) \ , \tag{3.47}$$

where L and M remain unchanged. It is easy to see that this new basis set is also a standard one in the *subspace* {1(1), 2(1), 3(1), $\cdots$}. It is referred to as the standard Fourier basis set (in the subspace), since Q^0 is just a Fourier sine transformation. Thus, the standard Fourier representations of the identity and diffusion operators (with the weight) are also diagonal in L and M with the diagonal elements being independent of M, so that we may write them as

$$<F^{M,j*}_{L,[k]} F^{M',j'}_{L',[k']}>_{\mathrm{eq}} = \delta_{LL'}\delta_{MM'} \overline{E}^{(j,j')}_{L,[k,k']} \ , \tag{2.48}$$

$$<F^{M,j*}_{L,[k]} \mathscr{L} F^{M',j'}_{L',[k']}>_{\mathrm{eq}} = \delta_{LL'}\delta_{MM'} \overline{L}^{(j,j')}_{L,[k,k']} \ . \tag{2.49}$$

By the use of Eq. (2.14) for $g^{jj'}_L(s)$ appearing in the elements of $E_{L(1)}$ and $L_{L(1)}$ given by Eqs. (3.13) and (3.14), respectively, and of the unitarity of $\overline{\mathscr{D}}^{jj'}_L$, we find for the elements of $\overline{E}_{L(1)}$ and $\overline{L}_{L(1)}$

$$\begin{aligned} \overline{E}^{(j,j')}_{L,[k,k']} &= \sum_{p,p'=1}^{N} \sum_{m,m'=-L}^{L} Q^0_{pk} Q^0_{p'k'} \overline{\mathscr{D}}^{mj*}_L(\Omega_a) \overline{\mathscr{D}}^{m'j'}_L(\Omega_a) E^{(m,m')}_{L,[p,p']} \\ &= \delta_{jj'} (8\pi^2)^{-N} S^{(0)j}_{L,kk'} \ , \end{aligned} \tag{3.50}$$

$$\begin{aligned} \overline{L}^{(j,j')}_{L,[k,k']} &= \sum_{p,p'=1}^{N} \sum_{m,m'=-L}^{L} Q^0_{pk} Q^0_{p'k'} \overline{\mathscr{D}}^{mj*}_L(\Omega_a) \overline{\mathscr{D}}^{m'j'}_L(\Omega_a) L^{(m,m')}_{L,[p,p']} \\ &= (8\pi^2)^{-N} \zeta_{\mathrm{r}}{}^{-1} \Big[\delta_{jj'}\delta_{kk'} L(L+1) \end{aligned}$$

$$- \sum_{\Delta l=-1}^{1} \sum_{j''=-L-\Delta l}^{L+\Delta l} T^{jj'j''}_{L,\Delta l} S^{(1)j''}_{L+\Delta l,kk'} \Bigg] , \tag{3.51}$$

with

$$S^{(n)j}_{L,kk'} = \sum_{p,p'=1}^{N} Q^0_{pk} Q^0_{p'k'} [\alpha^2 (C^{-1})_{pp'}]^n$$

$$\times \exp\{-[L(L+1)|p'-p| - ij\nu(p'-p)]\Delta s\} \quad (n = 0, 1) , \tag{3.52}$$

$$T^{jj'j''}_{L,\Delta l} = [32\pi^4/(2L+1)] \sum_{m,m'=-L}^{L} f(L, m; \Delta l) f(L, m'; \Delta l)$$

$$\times \mathscr{D}^{mj*}_{L}(\Omega_a) \mathscr{D}^{m'j'}_{L}(\Omega_a) \mathscr{D}^{mj''*}_{L+\Delta l}(\Omega_a) \mathscr{D}^{m'j''}_{L+\Delta l}(\Omega_a) , \tag{3.53}$$

where $f(L, j; \Delta l)$ is given by Eq. (3.15).

If we take the sums over p and p' in Eq. (3.52) by the use of Eq. (3.43) with the approximation given by Eq. (3.45), we can show that $S^{(n)j}_{L,kk'}$ with $k \neq k'$ are of $\mathcal{O}(N^{-1})$ in relation to $S^{(n)j}_{L,kk}$ (with $k = k'$), and obtain for the latter,

$$S^{(0)j}_{L,kk} = 1 + \sum_{i_1=-1}^{1} (1 - \delta_{i_1 0}) \{ S_c[L(L+1)\Delta s, k\theta + i_1 j\nu\Delta s]$$

$$+ (N+1)^{-1} \cot(k\theta) S_s[L(L+1)\Delta s, k\theta + i_1 j\nu\Delta s] \} , \tag{3.54}$$

$$S^{(1)j}_{L,kk} = [2(N+1)]^{-1} \sum_{k'=1}^{N} (\lambda^C_{k'})^{-1} \sum_{i_1,i_2=-1}^{1} (1 - \delta_{i_1 0})(1 - \delta_{i_2 0})$$

$$\times \Big([1 + \delta_{k+i_1 k', m(N+1)}] \{ \tfrac{1}{2} + S_c[L(L+1)\Delta s, (k + i_1 k')\theta + i_2 j\nu\Delta s] \}$$

$$+ (N+1)^{-1} \{ \cot k\theta + \cot i_1 k'\theta - [1 - \delta_{k+i_1 k', m(N+1)}] \cot(k + i_1 k')\theta \}$$

$$\times S_s[L(L+1)\Delta s, (k + i_1 k')\theta + i_2 j\nu\Delta s] \Big) , \tag{3.55}$$

where $\theta = \pi/(N+1)$,

$$S_c(x, y) \equiv \sum_{p=1}^{N-1} \left(1 - \frac{p}{N+1}\right) e^{-px} \cos py$$

$$= (N^2 + N - 2)/2(N+1) ,$$

$$\text{if } x = 0 \text{ and } y = 2n\pi \text{ (with } n \text{ integer)}$$

$$= \{e^{-x}\cos y - e^{-2x} - (N+1)^{-1}\{2e^{-Nx}\cos Ny$$

$$- 2e^{-(N+1)x}\cos(N-1)y + [e^{-x}\cos y - 2e^{-2x}$$

$$+ e^{-3x}\cos y - e^{-Nx}\cos Ny + 2e^{-(N+1)x}\cos(N-1)y$$

$$- e^{-(N+2)x}\cos(N-2)y](1 - 2e^{-x}\cos y + e^{-2x})^{-1}\}\}$$

$$\times (1 - 2e^{-x}\cos y + e^{-2x})^{-1} , \quad \text{otherwise} , \tag{3.56}$$

$$S_s(x, y) \equiv \sum_{p=1}^{N-1} e^{-px} \sin py$$

$$= 0 , \quad \text{if } x = 0 \text{ and } y = 2n\pi \text{ (with } n \text{ integer)}$$

$$= [e^{-x}\sin y - e^{-Nx}\sin Ny + e^{-(N+1)x}\sin(N-1)y]$$

$$\times (1 - 2e^{-x}\cos y + e^{-2x})^{-1} , \quad \text{otherwise} . \tag{3.57}$$

In Eq. (3.55), λ_k^C is given by Eq. (3.46), and $m(N+1)$ denotes multiples of $N+1$.

Thus, for $N \gg 1$, the matrices $\overline{E}_{L(1)}$ and $\overline{L}_{L(1)}$ become approximately diagonal in k, so that the $(2N+1)N$-dimensional eigenvalue problem in the $L(1)$ subspace approximation given by Eqs. (3.27) and (3.28) may be reduced to N eigenvalue problems for the $(2L+1)\times(2L+1)$ matrices $\overline{E}_{L(1),[k]}$ and $\overline{L}_{L(1),[k]}$ ($k = 1, 2, \cdots, N$) whose j, j' elements are $\overline{E}^{(j,j')}_{L,[k,k]}$ and $\overline{L}^{(j,j')}_{L,[k,k]}$, respectively,

$$Q^{\dagger}_{L(1),[k]}\overline{E}_{L(1),[k]}Q_{L(1),[k]} = 1_{L(1),[k]} , \tag{3.58}$$

$$Q^{\dagger}_{L(1),[k]}\overline{L}_{L(1),[k]}Q_{L(1),[k]} = \Lambda_{L(1),[k]} , \tag{3.59}$$

where $1_{L(1),[k]}$ and $\Lambda_{L(1),[k]}$ are $(2L+1)\times(2L+1)$ diagonal matrices with diagonal elements 1 and $\lambda^{j}_{L,k}$ $(j = -L, -L+1, \cdots, L)$, respectively, and $Q_{L(1),[k]}$ is a diagonalizing matrix (not unitary). This is the block-diagonal approximation.

Now, recalling that $\overline{E}_{L(1)}$ is already diagonal in j, we may readily reduce the eigenvalue problem given by Eqs. (3.58) and (3.59) to that for a $(2L+1)\times(2L+1)$ self-adjoint matrix as in Eq. (3.35); i. e.,

$$Q^{L\dagger}_{L(1),[k]}[(\overline{E}_{L(1),[k]})^{-1/2}\overline{L}_{L(1),[k]}(\overline{E}_{L(1),[k]})^{-1/2}]Q^{L}_{L(1),[k]} = \Lambda_{L(1),[k]} , \tag{3.60}$$

where $(\overline{E}_{L(1),[k]})^{-1/2}$ is the diagonal matrix with diagonal elements $(\overline{E}^{(j,j)}_{L,[k,k']})^{-1/2}$, and $Q^{L}_{L(1),[k]}$ is a unitary, diagonalizing matrix. Since the right-hand sides of Eqs. (3.59) and (3.60) are identical, the above two diagonalizing matrices are related to each other by

$$Q_{L(1),[k]} = (\overline{E}_{L(1),[k]})^{-1/2}Q^{L}_{L(1),[k]} . \tag{3.61}$$

The analytical solutions of the three-dimensional $(L = 1)$ eigenvalue problem given by Eq. (3.60) with Eqs. (3.50)-(3.57) are given in Appendix 3-A.

Finally, the correlation matrix $C_{L(1)}(t)$ in the subspace and block-diagonal approximations is obtained, from Eq. (3.29) with the elements $\overline{E}^{(j,j)}_{L,[k,k]}$ and the solution of Eq. (3.60), $\lambda^{j}_{L,k}$ and $Q^{L}_{L(1),[k]}$,

as follows:

$$C^{(j,j')}_{L,[p,p']}(t) = \sum_{k=1}^{N} \sum_{m,m',j''=-L}^{L} \overline{\mathscr{D}}^{jm}_{L}(\Omega_a)\overline{\mathscr{D}}^{j'm'*}_{L}(\Omega_a)Q^{0}_{pk}Q^{0}_{p'k}$$

$$\times Q^{L,mj''}_{L,k}Q^{L,m'j''*}_{L,k}(\overline{E}^{(m,m)}_{L,[k,k]}\overline{E}^{(m',m')}_{L,[k,k]})^{1/2}\exp(-\lambda^{j''}_{L,k}t) \ , \tag{3.62}$$

where $Q^{L,jj'}_{L,k}$ are the j, j' elements of the unitary matrix $Q^{L}_{L(1),[k]}$. In contrast to the subspace approximation of Eq. (3.29) alone, the $C_{L(1)}(0)$ given by Eq. (3.62) is already approximated because of the block-diagonal approximation.

For the KP chain ($\kappa_0 = 0$), both $\overline{E}_{L(1)}$ and $\overline{L}_{L(1)}$ are diagonal in j since then $g^{jj'}_{L}$ is given by Eq. (3.42), so that we need not solve the eigenvalue problem given by Eqs. (3.58) and (3.59); i. e., $Q^{L,jj'}_{L,k} = \delta_{jj'}$. Since we then also have $\overline{\mathscr{D}}^{jj'}_{L}(\Omega_a) = \delta_{jj'}$, Eq. (3.62) reduces to

$$C^{(j,j')}_{L,[p,p']}(t) = \delta_{jj'}\sum_{k=1}^{N} Q^{0}_{pk}Q^{0}_{p'k}\overline{E}^{(j,j)}_{L,[k,k]}\exp(-\lambda^{j}_{L,k}t) \quad \text{(KP)} \ , \tag{3.63}$$

where

$$(8\pi^2)^N\overline{E}^{(j,j)}_{L,[k,k]} = S^{(0)j}_{L,kk} = S^{(0)-j}_{L,kk} \ , \tag{3.64}$$

$$\lambda^{j}_{L,k} = \lambda^{-j}_{L,k} \ (j \neq 0) = (\overline{E}^{(j,j)}_{L,[k,k]})^{-1}\overline{L}^{(j,j)}_{L,[k,k]} \ , \tag{3.65}$$

so that

$$C^{(j,j)}_{L,[p,p']}(t) = C^{(-j,-j)}_{L,[p,p']}(t) \ . \tag{3.66}$$

3-5. Conditions on the Model Parameters

In order to find conditions to be imposed on ζ_t and ζ_r, it is convenient to introduce instead of them the dimensionless parameters r_1 and r_2 defined by

$$r_1 = \zeta_t/3\pi\eta_0 a \ , \tag{3.67}$$

$$r_2 = \zeta_r/a^2\zeta_t \ , \tag{3.68}$$

with η_0 the solvent viscosity. Note that for touched Stokes bead models, $r_1 = 1$ and $r_2 = 1/3$, and that a is uniquely related to Δs by Eq. (2.26). For convenience, we restore k_BT in this section.

a. The diffusion matrix B

We begin by examining the accuracy of the approximate eigenvalues $\lambda_k^B = \zeta_t(Q^0BQ^0)_{kk}$ of ζ_tB, where Q^0 is the Fourier sine transformation matrix given by Eq. (3.43). In particular, in the coil limit of $N \gg 1$ and $k/N \ll 1$ (for both flexible and stiff chains), they are the Rouse-Zimm eigenvalues in the Hearst version,[18,19] and are given by

$$\lambda_k^B = \frac{\pi^2}{N^2}\left(k^2 + \frac{4h\lambda_k'}{\pi^2}\right) \tag{3.69}$$

with

$$\lambda_k' = \pi k^{1/2}[\pi kC(\pi k) - \tfrac{1}{2}S(\pi k)] \ , \tag{3.70}$$

where $C(x)$ and $S(x)$ are the Fresnel integrals defined by

$$\begin{Bmatrix} C \\ S \end{Bmatrix}(x) = (2\pi)^{-1/2} \int_0^x t^{-1/2} \begin{Bmatrix} \cos \\ \sin \end{Bmatrix} t dt \ . \tag{3.71}$$

In Eq. (3.69), h is the conventional draining parameter, and for the present model, it is given by

$$\begin{aligned} h &= \zeta_t N^{1/2} / (12\pi^3)^{1/2} \eta_0 \bar{a} \\ &= (3/4\pi)^{1/2} (a/\bar{a}) r_1 N^{1/2} \ , \end{aligned} \tag{3.72}$$

where $\bar{a}$ is the (unperturbed) effective bond length of the discrete HW chain, and is defined, from Eq. (2.18) with Eq. (2.25) for its equilibrium mean-square end-to-end distance $<R^2(N)>_{eq}$, by

$$\bar{a}^2 \equiv \lim_{N \to \infty} [<R^2(N)>_{eq} / N] = c_\infty \Delta s \tag{3.73}$$

with c_∞ being given by Eq. (2.23). It is well known that the λ_k^B given by Eq. (3.69) are very good approximations in the coil limit.

Next, we examine the case of small N. Figure 3.2 shows plots of λ_k^B ($k = 1, 2, \cdots, N$) against reduced wave number $\tilde{k} \equiv k/(N+1)$ for isotactic polystyrene (i-PS; $\kappa_0 = 11$ and $\tau_0 = 15$)[16,20] and the KP chain ($\kappa_0 = 0$), both with $N = 9$. (Note that in the case of $\kappa_0 = 0$, the mean reciprocal distance between two subbodies and therefore the matrix B are independent of τ_0.) The open circles represent the exact eigenvalues, and the full and broken line segments connect the corresponding approximate values. In the case of i-PS, the lower and upper points correspond to $\Delta s = 0.4$ and 0.08, its upper and lower bounds, respectively, where the lower bound corresponds to two skeletal bonds and we have

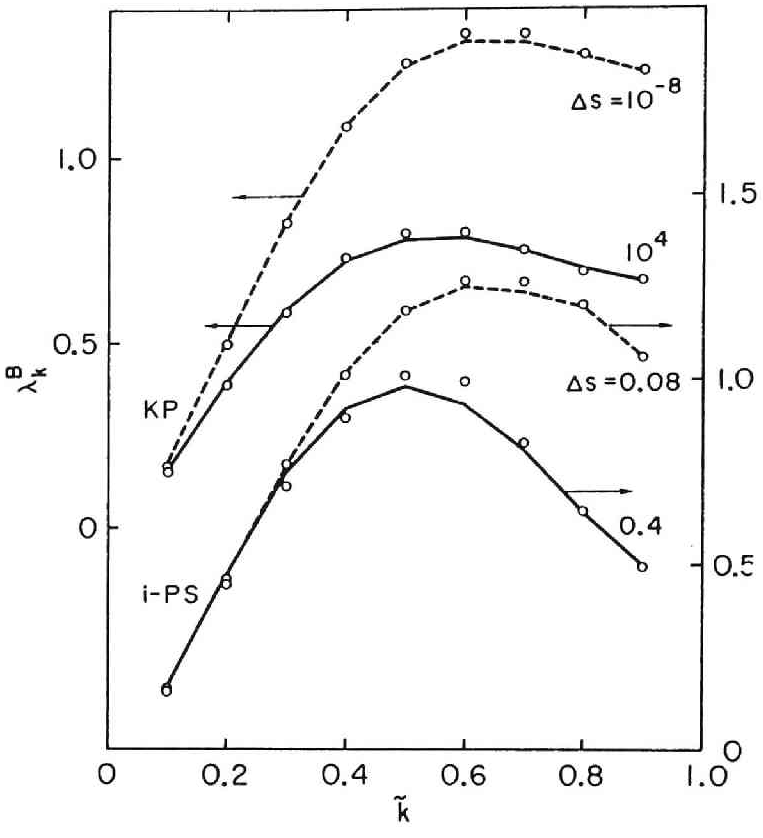

Fig. 3.2. Eigenvalues λ_k^B of $\zeta_t B$ plotted against the reduced wave number $\tilde{k}$ for isotactic polystyrene and the KP chain with $N=9$ and the indicated values of Δs. The open circles represent the exact eigenvalues, and full and broken line segments connect the corresponding approximate values.

taken $\lambda^{-1}= 26.4$ Å.[16,20] In the case of KP, the lower and upper points represent the values for $\Delta s = 10^4$ and 10^{-8}, respectively, which do not necessarily correspond to the upper and lower bounds on Δs for any real chain, but to very flexible and very stiff (KP) chains,

respectively. In any case, there is good agreement between the exact and approximate eigenvalues, the error becoming the largest at $k = 1$, 4–6%, depending on the model parameters. We note that for small N, it is easy to make the approximate eigenvalues correspond to the exact ones, as above, by comparing the respective eigenvectors, while for large N, this is difficult in the range of $\tilde{k} \gtrsim 0.2$. In the range of $\tilde{k} \lesssim 0.2$, we have found that the agreement between the exact and approximate eigenvalues becomes better as N is increased. Thus, the approximate eigenvalues λ_k^B may be used safely as a first approximation for all possible cases of the discrete HW chain.

Now, λ_k^B depend on only r_1 and N for given κ_0, τ_0, and Δs. As r_1 is increased, λ_k^B with large $\tilde{k}$ become small, and λ_N^B, λ_{N-1}^B, $\cdots$ become negative successively; the matrix B is then not positive definite. Let $r_1^{(u)}$ be the upper bound on r_1 such that $\lambda_k^B \geq 0$ for all k when $r_1 \leq r_1^{(u)}$. Figure 3.3 shows plots of $r_1^{(u)}$ against Δs not only for the KP chain and i–PS but also for syndiotactic polystyrene (s–PS; $\kappa_0 = 0.8$ and $\tau_0 = 2.3$), isotactic poly(methyl methacrylate) (i–PMMA; $\kappa_0 = 1.7$ and $\tau_0 = 1.4$), and syndiotactic poly(methyl methacrylate) (s–PMMA; $\kappa_0 = 4.4$ and $\tau_0 = 0.8$),[16,20] all with $N = 99$. The vertical line segments indicate the upper and lower bounds on Δs. The upper bound is taken as 0.4 for all cases, and the lower bound for flexible chains corresponds to two skeletal bonds and is equal to ~ 0.05 for s–PS ($\lambda^{-1} = 40.4$ Å), ~ 0.06 for

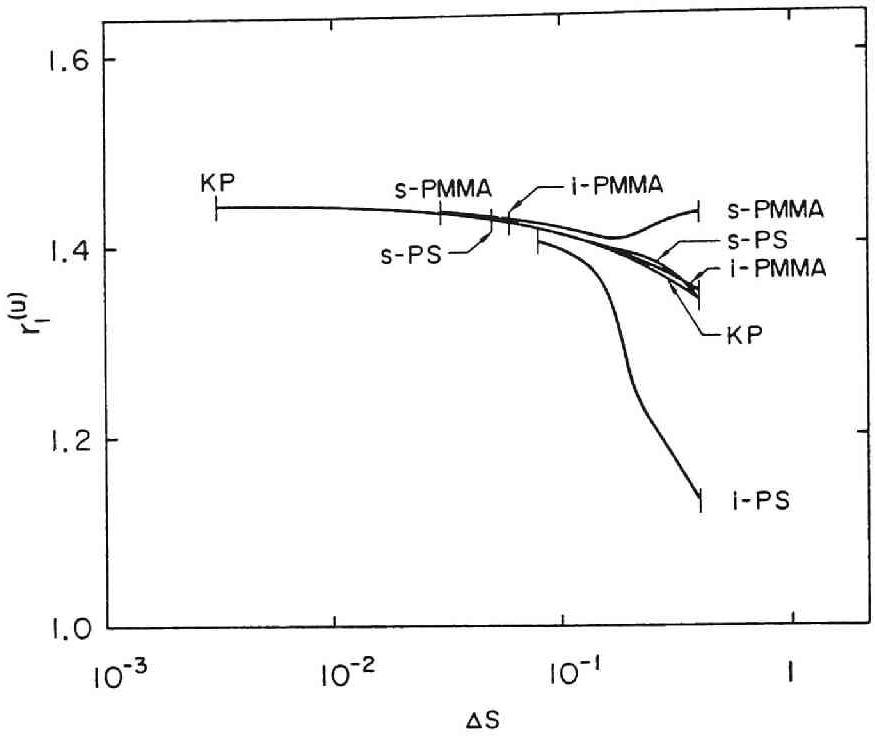

Fig. 3.3. The upper bound $r_1^{(u)}$ on r_1 plotted against Δs in its allowed range for isotactic and syndiotactic polystyrenes, isotactic and syndiotactic poly(methyl methacrylate)s, and the KP chain, all with $N=99$. The lower bound on Δs for the KP chain corresponds to the case of DNA.

i-PMMA ($\lambda^{-1}=$ 32.7 Å), and $\sim$ 0.03 for s-PMMA ($\lambda^{-1}=$ 65.6 Å). We have taken as an example of the lower bound for the KP chain the one which corresponds to the distance between base pairs 3.4 Å of DNA and is equal to $\sim$ 0.0031 if we adopt $\lambda^{-1}=$ 1100 Å (in 0.2 M NaCl).[21-24] It is seen that $r_1^{(u)}$ becomes almost independent of the model parameters as Δs is decreased. We also note that $r_1^{(u)}$ is almost independent of N for $N \gtrsim 50$. Anyway, it appears that

the positive definiteness of the diffusion matrix B is always guaranteed provided that $r_1 \lesssim 1$.

b. The lowest branch

We make an analysis of the eigenvalues $\lambda^0_{1,k}$ in the $j = 0$ branch of the spectrum for the diffusion operator in the subspace 1(1) (in the block-diagonal approximation). According to the j indexing of the $L = 1$ branches mentioned in Appendix 3-A, we always have $\lambda^0_{1,1} < \lambda^{-1}_{1,1}$. Further, it can be shown, from Eqs. (3A.5), that $\lambda^0_{1,1} < \lambda^1_{1,1}$ for $N \gg 1$. In other words, the eigenvalues $\lambda^0_{1,k}$, form the lowest of the $L = 1$ branches for small k provided that N is large. These eigenvalues are related to a slow part of the dielectric relaxation rates of the entire chain, and are explicitly given, from the first of Eqs. (3A.5), by

$$\lambda^0_{1,k} = (k_B T/2\zeta_r)[f_k - (f_k{}^2 - g_k)^{1/2}] , \tag{3.74}$$

with

$$\begin{aligned} f_k = {} & [(S_1^{(0)0})^{-1} + (S_1^{(0)1})^{-1}](2 - \tfrac{2}{3}S_0^{(1)0} - \tfrac{1}{4}S_1^{(1)1} - \tfrac{1}{3}S_2^{(1)0} - \tfrac{1}{4}S_2^{(1)1}) \\ & + (\kappa_0{}^2 + \tau_0{}^2)\nu^{-2}[(S_1^{(0)0})^{-1} - (S_1^{(0)1})^{-1}](\tfrac{2}{3}S_0^{(1)0} - \tfrac{1}{4}S_1^{(1)1} + \tfrac{1}{3}S_2^{(1)0} - \tfrac{1}{4}S_2^{(1)1}) \\ & + \tfrac{1}{2}\kappa_0{}^2\nu^{-2}(S_1^{(0)1})^{-1}(S_2^{(1)0} - S_2^{(1)2}) , \end{aligned} \tag{3.75}$$

$$\begin{aligned} g_k = {} & 4(S_1^{(0)0}S_1^{(0)1})^{-1}\{4 - \tfrac{8}{3}S_0^{(1)0}[1 - \tfrac{1}{4}(S_1^{(1)1} + S_2^{(1)1}) \\ & - \kappa_0{}^2\tau_0{}^2\nu^{-4}(\tfrac{3}{4}S_2^{(1)0} - S_2^{(1)1} + \tfrac{1}{4}S_2^{(1)2})] - S_1^{(1)1} - (\tfrac{4}{3} - \kappa_0{}^2\nu^{-2})S_2^{(1)0} \end{aligned}$$

$$- S_2^{(1)1} - \kappa_0{}^2\nu^{-2}S_2^{(1)2} + \tfrac{1}{12}(\kappa_0{}^2 - 2\tau_0{}^2)^2\nu^{-4}S_1^{(1)1}S_2^{(1)0}$$

$$+ \tfrac{1}{12}(\kappa_0{}^2 + 2\tau_0{}^2)^2\nu^{-4}S_2^{(1)0}S_2^{(1)1} + \kappa_0{}^2\tau_0{}^2\nu^{-4}(S_1^{(1)1}S_2^{(1)1} + \tfrac{1}{3}S_2^{(1)0}S_2^{(1)2})$$

$$+ \tfrac{1}{4}\kappa_0{}^4\nu^{-4}S_2^{(1)2}(S_1^{(1)1} + S_2^{(1)1})\} \ , \tag{3.76}$$

where $S_L^{(0)j} \equiv S_{L,kk}^{(0)j}$ and $S_L^{(1)j} \equiv S_{L,kk}^{(1)j}$ are given by Eqs. (3.54) and (3.55), respectively, and ν is given by Eq. (2.19).

Now we regard $S_{L,kk}^{(n)j}$ $(n = 0, 1)$ as continuous functions of k to find them in the limit of $k \longrightarrow 0$,

$$S_{1,00}^{(0)j} = (1 - e^{-4\Delta s})[1 - 2e^{-2\Delta s}\cos(j\nu\Delta s) + e^{-4\Delta s}]^{-1} \ , \quad (j = 0, 1), \tag{3.77}$$

$$S_{0,00}^{(1)0} = \frac{3}{2} - \frac{1 + 3(-1)^{N+1}}{4(N+1)^2}(\lambda_{N+1}^C)^{-1} \ , \tag{3.78}$$

$$S_{L,00}^{(1)j} = [4(N+1)]^{-1}(1 - e^{-2x}) \sum_{k=0}^{N+1} (2 - \delta_{0k} - \delta_{N+1,k})(\lambda_k^C)^{-1}$$

$$\times \sum_{i=-1}^{1} (1-\delta_{0i})[1 - 2e^{-x}\cos(k\theta + ij\nu\Delta s) + e^{-2x}]^{-1} \ , \quad (L \neq 0), \tag{3.79}$$

where $x = L(L+1)\Delta s$, $\theta = \pi/(N+1)$, and λ_k^C is given by Eq. (3.46). In Eq. (3.79) with Eq. (3.46), we may put $\lambda_0^B = 0$ and $\lambda_{N+1}^B \simeq \lambda_N^B$, so that

$$\lambda_0^C = \tfrac{2}{3}, \ \lambda_{N+1}^C \simeq \lambda_N^C \ . \tag{3.80}$$

Correspondingly, we regard $\lambda_{1,k}^0$ as a continuous function of k. Then, the ordinate intercept $\lambda_{1,0}^0$ of a plot of $\lambda_{1,k}^0$ against the reduced wave number is given by Eq. (3.74) with Eq. (3.75)–(3.80).

Next, we consider the coil limit of $N \gg 1$ and

$k/(N+1) \ll 1$. We then have

$$S^{(0)j}_{1,kk} = \alpha_j - \gamma^j_1(0)(k\theta)^2 + \cdots , \quad (j = 0, 1) , \tag{3.81}$$

$$S^{(1)0}_{0,kk} = \tfrac{3}{2} - \tfrac{9}{4} r_2 \lambda^B_k + \cdots , \tag{3.82}$$

$$S^{(1)j}_{L,kk} = a^j_L - b^j_L(k\theta)^2 + \cdots , \quad (L \neq 0) , \tag{3.83}$$

where

$$\alpha_j \equiv S^{(0)j}_{1,00} , \tag{3.84}$$

$$\begin{aligned} \gamma^j_L(\theta) = {} & e^{-x}(1 - e^{-2x})\{\cos(\theta + j\nu\Delta s) - 4e^{-x}\sin^2(\theta + j\nu\Delta s) \\ & \times [1 - 2e^{-x}\cos(\theta + j\nu\Delta s) + e^{-2x}]^{-1}\} \\ & \times [1 - 2e^{-x}\cos(\theta + j\nu\Delta s) + e^{-2x}]^{-2} , \end{aligned} \tag{3.85}$$

$$a^j_L = \lim_{N\to\infty} S^{(1)j}_{L,00} , \quad (L \neq 0) , \tag{3.86}$$

$$b^j_L = \lim_{N\to\infty} [2(N+1)]^{-1} \sum_{k=1}^{N} (\lambda^C_k)^{-1} [\gamma^j_L(k\theta) + \gamma^{-j}_L(k\theta)] , \quad (L \neq 0) \tag{3.87}$$

with $x = L(L+1)\Delta s$ and $\theta = \pi/(N+1)$. We note that the λ^B_k in Eq. (3.82) is given by Eq. (3.69) and becomes proportional to $(k\theta)^2$ in the free-draining limit $h \longrightarrow 0$ and to $(k\theta)^{3/2}$ in the nondraining limit $h \longrightarrow \infty$, and that in Eqs. (3.81)–(3.83), we have neglected terms of order N^{-1} and $e^{-N\Delta s}$.

The eigenvalues $\lambda^0_{1,k}$ in the lowest branch in the coil limit may then be written in the form

$$\lambda^0_{1,k} = \lambda^0_{1,0} + \overline{f}_D(3k_BT/\overline{a}^2\overline{\zeta})\overline{\lambda}^B_k , \quad \text{(coil limit)} , \tag{3.88}$$

where $\overline{\lambda}_k^B$ is given by Eq. (3.69) with the effective translational friction coefficient $\overline{\zeta}$ in place of ζ_t, and

$$\overline{\zeta} = (1 + A_2/A_1)^{-1}\zeta_t \ , \tag{3.89}$$

$$\begin{aligned}\overline{f}_D &= A_1(\overline{a}/a)^2 \\ &= A_1[1 + 2\tau_0{}^2\nu^{-2}e^{-2\Delta s}(1 - e^{-2\Delta s})^{-1} + 2\kappa_0{}^2\nu^{-2}e^{-2\Delta s} \\ &\quad \times (\cos\nu\Delta s - e^{-2\Delta s})(1 - 2e^{-2\Delta s}\cos\nu\Delta s + e^{-4\Delta s})^{-1}] \ ,\end{aligned} \tag{3.90}$$

with

$$\begin{aligned}A_1 &= 2(\alpha_0\alpha_1)^{-1}(f_0{}^2 - g_0)^{-1/2}[1 - \tfrac{1}{4}(a_1^1 + a_2^1) \\ &\quad - \kappa_0{}^2\tau_0{}^2\nu^{-4}(\tfrac{3}{4}a_2^0 - a_2^1 + \tfrac{1}{4}a_2^2)] + \tfrac{1}{4}[1 - f_0(f_0{}^2 - g_0)^{-1/2}] \\ &\quad \times [\alpha_0^{-1} + \alpha_1^{-1} - (\kappa_0{}^2 - \tau_0{}^2)\nu^{-2}(\alpha_0^{-1} - \alpha_1^{-1})] \ .\end{aligned} \tag{3.91}$$

In Eq. (3.89), A_2 may be written in terms of κ_0, τ_0, f_0, g_0, α_j, $\gamma_1^j(0)$, a_L^j, and b_L^j, but is unnecessary in later numerical computations, and its explicit expression is not given here. We note that the f_0 and g_0 appearing in $\lambda_{1,0}^0$, A_1, and A_2 in Eq. (3.88) should be evaluated in the limit $N \longrightarrow \infty$, and that in the second line of Eqs. (3.90), we have used Eqs. (3.73) and (2.26).

Now, the intercept $\lambda_{1,0}^0$ in general becomes positive or negative depending on N and r_2 (and also on r_1 weakly), the negative $\lambda_{1,0}^0$ giving definitely the negative eigenvalues $\lambda_{1,k}^0$ at small wave numbers. (We note that the negative eigenvalues occur even without the block-diagonal approximation.) It is interesting to see that if $\lambda_{1,0}^0$

vanish and if $\overline{f}_D$ were equal to unity, the inverse of $\lambda_{1,k}^0$ given by Eq. (3.88) would be just the Rouse–Zimm dielectric relaxation times. (Note then that the appearance of $\overline{\zeta}$ in place of ζ_t is immaterial, since it is known that the values to be assigned to $\overline{\alpha}$ and $\overline{\zeta}$ are, to some extent, arbitrary in the *two–parameter* theory for polymer chain dynamics.[19]) However, this is not generally the case , though $\overline{f}_D \equiv 1$ in particular case of $\kappa_0 = 0$ or $\tau_0 = 0$ since then $A_1 = \alpha_0^{-1}$ or α_1^{-1}. Such failure in reproducing long–wavelength (slow) motions may be regarded as arising from the preaveraging approximation made in the matrix **C** given by Eq. (2.94) and contained in matrix **M** given by Eq. (2.92), and therefore from the approximation of the matrix **M** by Eq. (2.113). For flexible chains, it is, however, possible to make $\lambda_{1,0}^0$ small in magnitude and $\overline{f}_D$ close to unity by choosing r_2 properly, as shown below. This determines its possible range. For typical stiff chains such as DNA, the possible range of r_2 must be determined in a different way, as mentioned in Sec. 3–1.

(i). Flexible chains

Figure 3.4 shows plots of the reduced intercept $\tilde{\lambda}_{1,0}^0 \equiv \zeta_r \lambda_{1,0}^0 / k_B T$ against r_2 for four polymers, i–PS, s–PS, i–PMMA, and s–PMMA, all with $r_1 = 1$ and $N = 99$. The full and broken curves represent the values for the values of Δs equal to its upper

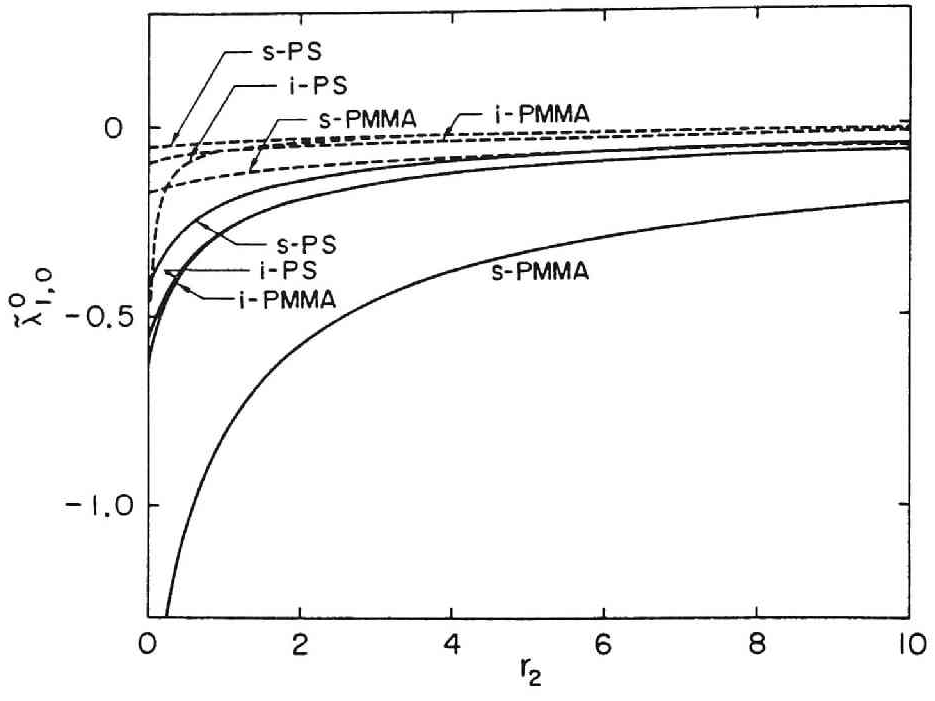

Fig. 3.4. The reduced intercept $\tilde{\lambda}_{1,0}^0$ of the lowest 1^0 branch of the eigenvalue spectrum plotted against r_2 for isotactic and syndiotactic polystyrenes and isotactic and syndiotactic poly(methyl methacrylate)s, all with $r_1=1$ and $N=99$. The full and broken curves represent the values for the values of Δs equal to its upper and lower bounds, respectively, for each polymer.

and lower bounds, respectively, for each polymer. In all cases, $\lambda_{1,0}^0$ increases monotonically with increasing r_2, and the larger Δs, the smaller $\lambda_{1,0}^0$ at given r_2. We note that although $\lambda_{1,0}^0$ is negative in the range of r_2 displayed, it becomes positive in some cases for very large r_2, and also that $\lambda_{1,0}^0$ is almost independent of N for $N \gtrsim 100$ in the range of r_2 displayed. It is then important to see that $\lambda_{1,0}^0$ in general decreases rapidly as r_2 is decreased to

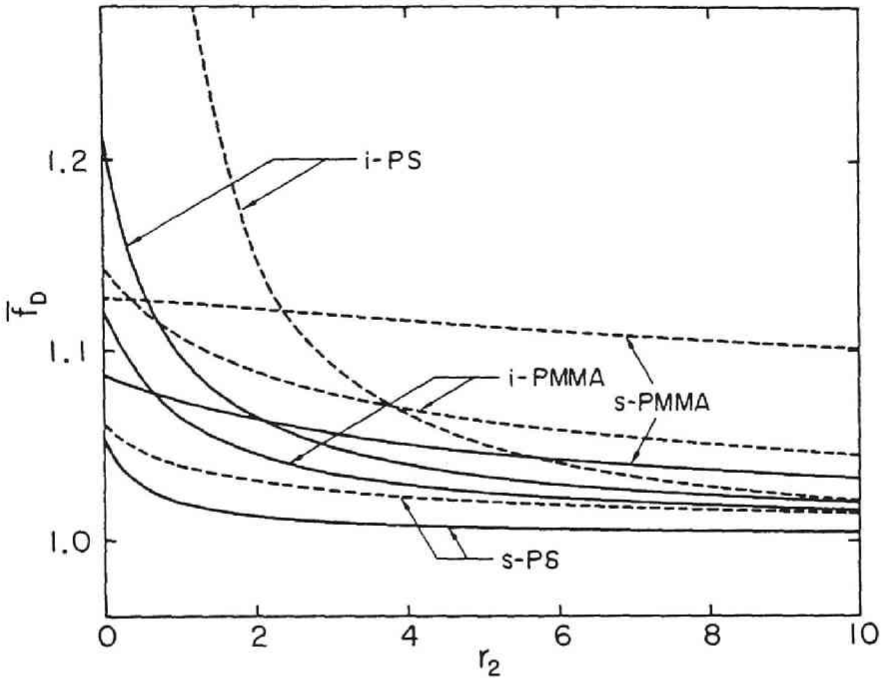

Fig. 3.5. The factor $\overline{f}_D$ plotted against r_2 for the four flexible polymers. The full and broken curves have the same meaning as in Fig. 3.4.

zero for $r_2 \lesssim 3$, but for $r_2 \gtrsim 3$, it depends on r_2 weakly, and is actually very small in magnitude.

Figure 3.5 shows plots of the factor $\overline{f}_D$ (appearing in the coil limit) against r_2 at $r_1 = 1$ for the same polymers, the meaning of the curves being the same as in Fig. 3.4. In all cases, $\overline{f}_D$ decreases to unity with increasing r_2, and the larger Δs, the closer to unity $\overline{f}_D$ at given r_2 in its range displayed. It is seen that for $r_2 \gtrsim 3$, $\overline{f}_D$ depends on r_2 weakly, and moreover $1.0 \lesssim \overline{f}_D \lesssim 1.1$; it is actually

very close to unity except for s-PMMA. These establish the allowed range of r_2, i. e., $r_2 \gtrsim 3$.

(ii). Stiff chains

We consider DNA as an example of typical stiff chains. It is well known that DNA may be represented by the KP chain ($\kappa_0 = 0$). However, in order to apply the present theory to it, we must also determine its τ_0. This can be achieved if a localized Cartesian coordinate system is affixed to each base pair, representing it by the KP-1 chain[25] with $\kappa_0 = 0$ and $\tau_0 \neq 0$ (see Fig. 2 of Ref. 25). Since its one helix turn contains 10 base pairs, we then have $\tau_0 \simeq 200$, assuming $\lambda^{-1} = 1100$ Å and the distance between base pairs equal to 3.4 Å. Further, if we take as Δs the distance between base pairs, we have $\Delta s = 0.0031$, as already mentioned. For DNA having such model parameters together with $r_1 = 1$, it has been found that the reduced intercept $\tilde{\lambda}^0_{1.0}$ is very small in magnitude ($\sim -2\times10^{-3}$) almost independently of r_2 and N for $0 \leq r_2 \lesssim 100$ and $N \gtrsim 100$. Therefore, we cannot limit the possible range of r_2 on the basis of $\lambda^0_{1.0}$, but must be resort to a classical-hydrodynamic model calculation. (Note that the coil limit is of no interest in the case of typical stiff chains, and moreover, for most of them, $\kappa_0 = 0$ and therefore $\overline{f}_D \equiv 1$.)

Now, the diameter d of DNA is much greater than Δs,

and therefore, for the present purpose, it is more adequate to regard its subbody as a circular disk of diameter d and width Δs rather than as a spherical bead. For convenience, we then replace the disk by a ring (regular plane polygon) such that n Stokes spherical beads of radius r are arranged in touch with each other on a circumference of diameter d. Its mean translational and rotatory diffusion coefficients D_t and D_r (for $n \gg 1$) are given, from Eqs. (72) and (81) of Ref. 26, by

$$D_t = (11k_BT/72\pi\eta_0 nr)[\ln n + \gamma_E - \ln(\pi/2) + 128/99] , \tag{3.92}$$

$$D_r = (k_BT/\pi\eta_0 nrd^2)[\ln n + \gamma_E - \ln(\pi/2) - 13/18] \tag{3.93}$$

with γ_E the Euler constant ($= 0.5772\cdots$). If we put $\zeta_t \simeq k_BT/D_t$ and $\zeta_r \simeq k_BT/D_r$ with $d = 25$ Å, $2r = a \simeq \Delta s = 3.4$ Å, and $n \simeq \pi d/2r$, we have $r_1 \simeq 5$ and $r_2 \simeq 15$, so that $r_1r_2 \simeq 75$. If we instead regard the disk as an oblate spheroid having major and minor axes 25 and 3.4 Å, respectively, and calculate its D_t and D_r,[27,28] we then have $r_1 \simeq 5$ and $r_2 \simeq 12$ so that $r_1r_2 \simeq 60$. In any case, the values of r_2 and r_1r_2 must be about two orders of magnitude greater than the value 1/3 for a touched Stokes spherical bead model. However, this value of r_1 exceeds its allowed range, as seen from the analysis in Sec. 3–5a. We therefore take $r_1 \simeq 1$ and $r_2 = 20$–80, so that $r_1r_2 = 20$–80. As shown later, the product r_1r_2, or ζ_r, plays an important role.

Finally, the above analysis requires some remarks. For DNA,

if we assume somewhat larger motional units, we must take larger Δs. Further, Δs will be larger for most of the other stiff chain than for DNA. As Δs is so increased, a Stokes spherical bead model for the subbody seems to become better. However, then, $\lambda_{1,0}^0$ decreases rapidly as r_2 is decreased to zero for $r_2 \lesssim 3$, as in the case of flexible chains (see Fig. 3.4). For such large Δs, we must therefore again impose the condition that $r_2 \gtrsim 3$.

3-6. Discussion and Concluding Remarks

a. The preaveraging approximation

The preaveraging approximation in the matrix $\mathbf{C}$ is the most serious in the present theory since it breaks, to some extent, the rigid constraints imposed and the components of the flux associated with the constrained coordinates are only on the average made to vanish. Now it must be recalled that the constraints are such that the magnitude of the bond vector $\mathbf{a}_p$ is fixed to be a and its direction coincides with the ζ_p axis of the localized coordinate system affixed to the pth subbody; i. e., $|\mathbf{a}_p| = a$ and $\mathbf{e}_{\zeta_p} \cdot \mathbf{a}_p = a$ for all p. It is also helpful to recall that the discrete HW chain is just equivalent to a system of coupled symmetric tops (subbodies) with constraints such that the rotation axis ($\mathbf{e}_{\zeta_p}$) of each points to the center of mass of its successor with the fixed distance a

between those of the two. In fact, if we suppress the term containing the (constraining) matrix $\mathbf{C}^{-1}$ in Eq. (2.92) for the matrix $\mathbf{M}$ so that $\mathbf{M} = \mathbf{I}_N$, then the diffusion equation reduces to the (rotational) one for a system of coupled tops without these constraints. Since it is the orientations Ω_p of the subbodies that evolve with time in the present model, the partial breakdown of these constraints must destroy, to some extent, the orientational correlations between subbodies. However, it seems to have no significant effect on the local motions, which are governed by the rather short-ranged correlations. On the other hand, in order that long-wavelength motions with large relaxation times take place, there must be correct, long-ranged strong correlations. For instance, end-over-end rotation of the entire chain is possible only when all Ω_p are varied without relative rotations of the subbodies with respect to each other. Therefore, if inhibited angular displacements of the subbodies are accumulated over a long range along the chain, such long-wavelength motions fail to take place. This is the reason why the eigenvalues in the lowest 1^0 branch, and also in the 2^0 branch in the case of stiff chain, become negative at small wave numbers. In this connection, we note that preaveraging approximations lead to the breakdown of the positive definiteness of the diffusion operator also in the case of the conventional bond chain, as shown by Fixman and Evans,[11] but then it causes errors in local chain motions rather than in

long-wavelength (slow) motions.

In the present theory, however, the proper choice of the parameter r_2 ($\gtrsim 3$) keeping the parameter $r_1 \simeq 1$ allows us to make the lowest 1^0 branch of the spectrum start from zero at zero wave number. For flexible chains, this makes it possible to remove the negative eigenvalues completely, and moreover the Rouse-Zimm dielectric relaxation times are then recovered in a very good approximation. The adjustable parameter r_2 also serves in its allowed and acceptable range to remove apparently the effect of the preaveraging approximation on local chain motions if any, and thus to give reasonable values for the correlation times. Thus, our hope mentioned in Sec. 1-1 has been more than realized.

b. Flexible constraints

Each subbody contains several skeletal bonds of the real chain, and moreover the interaction between two adjacent subbodies is governed by the soft potential derived from the free energy of the continuous HW chain. Therefore, the present model may be regarded as corresponding to a level of coarse graining of the realistic chain with flexible constraints on bond lengths and angles. The recent Brownian dynamic simulation study of Helfand and his co-workers[29-31] demonstrates the adequacy of such a bond chain with flexible constraints, especially on bond angles. However, owing

to the rejection of Boyer- and Schatzki-type crankshaft motions, it is no longer easy to image a detailed picture of chain motions clearly in the present model as well as in the bond chain.

c. Periodic vs nonperiodic boundary conditions

The equilibrium and also time-dependent distribution functions for the present discrete model have been expanded in terms of the Wigner functions $\mathscr{D}_l^{mj}$ (with l integer), and therefore satisfy periodic boundary conditions. Although this is a natural consequence of the construction of the present model from the continuous HW chain whose Green's function satisfies similar boundary conditions, it has a far more important meaning. That is, it makes the present model correspond to the real (flexible) bond chain whose potential energy is a periodic function of internal rotation (torsion) angles. On the contrary, Barkley and Zimm[32] have adopt nonperiodic boundary conditions in their treatment of the continuous elastic and also spring-bead models for DNA (near the rod limit). In fact, the nonperiodic boundary conditions are required when we consider, for instance, the super-coiling of constrained DNA,[33] or the linking number and the twist of closed DNA.[34] However, the periodic boundary conditions lead to no incorrect results as far as the properties of our present interest such as dielectric relaxation are concerned even for DNA and other

stiff chains. It is very difficult to impose the nonperiodic boundary conditions on the distribution functions for the HW chain whether it is continuous or discrete.

d. Conclusion

We have presented a method of decoupling the eigenvalue problem for the representation of the diffusion operator $\mathscr{L}$ of the discrete HW chain by introducing the standard representations by analogy with quantum mechanics, and have also given approximate expressions for the time-correlation functions in the subspace $L(1)$ for the discrete HW chains. All the results presented here encourage us to make a further detailed study of the present model. Thus, in the next chapter, we shall consider dielectric relaxation. The problem that will then follow is to obtain the eigenvalue spectra and the time-correlation functions in the subspace $\{2(1), 2(2)\}$ in order to treat the intrinsic viscosity. This will be done in Chap. 5.

Appendix 3-A. The Three-Dimensional Eigenvalue Problem

In this Appendix, we give the analytical solution of the three-dimensional ($L = 1$) eigenvalue problem given by Eq. (3.60) (with $\kappa_0 \neq 0$).

The 3×3 matrices $\overline{E}_{1(1),[k]}$ and $\overline{L}_{1(1),[k]}$ are explicitly given by

$$\overline{E}_{1(1),[k]} = (8\pi^2)^{-N}\mathrm{diag}(\alpha, \beta, \alpha) , \tag{3A.1}$$

$$\overline{L}_{1(1),[k]} = (8\pi^2)^{-N}\zeta_r{}^{-1}\begin{pmatrix} a & -ic & d \\ ic & b & ic \\ d & -ic & a \end{pmatrix} \tag{3A.2}$$

with

$$\alpha = S_1^{(0)1} ,$$

$$\beta = S_1^{(0)0} , \tag{3A.3}$$

and

$$\begin{aligned} a &= 2 - \tfrac{1}{2}\tau_0{}^2\nu^{-2}(S_1^{(1)1} + S_2^{(1)1}) \\ &\quad - \tfrac{2}{3}\kappa_0{}^2\nu^{-2}(S_0^{(1)0} + \tfrac{3}{8}S_1^{(1)0} + \tfrac{1}{8}S_2^{(1)0} + \tfrac{3}{4}S_2^{(1)2}) , \\ b &= 2 - \tfrac{4}{3}\tau_0{}^2\nu^{-2}(S_0^{(1)0} + \tfrac{1}{2}S_2^{(1)0}) - \tfrac{1}{2}\kappa_0{}^2\nu^{-2}(S_1^{(1)1} + S_2^{(1)1}) , \\ c &= \frac{2\sqrt{2}}{3}\kappa_0\tau_0\nu^{-2}(S_0^{(1)0} - \tfrac{3}{8}S_1^{(1)1} - \tfrac{1}{4}S_2^{(1)0} + \tfrac{3}{8}S_2^{(1)1}) , \\ d &= -\tfrac{2}{3}\kappa_0{}^2\nu^{-2}(S_0^{(1)0} - \tfrac{3}{8}S_1^{(1)0} + \tfrac{1}{8}S_2^{(1)0}) , \end{aligned} \tag{3A.4}$$

where ν, $S_L^{(0)j} \equiv S_{L,kk}^{(0)j}$, and $S_L^{(1)j} \equiv S_{L,kk}^{(1)j}$ are given by Eq. (2.19), (3.54), and (3.55), respectively, and we have used the relation $S_L^{(n)-j} = S_L^{(n)j}$ [as seen from Eqs. (3.54) and (3.55)], and expressed $T_{LM}^{jj'j''}$ in Eq. (3.51) explicitly in terms of κ_0 and τ_0.

Then, the desired eigenvalues $\lambda_{1,k}^j$ ($j = -1, 0, 1$) are

$$\begin{aligned} \lambda_{1,k}^j &= (2\zeta_r)^{-1}[\,\alpha^{-1}(a + d) + \beta^{-1}b - (-1)^j A\,] \quad \text{for } j = -1, 0 \\ &= (\zeta_r\alpha)^{-1}(a - d) \qquad \text{for } j = 1 , \end{aligned} \tag{3A.5}$$

with

$$A = \{\,[\,\alpha^{-1}(a + d) - \beta^{-1}b\,]^2 + 8(\alpha\beta)^{-1}c^2\,\}^{1/2} . \tag{3A.6}$$

The corresponding eigenvectors $\mathbf{v}_{1,k}^{j}$, which are the column vectors of the diagonalizing matrix $Q^{L}_{1(1),[k]}$ in Eq. (3.60), are

$$\mathbf{v}_{1,k}^{j\,T} = [\,-\tfrac{1}{2}(-1)^{j}(B_j/A)^{1/2},\ 2i(\alpha\beta)^{-1/2}c(AB_j)^{-1/2},$$

$$-\tfrac{1}{2}(-1)^{j}(B_j/A)^{1/2}\,] \quad \text{for } j = -1,\ 0$$

$$= (1/\sqrt{2},\ 0,\ -1/\sqrt{2}) \quad \text{for } j = 1, \tag{3A.7}$$

with

$$B_j = A - (-1)^{j}[\,\alpha^{-1}(a + d) - \beta^{-1}b\,] \quad (j = 0,\ -1)\,. \tag{3A.8}$$

We note that the indexing of the above eigenvalues and eigenvectors is arbitrary, and does not affect the value of the time-correlation function given by Eq. (3.62). In the above, for convenience, the indexing has been made in such a way that $j = 0$ and -1 for $v_{-1}^{j} = v_{1}^{j}$, and $j = 1$ for $v_{-1}^{j} = -v_{1}^{j}$, where $\mathbf{v}_{1,k}^{j\,T} = (v_{-1}^{j},\ v_{0}^{j},\ v_{1}^{j})$, and that $\lambda_{1,1}^{0} < \lambda_{1,1}^{-1}$ in the former.

Appendix 3-B. The Mean Reciprocal Distance

In this Appendix, we give an interpolation formula for the mean reciprocal distance $<R_{pq}^{-1}>_{\mathrm{eq}}$ between the pth and qth subbodies appearing in the diffusion matrix B. As noted before, it may be replaced by the mean reciprocal (end-to-end) distance $<R^{-1}(s)>$ of the corresponding continuous HW chain of contour length $s = |q - p|\Delta s$. Here and hereafter, the subscript eq is

suppressed, for simplicity. For the cylinder model used for the evaluation of the steady-state transport coefficients,[35,36] an interpolation formula for the mean reciprocal distance between a contour point and a point on the cylinder surface as a function of s and diameter d has already been given by Yamakawa et al.[37] on the basis of the $\varepsilon 3$ values by the epsilon method, the WI3, WII3, or FS3 values by the weighting function method, and the second Daniels approximation values.[37] For the present case of $d = 0$, we can construct an interpolation formula in a similar way but as a function of s, κ_0, and τ_0 covering almost all important ranges of κ_0 and τ_0.

It has been found to be convenient to construct an interpolation formula, instead of for $\langle R^{-1}(s)\rangle$ itself as in Eq. (66) of Ref. 37, for a function $\Gamma(s)$ defined by

$$\langle R^{-1}(s)\rangle = [\langle R^2(s)\rangle_{KP}/\langle R^2(s)\rangle]^{1/2}\langle R^{-1}(s)\rangle_{KP}[1 + \kappa_0{}^2\Gamma(s)] , \qquad (3B.1)$$

where $\langle R^2(s)\rangle$ is the mean-square end-to-end distance of the same continuous HW chain and given by Eq. (2.22), $\langle R^2(s)\rangle_{KP}$ is the mean-square end-to-end distance of the KP chain of the same contour length and given by Eq. (2.22) with $\kappa_0 = 0$ ($c_\infty = 1$ and $\tau_0/\nu = 1$), and $\langle R^{-1}(s)\rangle_{KP}$ is the mean reciprocal distance of the same KP chain and approximately given by[35]

$$\langle R^{-1}(s)\rangle_{KP} = \left(\frac{6}{\pi s}\right)^{1/2}\left(1 - \frac{1}{40s} - \frac{73}{4480s^2}\right) , \quad \text{for } s > 2.278 ,$$

$$= s^{-1}(1 + \tfrac{1}{3}s + 0.1130s^2 - 0.02447s^3) ,$$

$$\text{for } s \leq 2.278 . \tag{3B.2}$$

A good approximation to $\Gamma(s)$ has been found to be of the form,

$$\Gamma(s) = \exp(-2/s) \sum_{k=1}^{2} A_k s^{-k} + \exp[-(2 + \tfrac{3}{4}\nu)s] \sum_{k=3}^{7} A_k s^k , \tag{3B.3}$$

with

$$A_1 = 3(4 + \tau_0^2)^{-1}(4 + \nu^2)^{-1} - \tfrac{3}{10}(9 + \nu^2)^{-1}(36 + \nu^2)^{-1}$$

$$\times [1 + (101 + \kappa_0^2)(4 + \tau_0^2)^{-1} + 3(160 + 7\kappa_0^2)(4 + \tau_0^2)^{-2}] , \tag{3B.4}$$

$$A_k = \{1 + \delta_{k2}[(4 + \nu^2)^{-1} - 1]\} \sum_{i=0}^{7} \sum_{j=0}^{6} a_{ij}^k \nu^i (\tau_0/\nu)^{2j} ,$$

$$(k = 2\text{–}7) , \tag{3B.5}$$

where a_{ij}^k are constants independent of s, κ_0, and τ_0.

For $s \ll 1$ and $s \gg 1$, $<R^{-1}(s)>$ given by Eq. (3B.1) with Eqs. (3B.2)–(3B.5) may be expanded as follows:

$$<R^{-1}(s)> = s^{-1}(1 + \tfrac{1}{3}s + \cdots) , \quad \text{for } s \ll 1$$

$$= \left(\frac{6}{\pi c_\infty s} \right)^{1/2} \left(1 - \left\{ \frac{1}{40} - \kappa_0^2(4 + \tau_0^2)^{-1}(4 + \nu^2)^{-1} + \frac{3\kappa_0^2}{10} \right.\right.$$

$$\times [1 + (101 + \kappa_0^2)(4 + \tau_0^2)^{-1} + 3(160 + 7\kappa_0^2)(4 + \tau_0^2)^{-2}]$$

$$\left.\left. \times (9 + \nu^2)^{-1}(36 + \nu^2)^{-1} \right\} s^{-1} + \cdots \right) , \quad \text{for } s \gg 1 . \tag{3B.6}$$

That is, Eq. (3B.1) gives the exact first-order correction for the rod limit for $s \ll 1$ and the first Daniels approximation for $s \gg 1$, as seen from Eq. (47) of Ref. 37 (for $s \ll 1$) and Eq. (55) with

Eq. (53) of Ref. 37 and Eq. (44) of Ref. 38 (for $s \gg 1$). We note that Eq. (3B.1) gives the approximate second-order term $(0.1130 + \kappa_0^2/24)s^2$ for $s \ll 1$, while the corresponding exact term is $(1/15 + \kappa_0^2/24)s^2$, as found from Eq. (34) of Ref. 37 and Eq. (17) of Ref. 39 with its appendix. When $\kappa_0 = 0$, this statement applies to the second line of Eqs. (3B.2).

The numerical coefficients a_{ij}^k n Eq. (3B.5) have been determined by the method of least squares from the WI3 values of $<R^{-1}(s)>$ by the weighting function method for $0.3 \leq s \leq 2.3$ and for various values of κ_0 and τ_0. The WI3 values in this range of s had already been obtained for the values of κ_0 and τ_0 indicated by the filled points in the (κ_0, τ_0) plane of Fig. 3 of Ref. 36. We have here added WI3 values in the same range of s at some points in the domains of $\nu \leq 1.5$ and $0 \leq \tau_0/\nu \leq 0.5$ and of $\nu \leq 8$ and $0.5 \leq \tau_0/\nu \leq 1$. The results for a_{ij}^k are given in Table 3.1. In the shaded domain of Fig. 3 of Ref. 36 and the above two added domains, the values of $<R^{-1}(s)>$ calculated from Eq. (3B.1) with Eqs. (3B.2)-(3B.5) and with these values of a_{ij}^k agree with the $\varepsilon 3$ values for $s < 0.3$, the WI3 values for $0.3 \leq s \leq 2.3$, and the second Daniels approximation values for $s > 2.3$ to within 2%.

Finally, we note that in the domain III of Fig. 2 of Ref. 37 for $\nu \gtrsim 20$, Eq. (3B.1) with Eqs. (3B.2)-(3B.4) and with $A_k = 0$ $k = 2-7$ gives very good approximations. Thus, this rather simple formula applies to, for instance, i-PS, polyoxymethylene ($\kappa_0 = 17$

Table 3.1. Values of the coefficients a_{ij}^{k} in Eq. (3B.5).

		k					
i	j	2	3	4	5	6	7
0	0	−2.7049	−7.5400(−1)	6.1401	−6.6199	2.6941	4.1447(−2)
0	1	1.5233(1)[a]	9.4768(−1)	−2.2437	−5.9720(1)	9.3801(1)	−4.2218(1)
0	2	−9.3705(1)	2.0811(1)	−8.8606(1)	3.6688(2)	−3.3357(2)	1.0364(2)
0	3	3.4199(2)	−2.0445(2)	6.7654(2)	−1.0032(3)	−1.2857(2)	3.7135(2)
0	4	−6.1943(2)	5.4622(2)	−1.6914(3)	1.3957(3)	1.9124(3)	−1.6006(3)
0	5	5.4254(2)	−5.6789(2)	1.7137(3)	−1.0037(3)	−2.5173(3)	1.8642(3)
0	6	−1.8490(2)	2.0504(2)	−6.1311(2)	3.1010(2)	9.7025(2)	−6.9619(2)
1	0	9.1142	3.4651	−2.5624(1)	2.9550(1)	−1.2770(1)	3.8899(−1)
1	1	−5.3595(1)	−6.9304	2.1913(1)	2.0709(2)	−3.5688(2)	1.6667(2)
1	2	3.0376(2)	−3.0288(1)	1.3036(2)	−1.0721(3)	1.2051(3)	−4.4621(2)
1	3	−1.0880(3)	5.4423(2)	−1.5530(3)	2.2622(3)	8.0190(2)	−1.1734(3)
1	4	1.9786(3)	−1.6278(3)	4.4380(3)	−2.4375(3)	−7.5809(3)	5.4732(3)
1	5	−1.7484(3)	1.7824(3)	−4.8472(3)	1.6007(3)	9.4110(3)	−6.3560(3)
1	6	6.0051(2)	−6.6501(2)	1.8343(3)	−5.9341(2)	−3.4610(3)	2.3325(3)
2	0	−1.0953(1)	−5.1542	3.6013(1)	−4.3831(1)	1.9952(1)	−1.1709
2	1	5.4313(1)	1.3826(1)	−3.1847(1)	−2.7059(2)	4.9588(2)	−2.3698(2)
2	2	−2.2099(2)	−3.2259(1)	−4.7715(1)	1.2764(3)	−1.8389(3)	7.8458(2)
2	3	6.8539(2)	−3.6187(2)	1.3094(3)	−2.2413(3)	1.1757(2)	6.0981(2)
2	4	−1.1983(3)	1.4531(3)	−4.4486(3)	2.2324(3)	6.9490(3)	−5.0433(3)
2	5	1.0698(3)	−1.7667(3)	5.3715(3)	−1.9864(3)	−8.7553(3)	6.0542(3)
2	6	−3.8042(2)	6.9945(2)	−2.1919(3)	1.0478(3)	2.9927(3)	−2.1592(3)
3	0	5.7440	3.4159	−2.2711(1)	2.9061(1)	−1.3378(1)	8.6677(−1)
3	1	−1.9872(1)	−1.0809(1)	1.0667(1)	1.8760(2)	−3.4288(2)	1.6405(2)
3	2	−3.7479	5.6583(1)	7.4575(1)	−9.6990(2)	1.5440(3)	−6.9034(2)
3	3	1.5736(2)	3.5420(1)	−8.7510(2)	2.1083(3)	−1.9366(3)	5.8246(2)
3	4	−3.5702(2)	−5.2768(2)	2.9171(3)	−3.1763(3)	−7.4079(1)	9.8854(2)
3	5	3.0368(2)	7.8272(2)	−3.6467(3)	3.4184(3)	9.2878(2)	−1.5527(3)
3	6	−8.6201(1)	−3.4025(2)	1.5476(3)	−1.6139(3)	−8.5762(1)	4.9886(2)

4	0	−1.4876	−1.1070	7.0707	−9.2818	4.0545	−1.1502(−1)
4	1	2.5094	3.7734	2.0359	−7.4027(1)	1.2920(2)	−6.0976(1)
4	2	3.8402(1)	−2.4593(1)	−6.8657(1)	4.5264(2)	−7.0566(2)	3.1418(2)
4	3	−2.0277(2)	2.4499(1)	4.4154(2)	−1.2793(3)	1.5600(3)	−6.0554(2)
4	4	4.0109(2)	9.9426(1)	−1.2757(3)	2.3455(3)	−2.0101(3)	5.8374(2)
4	5	−3.4870(2)	−1.9649(2)	1.5435(3)	−2.5035(3)	1.7772(3)	−4.0787(2)
4	6	1.1115(2)	9.4812(1)	−6.5280(2)	1.0764(3)	−7.6449(2)	1.8051(2)
5	0	2.0156(−1)	1.8587(−1)	−1.1416	1.4900	−5.5695(−1)	−4.5479(−2)
5	1	1.0037(−1)	−6.4465(−1)	−1.5497	1.5971(1)	−2.6405(1)	1.2233(1)
5	2	−1.1430(1)	4.6045	2.2698(1)	−1.1165(2)	1.6633(2)	−7.2814(1)
5	3	5.4302(1)	−6.9392	−1.1903(2)	3.6679(2)	−4.6797(2)	1.8802(2)
5	4	−1.0524(2)	−1.1949(1)	3.1002(2)	−7.1974(2)	7.7277(2)	−2.7903(2)
5	5	9.1596(1)	3.0585(1)	−3.6016(2)	7.5604(2)	−7.3586(2)	2.4845(2)
5	6	2.9583(1)	−1.5919(1)	1.4990(2)	−3.1092(2)	2.9400(2)	−9.7735(1)
6	0	−1.3692(−2)	−1.5546(−2)	9.1506(−2)	−1.1498(−1)	3.0642(−2)	1.1544(−2)
6	1	−4.5337(−2)	5.2776(−2)	2.5063(−1)	−1.7173	2.7092	−1.2318
6	2	1.3124	−3.9410(−1)	−3.0626	1.3099(1)	−1.8776(1)	8.0822
6	3	−5.9817	6.4804(−1)	1.4823(1)	−4.6670(1)	5.9690(1)	−2.4081(1)
6	4	1.1478(1)	9.8534(−1)	−3.6396(1)	9.4233(1)	−1.0758(2)	4.0635(1)
6	5	−9.9799	−2.7398	4.1058(1)	−9.8016(1)	1.0452(2)	−3.7915(1)
6	6	3.2356	1.4718	−1.6848(1)	3.9416(1)	−4.0848(1)	1.4602(1)
7	0	3.6668(−4)	5.1292(−4)	−2.8821(−3)	3.3886(−3)	−3.7515(−4)	−6.7520(−4)
7	1	2.5887(−3)	−1.6554(−3)	−1.2765(−2)	7.1257(−2)	−1.0837(−1)	4.8466(−2)
7	2	−5.3926(−2)	1.2641(−2)	1.4489(−1)	−5.7451(−1)	8.0042(−1)	−3.3976(−1)
7	3	2.4002(−1)	−2.0081(−2)	−6.7528(−1)	2.1445	−2.7276	1.0976
7	4	−4.5749(−1)	−4.0030(−2)	1.6025	−4.3922	5.1268	−1.9646
7	5	3.9713(−1)	1.0440(−1)	−1.7729	4.5412	−5.0238	1.8683
7	6	−1.2890(−1)	−5.6148(−2)	7.1994(−1)	−1.8035	1.9439	−7.1361(−1)

[a] $a(n)$ means $a \times 10^n$.

and $\tau_0 = 25$), and syndiotactic polypropylene ($\kappa_0 = 7.5$ and $\tau_0 = 30$) (see Table I of Ref. 20).

References

[1]See, for example, A. S. Davydov, *Quantum Mechanics* (Pergamon, Oxford, 1965), Chap. IV.

[2]A. Messiah, *Quantum Mechanics* (North–Holland, Amsterdam, 1970), Vol. II, Chap. XIII.

[3]A. R. Edmonds, *Angular Momentum in Quantum Mechanics* (Princeton University, Princeton, 1974).

[4]A. P. Yutsis, I. B. Levinson, and V. V. Vanagas, *The Theory of Angular Momentum* (Israel Program for Scientific Translations, Jerusalem, 1962), Secs. 6 and 21.

[5]H. Mori, Prog. Theor. Phys. (Kyoto), **33**, 423 (1965).

[6]R. Zwanzig, J. Chem. Phys., **60**, 2717 (1974); Les Houches Lectures (1973) in *Molecular Fluids——Fluides Moleculaires*, edited by R. Balian and G. Weill (Gordon and Breach, New York, 1976), p. 1.

[7]G. T. Evans, Mol. Phys., **36**, 1199 (1978); J. Chem. Phys., **69**, 3363 (1978); and succeeding papers.

[8]G. T. Evans, J. Chem. Phys., **70**, 2362 (1979).

[9]R. Zwanzig, J. Kiefer, and G. H. Weiss, Proc. Natl. Acad. Sci. USA, **60**, 381 (1968).

[10]H. Yamakawa, Annu. Rev. Phys. Chem., **25**, 179 (1974).

[11]M. Fixman and G. T. Evans, J. Chem. Phys., **68**, 195 (1978).

[12]P. E. Rouse, Jr., J. Chem. Phys., **21**, 1272 (1953).

[13]B. H. Zimm, J. Chem. Phys., **24**, 269 (1956).

[14]See, for example, Ref. 1, Sec. 44.

[15]O. Kratky and G. Porod, Rec. Trav. Chim. Pays-Bas, **68**, 1106 (1949).

[16]H. Yamakawa and J. Shimada, J. Chem. Phys., **70**, 609 (1979).

[17]M. Fixman and J. Kovac, J. Chem. Phys., **61**, 4939 (1974); and succeeding papers.

[18]J. E. Hearst, J. Chem. Phys., **37**, 2547 (1962).

[19]H. Yamakawa, *Modern Theory of Polymer Solutions* (Harper & Row, New York, 1971).

[20]H. Yamakawa and T. Yoshizaki, Macromolecules, **15**, 1444 (1982).

[21]H. Yamakawa and M. Fujii, Macromolecules, **7**, 128 (1974); **7** 649 (1974).

[22]J. E. Godfrey and H. Eisenberg, Biophys. Chem., **5**, 301 (1976).

[23]R. T. Kovacic and K. E. van Holde, Biochemistry, **16**, 1490 (1977).

[24]D. P. Millar, R. J. Robbins, and A. H. Zewail, J. Chem. Phys., **76**, 2080 (1982).

[25]H. Yamakawa, M. Fujii, and J. Shimada, J. Chem. Phys., **71**, 1611 (1979).

[26]H. Yamakawa and J. Yamaki, J. Chem. Phys., **58**, 2049 (1973).

[27]G. B. Jeffery, Proc. R. Soc. London Ser. A, **102**, 161 (1922).

[28]F. Perrin, J. Phys. Rad., **7**, 1 (1936).

[29]E. Helfand, Z. R. Wasserman, and T. A. Weber, J. Chem. Phys., **70**,

2016 (1979); Macromolecules, **13**, 526 (1980).

[30]J. Skolnick and E. Helfand, J. Chem. Phys., **72**, 5489 (1980).

[31]E. Helfand, Z. R. Wasserman, T. A. Weber, J. Skolnick, and J. H. Runnels, J. Chem. Phys., **75**, 4441 (1981).

[32]M. D. Barkley and B. H. Zimm, J. Chem. Phys., **70**, 2991 (1979).

[33]C. J. Benham, Proc. Natl. Acad. Sci. USA, **74**, 2397 (1977); Biopolymers, **18**, 609 (1979).

[34]F. H. C. Crick, Proc. Natl. Acad. Sci. USA, **73**, 2639 (1976).

[35]H. Yamakawa and M. Fujii, Macromolecules, **6**, 407 (1973).

[36]H. Yamakawa and T. Yoshizaki, Macromolecules, **12**, 32 (1979).

[37]H. Yamakawa, J. Shimada, and M. Fujii, J. Chem. Phys., **68**, 2140 (1978).

[38]J. Shimada and H. Yamakawa, J. Chem. Phys., **67**, 344 (1977).

[39]M. Fujii and H. Yamakawa, J. Chem. Phys., **72**, 6005 (1980).

CHAPTER 4

DIELECTRIC RELAXATION

4-1. Introduction

In Chap. 3, we have given an approximate scheme for partially decoupling the eigenvalue problem for the representation of the diffusion operator of the discrete helical worm-like (HW) chain and found the general solutions in the decoupled subspaces $L(1)$ of the basis functions. In this chapter, we proceed to study the dielectric relaxation that can be described in terms of the $L = 1$ correlation functions.

We first give a brief historical survey of dielectric theories for chain polymers in dilute solution. The foremost of the development is a diffusion equation approach for the conventional bond chain with constraints by Kirkwood and his co-workers,[1-3] in which the dielectric dispersion broader than a Debye one[4] has been obtained but the results are far from realistic because of drastic mathematical approximations. Subsequently, significant advances have been made by Zimm[5] and Stockmayer and Baur[6,7] on the basis of the simple tractable spring-bead model. These provide an understanding of the long-wavelength motions of a chain, especially having parallel dipoles.[7,8] However, the model fails

to treat dielectric relaxation arising from the local motions of a chain having perpendicular dipoles. An analysis of this type of relaxation can be made, to some extent, on the basis of very simple models such as a one-dimensional array of perpendicular dipoles, as done by Clark and Zimm[9,10] and Shore and Zwanzig.[11] (Mansfield[12] has recently considered a modification of the Clark-Zimm model, and Cook and Livornese[13] have made a Brownian dynamics simulation study.) These and also stochastic models, including Ising and lattice systems,[14,15] serve to understand the basic local processes in chains having perpendicular dipoles and to derive broad and asymmetric loss curves. However, there is a great gap between them and real chains, and therefore it is impossible to evaluate dielectric correlation times, as determined from loss peaks, in terms of well-defined molecular parameters. In the meanwhile, Fixman and his co-workers[16] have elaborated the diffusion equation approach for the bond chain with constraints. In particular, Fixman and Evans[17] have made a semiquantitative analysis of the interaction between global and local modes by a physical insight, although the numerical results for, for instance, correlation times are not always satisfactory because of various preaveraging approximations.

Thus the main purposes of this chapter are threefold: (i) to make a mode analysis of the dielectric branches of the eigenvalue spectrum in order to inquire into the interaction between global

and local modes; (ii) to explain the broad and asymmetric dielectric loss and also even two loss peaks in some cases; and (iii) to evaluate dielectric correlation times for a wide variety of polymers. All these are done for both flexible and stiff chains on the basis of the discrete HW model such that an electric dipole moment is attached rigidly or with a rotational degree of freedom to each of the subbodies composing the chain.

The plan of this chapter is as follows: In the next section, the complex dielectric constant is formulated with the dipole correlation function and dielectrically active branches of the eigenvalue spectrum are identified for a given type of dipoles. In Sec. 4–3, we make a mode analysis of these branches, and also examine their dependences on chain length (or N). In Sec. 4–4, we examine the decay behavior of the dipole correlation function. In Sec. 4–5, we evaluate the dispersion (permittivity) $\varepsilon'(\omega)$ and loss $\varepsilon''(\omega)$ as functions of angular frequency ω to construct Cole–Cole plots for some polymers, and also compute correlation times for various polymers. Then a comparison with experiment is made. For stiff chains, the dependence on N of the correlation time is examined in some detail. In Sec. 4–6, we discuss discrepancies between theory and experiment, especially those, although not very large, found systematically for flexible chains, and suggest a possible direction toward improvement of the theory.

4-2. Formulation

Let $\varepsilon^* = \varepsilon' - i\varepsilon''$ be the excess complex dielectric constant of the dilute solution over that of the solvent alone. If the effect of local fields is ignored, it may be expressed in terms of the Fourier-Laplace transform of the dipole correlation function $M(t)$ as follows[11,18]:

$$(\varepsilon^* - \varepsilon_\infty)/(\varepsilon_0 - \varepsilon_\infty) = 1 - i\omega \int_0^\infty e^{-i\omega t} [M(t)/M(0)] dt , \tag{4.1}$$

where ε_0 and ε_∞ are the excess limiting low and high frequency dielectric constants, respectively, and t is the time. If $\boldsymbol{\mu}(t)$ is the instantaneous, field-free, dipole moment vector of the entire chain expressed in an external coordinate system, $M(t)$ is given by

$$M(t) = <\boldsymbol{\mu}(0) \cdot \boldsymbol{\mu}(t)>_{eq} , \tag{4.2}$$

where $<\cdots>_{eq}$ denotes an equilibrium average. Note that Eq. (4.1) with Eq. (4.2) is a good approximation in the case of nonpolar solvents. Thus our first problem is to evaluate $M(t)$. In what follows, all lengths are measured in units of λ^{-1} and $k_B T$ (with k_B the Boltzmann constant and T the absolute temperature) is chosen to be unity, unless noted otherwise.

Now let $\Omega_p = (\theta_p, \varphi_p, \psi_p)$ $(p = 1, 2, \cdots, N)$ be the Euler angles defining the orientation of the pth localized Cartesian coordinate system $(\mathbf{e}_{\xi_p}, \mathbf{e}_{\eta_p}, \mathbf{e}_{\zeta_p})$ affixed to the pth subbody of the discrete HW chain with respect to the external coordinate system

$(\mathbf{e}_x, \mathbf{e}_y, \mathbf{e}_z)$. Let $\mathbf{m}_p$ and $\tilde{\mathbf{m}}_p$ be the local electric dipole moment vectors attached to the pth subbody, expressed in the pth localized and external coordinate systems, respectively. We assume that their magnitudes are independent of p so that $|\mathbf{m}_p| = |\tilde{\mathbf{m}}_p| = m$. Further, suppose that the vector $\mathbf{m}_p$ is permitted to rotate about an axis, making a constant angle Δ with the axis, which has constant polar and azimuthal angles α and β (independent of p) in the pth localized system, as depicted in Fig. 4.1. Let $\gamma_p(t)$ be the (time-dependent) dihedral angle between the two planes containing the rotation axis and $\mathbf{e}_{\zeta_p}$, and the rotation axis and $\mathbf{m}_p$, respectively. The pth dipole moment vector expressed in a Cartesian coordinate system having the orientation defined by the Euler angles $(\alpha, \beta, \gamma_p)$ with respect to the pth localized system is independent of p. If we designate it by $\bar{\mathbf{m}}$, we have $\bar{\mathbf{m}} = (m \sin\Delta, 0, m \cos\Delta)$.

The coordinate transformation of a vector may easily be performed by using its spherical components rather than its Cartesian components, as done by Yamakawa et al.[19] For example, the spherical components $m_p^{(j)}$ $(j = 0, \pm 1)$ of $\mathbf{m}_p$ may be written in terms of the Cartesian components $(m_{p\xi}, m_{p\eta}, m_{p\zeta})$

$$m_p^{(\pm 1)} = \frac{1}{\sqrt{2}}(\mp m_{p\xi} - i m_{p\eta}) ,$$

$$m_p^{(0)} = m_{p\zeta} , \tag{4.3}$$

so that the spherical components $(\bar{\mathbf{m}})^{(j)}$ $(j = 0, \pm 1)$ of $\bar{\mathbf{m}}$ are given by

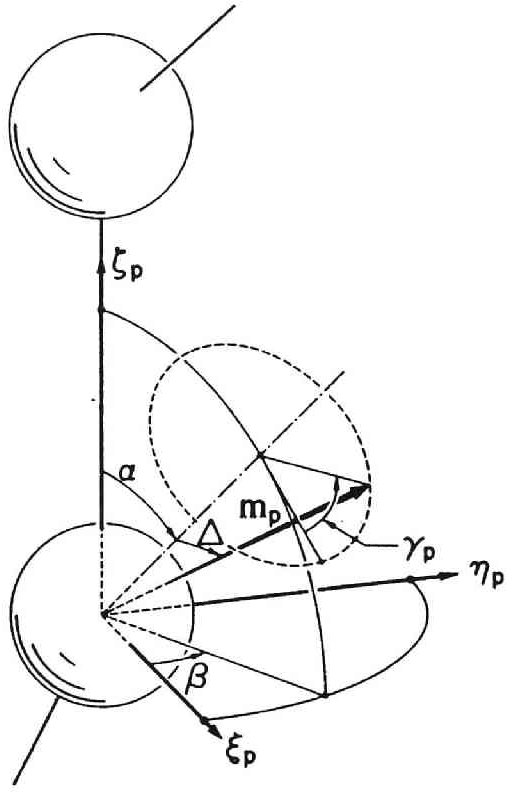

Fig. 4.1. Local dipole moment vector $\mathbf{m}_p$ in the pth localized Cartesian coordinate system.

$$\bar{m}^{(\pm 1)} = \mp \frac{m}{\sqrt{2}} \sin \Delta \ ,$$

$$\bar{m}^{(0)} = m \cos \Delta \ . \tag{4.4}$$

Since the spherical components of a vector obey the same transformation rule as the first-order spherical harmonics, we have for the spherical components $\tilde{m}_p^{(j)}$ $(j = 0, \pm 1)$ of $\tilde{\mathbf{m}}_p$:

$$\tilde{m}_p^{(j)} = (8\pi^2/3)^{1/2} \sum_{k=-1}^{1} \mathscr{D}_1^{jk}(\Omega_p) m_p^{(k)}$$

$$= (8\pi^2/3) \sum_{k_1,k_2=-1}^{1} \mathscr{D}_1^{jk_1}(\Omega_p) \mathscr{D}_1^{k_1k_2}(\alpha, \beta, \gamma_p) \bar{m}^{(k_2)} , \tag{4.5}$$

where $\mathscr{D}_l^{jj'}$ is the normalized Wigner functions as defined by Eq. (2.5).

Noting that

$$\boldsymbol{\mu} = \sum_{p=1}^{N} \tilde{\mathbf{m}}_p , \tag{4.6}$$

and that a scalar product of vectors may be expressed in terms of spherical components as in Eq. (9) of Ref. 19, we may write $M(t)$, from Eqs. (4.2) and (4.5), as

$$M(t) = \sum_{p,p'=1}^{N} <\tilde{\mathbf{m}}_p(0) \cdot \tilde{\mathbf{m}}_{p'}(t)>_{eq}$$

$$= \sum_{p,p'=1}^{N} \sum_{j=-1}^{1} <\tilde{m}_p^{(j)*}(0) \tilde{m}_{p'}^{(j)}(t)>_{eq}$$

$$= (8\pi^2/3)^2 \sum_{p,p'=1}^{N} \sum_{j,k_1,k_2,k_1',k_2'=-1}^{1} <\mathscr{D}_1^{jk_1*}(\Omega_p,0) \mathscr{D}_1^{k_1k_2*}[\alpha, \beta, \gamma_p(0)]$$

$$\times \mathscr{D}_1^{jk_1'}(\Omega_p,t) \mathscr{D}_1^{k_1'k_2'}[\alpha, \beta, \gamma_{p'}(t)]>_{eq} \bar{m}^{(k_2)} \bar{m}^{(k_2')} , \tag{4.7}$$

where the asterisk indicates the complex conjugate and in the third equality we have used the fact that $\bar{m}^{(j)}$ are real.

Now, in order to evaluate the average of the products of the $\mathscr{D}$ functions in Eq. (4.7), we assume that there are no

correlations between the motion of each subbody (main chain motion) and the rotational motion of the dipole moment about the rotation axis in it (side chain motion) and also between the latter motions in different subbodies. Then Eq. (4.7) reduces to

$$M(t) = m^2\cos^2\Delta \sum_{j,j'=-1}^{1} e^{-i(j-j')\beta} d_1^{j0}(\alpha) d_1^{j'0}(\alpha) M^{jj'}(t)$$

$$+ \sum_{jj'=-1}^{1} e^{-i(j-j')\beta} M_s^{jj'}(t) \sum_{k,k'=-1}^{1} (1 - \delta_{k0}\delta_{k'0})$$

$$\times d_1^{jk}(\alpha) d_1^{j'k'}(\alpha) \overline{m}^{(k)} \overline{m}^{(k')} C_{s1}^{kk'}(t) , \tag{4.8}$$

where $\delta_{kk'}$ is the Kronecker delta, $d_l^{jj'}$ is defined by Eq. (2.7) and $M^{jj'}$, $M_s^{jj'}$, and $C_{s1}^{jj'}$ are correlation functions defined by

$$M^{jj'}(t) = (8\pi^2)^N \sum_{p,p'=1}^{N} C_{1,[p,p']}^{(j,j')}(t) , \tag{4.9}$$

$$M_s^{jj'}(t) = (8\pi^2)^N \sum_{p=1}^{N} C_{1,[p,p]}^{(j,j')}(t) , \tag{4.10}$$

$$C_{s1}^{jj'}(t) = \langle \exp[-ij\gamma_p(0)] \exp[ij'\gamma_p(t)] \rangle_{eq} . \tag{4.11}$$

In Eqs. (4.9) and (4.10), $C_{1,[p,p']}^{(j,j')}$ is the (1, 1)-body standard correlation function defined in Chap. 3 with the "total angular momentum quantum number" $L = 1$.

We first consider $M^{jj'}(t)$ and $M_s^{jj'}(t)$. Taking the sums in Eqs. (4.9) and (4.10) by the use of Eq. (3.62) for $C_{1,[p,p']}^{(j,j')}$ (for $\kappa_0 \neq 0$), we find

$$M^{jj'}(t) = 2(N+1)^{-1} \sum_{k \text{ odd}} \cot^2[k\pi/2(N+1)]$$

$$\times \sum_{j''=-1}^{1} R_{1,k}^{j''j*} R_{1,k}^{j''j'} \exp(-\lambda_{1,k}^{j''} t) , \tag{4.12}$$

$$M_s^{jj'}(t) = \sum_{k=1}^{N} \sum_{j''=-1}^{1} R_{1,k}^{j''j*} R_{1,k}^{j''j'} \exp(-\lambda_{1,k}^{j''} t) \tag{4.13}$$

with

$$R_{1,k}^{jj'} = (8\pi^2)^{N/2} \sum_{m=-1}^{1} Q_{1,k}^{L,mj*} (\overline{E}_{1,[k,k]}^{(m,m)})^{1/2} \overline{\mathscr{D}}_1^{j'm*}(\Omega_a) , \tag{4.14}$$

where $\lambda_{1,k}^{j}$ are the eigenvalues given by Eqs. (3A.5), $Q_{1,k}^{Ljj'}$ are the j, j' elements of the unitary diagonalizing matrix $Q_{1(1),[k]}^{L}$ in Eq. (3.60), $\overline{E}_{1,[k,k]}^{(j,j)}$ are the diagonal elements of the standard representation $\overline{E}_{1(1),[k]}$ of the identity operator in Eq. (3.58), and $\overline{\mathscr{D}}_1^{jj'}(\Omega_a)$ is the unnormalized Wigner function defined by Eq. (2.11) with Ω_a given by Eq. (2.12). Recalling that $\overline{E}_{1,[k,k]}^{(j,j)}$ and the jth column vector $\mathbf{v}_{1,k}^{j}$ of $Q_{1(1),[k]}^{L}$ with $\mathbf{v}_{1,k}^{j\,T} \equiv (a_j, ib_j, a_j)$ are given by Eq. (3.50) and (3A.7), respectively, and writing $\overline{\mathscr{D}}_1^{jj'}(\Omega_a)$ explicitly in terms of κ_0 and τ_0, we obtain for $R_{1,k}^{jj'}$:

$$R_{1,k}^{j(-1)} = R_{1,k}^{j1} = \tau_0 \nu^{-1} (S_{1,kk}^{(0)1})^{1/2} a_j + \frac{1}{\sqrt{2}} \kappa_0 \nu^{-1} (S_{1,kk}^{(0)0})^{1/2} b_j \quad (j = 0, -1) ,$$

$$R_{1,k}^{j0} = i[\sqrt{2}\,\kappa_0 \nu^{-1} (S_{1,kk}^{(0)1})^{1/2} a_j - \tau_0 \nu^{-1} (S_{1,kk}^{(0)0})^{1/2} b_j] \quad (j = 0, -1) , \tag{4.15}$$

$$R_{1,k}^{1(-1)} = -R_{1,k}^{11} = \frac{1}{\sqrt{2}} (S_{1,kk}^{(0)1})^{1/2} , \quad R_{1,k}^{10} = 0 ,$$

where $S_{1,kk}^{(0)j}$ $(j = 0, 1)$ are given by Eq. (3.54), and ν is given by

Eq. (2.19).

For the KP chain ($\kappa_0 = 0$), $C_{1,[p,p']}^{(j,j')}$ is given by Eq. (3.63), so that Eqs. (4.14) and (4.15) become

$$R_{1,k}^{jj'} = \delta_{jj'}(8\pi^2)^{N/2}(\overline{E}_{1,[k,k]}^{(j,j)})^{1/2}$$

$$= \delta_{jj'}(S_{1,kk}^{(0)j})^{1/2} , \qquad \text{(KP)} , \tag{4.16}$$

and the eigenvalues $\lambda_{1,k}^{j}$ are given by Eq. (3.65). When $\sigma \neq 0$, we must use the expression for $g_L^{jj'}(s)$ derived by Yamakawa and Shimada,[20] i. e.,

$$g_L^{jj'}(s) = \delta_{jj'}\exp\{-[L(L+1) + ij\tau_0 + \sigma j^2]s\} , \quad \text{(KP)} , \tag{4.17}$$

instead of Eq, (3.42) (with $\sigma = 0$). The final results for the KP chain with $\sigma \neq 0$ may then be obtained from those with $\sigma = 0$ only if $L(L+1)$ is replaced by $L(L+1) + \sigma j^2$ in the quantities $S_{L,kk}^{(n)j}$ given by Eqs. (3.54) and (3.55).

Next we consider the correlation function $C_{s1}^{jj'}(t)$. This is associated with the rotational motion of the dipole moment vector about the rotation axis, and no information about it is contained in the present model. However, since it has been assumed to be independent of other motions, it may be regarded as equivalent to that of a single-axis rotor. Whether its relaxation is due to stochastic diffusion among a very large number of equilibrium positions[4.21] or to random jumps between two or three equivalent equilibrium positions to either of the two adjacent ones,[21,22] $C_{s1}^{jj'}(t)$ may then be written in the form

$$C_{s1}^{jj'}(t) = \delta_{jj'}\,, \qquad \text{for } j = 0$$

$$= \delta_{jj'}e^{-t/\tau_{s1}}\,, \qquad \text{for } j = \pm 1 \tag{4.18}$$

with τ_{s1} the corresponding correlation time. Note that the jump rate is equal to $(n\tau_{s1})^{-1}$ for the n-state jump process ($n = 2, 3$).

If we substitute Eq. (4.18) into Eq. (4.8) and write $M(t)$ explicitly in terms of trigonometric functions, we obtain

$$\begin{aligned} M(t) = {} & m^2\cos^2\Delta\,[\cos^2\alpha\; M^{00}(t) + \sin^2\alpha\; M^{11}(t) \\ & - \sin^2\alpha\,\cos 2\beta\; M^{1(-1)}(t) + \sqrt{2}\,i\,\sin 2\alpha\,\sin\beta\; M^{10}(t)] \\ & + \tfrac{1}{2}m^2\sin^2\Delta\; e^{-t/\tau_{s1}}[\sin^2\alpha\; M_s^{00}(t) + (1 + \cos^2\alpha)M_s^{11}(t) \\ & + \sin^2\alpha\,\cos 2\beta\; M_s^{1(-1)}(t) - \sqrt{2}\,i\,\sin 2\alpha\,\sin\beta\; M_s^{10}(t)]\,, \end{aligned} \tag{4.19}$$

where we have used the relations $M^{(-1)(-1)} = M^{11}$, $M^{(-1)1} = M^{1(-1)}$, and $M^{(-1)0} = -M^{0(-1)} = -M^{01} = M^{10}$ and also similar relations for $M_s^{jj'}$. When the dipole moment vectors are affixed rigidly to the subbodies ($\Delta = 0$), $M(t)$ may be written in terms of $M^{00}(t)$ if $\mathbf{m}_p$ is parallel to $\mathbf{e}_{\xi_p}$ ($\alpha = 0$), in terms of $M^{11}(t)$ and $M^{1(-1)}(t)$ if $\mathbf{m}_p$ is perpendicular to $\mathbf{e}_{\xi_p}$ ($\alpha = \pi/2$), and in terms of $\Delta M(t) \equiv M^{11}(t) - M^{1(-1)}(t)$ if $\mathbf{m}_p$ is parallel to $\mathbf{e}_{\xi_p}$ ($\alpha = \pi/2$ and $\beta = 0$ or π).

Substitution of Eqs. (4.12) and (4.13) with Eq. (4.15) into Eq. (4.19) leads to

$$\begin{aligned} M(t) = {} & 2(N+1)^{-1}m^2\cos^2\Delta \sum_{k\ \text{odd}} \cot^2[k\pi/2(N+1)] \sum_{j=-1}^{1} A_{1,k}^{j}\exp(-\lambda_{1,k}^{j}t) \\ & + \frac{1}{2}m^2\sin^2\Delta \sum_{k=1}^{N}\sum_{j=-1}^{1} A_{s1,k}^{j}\exp[-(\lambda_{1,k}^{j} + \tau_{s1}^{-1})t]\,, \end{aligned} \tag{4.20}$$

where the coefficients $A^j_{1,k}$ and $A^j_{s1,k}$ are real and nonnegative, and given by

$$A^j_{1,k} = (\sqrt{2}\sin\alpha\,\sin\beta\; R^{j1}_{1,k} + i\cos\alpha\; R^{j0}_{1,k})^2\,, \quad \text{for } j = 0, -1$$
$$= \sin^2\alpha\,\cos^2\beta\; S^{(0)1}_{1,kk}\,, \quad \text{for } j = 1\,, \tag{4.21}$$

$$A^j_{s1,k} = (\sqrt{2}\cos\alpha\,\sin\beta\; R^{j1}_{1,k} - i\sin\alpha\; R^{j0}_{1,k})^2 + 2\cos^2\beta\,(R^{j1}_{1,k})^2\,, \quad \text{for } j = 0, -1$$
$$= (\sin^2\beta + \cos^2\alpha\,\cos^2\beta)S^{(0)1}_{1,kk}\,, \quad \text{for } j = 1\,. \tag{4.22}$$

For the case of $\Delta = 0$, we note that if $\mathbf{m}_p$ is parallel to $\mathbf{e}_{\zeta_p}$ ($\alpha = 0$), then $A^1_{1,k} = 0$, and therefore the $j = 0$ and -1 branches of the eigenvalue spectrum make contribution to dielectric relaxation, and also that if $\mathbf{m}_p$ is parallel to $\mathbf{e}_{\xi_p}$ ($\alpha = \pi/2$ and $\beta = 0$ or π), then only the $j = 1$ branch makes contribution.

For the KP chain, there is degeneracy such that $\lambda^1_{1,k} = \lambda^{-1}_{1,k}$, as shown in Eq. (3.65). Therefore, if the second line of Eqs. (4.16) instead of Eqs. (4.15) is used, then Eqs. (4.21) and (4.22) become

$$A^j_{1,k} = \frac{1}{2}[1 + (-1)^j\cos 2\alpha]\,S^{(0)j}_{1,kk}\,, \quad \text{for } j = 0, 1$$
$$= 0\,, \quad \text{for } j = -1, \quad \text{(KP)}\,, \tag{4.23}$$

$$A^j_{s1,k} = (\sin^2\alpha + 2j\cos^2\alpha)S^{(0)j}_{1,kk}\,, \quad \text{for } j = 0, 1$$
$$= 0, \quad \text{for} j = -1\,, \quad \text{(KP)}\,. \tag{4.24}$$

When $\Delta = 0$, only the $j = 0$ or 1 branch is seen to make contribution if $\mathbf{m}_p$ is parallel or perpendicular to $\mathbf{e}_{\zeta_p}$.

Finally, if we substitute Eq. (4.20) into Eq (4.1) and perform the integration over t, we obtain

$$\frac{\varepsilon^* - \varepsilon_\infty}{\varepsilon_0 - \varepsilon_\infty} = \frac{m^2}{M(0)}\left\{\frac{2\cos^2\Delta}{N+1}\sum_{k\ \mathrm{odd}}\sum_{j=-1}^{1}\cot^2\left[\frac{k\pi}{2(N+1)}\right]\frac{A^j_{1,k}}{1+i\omega\tau^j_{1,k}}\right.$$

$$\left. + \frac{1}{2}\sin^2\Delta\sum_{k=1}^{N}\sum_{j=-1}^{1}\frac{A^j_{s1,k}}{1+i\omega\tau^j_{s1,k}}\right\}, \tag{4.25}$$

where

$$\tau^j_{1,k} = (\lambda^j_{1,k})^{-1}, \tag{4.26}$$

$$\tau^j_{s1,k} = (\lambda^j_{1,k} + \tau_{s1}^{-1})^{-1}, \tag{4.27}$$

and $M(0)$ is given by Eq. (4.20) with $t = 0$. We note that although $M(0) = <\mu^2>_{eq}$ as seen from Eq. (4.2), this $M(0)$ does not exactly agree with $<\mu^2>_{eq}$ for the continuous chain[19] because of its replacement by the discrete chain and also of the block-diagonal approximation introduced in Chap. 3. The final results in this form is seen, from Eq. (4.25), not to depend on the magnitude m of the dipole moment vector but on its orientation in the localized coordinate system, and can also be seen to be independent of the sign of the model parameter τ_0 for $\alpha = 0$ or $\pi/2$. However, it is more important to see that the eigenvalues with small k make the main contribution because of the factor $\cot^2[k\pi/2(N+1)]$ as far as the main chain motion is concerned.

4-3. Eigenvalue Spectra

Now, we examine the behavior of the three dielectric ($j = 0, \pm 1$) branches of the spectrum in detail, especially their mode

character and dependences on chain length at small wave number k. The mode analysis can be made by the use of the eigenfunctions corresponding to $\lambda^j_{l,k}$.

Before proceeding to the analysis, some remarks must be made on the model parameters. We introduce as in Chap. 3 the dimensionless parameter r_1 and r_2 defined by Eqs. (3.67) and (3.68), respectively. Further, it is convenient to use instead of Δs the number n_b of skeletal bonds of a given real chain (except DNA) corresponding to one subbody of the discrete HW chain. We may relate the unreduced Δs to n_b by the equation

$$\Delta s = (M_b/M_L)n_b \ , \tag{4.28}$$

where M_L is the well-known shift factor as defined as the molecular weight per unit (unreduced) contour length of the HW chain, and M_b is the molecular weight per bond, i. e., the molecular weight of the monomer unit divided by the number of skeletal bonds in it. In the case of DNA, it is convenient to let n_b be the number of base pairs in one subbody. As for the model parameters κ_0, τ_0, λ^{-1}, and M_L, we adopt the ones determined recently by Fujii et al.[23] and listed in Table I of Ref. 23. We consider flexible chains ($\kappa_0 \neq 0$) and KP stiff chains ($\kappa_0 = 0$). Note that in general, for stiff chains, λ^{-1} is large, and therefore the reduced Δs is very small. All numerical work has been done by the use of a FACOM M-382 digital computer in this university.

a. Flexible chains

We take as examples of flexible chains ($\kappa_0 \neq 0$) syndiotactic polystyrene (s–PS; $\kappa_0 = 0.8$ and $\tau_0 = 2.3$) and syndiotactic poly(methyl methacrylate) (s–PMMA; $\kappa_0 = 4.4$ and $\tau_0 = 0.8$). Figure 4.2 shows plots of the reduced eigenvalues $\tilde{\lambda}^j_{1,k} \equiv \zeta_r \lambda^j_{1,k}/k_B T = 3\pi\eta_0 a^3 r_1 r_2 \lambda^j_{1,k}/k_B T$ (with $\lambda^j_{1,k}$ and a unreduced) against the reduced wave number $\tilde{k} \equiv k/(N+1)$ for s–PS (full curves) with $n_b = 2$, $N = 999$, $r_1 = 1$, and $r_2 = 80$ and for s–PMMA (broken curves) with

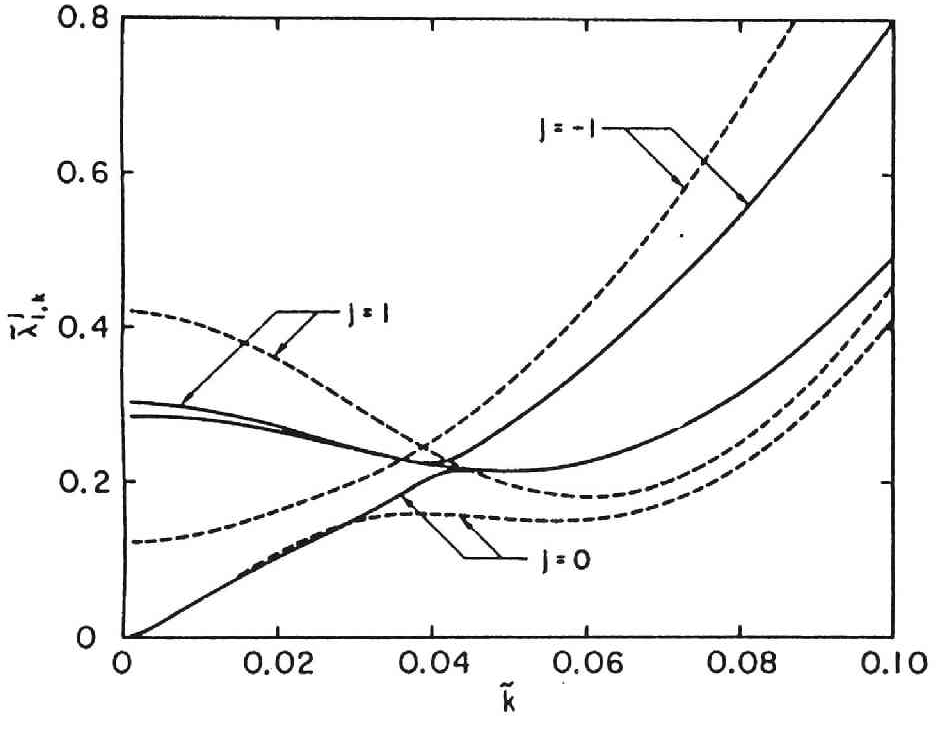

Fig. 4.2. The reduced eigenvalues $\tilde{\lambda}^j_{1,k}$ plotted against the reduced wave number $\tilde{k}$ for syndiotactic polystyrene (full curves) with n_b=2, N=999, r_1=1, and r_2=80 and for syndiotactic poly(methyl methacrylate) (broken curves) with n_b=2, N=999, r_1=1, and r_2=20.

$n_b = 2$, $N = 999$, $r_1 = 1$, and $r_2 = 20$. We have neglected the small intercept $\tilde{\lambda}^0_{1,0}$ of the lowest ($j = 0$) branch [given by Eq. (3.74)] to make $\tilde{\lambda}^0_{1,k}$ start just from zero at $\tilde{k} = 0$, and thus plotted the corrected values $\tilde{\lambda}^j_{1,k} - \tilde{\lambda}^0_{1,0}$. This correction is made throughout the remainder of this chapter. An avoided crossing between the $j = 0$ and -1 branches is seen to occur at $\tilde{k} \simeq 0.04$ for s-PS and at $\tilde{k} \simeq 0.02$ for s-PMMA.

It is important to see that the avoided crossing is remarkable for s-PS but not, or weak, for s-PMMA. In general, it is remarkable for monosubstituted syndiotactic chains which are close to s-PS in the model parameters κ_0 and τ_0, and also for chains such as monosubstituted isotactic chains having relatively large τ_0/κ_0 (see Table I and Fig. 10 of Ref. 23). On the other hand, it is weak for chains such as s-PMMA having relatively small τ_0/κ_0. Disubstituted isotactic chains are intermediate.

Now we examine the change of the mode character of each branch of the dielectric spectrum as $\tilde{k}$ is changed across the avoided crossing between the $j = 0$ and -1 branches. This can be done by using the eigenfunctions corresponding to the $L = 1$ eigenvalues $\lambda^j_{1,k}$, which we designate by $\psi^{M,j}_{1,[k]}$ with M ($= 0, \pm 1$) the "total magnetic quantum number." As shown in the Appendix 4-A, they may be written (for $\kappa_0 \neq 0$) in the form

$$
\begin{aligned}
\psi^{M,j}_{1,[k]} &= \sqrt{2}\, i\,[\, c^j_1(k) q^{\eta}_{k,z} + c^j_2(k) q^{\xi}_{k,z}\,] \ , \quad \text{for } M = 0 \\
&= c^j_1(k)(\mp i q^{\eta}_{k,x} + q^{\eta}_{k,y}) \qquad\qquad\qquad\qquad (j = 0, -1) \\
&\quad + c^j_2(k)(\mp i q^{\xi}_{k,x} + q^{\xi}_{k,y}) \qquad \text{for } M = \pm 1 \ , \qquad\qquad (4.29) \\
\psi^{M,j}_{1,[k]} &= \sqrt{2}\, c^1_1(k) q^{\xi}_{k,z} \ , \qquad\qquad \text{for } M = 0 \\
&= c^1_1(k)(\mp q^{\xi}_{k,x} - i q^{\xi h}_{k,y}) \ , \qquad \text{for } M = \pm 1 \ , \qquad (j = 1)
\end{aligned}
$$

where $c^j_1(k)$ and $c^j_2(k)$ are real coefficients given as functions of k by Eqs. (4A.6), and $q^{\xi}_{k,i}$ $(i = x, y, z)$ and so on are the components of vectors $\mathbf{q}^{\xi}_k$ and so on in the external coordinate system, which are given by

$$
\mathbf{q}^{\xi}_k = \sum_{p=1}^{N} Q^0_{pk} \mathbf{e}_{\xi_p} \ , \qquad (4.30)
$$

and similar equations for $\mathbf{q}^{\eta}_k$ and $\mathbf{q}^{\zeta}_k$ with Q^0_{pk} the orthogonal symmetric matrix defined by Eq. (3.43). Since $a\mathbf{e}_{\zeta_p}$ is the pth bond vector, $a\mathbf{q}^{\zeta}_k$ are just the Rouse global, vector (normal) modes. On the other hand, $\mathbf{e}_{\xi_p}$ and $\mathbf{e}_{\eta_p}$ are perpendicular to the bond vector and therefore $\mathbf{q}^{\xi}_k$ and $\mathbf{q}^{\eta}_k$ may be regarded as representing local, vector (although not normal) modes. Thus Eqs. (4.29) indicate that the $L = 1$ eigenfunctions may be written as linear combinations of the global and local vector modes.

Specifically, however, $\psi^{M,1}_{1,[k]}$ may be written in terms of only $\mathbf{q}^{\xi}_k$, so that the $j = 1$ branch is of the purely local nature, while there is a mixing of global and local modes in each of the $j = 0$ and -1 branches. Then the fractions $x^j_{\mathrm{glob}}(k)$ and $x^j_{\mathrm{loc}}(k)$ of global and local mode contributions to the j $(= 0$ or $-1)$ branch may

be expressed conveniently as

$$x^j_{loc} = (c^j_1)^2/[(c^j_1)^2 + (c^j_2)^2] \qquad (j = 0, -1) \tag{4.31}$$

with $x^j_{glob} = 1 - x^j_{loc}$. Figure 4.3 shows plots of x^j_{loc} $(j = 0, -1)$ against the reduced wave number $\tilde{k}$ for s-PS (full curves) and s-PMMA (broken curves) with the same respective model parameters as in Fig. 4.2. It is seen that at small $\tilde{k}$, for both polymers, x^0_{loc} is very small and x^{-1}_{loc} is close to unity, so that there the $j = 0$ branch is mainly global, while the $j = -1$ branch is mainly local.

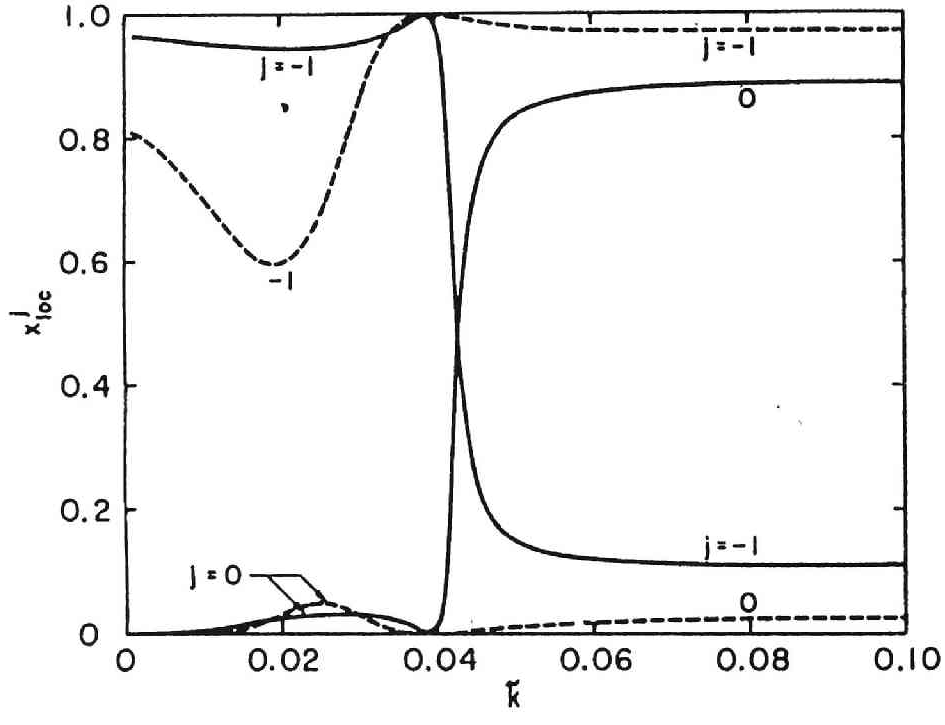

Fig. 4.3. The local mode fractions x^j_{loc} in the j=0 and −1 branches plotted against the reduced wave number $\tilde{k}$ for syndiotactic polystyrene (full curves) and syndiotactic poly(methyl methacrylate) (broken curves) with the same respective model parameters as in Fig. 4.2.

Recall that in Chap. 3, we have regarded the $\tau^0_{1,k}$ given by Eq. (4.26) with small k as the Rouse–Zimm dielectric relaxation times.[8] Further, in the case of s–PS, for which the avoided crossing is remarkable, the global and local mode contributions to each branch are seen to be reversed at $\tilde{k} \simeq 0.04$ at which it occurs. This is consistent with the conjecture of Fixman and Evans.[17] For s–PMMA, however, such reversal does not occur, although there is a weak interaction between global and local modes at $\tilde{k} \simeq 0.02$ at which the weak avoided crossing occurs.

Next we examine the dependence on N of the eigenvalues. Figure 4.4 shows plots of the reduced eigenvalues $\tilde{\lambda}^j_{1,k}$ ($j = 0, -1$) against the reduced wave number $\tilde{k}$ for s–PS with $n_b = 2$, $r_1 = 1$, and $r_2 = 80$. The full curve represent the values for $N = 999$ as in Fig. 4.2, and the broken and dotted line segments connect the values for $N = 99$ and 49, respectively. The open circles at $\tilde{k} = 0.001$, 0.01, and 0.02 represent the values of $\tilde{\lambda}^0_{1,1}$ and $\tilde{\lambda}^{-1}_{1,1}$, i. e., the end values for $N = 999$, 99, and 49, respectively. As seen from Fig. 4.2, the $j = 1$ branch is very close to the $j = -1$ branch for $\tilde{k} \lesssim 0.04$ and to the $j = 0$ branch for $\tilde{k} \gtrsim 0.04$, and therefore it has been omitted. From Fig. 4.4, the shape of the spectra is seen to be not strongly depend on N. However, it is interesting to see that $\lambda^1_{1,1}$ and also $\lambda^{-1}_{1,1}$ are almost independent of N ($\gtrsim 50$), while $\lambda^0_{1,1}$ decreases to zero with increasing N. The results seem reasonable since $\lambda^0_{1,1}$ and $\lambda^{\pm 1}_{1,1}$ are essentially the relaxation rates

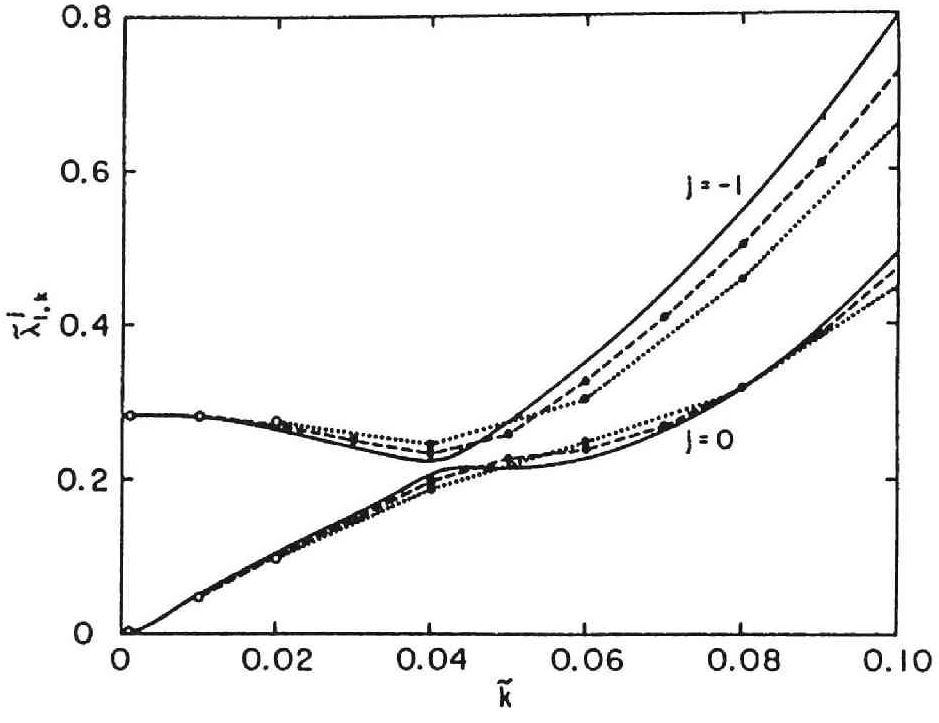

Fig. 4.4. The reduced eigenvalues $\tilde{\lambda}^{j}_{1,k}$ plotted against the reduced wave number $\tilde{k}$ for syndiotactic polystyrene with $n_b=2$, $r_1=1$, and $r_2=80$. The full curve represents the values for $N=999$, and the broken and dotted line segments connect the values for $N=99$ and 49, respectively. The open circles represent the values of $\tilde{\lambda}^{j}_{1,1}$.

associated with the global and local motions, respectively. A further discussion is deferred to Sec. 4–5*a*.

b. Stiff chains

All typical stiff chains such as DNA have complete helical structures, and may be represented by the KP1 chain ($\kappa_0 = 0$ and

$\tau_0 \neq 0$),[24] whose contour is taken along the helix axis. Because of a structural symmetry about it (the ζ axis), the local dipole moment vectors $\mathbf{m}_p$ may be regarded as parallel to it; i. e., $a = \Delta = 0$. As noted in Sec. 4–2, the dielectric relaxation may then be written in terms of only the eigenvalues $\lambda^0_{1,k}$ in the $j = 0$ branch unless the side chain motion exists. As seen from Eqs. (4A.7) in the Appendix 4–A, for the KP chain, the eigenfunctions $\psi^{M,0}_{1,\{k\}}$ corresponding to $\lambda^0_{1,k}$ may be written in terms of only $\mathbf{q}^\zeta_k$, so that the $j = 0$ branch is purely global. Furthermore, it can easily be seen, from Eq. (4.12) and the succeeding development for the KP chain with Poisson's ratio $\sigma \neq 0$, that the dielectric relaxation of such stiff chains is independent of τ_0 and σ.

Thus we examine the behavior of the $j = 0$ branch, taking DNA ($\kappa_0 = 0$ and $\tau_0 = 200$) as an example. As mentioned in Sec. 3–5*b*, even if $\lambda^0_{1,0}$ is subtracted, the first two corrected eigenvalues $\lambda^0_{1,1}$ and $\lambda^0_{1,2}$ are still negative, although very small in magnitude, for $n_b = 1$ ($\Delta s = 0.0031$), $N = 199$, $r_1 = 1$, and $\rho_2 = 50$. (Recall that this arises from the preaveraging approximation.) It is therefore important to find those ranges of n_b and r_2 over which the negative eigenvalues can be removed. Figure 4.5 shows plots of the reduced eigenvalues $\tilde{\lambda}^0_{1,k}$ against the reduced wave number $\tilde{k}$ for DNA with $N = 199$ and $r_1 = 1$ for various values of n_b and r_2. Note that the points connected by the dotted line segment are just the results obtained previously and that $n_b = 10$ corresponds

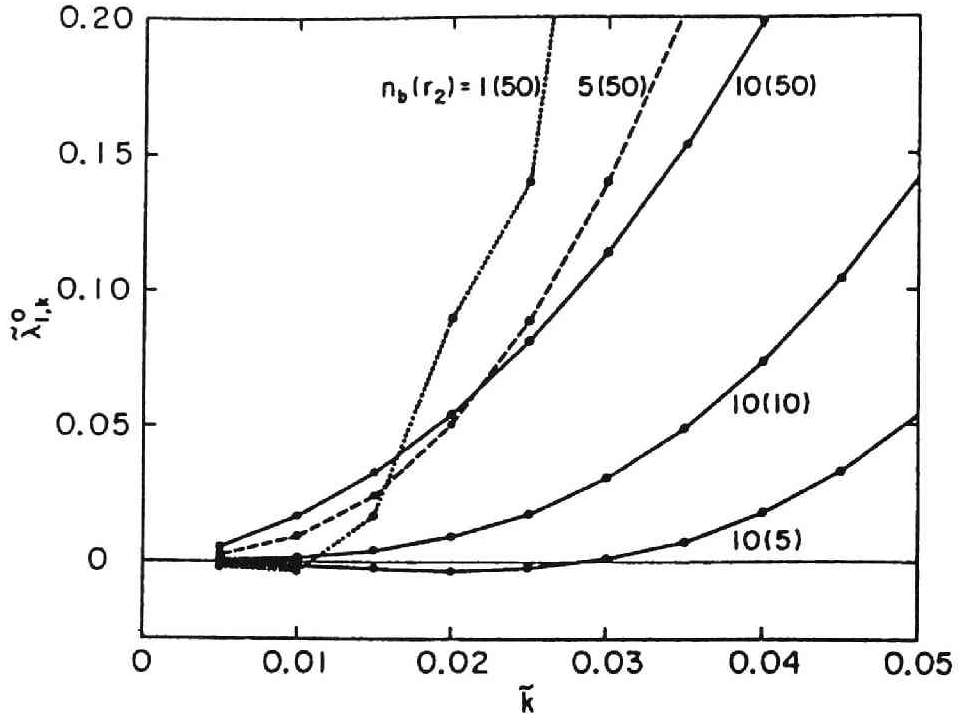

Fig. 4.5. The reduced eigenvalues $\tilde{\lambda}^0_{1,k}$ plotted against the reduced wave number $\tilde{k}$ for DNA with N=199 and r_1=1, for the indicated value of n_b and r_2 as $n_b(r_2)$.

nearly to one turn of the double helix. It is seen that all eigenvalues are safely positive for $n_b \gtrsim 5$ at $r_2 = 50$ or for $r_2 \gtrsim 10$ at $n_b = 10$. In any case, n_b must be chosen to be relatively large. It is clear that such a choice is permitted in the case of dielectric relaxation associated with the global motion, although Δs must be chosen to be close to the distance between base pairs in the case of nuclear magnetic relaxation and fluorescence depolarization associated with the local motion or torsion dynamics.

As in the case of s-PS shown in Fig. 4.4, the shape of the spectra in Fig. 4.5 except for the case of $n_b = 1$ and $r_2 = 50$ (dotted line) is almost independent of N, and $\lambda^0_{1,1}$ decreases to zero with increasing N provided that all eigenvalues $\lambda^0_{1,k}$ are positive. A further analysis of the N dependence is deferred to Sec. 4-5*b*.

4-4. Correlation Functions

In this section, we examine the decay behavior of the dipole correlation function $M(t)$ for both flexible chains ($\kappa_0 \neq 0$) and stiff chains ($\kappa_0 = 0$). In general, it is governed not only by the eigenvalues but also by the amplitudes, especially for the former.

a. Flexible chains

We begin by making some general remarks. If side chain motions do not exist ($\Delta = 0^\circ$) and if the dipole moment vector $\mathbf{m}_p$ is parallel to $\mathbf{e}_{\xi_p}$ ($\alpha = 90^\circ$ and $\beta = 0^\circ$ or 180°), then the dipole correlation function $M(t)$ given by Eq. (4.20) with Eqs. (4.21) and (4.22) may be written in terms of the eigenvalues $\lambda^1_{1,k}$ in the $j = 1$ branch with small k, which are there almost independent of k (see Fig. 4.2), and therefore it obeys a single exponential decay low. On the other hand, if two or three branches make contribution, or if the $j = 0$ branch makes always contribution, then $M(t)$ may

be written in terms of two or more different eigenvalues, and therefore does not obey the single exponential law irrespective of the value of Δ. This is always the case with chains with side chain motions ($\Delta \neq 0^\circ$). Thus the behavior of $M(t)$ in general depends strongly on the orientation (α, β) of the dipole moment vector with respect to the localized coordinate system and on the degree (Δ) of side chain motion through the amplitudes. We must therefore consider the choice of α, β, and Δ for a given polymer. For convenience, they are determined for the case of the smallest possible subbody ($n_b = 2$), and the same values are assumed for the case of larger subbodies ($n_b = 4$ or 6). (Recall that $n_b \geq 2$ since, otherwise, the HW chain cannot mimic the real chain.)

We first take poly(oxyethylene) (POE; $\kappa_0 = 2.4$ and $\tau_0 = 0.5$) as an example of symmetric chains. The local dipole moment vector arising from the C–O and O–C bonds is in the negative direction of the ξ axis if the localized coordinate system corresponding to that of the HW chain is affixed to the rigid body part composed of the successive C–O and O–C bonds in its monomer unit, which is composed of three skeletal bonds, as done by Fujii et al.[23] Therefore we choose $\alpha = 90^\circ$, $\beta = 180^\circ$, and $\Delta = 0^\circ$ for POE irrespective of the value of n_b (≥ 2).

For monosubstituted and disubstituted asymmetric chains, we take the monomer unit composed of the successive C–C$^\alpha$ and C$^\alpha$–C bonds as the subbody with $n_b = 2$ and affix the localized

coordinate system in such a way as mentioned by Yamakawa et al.[20,23] [For PMMA, e. g., see case (i) of Fig. 9 of Ref. 20.] Since the ζ axis is parallel to the resultant vector of the two successive bond vectors $C \rightarrow C^{\alpha}$ and $C^{\alpha} \rightarrow C$, the local dipole moment vector arising from the side group attached to the α carbon is perpendicular to the ζ axis or permitted to rotate about an axis perpendicular to the ζ axis, so that $\alpha = 90^{\circ}$. In order to determine β, it is necessary to specify the angle $\hat{\psi}$ between the ξ axis and the plane containing the $C-C^{\alpha}$ and $C^{\alpha}-C$ bonds. We choose $\hat{\psi} = 270^{\circ}$ and 0° for monosubstituted isotactic and syndiotactic chains, respectively, and $\hat{\psi} = 180^{\circ}$ for both disubstituted isotactic and syndiotactic chains.[23] Then, if all bond angles are assumed to be equal to 110°, we have $\beta = 145^{\circ}$ and 325° for monosubstituted isotactic chains, $\beta = \pm 55^{\circ}$ (or $\pm 125^{\circ}$) alternately for monosubstituted syndiotactic chains, $\beta = \pm 55^{\circ}$ or $\pm 125^{\circ}$ for disubstituted isotactic chains, and $\beta = \pm 55^{\circ}$ (or $\pm 125^{\circ}$) alternately for disubstituted syndiotactic chains. Thus the direction of the local dipole moment vector changes alternately along the chain for syndiotactic chains. For the present discrete HW chain, however, β must be independent of the subbody number p since $\mathbf{m}_p$ is assumed so. Therefore, for both monosubstituted and disubstituted syndiotactic chains, we choose $\mathbf{m}_p$ to be the average of the two successive local dipole moment vectors (of the real chain); i. e., $\beta = 0^{\circ}$ or 180°.

The asymmetric chains (with $\alpha = 90^\circ$) we consider in this chapter are the following: isotactic poly(p-halostyrene) with $\beta = 325^\circ$, syndiotactic poly(p-halostyrene) with $\beta = 180^\circ$, syndiotactic poly(methyl acrylate) (s-PMA) with $\beta = 180^\circ$, syndiotactic poly(methyl vinyl ketone) (s-PMVK) with $\beta = 180^\circ$, syndiotactic poly(vinyl acetate) (s-PVAc) with $\beta = 0^\circ$, and syndiotactic poly(vinyl halide) with $\beta = 180^\circ$ as monosubstituted chains; and i-PMMA with $\beta = 55^\circ$ (or -55°) and s-PMMA with $\beta = 180^\circ$ as disubstituted chains. For these polymers except s-PMVK,[25] side chain motions have not been observed in dielectric relaxation experiments, so that we choose $\Delta = 0^\circ$ except for it. [Note that in fact $\Delta = 0^\circ$ for poly(p-halostyrene) and poly(vinyl halide).] Further, we assume that isotactic and syndiotactic poly(p-halostyrene)s have the same model parameters κ_0, τ_0, and λ^{-1} as isotactic polystyrene (i-PS) and s-PS, respectively, and identify the former with the latter in this section.

Now we can examine the behavior of $M(t)$. Figure 4.6 shows plots of the natural logarithm of the normalized dipole correlation function $M(t)/M(0)$ against t for i-PS ($\kappa_0 = 11$ and $\tau_0 = 15$) and s-PS with $r_2 = 80$ (full curves), i-PMMA ($\kappa_0 = 1.7$ and $\tau_0 = 1.4$) and s-PMMA with $r_2 = 20$ (broken curves), and s-PMVK ($\kappa_0 = 0.1$ and $\tau_0 = 2.0$) with $r_2 = 10$ and the indicated values of Δ and with $k_B T \tau_{s1}/\zeta_r = 0.5$ ($\simeq 1/20\tilde{\lambda}^1_{1,1}$) (chain curves), all with $n_b = 2$, $N = 999$, and $r_1 = 1$, where $M(t)$ has been computed at $T = 300$ K and

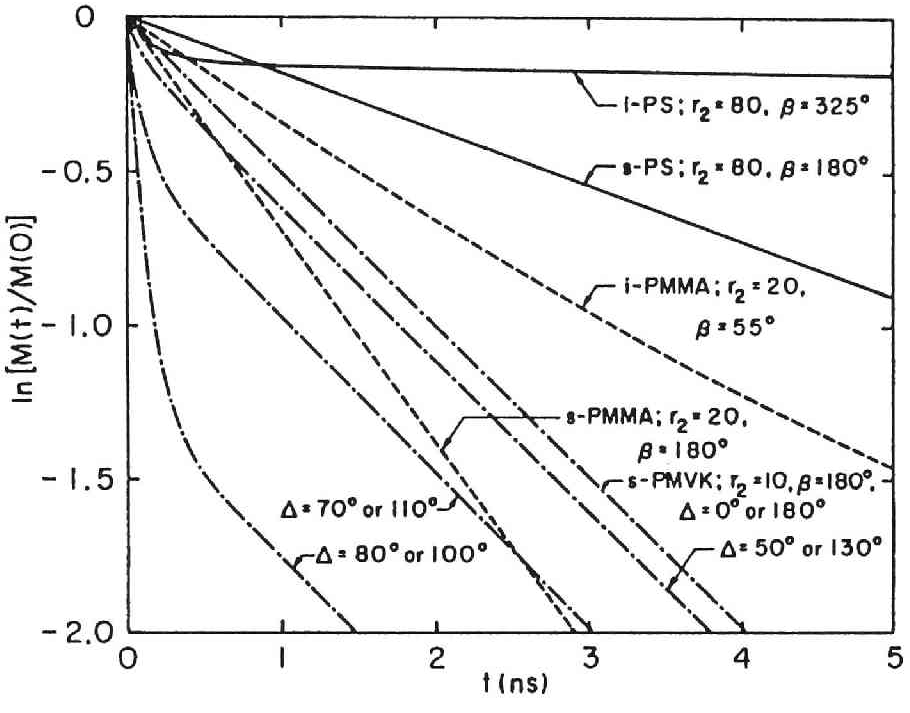

Fig. 4.6. The natural logarithm of the normalized dipole correlation function $M(t)/M(0)$ plotted against t for various flexible chains, all with $n_b=2$, $N=999$, $r_1=1$, and $\alpha=90^\circ$, at $T=300$ K and $\eta_0=0.006$ P, s-PMVK with side chain motions ($\Delta\neq 0^\circ$) having $k_BT\tau_{s1}/\zeta_r=0.5$.

η_0 = 0.006 P (corresponding to benzene). (The model parameters κ_0 and τ_0 of s-PS and s-PMMA are the same as those in Fig. 4.2.)

For the syndiotactic chains (s-PS, s-PMMA, and s-PMVK with $\Delta = 0^\circ$) without side chain motions, it is seen that $M(t)$ obeys the single exponential law, as expected from the general remarks at the beginning of this subsection. For the isotactic chains (i-PS and i-PMMA) without side chain motions, all the branches of the

eigenvalue spectrum make contributions, and therefore it is necessary to examine the amplitudes in each branch in order to understand the behavior of $M(t)$. In the case of i-PS, the contributions of $\lambda_{1,1}^{0}$, $\lambda_{1,1}^{1}$, and $\lambda_{1,1}^{-1}$ to the relaxation have been found to be 71 %, 6 %, and 5 %, respectively. That is, the contribution of the $j = 0$ branch (global motion) is large despite the fact that i-PS has perpendicular dipoles ($\alpha = 90^{\circ}$), and thus the decay of its $M(t)$ is very slow in comparison with other polymers. This may be regarded as arising from the fact that for monosubstituted isotactic chains such as i-PS having large κ_0 and τ_0, there exist locally rather tight helices (of small radius),[20] which give rise to the parallel components of the local dipole moment vectors along the helix axis with the cancellation of the perpendicular components. On the other hand, in the case of i-PMMA, the contributions of $\lambda_{1,1}^{0}$, $\lambda_{1,1}^{1}$, and $\lambda_{1,1}^{-1}$ are 7 %, 18 %, and 56 %, respectively, the $j = \pm 1$ branches (local motion) making main contribution, and moreover the eigenvalues in these two branches are almost independent of k for small k. Therefore its $M(t)$ obeys nearly the single exponential law. For s-PMVK with side chain motions, $M(t)$ exhibits an initial rapid decay due to those motions and then relaxes by main chain motions. The initial decay is more rapid if Δ is closer to 90°, while the rate of the latter part is independent of Δ, as expected.

Finally, it is pertinent to make some remarks on the

dependence on N of the normalized correlation function. As far as main chain motions are concerned, the amplitudes in each branch have been found to be almost independent of N for $N \gtrsim 50$, so that $M(t)/M(0)$ depends on N only through the eigenvalues in the $j = 0$ branch. Therefore, except for monosubstituted isotactic chains having local helices, its N dependence is negligibly small for large N. Furthermore, the decay due to side chain motions is independent of N, as is evident from their nature.

b. Stiff chains

As mentioned in Sec. 4–3*b*, typical stiff chains may be represented by the KP chain ($\kappa_0 = 0$) having parallel dipoles ($\alpha = \Delta = 0^\circ$), whose correlation function may be written in terms of the eigenvalues $\lambda^0_{1,k}$ in the $j = 0$ branch, so that it is enough to consider the amplitudes only in this branch. We examine the behavior of $M(t)/M(0)$ within the ranges of n_b and r_2 for positive eigenvalues.

Figure 4.7 shows plots of the natural logarithm of $M(t)/M(0)$ against t for DNA with $r_1 = 1$ and the indicated values of n_b and r_2, where $M(t)$ has been computed at $T = 300$ K and $\eta_0 = 0.01$ P (0.2 M NaCl). The light and heavy curves represent the values for $(N + 1)n_b = 5000$ and 10000, respectively. It is seen

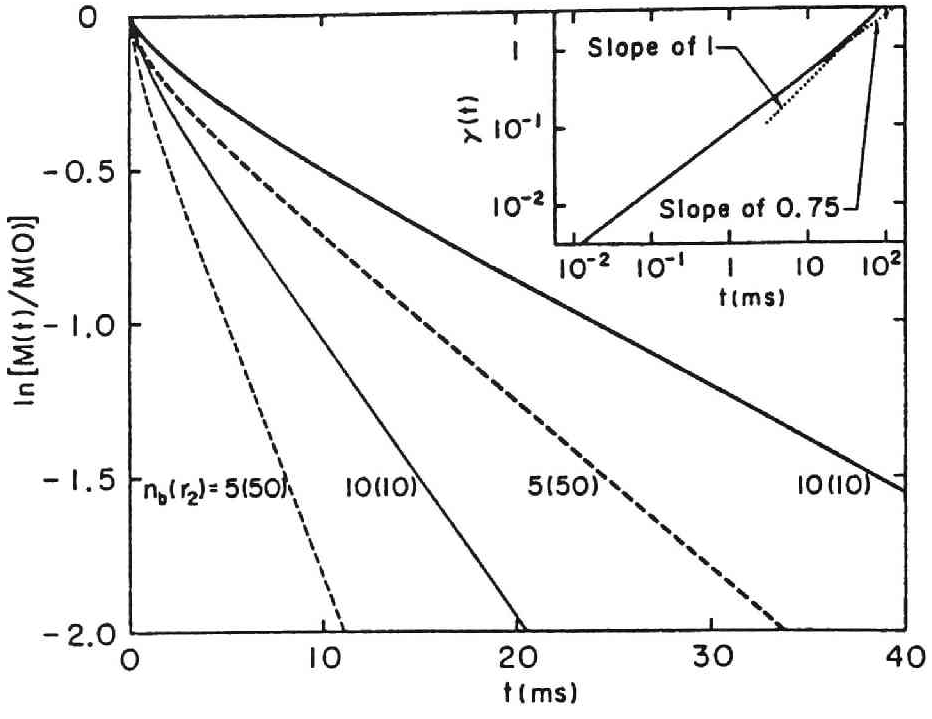

Fig. 4.7. The natural logarithm of the normalized dipole correlation function $M(t)/M(0)$ plotted against t for DNA ($\alpha=\Delta=0^\circ$) with $r_1=1$ and the indicated values of n_b and r_2 at $T=300$ K and $\eta_0=0.01$ P. The light and heavy curves represent the values for $(N+1)n_b=5000$ and 10000, respectively. The insert shows a double logarithmic plot of the function $\gamma(t)$ defined by Eq. (4.32) against t for the case of the heavy full curve.

that the decay is slower for larger $(N+1)n_b$, i. e., for larger chain length, as expected. We note that the amplitudes of $M(t)/M(0)$ are almost independent of N for $N \gtrsim 50$, and moreover the contribution of $\lambda_{1,1}^0$ is 86 %, so that the dependence of $M(t)/M(0)$ on N arises mainly from $\lambda_{1,1}^0$. In any case, it is seen that the decay is not single exponential except at large t. This is due to the fact

that the strong dependence of $\lambda_{1,k}^0$ on k at small k is effective at small t, while only $\lambda_{1,1}^0$ governs the decay at large t.

For a more quantitative examination, it is convenient to introduce a function $\gamma(t)$ defined by

$$M(t)/M(0) = e^{-\gamma(t)} . \tag{4.32}$$

The insert of Fig. 4.7 shows a double logarithmic plot of $\gamma(t)$ against t for $n_b = 10$, $N = 999$, $r_1 = 1$, and $r_2 = 10$ (the same model parameters as for the heavy full curve), the dotted straight lines having slopes of 0.75 and 1. It is seen that $\gamma(t)$ is proportional to $t^{0.75}$ for $t \lesssim 10$ ms and to t for larger t.

4-5. Comparison with Experiment

In this section, we make a comparison between theory and experiment with respect to the frequency dependences of the excess dielectric dispersion ε' and loss ε'', and the dielectric correlation time τ_D as defined as the inverse of ω_{max} corresponding the maximum loss ε''_{max} associated with the (net) main chain motion. Their theoretical values are computed from Eq. (4.25). The parameters n_b and r_2 (and also Δ and τ_{sl} in the presence of side chain motion) are then determined to give agreement between theory and experiment, assuming that $r_1 = 1$. We estimate the size (or diameter) of the subbody from r_1 and r_2 thus determined and compare the results with those from chemical structures. For stiff

chains, attention is given also to the dependence of τ_D on the molecular weight.

a. Flexible chains

In this subsection, we make an analysis for all flexible chains for which the angles α and β have already been determined in Sec. 4–4*a*. As for monosubstituted asymmetric chains, we must note that experimental data have been obtained for atactic polymers, while the HW model parameters κ_0, τ_0, λ^{-1}, and M_L have been determined for isotactic and syndiotactic chains. However, these atactic samples for which we analyze the data have been prepared by free radical polymerization, and have the fractions of meso dyads less than 0.5, and therefore we regard them as having the HW model parameters for syndiotactic chains, for convenience.

First, we take atactic poly(vinyl acetate) (a–PVAc) as an example of chains without side chain motions. Figure 4.8 shows plots of its reduced dispersion $\varepsilon_r' \equiv (\varepsilon' - \varepsilon_\infty)/(\varepsilon_0 - \varepsilon_\infty)$ and reduced loss $\varepsilon_r'' \equiv \varepsilon''/(\varepsilon_0 - \varepsilon_\infty)$ against the logarithm of frequency $f = \omega/2\pi$. The open and filled circles represent the experimental values of ε_r' and ε_r'', respectively, obtained recently by Cole et al.[26] by time domain reflectometry in toluene at 23 ℃, and the curves represent the corresponding theoretical values for s–PVAc ($\kappa_0 = 0.4$ and $\tau_0 = 2.5$) with $n_b = 2$, $N = 999$, $r_1 = 1$, and $r_2 = 27$. The insert shows

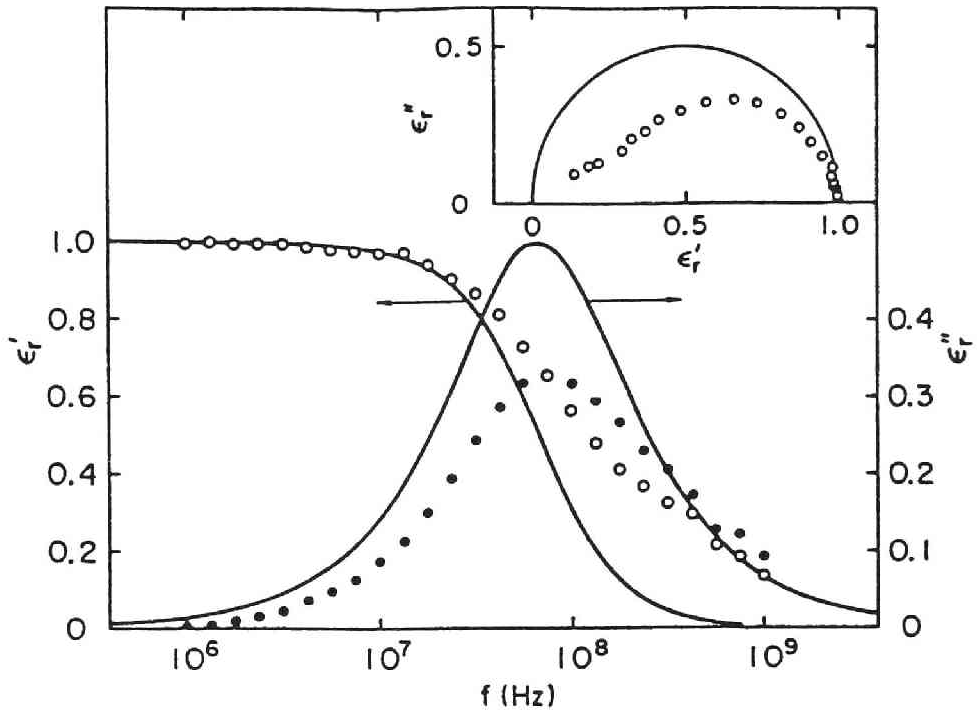

Fig. 4.8. The reduced dispersion ε_r' and reduced loss ε_r'' plotted against the logarithm of frequency f for atactic poly(vinyl acetate) in toluene at 23℃. The points represent the experimental values of Cole et al. (Ref. 26) and the curves the theoretical values for the syndiotactic chain ($\alpha=90^\circ$ and $\beta=0^\circ$) with $n_b=2$, $N=999$, $r_1=1$, and $r_2=27$. The insert shows the corresponding Cole–Cole plots.

the corresponding Cole–Cole plots, the open circles and curve representing the experimental and theoretical values, respectively. The value r_2 has been determined so that the calculated value of τ_D agrees with the observed value of 2.1 ns. The observed ε_r'' is seen to be asymmetric about f_{max}, i. e., somewhat broader on the high-frequency side, indicating that the dispersion is not strictly

of the Debye type, there being several absorption on that side. On the other hand, the theoretical values exhibit nearly a Debye dispersion. This corresponds to the fact that for monosubstituted syndiotactic chains, the theoretical dipole correlation function obeys the single exponential law, as mentioned in Sec. 4–4*a*. The disagreement between the theoretical and experimental ε_r' and ε_r'' indicates a defect of the theory, and it is discussed in Sec. 4–6.

Next, Fig. 4.9 shows similar plots for a–PMVK as an example of chains with side chain motions. The experimental values are those obtained very recently by Mashimo et al.[25] by the same method in dioxane at 20 C. The full curves represent the corresponding theoretical values for s–PMVK with $n_b = 2$, $N = 999$, $r_1 = 1$, $r_2 = 7$, $\Delta = 103^\circ$, and $k_B T \tau_{s1}/\zeta_r = 0.5$, and the broken curve represents the theoretical values of ε_r'' for $\Delta = 0^\circ$ but with the other parameters remaining unchanged. (Note that $\Delta = 120^\circ$ from chemical structures.) The loss peaks on the low– and high–frequency sides correspond to the main chain and side chain motions with the correlation times of 2.7 and 0.16 ns, respectively. However, the correlation time τ_D associated with the net main–chain motion is estimated to be 3.2 ns from the loss peak (of the broken curve) that would be obtained if the side chain motion were absent ($\Delta = 0^\circ$). We also find $\tau_{s1} = 0.17$ ns from $k_B T \tau_{s1}/\zeta_r = 0.5$. These correlation times τ_D and τ_{s1} are to be compared with the corresponding values 3.70 and 0.155 ns obtained by Mashimo et al.[25]

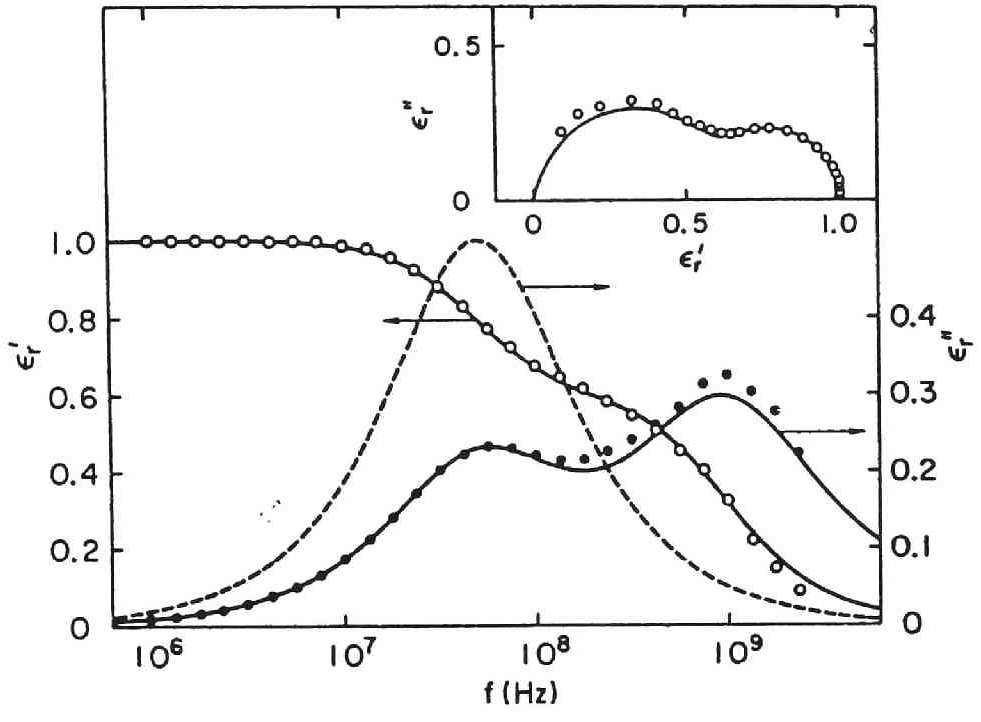

Fig. 4.9. The reduced dispersion ϵ_r' and reduced loss ϵ_r'' plotted against the logarithm of frequency f for atactic poly(methyl vinyl ketone) in dioxane at 20°C. The points represent the experimental values of Mashimo et al. (Ref. 25). The full curves represent the theoretical values for the syndiotactic chain ($\alpha=90^\circ$ and $\beta=180^\circ$) with $n_b=2$, $N=999$, $r_1=1$, $r_2=7$, $\Delta=103^\circ$, and $k_BT\tau_{s1}/\zeta_r=0.5$, and the broken curve represents the theoretical values of ϵ_r'' for the net main-chain motion ($\Delta=0^\circ$).

from an analysis with a superposition to the two Havriliak-Negami functions[27] for ϵ^*. In any case, the correlation time τ_D for the net main-chain motion is somewhat larger than the correlation time determined from the loss peak on the low-frequency side without correction for side chain motion. In contrast to the case of a-PVAc, the theory can well explain the experimental ϵ_r' and

ϵ_r''. The reason for this is that the lack of the absorptions due to the main-chain motion on the high-frequency side has been compensated by the absorption due to the side chain motion.

In Table 4.1 are given observed values of τ_D thus determined for POE,[28,29] atactic poly(p-chlorostyrene) (a-PPCS),[30,31] a-PMA,[32] a-PMVK,[25] a-PVAc,[26] atactic poly(vinyl chloride) (a-PVC),[33] i-PMMA,[34] and s-PMMA.[34] We also give values of r_2 that give agreement between the calculated and observed values of τ_D for $n_b = 2$ and 6, all for $r_1 = 1$ and $N = 999$. The observed values of τ_D determined as above for a-PMVK with $n_b = 2$ and 6 are the same. We have omitted the value of r_2 for POE with $n_b = 6$ since then Δs exceeds the allowed upper bound 0.4, as given in Chap. 2. However, we have ignored the lower bound of r_2 ($\gtrsim 3$), which is less

Table 4.1. Observed values of the dielectric correlation time τ_D and estimates of the parameter r_2 for the flexible chain polymers.

Polymer	Solvent	Temperature (℃)	τ_D, obs (ns)	r_2		Observed values (Ref.)
				n_b=2	n_b=6	
POE	Benzene	25	0.013	0.3	···	28,29
a-PPCS	Benzene	25	4.7	65	6.8	30
		25.5	6.6	95	10	31
a-PMA	Benzene	20	0.25	2	0.2	32
a-PMVK	Dioxane	20	3.2[a]	7	0.8	25
a-PVAc	Toluene	23	2.1	27	2.7	26
a-PVC	Dioxane	30	2.6	6	0.6	33
i-PMMA	Toluene	30	1.0	8	0.9	34
s-PMMA	Toluene	30	4.1	70	7.5	34

[a]Corresponding to the net main-chain motion.

important.

Now we estimate the size of the subbody from r_2. As noted in Chap. 3, the product of r_1 and r_2 rather than their individual values (or ζ_r rather than ζ_t) plays an important role as far as the local motions are concerned. (The reduced eigenvalues are almost independent of r_2.) From Eqs. (3.67) and (3.68), we have

$$r_1 r_2 \equiv r = \zeta_r / 3\pi\eta_0 a^3 . \tag{4.33}$$

It is reasonable here to regard the subbody as a spheroid (ellipsoid of revolution) having rotation axis of length a and diameter d. Then ζ_r must be then the mean rotatory friction coefficient, and is given by

$$\zeta_r = \frac{k_B T}{3}\left(\frac{2}{D_{r,1}} + \frac{1}{D_{r,3}}\right) , \tag{4.34}$$

where $D_{r,1}$ and $D_{r,3}$ are the rotatory diffusion coefficients of the spheroid about the transverse axis and rotation axis, respectively. With the well-known results for them,[35,36] we obtain from Eqs. (4.33) and (4.34)

$$r = \frac{2(1 - x^2)}{27x^3}\left[\frac{2(1 + x^2)}{(1 - 2x^2)F(x) + x} + \frac{1}{F(x) - x}\right] , \quad \text{for } x \neq 1$$

$$= 1/3 , \qquad \text{for } x = 1 , \tag{4.35}$$

where

$$F(x) = (x^2 - 1)^{-1/2}\cosh^{-1}x , \quad \text{for } x > 1$$

$$= (1 - x^2)^{-1/2}\cos^{-1}x , \quad \text{for } x < 1 \tag{4.36}$$

with $x \equiv a/d$. Thus we may determine d from Eqs. (4.35) with

the values of r and a, where the bond length a may be computed from Eq. (2.26) with Eq. (4.28).

The values of d thus determined and also those from chemical structures are given in Table 4.2. The latter values have been calculated on the assumption that this d is approximately equal to the diameter of a circumscribed circle of the projection of the monomer unit composed of the atoms having van der Waals radii onto the plane perpendicular to the end-to-end vector C⟶C of the sequence of two successive skeletal bonds C⟶C^a⟶C (C⟶O⟶C for POE). Except for POE and a-PMA, the values of d from r are seen to be 1.2-2 times as large as those from chemical structures for $n_b = 2$, and even larger for $n_b = 6$. This

Table 4.2. Values of the diameter d (Å) determined from chemical structures and from the estimates of the parameter $r = r_1 r_2$ for flexible chain polymers.

Polymer	From chemical structures	From r	
		n_b=2	n_b=6
POE	4.5	3.1	・・・
a-PPCS	12.0	18.7[a]	25.3[a]
		21.3[b]	29.0[b]
a-PMA	8.5	5.5	5.7
a-PMVK	7.5	8.8	11.3
a-PVAc	9.0	13.8	17.9
a-PVC	6.0	8.2	9.9
i-PMMA	9.0	10.8	13.8
s-PMMA	9.0	21.6	29.3

[a]From τ_D(obs) = 4.7 ns (Ref. 30).
[b]From τ_D(obs) = 6.6 ns (Ref. 31).

indicates that if τ_D are calculated with the diameters from chemical structures, the results are smaller than the observed τ_D. It is also a defect of the theory.

It is then instructive to consider the ratio of τ_D to the dielectric correlation time τ_D^0 of the isolated spheroid above having a dipole moment vector parallel to the transverse axis, assuming that $n_b = 2$. τ_D^0 can easily be shown to be given by

$$\tau_D^0 = (D_{r,1} + D_{r,3})^{-1}$$

$$= \frac{2\pi\eta_0 a^3}{3k_B T} \frac{x^4 - 1}{x^3[(x^2-2)F(x) + x^3]}, \quad \text{for } x \neq 1$$

$$= \frac{\pi\eta_0 a^3}{2k_B T}, \quad \text{for } x = 1, \tag{4.37}$$

where $F(x)$ is again given by Eqs. (4.36) with $x = a/d$. In Table 4.3 are given values of $\tau_D(\text{obs})/\tau_D^0$ and $\tau_D(\text{calc})/\tau_D^0$, where $\tau_D(\text{calc})$ and τ_D^0 have been calculated with the diameters d from chemical structures. The latter ratio is seen to be smaller than the former except for POE and a-PMA, as expected, but larger than unity for all cases. The result that $\tau_D > \tau_D^0$ seems quite reasonable, considering the fact that if the isolated subbody or monomer unit is incorporated into the chain, its correlation time will be appreciably increased because of the constraints and the interactions with its neighbors. Thus the ratio τ_D/τ_D^0 may be regarded as a measure of dynamic chain stiffness. For comparison, the values of the (static) stiffness parameter λ^{-1} (reproduced from Ref. 23)

Table 4.3. Dynamic stiffness τ_D/τ_D^0 and static stiffness λ^{-1} for flexible chain polymers.

Polymer	$\tau_D(obs)/\tau_D^0$	$\tau_D(calc)/\tau_D^0$	λ^{-1}(Å)
POE	0.8	1.9	12.0
a-PPCS	24[a](34[b])	7.2	37.5
a-PMA	3.1	9.0	35.8
a-PMVK	28[c]	18.6[c]	65.1
a-PVAc	26	8.4	42.0
a-PVC	50	24.1	78.0
i-PMMA	13	7.8	32.7
s-PMMA	54	5.0	65.6

[a]From $\tau_D(obs)$ = 4.7 ns (Ref. 30).
[b]From $\tau_D(obs)$ = 6.6 ns (Ref. 31).
[c]Corresponding to the net main-chain motion.

are given in the last column of Table 4.3. It is interesting to see that there is strong correlation between $\tau_D(obs)/\tau_D^0$ and λ^{-1} except for a-PMA. For this polymer, the observed τ_D is of the same order of magnitude as τ_{s1} of a-PMVK (see Table 4.1), and moreover the dispersion has been found to be nearly of the Debye type,[26] so that the observed τ_D does not seem to reflect strictly the main-chain motion. As for other polymers, there is also strong correlation between $\tau_D(obs)/\tau_D^0$ (or λ^{-1}) and $\tau_D(calc)/\tau_D^0$ except for s-PMMA. The reason for the large discrepancy between theory and experiment for this polymer is not clear.

Finally, some remarks should be made on the dependence of τ_D on the molecular weight M. The experimental results obtained by Stockmayer and Matsuo[30] for a-PPCS show that τ_D increases with increasing M for $M \lesssim 2\times10^4$ and then levels off.

According to our computations for s-PPCS with $n_b = 2$, $r_1 = 1$, $r_2 = 65$, and $N + 1 = 10$, 20, 50, 100, 200, 500, and 1000, τ_D is independent of N for $N \gtrsim 19$, the value for $N = 9$ being somewhat smaller. We note that $N = 9$ corresponds to $M \simeq 1200$, so that the calculated τ_D levels off more rapidly. This disagreement between theory and experiment may be regarded as arising from the fact that the diagonal approximation (see Chap. 3) becomes asymptotically valid only for large N.

b. Stiff chain

For flexible chains with perpendicular dipoles, the dielectric correlation time τ_D is associated with the local main-chain motion, while for stiff chains ($\kappa_0 = 0$) with parallel dipoles ($\alpha = \Delta = 0^\circ$), it reflects the global motion (end-over-end rotation, etc.) and its molecular weight dependence becomes very important. In this subsection, we consider primarily this problem.

Before making a comparison with experiment, we must establish the calculated values of τ_D within the ranges of the parameters for positive eigenvalues as determined in Sec. 4-3*b*. For this purpose, we examine its dependence on r_2. It is then convenient to use again the parameter a (or Δs) instead of n_b. Furthermore, we assume that $r_1 = 1$ as before, and do not consider the model parameters τ_0 and σ, since in this case the results are

independent of them, as mentioned in Sec. 4–3*b*. Figure 4.10 shows double logarithmic plots of $k_B T\tau_D/3\pi\eta_0 a^3$ against r_2 for stiff chains with $N = 99$ and 249. The full and broken curves represent the values for $a = 0.01$ and 0.05, respectively. It is seen that if r_2 decreases and approaches the range for negative eigenvalues, τ_D becomes very large rapidly, but otherwise, it is almost independent of r_2 over a relatively wide range. This independence is rather reasonable since the τ_D associated with the global motion should not depend on ζ_r (related to r_2) but on ζ_t for large N, as predicted by the conventional theory for bead models. (Compare with the case of the local motion.) Indeed, the contribution of ζ_r to τ_D or the rotatory friction coefficient of the entire chain is of order $N\zeta_r$ and negligibly small compared to that of ζ_t. Recall that the conventional theory predicts that when $\alpha = \Delta = 0^\circ$, τ_D is proportional to $N^3/\ln N$ in the long rod limit[37] and to $N^{3/2}$ in the coil limit.[5,6] Thus, for convenience, we adopt as the calculated values of $k_B T\tau_D/3\pi\eta_0 a^3$ independent of r_2 the minimum values as indicated by the open circles in Fig. 4.10. (We neglect the slight increase in this ratio for larger r_2. Note that if the theory is exact, it will be independent of r_2 over the whole range.) Then, since $r_1 = 1$, i. e., $\zeta_t = 3\pi\eta_0 a$, the τ_D thus evaluated may be regarded as the correlation time for a touched bead model, each bead being a Stokes sphere of diameter a.

Next we replace the bead model by an equivalent cylinder

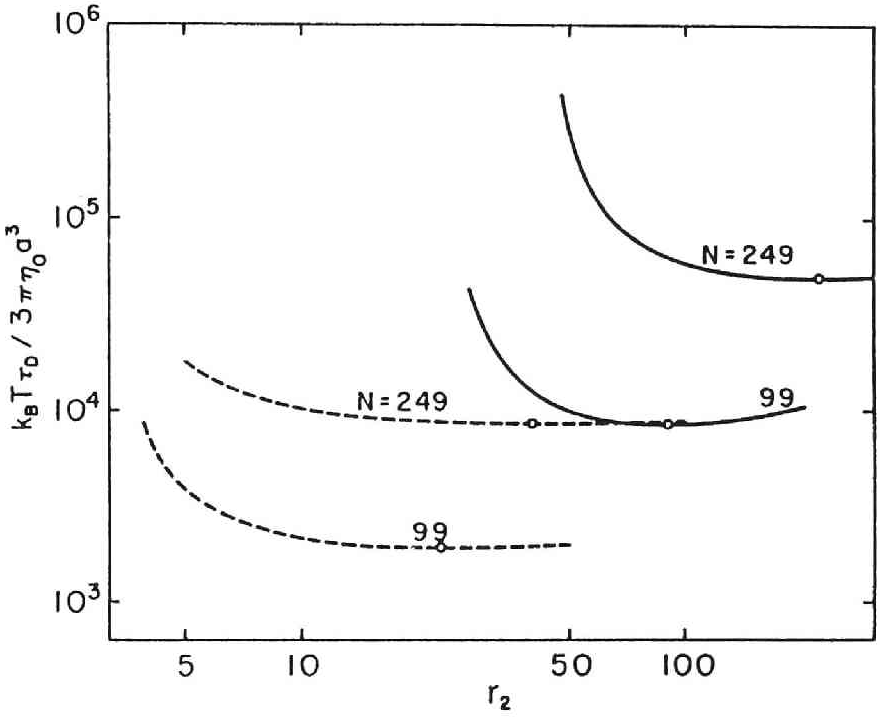

Fig. 4.10. Double logarithmic plots of $k_BT\tau_D/3\pi\eta_0 a^3$ for stiff chains ($\kappa_0=0$ and $\alpha=\Delta=0^\circ$). The full and broken curves represent the values for $a=0.01$ and 0.05, respectively, and the open circles indicate the minimum points.

model of diameter d, for which we have previously evaluated steady-state transport coefficients. This can be done by the use of a shift factor[38] we have recently determined to convert a to d for the case of the touched bead model for a rigid rod with the nonpreaveraged original or modified Oseen tensor. Although the present theory uses the preaveraged original Oseen tensor, we may adopt the shift factor for its nonpreaveraged case since the effects of this preaveraging are rather small near the rod limit.[39] For

the case of τ_D (or the rotatory diffusion coefficient), d is then related to a by

$$d = 0.861a \ . \tag{4.38}$$

Values of $2k_BT\tau_D//\pi\eta_0 d^3$ thus calculated as a function of L/d for various values of a are represented by the open circles in Fig. 4.11 for the KP cylinder of contour length L $(= N\Delta s \simeq Na)$ and diameter d.

With these values, we have constructed an interpolation formula, as in the case of the intrinsic viscosity.[40] The results reads

$$\tau_D = \tau_{D.rod} L^{-3}[\, L + \tfrac{1}{2}(e^{-2L} - 1)\,]^{3/2}$$

$$\times\, [1 + 0.539526 \ln(1 + L)] \ , \quad (L \lesssim 30) \ , \tag{4.39}$$

where $\tau_{D.rod}$ is the dielectric correlation time of a spherocylinder (spheroid cylinder with $\varepsilon = 1$) as given by $\tau_D = 1/2D_{r.1}$ with Eq. (120) of Ref. 41 for $D_{r.1}$; i. e.,

$$\tau_{D.rod} = \tau\eta_0 L^3 F_r(L/d)/6k_BT \tag{4.40}$$

with

$$\begin{aligned} F_r(x)^{-1} = {} & \ln x + 2\ln 2 - 11/6 - 8.25644[\ln(1 + x)]^{-1} \\ & + 13.0447x^{-1/4} - 62.6084x^{-1/2} \\ & + 174.0921x^{-3/4} - 218.8356x^{-1} \\ & + 140.2699x^{-5/4} - 32.2708x^{-3/2} \ . \end{aligned} \tag{4.41}$$

In Fig. 4.11, the full curves represent the values calculated from Eq. (4.39), and the dotted curve R those from Eq. (4.40) for the spherocylinder.

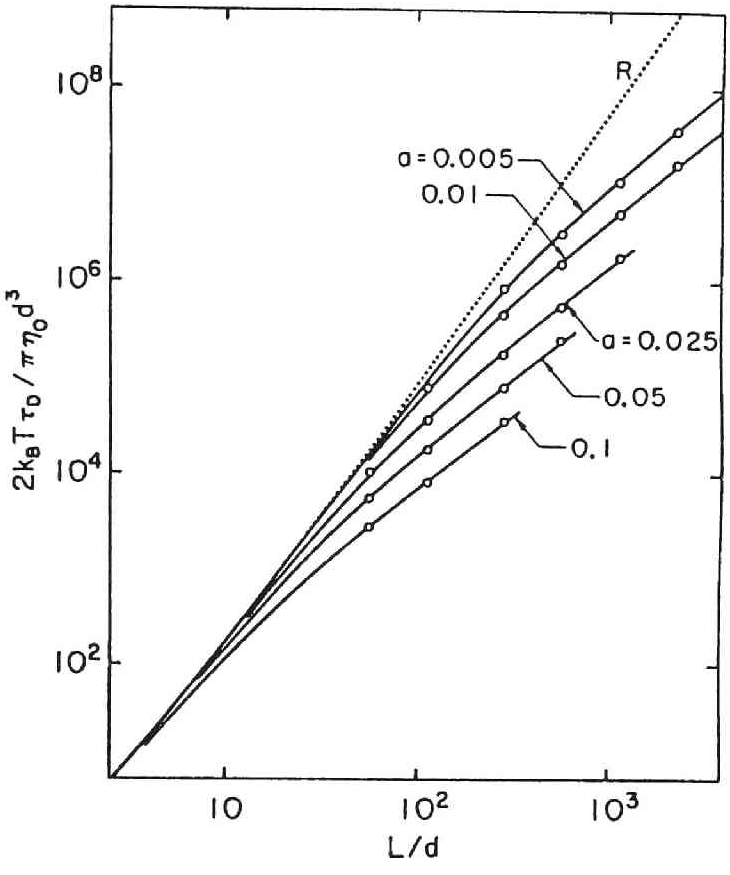

Fig. 4.11. Double logarithmic plots of $2k_BT\tau_D/\pi\eta_0d^3$ against L/d for the KP cylinder ($\kappa_0=0$ and $\alpha=\Delta=0^\circ$) of contour length L and diameter d. The points represent the original theoretical values. The full curves represent the values calculated from the interpolation formula [Eq. (4.39)] and the dotted curve R those from Eq. (4.40) for the spherocylinder.

Now we are in position to make a comparison with experiment. Fig. 4.12 shows its example with double logarithmic plots of $2k_BT\tau_D/\pi\eta_0d^3$ against L/d ($= M/dM_L$ with d unreduced). The open and filled circles and triangles represent the observed

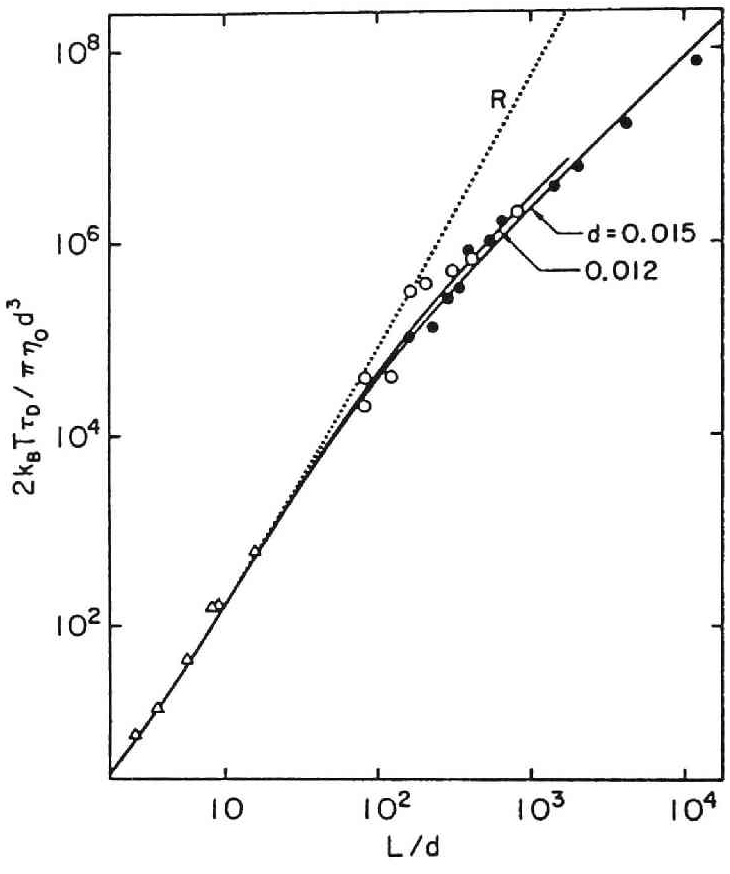

Fig. 4.12. Double logarithmic plots of $2k_BT\tau_D/\pi\eta_0d^3$ against L/d for stiff chains ($\kappa_0=0$ and $\alpha=\Delta=0^\circ$). The open and filled circles and triangles represent the experimental values of Sakamoto et al. (Ref. 42) for DNA in 1 mM NaCl at 10°C, of Bur and Roberts (Ref. 43) for poly(n-butyl isocyanate) in carbon tetrachloride at 22.9°C, and of Matsumoto et al. (Ref. 44) for poly(γ-benzyl L-glutamate) in m-cresol at 25°C, respectively. The full curves represent the best fit theoretical values calculated from Eq. (4.39), and the dotted curve R the values from Eq. (4.40) for the spherocylinder.

values obtained by Sakamoto et al.[42] for DNA in 1 mM NaCl at 10°C, by Bur and Roberts[43] for poly(n-butyl isocyanate) (PBIC) in

carbon tetrachloride at 22.9℃, and by Matsumoto et al.[44] for poly(γ-benzyl L-glutamate) (PBLG) in m-cresol at 25℃, respectively. The model parameters determined from a best fit of the theoretical values to the observed ones are λ^{-1}= 2100 Å for DNA assuming d = 25 Å and M_L = 195 Å^{-1}; λ^{-1}= 1000 Å for PBIC assuming d = 15 Å and M_L = 55.1 Å^{-1};[19] and d = 28 Å for PBLG assuming M_L = 146 Å^{-1}.[45] These values of d and M_L have been used to plot the data points. [We note that the assumed value of d for PBIC is intermediate between the value 13 Å determined from crystallographic data[46] and the value 16 Å for poly(n-hexyl isocyanate) from intrinsic viscosity data.[47]] The full curve represent the theoretical values calculated from Eq. (4.39) with the indicated values of (reduced) d, and the dotted curve R those from Eq. (4.40) for the spherocylinder. The above estimate of λ^{-1} for DNA (in 1 mM NaCl) seems reasonable, compared with literature values,[48-50] while that for PBIC is somewhat smaller than the value 1440 Å determined[19] from dipole moments for the same samples.[43] (For PBLG, λ^{-1}cannot be determined since the data are confined to the range of rigid rods.) Thus we may conclude that there is good agreement between theory and experiment as far as τ_D for stiff chains is concerned.

Finally, we make a comparison of theory with experiment with respect to the dispersion and loss curves, taking as an example a fraction of the above PBIC with the weight-average molecular

weight $M_w = 23.5\times10^4$. Figure 4.13 shows plots of ε_r' and ε_r'' against the logarithm of frequency f, and the insert shows the Cole–Cole plots. As in Figs. 4.8 and 4.9, the points represent the experimental values and the curves the theoretical values calculated with $n_b = 19.4$ (or $a = 0.0174$) and $N = 245$ (corresponding to the above values of λ^{-1}, d, M_L, and M_w) and with $r_1 = 1$ and $r_2 = 30$. The observed ε_r'' is asymmetric and broader on the high-frequency side,

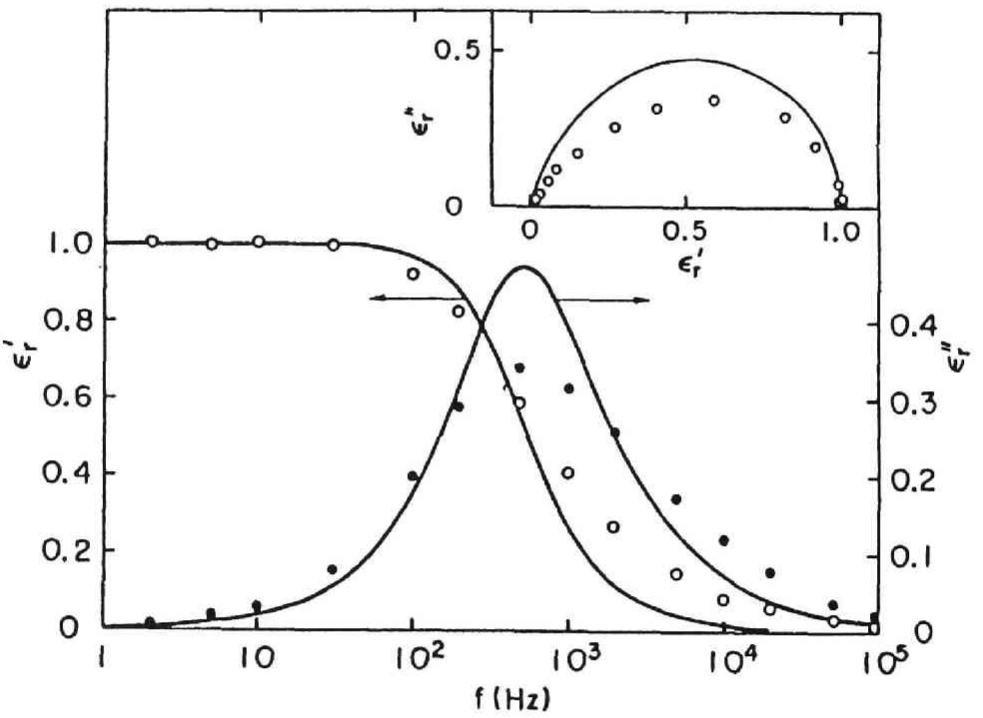

Fig. 4.13. The reduced dispersion ε_r' and reduced loss ε_r'' plotted against the logarithm of frequency f for poly(n-butyl isocyanate) with $M_w=23.5\times10^4$ in carbon tetrachloride at 22.9℃. The points represent the experimental values of Bur and Roberts (Ref. 43) and the curves the theoretical values calculated with $n_b=19.4$, $N=245$, $r_1=1$, and $r_2=30$ (the same model parameters as in Fig. 4.12). The insert shows the Cole–Cole plots.

although less remarkably than for PVAc. The theory can explain, to some extent, this feature, but the agreement with experiment is not complete.

4-6. Discussion

Among the three main purpose of this chapter, we have almost completely achieved the first regarding the mode analysis of the dielectric branches of the eigenvalue spectrum. As for the other two, which are more important, however, the results are not always satisfactory. In particular, we have failed to completely explain the asymmetric dielectric loss, especially for flexible chains without side chain motions. On the other hand, we have been able to evaluate the dielectric correlation time τ_D in terms of the well-defined model parameters for a wide variety of flexible and stiff chain polymers. The significant results for τ_D are the following two: (i) For flexible chains, there is strong correlation between the dynamic stiffness τ_D/τ_D^0 and the static stiffness λ^{-1} and also between the observed and calculated τ_D; and (ii) for stiff chains, there is good agreement between theory and experiment with respect to the molecular weight dependence of τ_D. For flexible chains, however, calculated values of τ_D are one half or one third of observed values. In order to remove these discrepancies between theory and experiment, we must search for possibilities of

improvement of the approximation used.

First we consider the case of flexible chains. We have made the preaveraging approximations in the Oseen tensor and the constraining matrix $\mathbf{C}^{-1}$. The former may be regarded as having no significant effect since ζ_r plays an important role as far as local motions are concerned, while the latter breaks, to some extent, the rigid constraints imposed and therefore may lead to an underestimate of τ_D. At present, however, it is almost impossible to improve this approximation. Another approximation, which is more serious for flexible chains, it is subspace approximation, i. e., the development in terms of only the one-body excitation basis functions. This approximation fails to take complete account of the (short-range) interactions between subbodies or more, thereby weakening the polymeric nature of the chain. This point can be improved by augmenting the 1(1) subset with two-body excitation basis functions. The augmentation will lead to perturbation of the present three dielectric branches of the eigenvalue spectrum and also addition of a few new branches. Therefore this will enable us to explain better the asymmetry of the loss curve and also τ_D. [We note that if τ_D^0 is evaluated with the slip boundary condition, values of $\tau_D(\mathrm{obs})/\tau_D^0$ become larger than those listed in Table 4.3.]

Next we consider stiff chains. In this case, only the $j = 0$ branch makes contribution, and the first few of the eigenvalues

$\lambda^0_{1,k}$ in it may possibly become negative because of the preaveraging approximation in the constraining matrix. Fortunately, however, we have found the maneuver to avoid its serious effects. Clearly the subspace approximation has much less significant effect, and the results (dependent on the $j = 0$ branch) will not greatly be altered by augmentation. On the other hand, the diagonal approximation is not very good for stiff chains except at very small wave number k. It is therefore easy to understand why the theory can well explain τ_D but not the asymmetry of the loss curve, if we recall that the former is determined mainly by $\lambda^0_{1,1}$ and the latter is caused by the first several eigenvalues. However, it is difficult to improve the diagonal approximation.

In conclusion, the present theory as a whole may be regarded as fairly satisfactory despite the fact that it is only a first-order approximation within the framework of the discrete HW model.

Appendix 4-A. Eigenfunctions

The eigenfunctions $\psi^{M,j}_{1,[k]}(\{\Omega_N\})$ $(M, j = 0, \pm 1; k = 1, 2, \cdots, N)$ corresponding to the eigenvalues $\lambda^j_{1,k}$ in the subspace 1(1) of the basis functions may be expressed, from Eqs. (3.47)-(3.49), (3.58), and (3.59), in the form

$$\psi^{M,j}_{1,[k]}(\{\Omega_N\}) = (8\pi^2)^{N/2} \sum_{p=1}^{N} \sum_{j'=-1}^{1} Q^0_{pk} (R^{-1}_{1,[k]})^{j'j} D^{M,j'}_{1,[p]}(\Omega_p) , \tag{4A.1}$$

where Q^0_{ph} is given by Eq. (3.43), $(R^{-1}_{1.[k]})^{jj'}$ are the j, j' elements of the inverse $R^{-1}_{1.[k]}$ of the 3×3 matrix $R_{1.[k]}$ whose j, j' elements $R^{jj'}_{1.k}$ are given by Eq. (4.14) for $\kappa_0 \neq 0$ or by Eq. (4.16) for $\kappa_0 = 0$, and $D^{M,j}_{1.[p]}(\Omega_p)$ are the one-body excitation standard basis functions defined by Eq. (3.3) (with omission of tilde on D).

For the HW chain with $\kappa_0 \neq 0$, we obtain, from Eq. (4.14) with the use of the unitarity of $Q^L_{1(1).[k]}$ and $\overline{\mathscr{D}}^{jj'}_1(\Omega_a)$:

$$(R^{-1}_{1.[k]})^{jj'} = (8\pi^2)^{-N/2} \sum_{m=-1}^{1} \overline{\mathscr{D}}^{jm}_1(\Omega_a)(\overline{E}^{(m,m)}_{1.[k,k]})^{-1/2} Q^{L,mj}_{1.k} , \tag{4A.2}$$

and therefore

$$\begin{aligned}
(R^{-1}_{1.[k]})^{(-1)j} &= (R^{-1}_{1.[k]})^{1j} \\
&= \tau_0 \nu^{-1} (S^{(0)1}_{1.kk})^{-1/2} a_j + \frac{1}{\sqrt{2}} \kappa_0 \nu^{-1} (S^{(0)0}_{1.kk})^{-1/2} b_j , \quad (j = 0, -1) , \\
(R^{-1}_{1.[k]})^{0j} &= i[-\sqrt{2}\,\kappa_0 \nu^{-1} (S^{(0)1}_{1.kk})^{-1/2} a_j + \tau_0 \nu^{-1} (S^{(0)0}_{1.kk})^{-1/2} b_j] , \\
& \qquad\qquad (j = 0, -1) , \\
(R^{-1}_{1.[k]})^{(-1)1} &= -(R^{-1}_{1.[k]})^{11} = \frac{1}{\sqrt{2}} (S^{(0)1}_{1.kk})^{-1/2} , \\
(R^{-1}_{1.[k]})^{01} &= 0 ,
\end{aligned} \tag{4A.3}$$

where the meaning of the symbols is the same as in Eqs. (4.15). For the KP chain ($\kappa_0 = 0$), we have, from Eq. (3.50) and Eq. (4.16),

$$(R^{-1}_{1.[k]})^{jj'} = \delta_{jj'} (S^{(0)j}_{1.kk})^{-1/2} , \qquad \text{(KP)} . \tag{4A.4}$$

The $\mathscr{D}$ functions $\mathscr{D}^{Mj}_1(\Omega_p)$ involved in $D^{M,j}_{1.[p]}(\Omega_p)$ may be expressed in terms of the Cartesian components of $\mathbf{e}_{\xi_p}$, $\mathbf{e}_{\eta_p}$, and $\mathbf{e}_{\zeta_p}$, in the external coordinate system, which we designate by

$\mathbf{e}_{\xi_p} = (x_{\xi_p}, y_{\xi_p}, z_{\xi_p})$ and so on, as follows:

$$\begin{aligned}
\mathscr{D}_1^{(-1)(\pm1)}(\Omega_p) &= (3/32\pi^2)^{1/2}[\mp(x_{\xi_p} - iy_{\xi_p}) + i(x_{\eta_p} - iy_{\eta_p})] , \\
\mathscr{D}_1^{0(\pm1)}(\Omega_p) &= (3/16\pi^2)^{1/2}(\mp z_{\xi_p} + iz_{\eta_p}) , \\
\mathscr{D}_1^{1(\pm1)}(\Omega_p) &= (3/32\pi^2)^{1/2}[\pm(x_{\xi_p} + iy_{\xi_p}) - i(x_{\eta_p} + iy_{\eta_p})] , \\
\mathscr{D}_1^{(\mp1)0}(\Omega_p) &= (3/16\pi^2)^{1/2}(\pm x_{\zeta_p} - iy_{\zeta_p}) , \\
\mathscr{D}_1^{00}(\Omega_p) &= (3/8\pi^2)^{1/2} z_{\zeta_p} .
\end{aligned} \tag{4A.5}$$

For the HW chain with $\kappa_0 \neq 0$, if we substitute Eqs. (4A.3) and (4A.5) into Eq. (4A.1), we find Eqs. (4.29) for $\psi_{1,[k]}^{M,j}$, where $c_1^j(k)$ and $c_2^j(k)$ are given by

$$\begin{aligned}
c_1^j(k) &= \sqrt{3}(R_{1,[k]}^{-1})^{(-1)j} , \qquad (j = 0, \pm1) , \\
c_2^j(k) &= -\sqrt{3/2}\, i(R_{1,[k]}^{-1})^{0j} , \qquad (j = 0, -1) .
\end{aligned} \tag{4A.6}$$

For the KP chain ($\kappa_0 = 0$), if we substitute Eqs. (4A.4) and (4A.5) into Eq. (4A.1), we find

$$\begin{aligned}
\psi_{1,[k]}^{M,0} &= \sqrt{3}(S_{1,kk}^{(0)0})^{-1/2} q_{k,z}^{\zeta} , \quad \text{for } M = 0 \\
&= \sqrt{3/2}(S_{1,kk}^{(0)0})^{-1/2}(\mp q_{k,x}^{\zeta} + iq_{k,y}^{\zeta}) , \quad \text{for } M = \pm1, \ (j = 0), \\
\psi_{1,[k]}^{M,j} &= \sqrt{3/2}(S_{1,kk}^{(0)j})^{-1/2}(-q_{k,z}^{\xi} + iq_{k,z}^{\eta}) , \quad \text{for } M = 0 \\
&= (\sqrt{3}/2)(S_{1,kk}^{(0)j})^{-1/2}[\, j(\pm q_{k,x}^{\xi} + iq_{k,y}^{\xi}) \mp iq_{k,x}^{\eta} + iq_{k,y}^{\eta}] , \\
&\qquad\qquad \text{for } M = \pm1, \ (j = \pm1), \ (\mathrm{KP}),
\end{aligned} \tag{4A.7}$$

where $q_{k,x}^{\xi}$, $q_{k,x}^{\eta}$, $q_{k,x}^{\zeta}$, and so on are defined by Eq. (4.30) and similar equations. In this case, $\psi_{1,[k]}^{M,0}$ may be written in terms of only the global modes $\mathbf{q}_k^{\zeta}$ and $\psi_{1,[k]}^{M,\pm1}$ in terms of the local modes $\mathbf{q}_k^{\xi}$ and $\mathbf{q}_k^{\eta}$.

References

[1]J. G. Kirkwood and R. M. Fuoss, J. Chem. Phys., **9**, 329 (1941).

[2]J. G. Kirkwood, J. Polym. Sci., **12**, 1 (1954).

[3]W. G. Hammerle and J. G. Kirkwood, J. Chem. Phys., **23**, 1743 (1955).

[4]P. Debye, *Polar Molecules* (Dover, New York, 1945).

[5]B. H. Zimm, J. Chem. Phys., **24**, 269 (1956).

[6]W. H. Stockmayer and M. E. Baur, J. Am. Chem. Soc., **86**, 3485 (1964).

[7]W. H. Stockmayer, Pure Appl. Chem., **15**, 539 (1967).

[8]H. Yamakawa, *Modern Theory of Polymer Solutions* (Harper & Row, New York, 1971).

[9]M. B. Clark and B. H. Zimm, in *Dielectric Properties of Polymers*, edited by F. Karasz (Plenum, New York, 1972), p. 45.

[10]M. B. Clark, in *Dielectric Properties of Polymers*, edited by F. Karasz (Plenum, New York, 1972), p. 73.

[11]J. E. Shore and R. Zwanzig, J. Chem. Phys., **63**, 5445 (1975).

[12]M. L. Mansfield, J. Polym. Sci., Polym. Phys. Ed., **21**, 773 (1983); **21**, 787 (1983).

[13]R. Cook and L. L. Livornese, Jr., Macromolecules, **16**, 920 (1983).

[14]J. T. Bendlar and R. Yaris, Macromolecules, **11**, 650 (1978).

[15]J. L. Skinner, J. Chem. Phys., **79**, 1955 (1983). See also papers cited in Refs. 8–15.

[16]M. Fixman and J. Kovac, J. Chem. Phys., **61**, 4939 (1974); and succeeding papers.

[17]M. Fixman and G. T. Evans, J. Chem. Phys., **68**, 195 (1978).

[18]G. Williams, Chem. Rev., **72**, 55 (1972).

[19]H. Yamakawa, J. Shimada, and K. Nagasaka, J. Chem. Phys., **71**, 3573 (1979).

[20]H. Yamakawa and J. Shimada, J. Chem. Phys., **70**, 609 (1979).

[21]D. E. Woessner, J. Chem. Phys., **36**, 1 (1962).

[22]J. D. Hoffman and H. G. Pfeiffer, J. Chem. Phys., **22**, 132 (1954).

[23]M. Fujii, K. Nagasaka, J. Shimada, and H. Yamakawa, Macromolecules, **16**, 1613 (1983).

[24]H. Yamakawa, M. Fujii, and J. Shimada, J. Chem. Phys., **71**, 1611 (1979).

[25]S. Mashimo, P. Winsor IV, R. H. Cole, K. Matsuo, and W. H. Stockmayer, Macromolecules, **16**, 965 (1983).

[26]R. H. Cole, S. Mashimo, and P. Winsor IV, J. Phys. Chem., **84**, 786 (1980).

[27]S. Havriliak and S. Negami, J. Polym. Sci., Part C, **14**, 99 (1966).

[28]W. H. Stockmayer, Pure Appl. Chem. Suppl., Macromol. Chem., **8**, 379 (1973).

[29]M. Davies, G. Williams, and G. D. Loveluck, Z. Elektrochem., **64**, 575 (1960).

[30]W. H. Stockmayer and K. Matsuo, Macromolecules, **5**, 766 (1972).

[31]S. Mashimo, Macromolecules, **9**, 91 (1976).

[32]S. Mashimo, H. Nakamura, and A. Chiba, J. Chem. Phys., **76**, 6342 (1982).

[33]S. Mashimo and A. Chiba, Polym. J., **5**, 41 (1973).

[34]Y. Iwasa, S. Mashimo, and A. Chiba, Polym. J., **8**, 401 (1976).

[35]G. B. Jeffery, Proc. R. Soc. London Ser. A, **102**, 161 (1922).

[36]F. Perrin, J. Phys. Rad., **7**, 1 (1936).

[37]J. G. Kirkwood and P. L. Auer, J. Chem. Phys., **19**, 281 (1951).

[38]H. Yamakawa, Macromolecules, **16**, 1928 (1983).

[39]G. Tanaka, T. Yoshizaki, and H. Yamakawa, Macromolecules, **17**, 767 (1984).

[40]H. Yamakawa and T. Yoshizaki, Macromolecules, **13**, 633 (1980).

[41]T. Yoshizaki and H. Yamakawa, J. Chem. Phys., **72**, 57 (1980).

[42]M. Sakamato, R. Hayakawa, and Y. Wada, Biopolymers, **17**, 1507 (1978).

[43]A. J. Bur and D. E. Roberts, J. Chem. Phys., **51**, 406 (1969).

[44]T. Matsumoto, N. Nishioka, A. Teramoto, and H. Fujita, Macromolecules, **7**, 824 (1974).

[45]S. Itou, N. Nishioka, T. Norisuye, and A. Teramoto, Macromolecules, **14**, 904 (1981).

[46]U. Shmueli, W. Traub, and K. Rosenheck, J. Polym. Sci., Part A, **27**, 515 (1969).

[47]H. Murakami, T. Norisuye, and H. Fujita, Macromolecules, **13**, 345 (1980).

[48]N. Borochov, H. Eisenberg, and Z. Kam, Biopolymers, **20**, 231 (1981).

[49]Z. Kam, N. Borochov, and H. Eisenberg, Biopolymers, **20**, 2671 (1981).

[50]C. B. Post, Biopolymers, **22**, 1087 (1983).

CHAPTER 5

DYNAMIC INTRINSIC VISCOSITY

5-1. Introduction

In Chap. 4, we have evaluated dielectric relaxation, which can be expressed in terms of the (1, 1)-body correlation functions. Now we proceed to study a new observable expressed in terms of (2, 2) or (1, 2)-body correlation functions, i. e., the dynamic intrinsic viscosity.

There have been many experimental and theoretical investigations on the dynamic intrinsic viscosity of flexible chains.[1] The foremost of the theoretical ones is the very famous Rouse-Zimm theory[2-4] using the spring-bead model. As is well known, it is in good agreement with experiment in the low-frequency region, but fails to explain the high-frequency plateau. Several attempts have been made to give a theoretical explanation of the latter.[1] Cerf[5] and Peterlin[6] have introduced phenomenologically the internal viscosity into the spring-bead model. (A rationale for the internal viscosity has been considered by Adelman and Freed.[7]) Doi et al.[8] and Fixman and Evans[9] have regarded the high-frequency plateau as arising from the constraints on the bond lengths and bond angles, and obtained the theoretical

values which lie far below the experimental values. Fixman and Evans[10] have conjectured that the plateau stems from the interaction between the local and global modes due to the constraints. Adler and Freed[11] have shown that the spring-bead model having side groups (or a comb-like spring-bead model) exhibits a high-frequency plateau. Despite these efforts, there is still a lack of complete understanding of the plateau. Thus, our major attention is given to it without considering the behavior over the whole frequency range.

From the studies cited above, it appears that there are two contributions to the high-frequency viscosity. One is the relaxation mechanism of a chain with constraints in the high-frequency region, and the other is the energy dissipation due to a bead (or monomer unit) having a finite hydrodynamic volume.[9] The former may be treated on the basis of our HW chain, i.e., the model that can describe the local chain motion. For the latter, we take into account its effect by distributing the frictional force on the surface of the bead instead of regarding it as a point force. As in the case of the dielectric relaxation treated in Chap. 4, we express the dynamic intrinsic viscosity in terms of certain correlation functions in the regime of linear response. In order to obtain an approximate solution for the correlation matrix, we use the crude subspace approximation, for simplicity. In this approximation, the problem may be reduced to N six-dimensional eigenvalue

problems with N the number of subbodies in the discrete HW chain. Note that we have encountered the three- or five-dimensional problems in the preceding chapters.

The plan of this chapter is as follows. In Sec. 5-2, the dynamic intrinsic viscosity of the discrete HW chain is expressed in terms of correlation functions of basis functions properly chosen, and approximate solutions for the correlation functions are obtained in terms of the solutions of relevant eigenvalue problems. In Sec. 5-3, we examine the behavior of the eigenvalues. In Sec. 5-4, we discuss the origin of the high-frequency viscosity. In Sec. 5-5, we make a comparison of theory with experiment with respect to the high-frequency viscosity for some flexible chains. Some mathematical details are given in the Appendices.

5-2. Formulation

In what follows, all lengths are measured in units of λ^{-1}, and $k_B T$ is chosen to be unity, as in the preceding chapters, unless noted otherwise.

Now, suppose that the (discrete) HW chain defined above is immersed in a solvent having an unperturbed oscillating shear flow field $\mathbf{V}^0$ at $\mathbf{R}$,

$$\mathbf{V}^0(\mathbf{R}) = \epsilon\, \mathbf{e}_x \mathbf{e}_y \cdot \mathbf{R} \ , \tag{5.1}$$

where ε is the oscillating rate of shear of angular frequency ω,

$$\varepsilon = \varepsilon_0 e^{i\omega t} \tag{5.2}$$

with ε_0 a constant, i the imaginary unit, and t the time. The intrinsic viscosity $[\eta]$ (in volume/weight) is given by

$$[\eta] = N_A<\sigma'>:\mathbf{e}_x\mathbf{e}_y/M\eta_0\varepsilon \ , \tag{5.3}$$

where N_A is the Avogadro number, σ' is the excess stress tensor due to the addition of one HW chain to the solvent of unit volume, $<\cdots>$ denotes an average with the time-dependent distribution function $\Psi(\{\Omega_N\};t)$, M is the polymer molecular weight, and η_0 is the viscosity coefficient of the solvent. Let $\mathbf{F}_p^{(S)}(\mathbf{r}_p)$ be the frictional force exerted on the fluid by the unit area at a point on the surface of the pth subbody of the vector distance $\mathbf{r}_p$ from the center of that subbody. The excess stress tensor may then be written as follows (see Appendix 5-A),

$$<\sigma'> = -\sum_{p=1}^{N+1} <\mathbf{R}_p\mathbf{F}_p> - \sum_{p=1}^{N} <\int_{S_p} \mathbf{r}_p\mathbf{F}_p^{(S)}(\mathbf{r}_p)d\mathbf{r}_p> \ , \tag{5.4}$$

where $\mathbf{R}_p$ is the vector position of the center of the pth subbody, $\mathbf{F}_p$ is the total frictional force exerted on the fluid by the pth subbody, and $\int_{S_p} d\mathbf{r}_p$ indicates the integration over its surface. Note that the term $<\mathbf{R}_{N+1}\mathbf{F}_{N+1}>$ comes from the $(N+1)$th bead having vanishing rotatory friction coefficient (see Sec. 2-2).

In Subsec. *a*, we find a formal solution for the time-dependent distribution function Ψ in order to evaluate the

averages in Eq. (5.4). In Subsec. *b*, we express the excess stress tensor $<\sigma'>$ in terms of certain time-correlation functions, and in Subsec. *c*, we evaluate them. In Subsec. *d*, we give a final expression for $[\eta]$.

a. Time-dependent distribution function

In the regime of linear response, the time-dependent distribution function Ψ may be written as

$$\Psi(\{\Omega_N\};t) = \Psi_{eq}(\{\Omega_N\})\ [1 + \varphi(\{\Omega_N\}; t)]\ , \tag{5.5}$$

where Ψ_{eq} is the equilibrium distribution function given by Eq. (2.15) or (2.103). The function φ is the solution of the (linearized) diffusion equation, as given by Eq. (2.98), i. e.,

$$(\partial/\partial t + \mathcal{L})\ \varphi = X, \tag{5.6}$$

where $\mathcal{L}$ is the diffusion operator given by Eq. (2.99), and X is the function (not an operator) given by Eq. (2.100) with the external potential $U_e = 0$.

In order to obtain an explicit expression for X, we need explicit forms of the generalized unperturbed fluid velocity $\mathbf{v}_p^0$ (expressed in the bond coordinates) associated with the pth bond vector $\mathbf{a}_p = \mathbf{R}_{p+1} - \mathbf{R}_p$, and of the unperturbed fluid angular velocity $\mathbf{W}_p^0$ at the point $\mathbf{R}_p$ (expressed in the external coordinates), as defined by Eqs. (2.48) and (2.37), respectively. From Eq. (5.1), these

velocities may be written as

$$\mathbf{v}_p^0 = \varepsilon\, \mathbf{e}_x\mathbf{e}_y \cdot \mathbf{a}_p \,, \tag{5.7}$$

$$\mathbf{W}_p^0 = -\tfrac{1}{2}\varepsilon\, \mathbf{e}_z \,. \tag{5.8}$$

Substitution of Eqs. (5.7) and (5.8) into Eq. (2.100) leads to

$$X = \tfrac{1}{2}\varepsilon\, (\mathscr{L}\Gamma + X') \tag{5.9}$$

with

$$\Gamma = \tfrac{1}{2}\left[\sum_{p_1,p_2=1}^{N} (B^{-1})_{p_1p_2}\mathbf{a}_{p_1}\mathbf{a}_{p_2}\right]:(\mathbf{e}_x\mathbf{e}_y + \mathbf{e}_y\mathbf{e}_x) \,, \tag{5.10}$$

$$X' = \sum_{p=1}^{N} \Psi_{\mathrm{eq}}^{-1}\, \mathbf{L}_p\, \Psi_{\mathrm{eq}} \cdot \mathbf{A}_p \cdot \mathbf{e}_z \,, \tag{5.11}$$

where $(B^{-1})_{pq}$ is the pq element of the inverse of the $N\times N$ preaveraged diffusion tensor B (expressed in the bond coordinates) whose pq element is given by Eq. (2.55), $\mathbf{L}_p$ is the angular momentum operator defined by Eqs. (2.86), and $\mathbf{A}_p$ is the 3×3 matrix for transformation from the external coordinate system to the pth localized coordinate system and is given by Eq. (2.31). The derivation of Eq. (5.9) with Eqs. (5.10) and (5.11) is given in Appendix 5-B. Note that the first and second terms on the right-hand side of Eq. (5.9) represent the contributions from the symmetric part (deformational flow) and the antisymmetric part (uniform rotational flow) of $\mathbf{e}_x\mathbf{e}_y$, respectively.

From Eqs. (5.2), (5.7), (5.8), and (5.9), Ψ may be formally written as

$$\Psi = \Psi_{eq}\left[1 + \tfrac{1}{2}\int_{-\infty}^{t} e^{-L(t-s)}\epsilon(s)(\mathcal{L}\Gamma + X')\mathrm{d}s\right] . \tag{5.12}$$

b. Correlation function formalism of the excess stress tensor

Now we consider the problem of expressing, in terms of time-correlation functions, the two sums on the right-hand side of Eq. (5.4).

By the use of the bond coordinates, the first sum $\sum_{p=1}^{N+1}<\mathbf{R}_p\mathbf{F}_p>$ may be rewritten as

$$\sum_{p=1}^{N+1} <\mathbf{R}_p\mathbf{F}_p> = \sum_{p=1}^{N} <\mathbf{a}_p\mathbf{f}_p> , \tag{5.13}$$

where $\mathbf{f}_p$ is the frictional force associated with the pth bond vector $\mathbf{a}_p$ and is defined by Eq. (2.49). Equation (5.13) has been obtained by the use of Eqs. (2.43) and (2.49) and of the fact that the total frictional force exerted by the chain on the solvent vanishes. From Eq. (2.60) with Eqs. (2.72), (2.73), and (2.81), $\mathbf{f}_p$ is given by

$$\mathbf{f}_p = -\sum_{q=1}^{N} [(\mathbf{N}^T)_{pq}\cdot\mathbf{L}_q \ \ln(\Psi/\Psi_{eq}) + \zeta_r(\mathbf{C}^{-1})_{pq}\cdot\mathbf{v}_q^0$$

$$- \zeta_r(\mathbf{N}^T)_{pq}\cdot\mathbf{A}_q\cdot\mathbf{W}_q^0] , \tag{5.14}$$

where $(\mathbf{N}^T)_{pq}$ is the 3×3 matrix which is the pq element of the transpose of the $3N\times3N$ matrix $\mathbf{N}$ given by Eq. (2.93), and $(\mathbf{C}^{-1})_{pq}$ is the 3×3 matrix which is the pq element of the inverse of the

$3N\times3N$ matrix $\mathbf{C}$ given by Eq. (2.94).

From Eqs. (5.12), (5.13), and (5.14), we then obtain in the regime of linear response

$$\sum_{p=1}^{N+1}\langle\mathbf{R}_p\mathbf{F}_p\rangle = -\tfrac{1}{2}\sum_{p_1,p_2=1}^{N}\langle\mathbf{a}_{p_1}(\mathbf{N}^T)_{p_1p_2}\cdot\mathbf{L}_{p_2}\int_{-\infty}^{t}e^{-L(t-s)}\varepsilon(s)(\mathscr{L}\Gamma + X')ds\rangle_{\mathrm{eq}}$$

$$-\tfrac{1}{2}\zeta_r\varepsilon\sum_{p_1,p_2=1}^{N}\langle\mathbf{a}_{p_1}(\mathbf{C}^{-1})_{p_1p_2}\mathbf{a}_{p_2}\rangle_{\mathrm{eq}}:(\mathbf{e}_x\mathbf{e}_y + \mathbf{e}_y\mathbf{e}_x)\ . \tag{5.15}$$

Since the excess stress tensor given by Eq. (5.4) is symmetric, we may assume that the tensor on the left-hand side of Eq. (5.15) is symmetric. Then, we have

$$\sum_{p=1}^{N+1}\langle\mathbf{R}_p\mathbf{F}_p\rangle:\mathbf{e}_x\mathbf{e}_y$$

$$= -\tfrac{1}{4}\varepsilon\left\{\int_0^{\infty}e^{-i\omega s}\left[\frac{\partial^2}{\partial s^2}\langle\Gamma(0)\Gamma(s)\rangle_{\mathrm{eq}} + \frac{\partial}{\partial s}\langle\Gamma(0)X'(s)\rangle_{\mathrm{eq}}\right]ds\right.$$

$$\left. + \zeta_r(\mathbf{e}_x\mathbf{e}_y + \mathbf{e}_y\mathbf{e}_x):\sum_{p_1,p_2=1}^{N}\langle\mathbf{a}_{p_1}(\mathbf{C}^{-1})_{p_1p_2}\mathbf{a}_{p_2}\rangle_{\mathrm{eq}}:(\mathbf{e}_x\mathbf{e}_y + \mathbf{e}_y\mathbf{e}_x)\right\}\ . \tag{5.16}$$

The functions Γ and X' may be written in terms of the normalized Wigner functions $\mathscr{D}$ defined by Eq. (2.5) as follows,

$$\Gamma = \tfrac{4}{3}\pi^2a^2i\sum_{p_1,p_2=1}^{N}(B^{-1})_{p_1p_2}[-\mathscr{D}_1^{10}(\Omega_{p_1})\mathscr{D}_1^{10}(\Omega_{p_2}) + \mathscr{D}_1^{(-1)0}(\Omega_{p_1})\mathscr{D}_1^{(-1)0}(\Omega_{p_2})]\ , \tag{5.17}$$

$$X' = \sum_{p=1}^{N}\Psi_{\mathrm{eq}}^{-1}\,\mathbf{L}_p\,\Psi_{\mathrm{eq}}\cdot\tfrac{2\sqrt{3}}{3}\pi\begin{pmatrix} -\mathscr{D}_1^{01}(\Omega_p) + \mathscr{D}_1^{0(-1)}(\Omega_p) \\ -i\mathscr{D}_1^{01}(\Omega_p) - i\mathscr{D}_1^{0(-1)}(\Omega_p) \\ \sqrt{2}\,\mathscr{D}_1^{00}(\Omega_p)\end{pmatrix}\ . \tag{5.18}$$

From these equations and Eqs. (3.3) and (3.4), it is seen that Γ is a function which belongs to a class of functions specified by the "total angular momentum quantum number" $L=2$ and the "total magnetic quantum number" $M=\pm 2$, and that X' is a function with $L=1$ and $M=0$ (see Sec. 3-2). Since there is no correlation between functions having different pairs of L and M [see Eq. (3.23)], the time-correlation function $<\Gamma(0)X'(s)>_{eq}$ in Eq. (5.16) vanishes, and we have

$$\sum_{p=1}^{N+1} <\mathbf{R}_p\mathbf{F}_p>:\mathbf{e}_x\mathbf{e}_y = -\frac{1}{4}\epsilon\left[\int_0^\infty e^{-i\omega s}\frac{\partial^2}{\partial s^2}<\Gamma(0)\Gamma(s)>_{eq}ds\right.$$

$$\left. + \zeta_r(\mathbf{e}_x\mathbf{e}_y + \mathbf{e}_y\mathbf{e}_x):\sum_{p_1,p_2=1}^{N} <\mathbf{a}_{p_1}(\mathbf{C}^{-1})_{p_1p_2}\mathbf{a}_{p_2}>_{eq}:(\mathbf{e}_x\mathbf{e}_y + \mathbf{e}_y\mathbf{e}_x)\right]. \qquad (5.19)$$

Integration by parts of the first term in the square brackets on the right-hand side of Eq. (5.19) leads to an alternative expression,

$$\sum_{p=1}^{N+1} <\mathbf{R}_p\mathbf{F}_p>:\mathbf{e}_x\mathbf{e}_y = -\frac{1}{4}\epsilon\left[i\omega\int_0^\infty e^{-i\omega s}\frac{\partial}{\partial s}<\Gamma(0)\Gamma(s)>_{eq}ds\right.$$

$$\left. + (\mathbf{e}_x\mathbf{e}_y + \mathbf{e}_y\mathbf{e}_x):\sum_{p_1,p_2=1}^{N} <\mathbf{a}_{p_1}(B^{-1})_{p_1p_2}\mathbf{I}\quad\mathbf{a}_{p_2}>_{eq}:(\mathbf{e}_x\mathbf{e}_y + \mathbf{e}_y\mathbf{e}_x)\right]. \qquad (5.20)$$

Next we consider the second sum $\sum_{p=1}^{N} <\int_{S_p}\mathbf{r}_p\mathbf{F}_p^{(S)}(\mathbf{r}_p)d\mathbf{r}_p>$ Under the nonslip boundary condition, the frictional forces $\mathbf{F}_p^{(S)}(\mathbf{r}_p)$ ($p = 1, 2, \cdots, N$) satisfy the coupled integral equations,

$$\mathbf{V}_p + \mathbf{W}_p\times\mathbf{r}_p - \mathbf{V}^0(\mathbf{R}_p + \mathbf{r}_p)$$

$$= (8\pi\eta_0)^{-1}\int_{S_p}\mathbf{K}_p(\mathbf{r}_p,\mathbf{r}_p')\cdot\mathbf{F}_p^{(S)}(\mathbf{r}_p')d\mathbf{r}_p'$$

$$+\sum_{\substack{q=1\\ \neq p}}^{N}\int_{S_q}\mathbf{T}(\mathbf{R}_p+\mathbf{r}_p-\mathbf{R}_q-\mathbf{r}_q)\cdot\mathbf{F}_q^{(S)}(\mathbf{r}_q)d\mathbf{r}_q$$

$$+\mathbf{T}(\mathbf{R}_p+\mathbf{r}_p-\mathbf{R}_{N+1})\cdot\mathbf{F}_{N+1}\qquad(p=1,2,\cdots,N)\,,\tag{5.21}$$

where $\mathbf{V}_p$ and $\mathbf{W}_p$ are the translational and angular velocities of the pth subbody, respectively, $\mathbf{T}(\mathbf{R})$ is the Oseen tensor[4] and

$$\mathbf{K}_p(\mathbf{r}_p,\mathbf{r}_p')=8\pi\eta_0\mathbf{T}(\mathbf{r}_p-\mathbf{r}_p')\,.\tag{5.22}$$

We expand $\mathbf{T}(\mathbf{R}_p+\mathbf{r}_p-\mathbf{R}_q-\mathbf{r}_q)$ in a Taylor series around $\mathbf{r}_p-\mathbf{r}_q=0$,

$$\mathbf{T}(\mathbf{R}_p+\mathbf{r}_p-\mathbf{R}_q-\mathbf{r}_q)=\mathbf{T}(\mathbf{R}_p-\mathbf{R}_q)+(\mathbf{r}_p-\mathbf{r}_q)\cdot\nabla\,\mathbf{T}(\mathbf{R}_p-\mathbf{R}_q)$$

$$+\tfrac{1}{2}(\mathbf{r}_p-\mathbf{r}_q)(\mathbf{r}_p-\mathbf{r}_q):\nabla\nabla\,\mathbf{T}(\mathbf{R}_p-\mathbf{R}_q)+\cdots,\tag{5.23}$$

where the nth term is of $\mathcal{O}(|\mathbf{R}_p-\mathbf{R}_q|^{-n})$, and we neglect terms of $n\geq 2$, as done in Chap. 2. This is equivalent to replacing $\mathbf{T}(\mathbf{R}_p+\mathbf{r}_p-\mathbf{R}_q-\mathbf{r}_q)$ by $T(\mathbf{R}_p-\mathbf{R}_q)$. Similarly, $\mathbf{T}(\mathbf{R}_p+\mathbf{r}_p-\mathbf{R}_{N+1})$ may be replaced by $\mathbf{T}(\mathbf{R}_p-\mathbf{R}_{N+1})$ Then, Eq. (5.21) becomes

$$(8\pi\eta_0)^{-1}\int_{S_p}\mathbf{K}_p(\mathbf{r}_p,\mathbf{r}_p')\cdot\mathbf{F}_p^{(S)}(\mathbf{r}_p')d\mathbf{r}_p'$$

$$=-\tfrac{1}{2}\varepsilon(\mathbf{e}_x\mathbf{e}_y+\mathbf{e}_y\mathbf{e}_x)\cdot\mathbf{r}_p+(\mathbf{W}_p-\mathbf{W}_p^0)\times\mathbf{r}_p$$

$$+\mathbf{V}_p-\varepsilon\mathbf{e}_x\mathbf{e}_y\cdot\mathbf{R}_p-\sum_{\substack{q=1\\ \neq p}}^{N+1}\mathbf{T}(\mathbf{R}_p-\mathbf{R}_q)\cdot\mathbf{F}_q\,.\tag{5.24}$$

Now we define the inverse $\mathbf{K}_p^{-1}(\mathbf{r}_p,\mathbf{r}_q')$ by

$$\delta^{(2)}(\mathbf{r}_p-\mathbf{r}_p')\mathbf{I}=\int_{S_p}\mathbf{K}_p^{-1}(\mathbf{r}_p,\mathbf{r}_p'')\cdot\mathbf{K}_p(\mathbf{r}_p'',\mathbf{r}_p')d\mathbf{r}_p''$$

$$= \int_{S_p} \mathbf{K}_p(\mathbf{r}_p,\mathbf{r}_p'') \cdot \mathbf{K}_p^{-1}(\mathbf{r}_p'',\mathbf{r}_p') d\mathbf{r}_p'' , \tag{5.25}$$

where $\delta^{(2)}(\mathbf{r})$ is the two-dimensional Dirac delta function on the surface of the pth subbody. [It is not to be confused with the inverse $\mathbf{K}_p(\mathbf{r}_p,\mathbf{r}_q')^{-1}$ of the 3×3 matrix $\mathbf{K}_p(\mathbf{r}_p,\mathbf{r}_q')$.] With this inverse, we have formally

$$\begin{aligned}
&- \int_{S_p} \mathbf{r}_p \mathbf{F}_p^{(S)}(\mathbf{r}_p) d\mathbf{r}_p \\
&= \tfrac{\varepsilon}{2} \left[8\pi\eta_0 \int_{S_p} d\mathbf{r}_p \int_{S_p} d\mathbf{r}_p' \mathbf{r}_p \mathbf{K}_p^{-1}(\mathbf{r}_p,\mathbf{r}_p') \mathbf{r}_p' \right] : (\mathbf{e}_x\mathbf{e}_y + \mathbf{e}_y\mathbf{e}_x) \\
&\quad + \left\{ 8\pi\eta_0 \int_{S_p} d\mathbf{r}_p \int_{S_p} d\mathbf{r}_p' \mathbf{r}_p \left[\mathbf{K}_p^{-1}(\mathbf{r}_p,\mathbf{r}_p') \times \mathbf{r}_p' \right] \right\} \cdot (\mathbf{W}_p - \mathbf{W}_p^0) \\
&\quad - \left[8\pi\eta_0 \int_{S_p} d\mathbf{r}_p \int_{S_p} d\mathbf{r}_p' \mathbf{r}_p \mathbf{K}_p^{-1}(\mathbf{r}_p,\mathbf{r}_p') \right] \\
&\quad \cdot \left[\mathbf{V}_p - \tfrac{1}{2}\varepsilon\, \mathbf{e}_x\mathbf{e}_y \cdot \mathbf{R}_p - \sum_{\substack{q=1 \\ \neq p}}^{N+1} \mathbf{T}(\mathbf{R}_p - \mathbf{R}_q) \cdot \mathbf{F}_q \right] .
\end{aligned} \tag{5.26}$$

Considering the fact that the stress tensor is symmetric, the xy component of the tensor on the left-hand side of Eq. (5.26) is found to be

$$\begin{aligned}
&\tfrac{1}{2}(\mathbf{e}_x\mathbf{e}_y + \mathbf{e}_y\mathbf{e}_x) : \left[- \int_{S_p} \mathbf{r}_p \mathbf{F}_p^{(S)}(\mathbf{r}_p) d\mathbf{r}_p \right] \\
&= \tfrac{\varepsilon}{4}(\mathbf{e}_x\mathbf{e}_y + \mathbf{e}_y\mathbf{e}_x) : \left[8\pi\eta_0 \int_{S_p} d\mathbf{r}_p \int_{S_p} d\mathbf{r}_p' \mathbf{r}_p \mathbf{K}_p^{-1}(\mathbf{r}_p,\mathbf{r}_p') \mathbf{r}_p' \right] : (\mathbf{e}_x\mathbf{e}_y + \mathbf{e}_y\mathbf{e}_x)
\end{aligned}$$

$$- \left[\mathbf{A}_p \cdot (\mathbf{W}_p - \mathbf{W}_p^0) \right] \cdot \tau_p : \left[\mathbf{A}_p^T \cdot \tfrac{1}{2}(\mathbf{e}_x\mathbf{e}_y + \mathbf{e}_y\mathbf{e}_x) \cdot \mathbf{A}_p \right]$$

$$+ \left\{ \mathbf{A}_p \cdot \left[\mathbf{V}_p - \tfrac{1}{2}\varepsilon\, \mathbf{e}_x\mathbf{e}_y \cdot \mathbf{R}_p - \sum_{\substack{q=1 \\ \neq p}}^{N+1} \mathbf{T}(\mathbf{R}_p - \mathbf{R}_q) \cdot \mathbf{F}_q \right] \right\}$$

$$\cdot \varphi_p : \left[\mathbf{A}_p^T \cdot \tfrac{1}{2}(\mathbf{e}_x\mathbf{e}_y + \mathbf{e}_y\mathbf{e}_x) \cdot \mathbf{A}_p \right] , \tag{5.27}$$

where φ_p and τ_p are triadics whose components are expressed in the pth localized coordinate system, and are defined by

$$\varphi_p = - 8\pi\eta_0 \int_{S_p} \Psi_1(\hat{\mathbf{r}}_p)^T \, \hat{\mathbf{r}}_p d\hat{\mathbf{r}}_p , \tag{5.28}$$

$$\tau_p = - 8\pi\eta_0 \int_{S_p} \Psi_2(\hat{\mathbf{r}}_p)^T \, \hat{\mathbf{r}}_p d\hat{\mathbf{r}}_p , \tag{5.29}$$

with the tensors Ψ_1 and Ψ_2 being the solutions of the integral equations,

$$\int_{S_p} \mathbf{K}(\hat{\mathbf{r}}_p, \hat{\mathbf{r}}_p') \cdot \Psi_1(\hat{\mathbf{r}}_p') d\hat{\mathbf{r}}_p' = \mathbf{I} , \tag{5.30}$$

$$\int_{S_p} \mathbf{K}(\hat{\mathbf{r}}_p, \hat{\mathbf{r}}_p') \cdot \Psi_2(\hat{\mathbf{r}}_p') d\hat{\mathbf{r}}_p' = \mathbf{B}_0(\hat{\mathbf{r}}_p) . \tag{5.31}$$

In Eqs. (5.28)–(5.31), the caret on $\mathbf{r}_p$ indicates that it is expressed in the pth localized coordinate system. Thus the triadics φ_p and τ_p are independent of the bead number p, and correspond to the shear force and torque triadics introduced by Brenner,[12] respectively.

In Chap. 2, we have characterized hydrodynamically the subbody by the translational friction coefficient ζ_t and the rotatory

friction coefficient ζ_r. This implies that the hydrodynamic anisotropy of the subbody is neglected as far as its motion is concerned, and it is replaced by a hypothetical sphere whose translational and rotatory friction tensors are isotropic but do not necessarily satisfy the relation for the sphere. Thus, it is consistent with this situation to use the values of φ_p and τ_p for the sphere. According to Brenner,[12] they vanish for spherically isotropic bodies. Therefore, Eq. (5.27) reduces to

$$\tfrac{1}{2}(\mathbf{e}_x\mathbf{e}_y + \mathbf{e}_y\mathbf{e}_x):\left[-\int_{S_p} \mathbf{r}_p\mathbf{F}_p^{(S)}(\mathbf{r}_p)d\mathbf{r}_p \right]$$

$$= \tfrac{\varepsilon}{4}(\mathbf{e}_x\mathbf{e}_y + \mathbf{e}_y\mathbf{e}_x):\left[8\pi\eta_0\int_{S_p} d\mathbf{r}_p\int_{S_p} d\mathbf{r}'_p\mathbf{r}_p\mathbf{K}_p^{-1}(\mathbf{r}_p,\mathbf{r}'_p)\mathbf{r}'_p \right]:(\mathbf{e}_x\mathbf{e}_y + \mathbf{e}_y\mathbf{e}_x) . \quad (5.32)$$

As shown in Appendix 5-C, the right-hand side of Eq. (5.32) represents the increment of the xy component of the stress tensor due to the single sphere, and is given by

$$\tfrac{1}{2}(\mathbf{e}_x\mathbf{e}_y + \mathbf{e}_y\mathbf{e}_x):\left[-\int_{S_p} \mathbf{r}_p\mathbf{F}_p^{(S)}(\mathbf{r}_p)d\mathbf{r}_p \right] = 5\pi\eta_0\varepsilon d_E^3/12 \quad (5.33)$$

with d_E the diameter of the sphere. This gives the intrinsic viscosity of the Einstein sphere.

c. Correlation function $<\Gamma(0)\Gamma(t)>_{eq}$

By the use of Eqs. (3.3), (3.44), and (3.47), the function Γ given by Eq. (5.17) may be written in terms of the one-body excitation

Fourier basis functions $F^{M,j}_{L,[k]}(\{\Omega_N\})$ defined by Eq. (3.47), as follows,

$$\Gamma = (8\pi^2)^N (a^2\zeta_t/6)i \sum_{k=1}^{N} (\lambda_k^B)^{-1} \sum_{j_1,j_2=-1}^{1} \overline{\mathscr{D}}_1^{0j_1*}(\Omega_a)\ \overline{\mathscr{D}}_1^{0j_2*}(\Omega_a)$$

$$\times\left(- F^{1,j_1}_{1,[k]}\ F^{1,j_2}_{1,[k]} + F^{(-1),j_1}_{1,[k]}\ F^{(-1),j_2}_{1,[k]}\right) , \tag{5.34}$$

where λ_k^B is the kth approximate eigenvalue of the matrix B defined by Eq. (3.44), $\overline{\mathscr{D}}^{mj}_L$ is the unnormalized Wigner function defined by Eq. (2.11), Ω_a is given by Eq. (2.12), and the asterisk indicates the complex conjugate.

From Eqs. (3.4) and (3.47) and Eqs. (5D.3) and (5D.4), it can be shown that the product $F^{(\pm1),j_1}_{1,[k]}F^{(\pm1),j_2}_{1,[k]}$ in Eq. (5.34) may be written in terms of $F^{(\pm2),j}_{2,[k]}$ $(j = -2,\ -1,\ \cdots,\ 2)$ and $F^{(\pm2),(j_1j_2)}_{2,(11)[kk]}$ with $F^{M,(j_1j_2)}_{L,(l_1l_2)[k_1k_2]}$ being the two-body excitation Fourier basis functions defined by Eq. (5D.3). Since both $\{F^{(\pm2),(j_1j_2)}_{2,(11)[kk]}\}$ and $\{F^{(\pm2),j}_{2,[k]}\}$ are the standard basis sets with $L = 2$ and $M = \pm2$ (see Sec. 3-2), $\{F^{(\pm1),j_1}_{1,[k]}F^{(\pm1),j_2}_{1,[k]}\}$ is also a standard one with $L = 2$ and $M = \pm2$, and therefore Γ is the function with $L = 2$ and $M = \pm2$, as already mentioned. Thus, in order to evaluate the correlation function $<\Gamma(0)\Gamma(t)>_{eq}$, it is convenient to use $\{F^{(\pm1),j_1}_{1,[k]}F^{(\pm1),j_2}_{1,[k]}\}$ as a basis set, which is a hybrid of the one- and two-body excitation basis functions.

The correlation functions of the standard basis functions are diagonal in L and M, and their values are independent of M (see Sec. 3-2). With these properties, $<\Gamma(0)\Gamma(t)>_{eq}$ may be simply

written as

$$<\Gamma(0)\Gamma(t)>_{eq} = (8\pi^2)^{2N}[(a^2\zeta_t)^2/18]\sum_{k,k'=1}^{N}(\lambda_k^B\lambda_{k'}^B)^{-1}$$

$$\times\sum_{j_1,j_2,j_1',j_2'=-1}^{1}\overline{\mathscr{D}}_1^{0j_1}(\Omega_a)\,\overline{\mathscr{D}}_1^{0j_2}(\Omega_a)\,\overline{\mathscr{D}}_1^{0j_1'*}(\Omega_a)\,\overline{\mathscr{D}}_1^{0j_2'*}(\Omega_a)\,C_{2,[k,k']}^{(j_1j_2;\,j_1'j_2')}(t) \qquad (5.35)$$

with

$$C_{2,[k,k']}^{(j_1j_2;\,j_1'j_2')}(t) = <F_{1,[k]}^{1;\,j_1^*}\,F_{1,[k]}^{1;\,j_2^*}\,e^{-Lt}\,F_{1,[k']}^{1;\,j_1'}\,F_{1,[k']}^{1;\,j_2'}>_{eq}\,. \qquad (5.36)$$

Now, the problem is to evaluate the correlation functions $C_{2,[k,k']}^{(j_1j_2;\,j_1'j_2')}(t)$. It is equivalent to the eigenvalue problem for the matrix representations of of the identity operator and the diffusion operator $\mathscr{L}$ with weight Ψ_{eq}. For this purpose, we use the subspace approximation i.e., evaluate the correlation functions without taking account of correlations between the subspace spanned by the basis set $\{F_{1,[k]}^{1;\,j_1}F_{1,[k]}^{1;\,j_2}\}$ and its complementary space. With this approximation, we need only the elements of the above matrix representations in this subspace. They are evaluated to be

$$<F_{1,[k]}^{1;\,j_1^*}\,F_{1,[k]}^{1;\,j_2^*}\,F_{1,[k']}^{1;\,j_1'}\,F_{1,[k']}^{1;\,j_2'}>_{eq}$$

$$= (8\pi^2)^{-N}\left[\overline{E}_{2,(11,11)[kk,\,k'k']}^{(j_1j_2,\,j_1'j_2')} + \mathscr{O}(N^{-1})\right], \qquad (5.37)$$

$$<F_{1,[k]}^{1;\,j_1^*}\,F_{1,[k]}^{1;\,j_2^*}\,\mathscr{L}\,F_{1,[k']}^{1;\,j_1'}\,F_{1,[k']}^{1;\,j_2'}>_{eq}$$

$$= (8\pi^2)^{-N}\left[\overline{L}_{2,(11,11)[kk,\,k'k']}^{(j_1j_2,\,j_1'j_2')} + \mathscr{O}(N^{-1})\right], \qquad (5.38)$$

where $\overline{E}^{(j_1 j_2,\, j_1' j_2')}_{L,(l_1 l_2,\, l_1' l_2')[k_1 k_2,\, k_1' k_2']}$ and $\overline{L}^{(j_1 j_2,\, j_1' j_2')}_{L,(l_1 l_2,\, l_1' l_2')[k_1 k_2,\, k_1' k_2']}$ are the standard Fourier representations of the identity and diffusion operators given by Eqs. (5D.6) and (5D.7), respectively.

For this case of $l_1=l_2=l_1'=l_2'=1$, $k_1=k_2=k$, and $k_1'=k_2'=k$, the independent elements of $\overline{E}^{(j_1 j_2,\, j_1' j_2')}_{2,(11,11)[kk,\,k'k']}$, $\overline{L}^{(j_1 j_2,\, j_1' j_2')}_{2,(11,11)[kk,\,k'k']}$, and $C^{(j_1 j_2,\, j_1' j_2')}_{2,[k,k']}$ are the ones with pairs of indices (j_1,j_2) and $(j_1',j_2')=(-1,-1)$, $(-1,0)$, $(-1,1)$, $(0,0)$, $(0,1)$, and $(1,1)$. We designate these pairs by J and $J'=1,2,\cdots,6$ in that order, for simplicity, and write, for instance, $\overline{E}^{(j_1 j_2,\, j_1' j_2')}_{2,(11,11)[kk,\,k'k']}$ as $\overline{E}^{(J,\,J')}_{2,(11,11)[kk,\,k'k']}$. Taking account of the fact that both $\overline{E}^{(J,\,J')}_{2,(11,11)[kk,\,k'k']}$ and $\overline{L}^{(J,\,J')}_{2,(11,11)[kk,\,k'k']}$ are diagonal in k [see Eqs. (5D.6) and (5D.7)], we have only to solve the following six-dimensional eigenvalue problem,

$$Q^{\dagger}_{2(2),[k]}\ \overline{E}_{2(2),[k]}\ Q_{2(2),[k]} \;=\; 1_{2(2),[k]}\ , \tag{5.39}$$

$$Q^{\dagger}_{2(2),[k]}\ \overline{L}_{2(2),[k]}\ Q_{2(2),[k]} \;=\; \Lambda_{2(2),[k]}\ , \tag{5.40}$$

where $\overline{E}_{2(2),[k]}$ and $\overline{L}_{2(2),[k]}$ are the 6×6 matrices whose JJ' elements are $\overline{E}^{(J,\,J')}_{2,(11,11)[kk,\,k'k']}$ and $\overline{L}^{(J,\,J')}_{2,(11,11)[kk,\,k'k']}$, respectively, $1_{2(2),[k]}$ and $\Lambda_{2(2),[k]}$ are 6×6 diagonal matrices with diagonal elements 1 and $\lambda^{J}_{2(2),k}$ ($J=1$–6), respectively, $Q_{2(2),[k]}$ is a diagonalizing matrix (not unitary), and the dagger indicates the adjoint.

Since $\overline{E}^{(J,\,J')}_{2,(11,11)[kk,\,k'k']}$ is diagonal in J, the eigenvalue problem given by Eqs. (5.39) and (5.40) reduces to the eigenvalue problem,

$$Q^{L\dagger}_{2(2),[k]}\left[(\overline{E}_{2(2),[k]})^{-1/2}\ \overline{L}_{2(2),[k]}\ (\overline{E}_{2(2),[k]})^{-1/2}\right] Q^{L}_{2(2),[k]} \;=\; \Lambda_{2(2),[k]}\ , \tag{5.41}$$

where $(\overline{E}_{2(2),[k]})^{-1/2}$ is the 6×6 diagonal matrix with diagonal elements $(\overline{E}^{(J,J)}_{2,(11,11)[kk,kk]})^{-1/2}$, and $Q^{L}_{2(2),[k]}$ is a unitary, diagonalizing matrix. From a comparison of the left-hand sides of Eqs. (5.50) and (5.41), we have a relation between the above two diagonalizing matrix, i. e.,

$$Q_{2(2),[k]} = (\overline{E}_{2(2),[k]})^{-1/2} Q^{L}_{2(2),[k]} . \tag{5.42}$$

The correlation functions $C^{(J,J')}_{2,[k,k']}$ may then be written in terms of the solutions of Eqs. (5.41) as

$$C_{2,[k]}(t) = (\overline{E}_{2(2),[k]})^{1/2} Q^{L}_{2(2),[k]} \exp(-\Lambda_{2(2),[k]}t) Q^{L\dagger}_{2(2),[k]} (\overline{E}_{2(2),[k]})^{1/2} , \tag{5.43}$$

where $C_{2,[k]}$ is the 6×6 matrix whose JJ' element is $C^{(J,J')}_{2,[k,k]}$, and $(\overline{E}_{2(2),[k]})^{1/2}$ is the 6×6 diagonal matrix with diagonal elements $(\overline{E}^{(J,J)}_{2,(11,11)[kk,kk]})^{1/2}$. Note that the correlation function $C^{(J,J')}_{2,[k,k']}$ is also diagonal in k, since both $\overline{E}^{(J,J')}_{2,(11,11)[kk,k'k']}$ and $\overline{L}^{(J,J')}_{2,(11,11)[kk,k'k']}$ are diagonal in k. By the use of Eqs. (5D.5), Eq. (5.43), and the solution of the eigenvalue problem given by Eq. (5.41) (which is given in Appendix 5-E), the correlation function $<\Gamma(0)\Gamma(t)>_{eq}$ given by Eq. (35) may be finally written as

$$<\Gamma(0)\Gamma(t)>_{eq} = \tfrac{1}{9}(a^2\zeta_t)^2 \sum_{k=1}^{N}(\lambda^B_k)^{-2}(\kappa_0^2\nu^{-2}g^1_{1,k} + \tau_0^2\nu^{-2}g^0_{1,k})^2$$

$$\times\sum_{J=1}^{3}(Q^{(1)}_{[k],1J})^2 e^{-\lambda^J_{2(2),k}t} , \tag{5.44}$$

where $g^j_{l,k}$ is given by Eq. (5D.9), $Q^{(1)}_{[k],1J}$ is $1J$ element of the 3×3 transformation matrix $Q^{(1)}_{[k]}$ defined by Eq. (5E.13), and $\lambda^J_{2(2),k}$ is given

by Eq. (5E.20). Note that the three eigenvalues $\lambda^{J}_{2(2),k}$ (J=1,2,3) make contribution to $<\Gamma(0)\Gamma(t)>_{eq}$.

d. Final expression for $[\eta]$

In order to obtain a final expression for $[\eta]$ suitable for numerical calculations, we rewrite the second terms in the square brackets on the right-hand sides of Eqs. (5.19) and (5.20) in the form,

$$\zeta_r(\mathbf{e}_x\mathbf{e}_y + \mathbf{e}_y\mathbf{e}_x):\sum_{p_1,p_2=1}^{N}<\mathbf{a}_{p_1}(\mathbf{C}^{-1})_{p_1p_2}\mathbf{a}_{p_2}>_{eq}:(\mathbf{e}_x\mathbf{e}_y + \mathbf{e}_y\mathbf{e}_x)$$

$$= \tfrac{2}{3}\zeta_r\sum_{k=1}^{N}(\lambda_k^C)^{-1}(\kappa_0^2\nu^{-2}S^{(0)1}_{1,kk} + \tau_0^2\nu^{-2}S^{(0)0}_{1,kk}) , \tag{5.45}$$

$$(\mathbf{e}_x\mathbf{e}_y + \mathbf{e}_y\mathbf{e}_x):\sum_{p_1,p_2=1}^{N}<\mathbf{a}_{p_1}(B^{-1})_{p_1p_2}\mathbf{a}_{p_2}>_{eq}:(\mathbf{e}_x\mathbf{e}_y + \mathbf{e}_y\mathbf{e}_x)$$

$$= \tfrac{2}{3}a^2\zeta_t\sum_{k=1}^{N}(\lambda_k^B)^{-1}(\kappa_0^2\nu^{-2}S^{(0)1}_{1,kk} + \tau_0^2\nu^{-2}S^{(0)0}_{1,kk}) , \tag{5.46}$$

where λ_k^C is the kth approximate eigenvalue of the matrix $a^{-2}C$ with C being the $N\times N$ matrix defined by Eq. (2.112) and is given by Eq. (3.46), and $S^{(0)J}_{L,kk}$ is given by Eq. (3.54). Note that in obtaining Eq. (5.45), we have replaced $(\mathbf{C}^{-1})_{p_1p_2}$ by $(C^{-1})_{p_1p_2}\mathbf{I}$ with $(C^{-1})_{p_1p_2}$ the p_1p_2 element of the inverse of C, i.e., preaveraged the constraining matrix $\mathbf{C}^{-1}$, as done in Sec. 2-3*c*.

Substitution of Eqs. (5.19) and (5.33) with Eqs. (5.44) and (5.45)

into Eq. (5.3) with Eq. (5.4) leads to the desired expression,

$$[\eta] = [N_A(a^2\zeta_t)^2/36\eta_0 M] \sum_{k=1}^{N}(\lambda_k^B)^{-2}(\kappa_0^2\nu^{-2}g_{1,k}^1 + \tau_0^2\nu^{-2}g_{1,k}^0)^2$$

$$\times\sum_{J=1}^{3}(Q_{[k],1J}^{(1)})^2(\lambda_{2(2),k}^J)^2/(\lambda_{2(2),k}^1 + i\omega) + [\eta]_\infty , \tag{5.47}$$

where $[\eta]_\infty$ is the value of $[\eta]$ in the limit of $\omega \longrightarrow \infty$ and is given by

$$[\eta]_\infty = (N_A\zeta_r/6\eta_0 M) \sum_{k=1}^{N}(\lambda_k^C)^{-1}(\kappa_0^2\nu^{-2}S_{1,kk}^{(0)1} + \tau_0^2\nu^{-2}S_{1,kk}^{(0)0})$$

$$+ 5\pi N_A N d_E^3/12M . \tag{5.48}$$

Substitution of Eqs. (5.20) and (5.33) with Eqs. (5.44) and (5.46) into Eq. (5.3) with Eq. (5.4) leads to the alternative expression,

$$[\eta] = [N_A(a^2\zeta_t)^2/36\eta_0 M] \sum_{k=1}^{N}(\lambda_k^B)^{-2}(\kappa_0^2\nu^{-2}g_{1,k}^1 + \tau_0^2\nu^{-2}g_{1,k}^0)^2$$

$$\times\sum_{J=1}^{3}(Q_{[k],1J}^{(1)})^2(-i\omega\lambda_{2(2),k}^J)/(\lambda_{2(2),k}^1 + i\omega) + [\eta]_0 , \tag{5.49}$$

where $[\eta]_0$ is the value of $[\eta]$ at $\omega = 0$ and is given by

$$[\eta]_0 = (N_A a^2\zeta_t/6\eta_0 M) \sum_{k=1}^{N}(\lambda_k^B)^{-1}(\kappa_0^2\nu^{-2}S_{1,kk}^{(0)1} + \tau_0^2\nu^{-2}S_{1,kk}^{(0)0})$$

$$+ 5\pi N_A N d_E^3/12M. \tag{5.50}$$

Note that in the Gaussian coil limit ($N \longrightarrow \infty$ and $\Delta s \longrightarrow \infty$,) a becomes equal to its effective bond length with $S_{1,kk}^{(0)J}=1$, and then $[\eta]_0$ given by Eq. (5.50) is the correct zero-frequency intrinsic viscosity of the spring-bead model,[4] apart from the second term

on the right-hand side of Eq. (5.50).

It is pertinent here to make two remarks on Eqs. (5.47)-(5.50). First, the second terms on the right-hand sides of Eqs. (5.48) and (5.50) arise from the contributions of the Einstein spherical subbodies (beads). Second, the two expressions for $[\eta]$, i.e., Eq. (4.47) with Eq. (5.48) and Eq. (5.49) with Eq. (5.50), are no longer equivalent to each other, since we have made the approximations to evaluate the correlation function $<\Gamma(0)\Gamma(t)>_{eq}$ and the $[\eta]_\infty$ given by Eq. (5.48). Therefore, $[\eta]$ given by Eq. (5.47) with $\omega=0$ is not identical with $[\eta]_0$ given by Eq. (5.50), nor is $[\eta]$ given by Eq. (5.49) with $\omega=\infty$ identical with $[\eta]_\infty$ given by Eq. (5.49).

5-3. Eigenvalue Spectra

As in the case of the eigenvalues $\lambda^0_{1,k}$, which form the lowest of the $L=1$ branches of the spectrum,[2] the eigenvalues $\lambda^1_{2(2),k}$, which form the lowest in the present case, may possibly become negative at small wave numbers k. Therefore, in order to eliminate the negative eigenvalues, we must first examine the behavior of the lowest branch in the coil limit of $N\gg1$ and $k/(N+1)\ll1$, as done in Sec. 3-5*b*.

In this limit, the functions $g^j_{l,k}$ defined by Eq. (5D.9) become equal to $S^{(0)j}_{l,kk}$, whose asymptotic form is explicitly given by Eq. (3.81). Similarly, the functions $S^j_{l,k}$ ($l\neq0$) defined by Eq. (5E.7)

become equal to $S^{(1)J}_{l,kk}$ defined by Eq. (3.55), whose asymptotic form is given by Eq. (3.83). Moreover, the term $(1-1/2N)(\lambda^C_k)^{-1}$ appearing in Eqs. (5E.3)–(5E.6) becomes equal to $S^{(1)0}_{0,kk}$, whose asymptotic form is given by Eq. (3.82). From these correspondences, we find that the function $a-2d$, b, and c with a, b, c, and d being defined by Eqs. (5E.3)–(5E.6) are equivalent to the functions $2\alpha^{-1}(a+d)$, $2\beta^{-1}b$, and $(\alpha\beta)^{-1/2}c$ defined in Appendix 3–A, respectively. Thus, in the coil limit, it can be shown that

$$\lambda^1_{2(2),k} = 2\lambda^0_{1,k} \qquad \text{(coil limit)}. \tag{5.51}$$

The eigenvalues $\lambda^0_{1,k}$ are relevant to dielectric relaxation of polymers having dipoles parallel to the chain contour, and therefore Eq. (5.51) agrees exactly with the relation between the viscoelastic and dielectric relaxation rates for the spring–bead model.[3,4,13]

Equation (5.51) suggests that we may eliminate the negative eigenvalues by the simple procedure as in Chap. 3, i. e., by replacing $\lambda^J_{2(2),k}$ by $\lambda^J_{2(2),k}-\lambda^J_{2(2),0}$, as far as the eigenvalues themselves are concerned. This is referred to as procedure A. In the case of $[\eta]$, however, we must also give attention to the behavior of the transformation matrix $Q^{(1)}_{[k]}$ at small wave numbers k, since it determines the relative amplitudes of the $J=2$ and 3 branches (relevant to the local motions). From Eq. (5.47) or (5.49), it is seen that the contributions of these branches diverge unless $Q^{(1)}_{[k],1J}$ ($J=2,3$) vanish in the limit of $k \longrightarrow 0$, since the factor $(\lambda^B_k)^{-2}/M$ diverges in this limit. Therefore, in addition to the requirement on the

lowest branch, it must be required that $Q^{(1)}_{[k],1J}$ (J=2,3) vanish in the limit of $k \longrightarrow 0$. [Because of the preaveraging of the constraining matrix, the $Q^{(1)}_{[k]}$ given by Eq. (5E.13) with Eqs. (5E.3)–(5E.6), (5E.11), (5E.12), (5E.15), (5E.16), (5E.18), and (5E.19) does not fulfil this requirement.] These two requirements may be explicitly expressed in terms of the functions a, b, c, and d defined by Eqs. (5E.3)–(5E.6) as follows

$$\lim_{k\to 0} [(a - 2d)b - 8c^2] = 0 , \tag{5.52}$$

$$\lim_{k\to 0} [\sqrt{\alpha\beta/2}(a - b - 2d) - 2(\alpha - \beta)c] = 0 \tag{5.53}$$

with α and β the functions defined by Eqs. (5E.11) and (5E.12), respectively. These requirements may be fulfilled by adding some constants $\overline{b}$ and $\overline{d}$ properly chosen to b and d, respectively. They are found to be

$$\overline{b} = 2(2\beta_0/\alpha_0)^{1/2}c_0 - b_0 , \tag{5.54}$$

$$\overline{d} = a_0/2 - (2\alpha_0/\beta_0)^{1/2}c_0 - d_0 , \tag{5.55}$$

where the subscript 0 indicates that the values at k=0 are taken. This procedure is referred to as procedure B.

Now, taking syndiotactic polystyrene (s–PS) as an example of flexible chains, we examine the behavior of the eigenvalues. We introduce as before the dimensionless parameters r_1 and r_2 defined by

$$r_1 = \zeta_t/3\pi\eta_0 a , \tag{5.56}$$

$$r_2 = \zeta_r/a^2\zeta_t , \tag{5.57}$$

and also use, instead of Δs, the number n_b of skeletal bonds of a given real chain corresponding to one subbody of the discrete HW chain. These are related to each other by Eq. (4.19). As for the necessary equilibrium model parameters, κ_0, τ_0, λ^{-1}, and the shift factor M_L, we adopt the ones listed in Table I of Ref. 14. All numerical work has been done by the use of FACOM M-380 and VP-200 digital computers in this university.

Figure 5.1 shows plots of the reduced eigenvalues $\tilde{\lambda}^J_{2(2),k} \equiv \zeta_r \lambda^J_{2(2),k}/k_BT = 3\pi\eta_0 a^3 r_1 r_2 \lambda^J_{2(2),k}/k_BT$ (with $\lambda^J_{2(2),k}$ and a unreduced) in the $J = 1$, 2, and 3 branches (relevant to $[\eta]$) against the reduced wave number $\tilde{k} = k/(N+1)$ for s-PS with $n_b = 2$, $N = 999$, $r_1 = 1$, and $r_2 = 15$. The full curves represent the values calculated following procedure B. As in the case of the $L(1)$ eigenvalues calculated in the crude subspace approximation, avoided crossings are seen to occur among the $J = 1$, 2,and 3 branches at $\tilde{k} \simeq 0.06$, as conjectured by Fixman and Evans.[10] For comparison, the values calculated following procedure A are also shown in the broken curves. The difference between the two procedures seems small as far as the eigenvalues are concerned. In what follows, all numerical results are obtained by procedure B.

5-4. High-Frequency Viscosity

In this section, we discuss the high-frequency behavior of

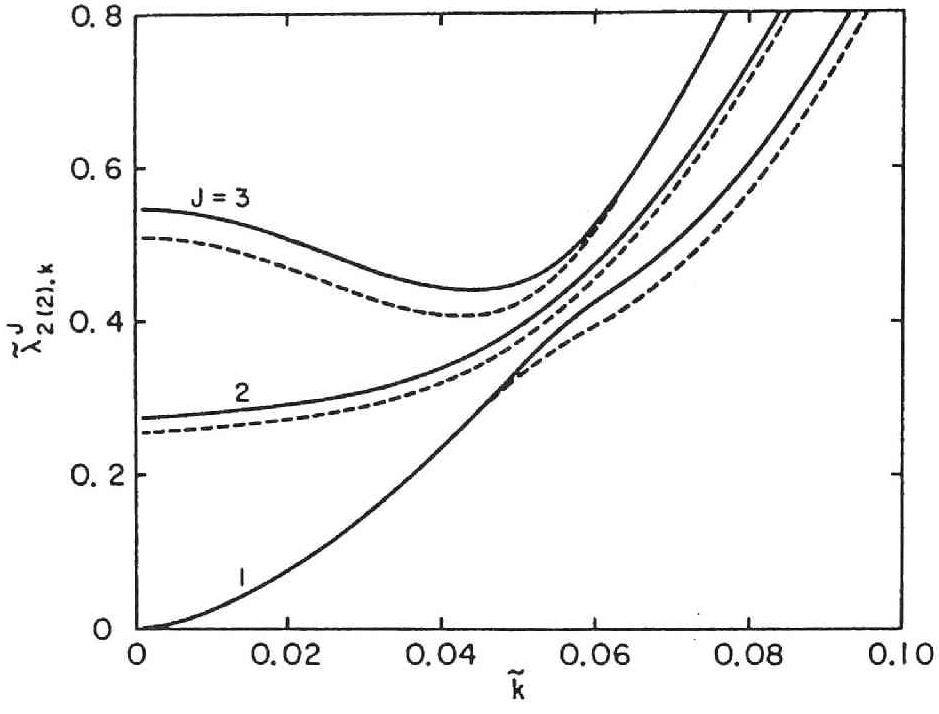

Fig. 5.1. The reduced eigenvalues $\tilde{\lambda}'_{2(2),k}$ ($J=1$, 2, 3) plotted against the reduced wave number $\tilde{k}$ for syndiotactic polystyrene with $n_b=2$, $N=999$, $r_1=1$, and $r_2=15$. The full and broken curves represent the values calculated following procedures B and A, respectively.

the dynamic intrinsic viscosity, i. e., the real part $[\eta']$ of $[\eta]=[\eta']-i[\eta'']$. From Eq. (5.47), $[\eta']$ may be written in the form,

$$[\eta'] = [\eta]^{glob} + [\eta]^{loc} + [\eta]_\infty , \tag{5.58}$$

where $[\eta]^{glob}$ and $[\eta]^{loc}$ are contributions from the global and local motions, respectively, and are given by

$$[\eta]^{glob} = [N_A(a^2\zeta_t)^2/36\eta_0 M] \sum_{k=1}^{N} (\kappa_0^2\nu^{-2}g^1_{1,k} + \tau_0^2\nu^{-2}g^0_{1,k})^2 \, (Q^{(1)}_{[k],11})^2$$

$$\times(\lambda_k^B)^{-2}\lambda^1_{2(2),k}[1+(\omega/\lambda^1_{2(2),k})^2]^{-1}\,, \tag{5.59}$$

$$[\eta]^{loc} = [N_A(a^2\zeta_t)^2/36\eta_0 M]\sum_{k=1}^{N}\sum_{J=2}^{3}(\kappa_0^2\nu^{-2}g^1_{1,k}+\tau_0^2\nu^{-2}g^0_{1,k})^2\,(Q^{(1)}_{[k],1J})^2$$

$$\times(\lambda_k^B)^{-2}\lambda^J_{2(2),k}[1+(\omega/\lambda^J_{2(2),k})^2]^{-1}\,. \tag{5.60}$$

As noted in Sec. 5-2*d*, $[\eta']$ given by Eq. (5.58) with $\omega = 0$ is not identical with the correct $[\eta]_0$ given by Eq. (5.50). In other words, Eq. (5.59) for $[\eta]^{glob}$ along with Eq. (5.60) for $[\eta]^{loc}$ cannot correctly describe the whole relaxation behavior of $[\eta']$ from $[\eta]_0$ to $[\eta]_\infty$. This defect arises from the approximate nature of the above expressions for $[\eta]^{glob}$, $[\eta]^{loc}$, and $[\eta]_\infty$. Among them, that for $[\eta]^{glob}$ is the worst. The reason for this is that as already discussed, the preaveraging approximation in the constraining matrix has significant effect on the global motions but not on the local motions. As for $[\eta]_\infty$, we have made this approximation only to evaluate the equilibrium moments at the stage of Eq. (5.45), so that Eq. (5.48) may rather be regarded as giving a good approximate value. Then, it is better to use Eq. (5.47) than Eq. (5.49) for $[\eta]$ as far as its behavior in the high-frequency region is concerned. If $[\eta]^{glob}$ is necessary, it is sufficient to replace it by the Rouse-Zimm theory result properly renormalized, as done by Brueggeman et al.[15] in the analysis of experimental data.

Now, we consider the origin of the high-frequency viscosity.

First, we make a remark on $[\eta]^{loc}$. It can be shown that as $k/(N+1)$ approaches zero, $Q^{(1)}_{[k],12}$ and $Q^{(1)}_{[k],13}$ obtained by procedure B become proportional to λ^B_k and $(\lambda^B_k)^2$, respectively, so that the ratio $Q^{(1)}_{[k],12}/\lambda^B_k$ approaches a non-zero finite value, while $Q^{(1)}_{[k],13}/\lambda^B_k$ approaches zero. This means that the interaction (coupling) $Q^{(1)}_{[k],1J}$ $(J=2,3)$ between the global and local motions becomes infinitely small as $k/(N+1)$ is decreased [so that the eigenvalues $\lambda^1_{2(2),k}$ remain unaffected for small k (and should there become identical with the Rouse-Zimm eigenvalues λ^B_k if there were no approximations)], but the contribution of $Q^{(1)}_{[k],12}$ to $[\eta']$ never vanishes because of the factor $(\lambda^B_k)^{-2}$ in Eq. (5.60). Moreover, we have found that the summand on the right-hand side of Eq. (5.60) becomes a function of $k/(N+1)$ when $N\gg1$, and that its amplitude for $J=2$ is much larger for smaller k. Thus, the total amplitude $[\eta]^{loc}_0$, i.e., the zero-frequency value of $[\eta]^{loc}$ is independent of M when $N\gg1$, and the terms in Eq. (5.60) with $J=2$ and with small k mainly contribute to it.

Since the eigenvalues (relaxation rates) in the $J=2$ and 3 branches are much larger (faster) than those in the $J=1$ branch at small wave numbers k (see Fig. 5.1), it is evident that $[\eta]^{loc}$ still remains finite after $[\eta]^{glob}$ (with small k) relaxes away. Then the sum $[\eta]^{loc}_0+[\eta]_\infty$ may be regarded as the high-frequency plateau observed in viscoelastic experiment, which we designate by $[\eta]^P$. For larger ω, $[\eta]^{loc}$ also relaxes, and only $[\eta]_\infty$ remains.

The latter seems to correspond to another high-frequency viscosity observed in the higher-frequency region.[1,16] Such relaxation mechanism is depicted schematically in Fig. 5.2. The full curve represents the values of $[\eta']$, the broken curves *glob* and *loc* represent the contributions of $[\eta]^{glob}$ and $[\eta]^{loc}$, respectively, and the horizontal dotted lines 1 and 2 indicate the values of $[\eta]^{P}$ and $[\eta]_{\infty}$, respectively.

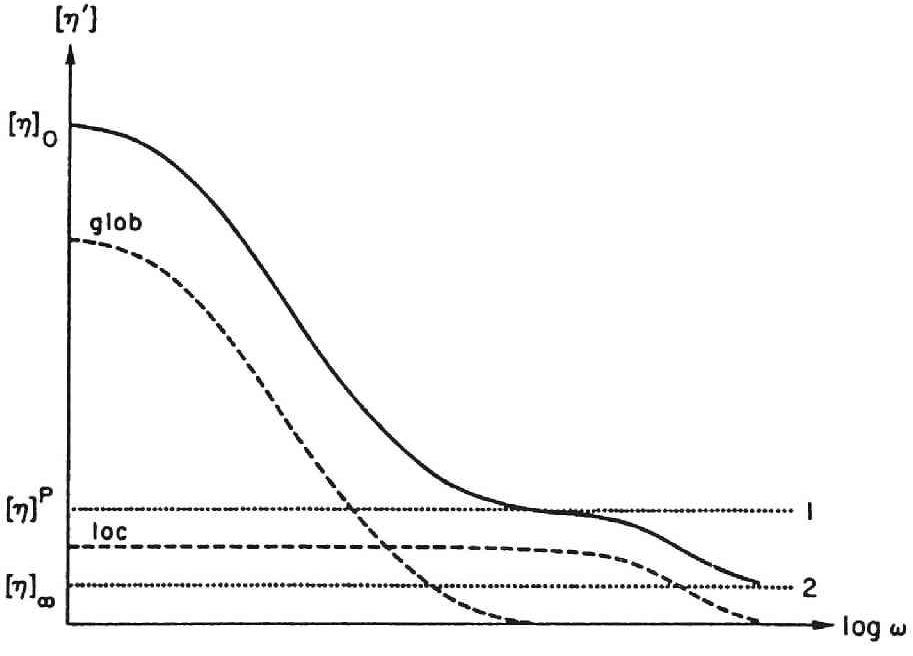

Fig. 5.2. Schematic depiction of the relaxation mechanism of $[\eta']$. The full curve represents the values of $[\eta']$, the broken curves *glob* and *loc* represent the contributions of $[\eta]^{glob}$ and $[\eta]^{loc}$, respectively, and the horizontal dotted lines 1 and 2 indicate the (frequency-independent) values of $[\eta]^{P}$ and $[\eta]_{\infty}$, respectively.

Thus, on the basis of the HW chain, it has been deduced that the high-frequency plateau $[\eta]^P$ is composed of the two parts $[\eta]_0^{loc}$ and $[\eta]_\infty$. $[\eta]_0^{loc}$ stems from the interaction between the global (Rouse-Zimm) motions and the local ones, since $[\eta]_0^{loc}$ would vanish if there were no interaction, i.e., $Q^{(1)}_{[k],1J}=0$ $(J=2,3)$. In this sense, the origin of $[\eta]_0^{loc}$ in the present theory is in accordance with that conjectured by Fixman and Evans.[10] In the two theories, however, the precise mechanisms by which the interaction makes contribution to the plateau value are somewhat different. In the latter, the plateau is due to the gap structure of the spectrum. As for $[\eta]_\infty$, it has two origins. One arises from the constraints [the first term on the right-hand side of Eq. (5.48)], and the other is the contribution of the Einstein spherical subbodies. (Such an effect of the constraints has already been considered by Doi et al.[8] and Fixman and Evans[9] for the bond chain.)

Finally, it should be noted that in our model, the interaction between the motions arises from the local helical nature of the chain contour, as possessed by almost all kinds of flexible polymers. In the case of the Kratky-Porod worm-like chain[17] $\kappa_0 = 0$ whose local chain contour is a straight rod, there is no interaction between them [$Q^{(1)}_{[k],1J}=0$ $(J=2,3)$], and therefore $[\eta]_0^{loc}=0$. The (first) plateau observed for very stiff chains, which may be well represented by the worm-like chain, arises by a different mechanism.[18-21$] In the case of rigid rods, it arises from the

constraints, and within the framework of the present theory, it corresponds to the part of $[\eta]_\infty$ due to the constraints.

5-5. Comparison with Experiment

We proceed to make a comparison between theory and experiment, giving attention only to $[\eta]^P$, since the theoretical expression for $[\eta]^{glob}$ given by Eq. (5.59) is not reliable, as mentioned in Sec. 5-4, and since available experimental data have not been obtained in the theta state. The theoretical value of $[\eta]^P = [\eta]_0^{loc} + [\eta]_\infty$ is computed from Eqs. (5.48) and (5.50), assuming that $n_b = 2$ and $r_1 = 1$.

In Chap. 4, we have regarded the subbody (corresponding to a monomer unit for almost all flexible polymers) as a spheroid (ellipsoid of revolution) having rotation axis of length a and diameter d, and related d to the product $r_1 r_2$ by Eq. (4.35). We must also relate d to the intrinsic viscosity of the Einstein sphere in order to calculate $[\eta]^P$. We simply assume that the Einstein sphere and this spheroid have the same hydrodynamic volume, i.e.,

$$d_E^3 = ad^2 . \tag{5.61}$$

In Table 5.1 are given observed values of $[\eta]^P$ for atactic polystyrene (a-PS),[1,15,22] atactic poly(methyl methacrylate) (a-PMMA)[1,15,23] and atactic poly(α-methylstyrene) (a-PαMS)[1,15,22] along with that of $[\eta]_\infty$ for a-PS,[16] the calculated values of $[\eta]^P$,

Table 5.1. Observed and calculated values of $[\eta]^P$.

Polymer	Temperature (°C)	Observed		Calculated					
		$[\eta]^P$(ml/g)	$[\eta]_\omega$(ml/g)	$[\eta]^P$(ml/g)	$[\eta]_0^{loc}$(ml/g)	$[\eta]_\omega$(ml/g)	κ_0	τ_0	r_2
a-PS	25	14.3[a]	7[b]	4.2	0.19	4.0	0.8	2.3	15
				10.8	0.31	10.5			60
				4.4	0.42	4.0	1.6	2.3	15
				11.4	0.85	10.5			60
a-PMMA	25	22.8[c]	——	4.0	1.1	2.9	4.4	0.8	6
				12.1	3.5	8.6			30
a-PαMS	25	22.2[a]	——	5.3	1.5	3.8	4.4	1.0	11
				15.9	4.6	11.3			60

[a]See Refs. 1, 15, and 22.
[b]See Ref. 16.
[c]See Refs. 1, 15, and 23.

$[\eta]_0^{loc}$, and $[\eta]_\infty$, and the assigned values of κ_0, τ_0, and r_2. For convenience, we regard the atactic polymers as syndiotactic, as done in the preceding chapters. The values of κ_0 and τ_0 are the same as those listed in Table I of Ref. 14 except for κ_0=1.6 and τ_0=2.3 for s-PS. This pair of values of κ_0 and τ_0 has been assigned to examine the dependence of $[\eta]^P$, $[\eta]_0^{loc}$, and $[\eta]_\infty$ on κ_0 and τ_0. The two values have been assigned for r_2; in every case, the smaller value has been computed by the use of the value of d determined from the chemical structure (see Table 4.2), and the larger value is the one determined previously from the analysis of experimental data in the crude-subspace approximation. The theoretical values of $[\eta]^P$ calculated with the larger r_2 are in better agreement with the observed ones than those calculated with the smaller r_2. As seen from the table, $[\eta]_0^{loc}$ is sensitive to the change of κ_0 and τ_0, while this is not the case with $[\eta]_\infty$; $[\eta]^P$ depends on κ_0 and τ_0 (helical nature) through $[\eta]_0^{loc}$. As for $[\eta]_\infty$, the calculated and observed values are rather in good agreement with each other. We note that in every case, about 60% of the calculated value of $[\eta]_\infty$ is the contribution of the Einstein spheres. In the case of a-PS, $[\eta]_0^{loc}$ may be estimated to be ~7 ml/g from the observed values of $[\eta]^P$ and $[\eta]_\infty$, and it is almost equal to the observed value of $[\eta]_\infty$. However, the calculated value of $[\eta]_0^{loc}$ is smaller than that of $[\eta]_\infty$, and therefore, the crude-subspace approximation seems to underestimate $[\eta]_0^{loc}$.

5–6. Concluding Remarks

We have evaluated the dynamic intrinsic viscosity of the discrete HW chain, and showed that it has the high-frequency plateau $[\eta]^P$ $(=[\eta]_0^{loc}+[\eta]_\infty)$ which is distinguished from the infinitely-high-frequency viscosity $[\eta]_\infty$. In our model, $[\eta]_0^{loc}$ or $[\eta]^{loc}$ arises from the interaction (coupling) between the global and local motions caused by the helical nature of the local chain contour, and $[\eta]_\infty$ arises from the constraints and the finite hydrodynamic volume of the subbody. The agreement between the theoretical and experimental values of $[\eta]^P$ is rather good, and the dependence of $[\eta]^P$ on the chemical structure of the chain may well be explained. It is evident that the incomplete agreement between theory and experiment is due to the crude-subspace approximation. On the other hand, the preaveraging approximation in the constraining matrix has significant effect on the global motions, and therefore we have not made an analysis of the $J = 1$ branch of the spectrum corresponding to the Rouse-Zimm eigenvalues.

In conclusion, our model has proved effective for a description of the relaxation behavior of $[\eta']$ in the high-frequency region which concerns the local motions, as in the cases of the $L(1)$ observable studied in Chap. 4.

Appendix 5-A. Excess Stress Tensor

In this Appendix, we derive an expression for the excess stress tensor due to the addition of one HW chain having its finite volume to an incompressible Stokes fluid.

It is reasonable to assume that the flow of the fluid is steady at every instant, since the relaxation of the velocity of the fluid is much faster than the local motion of the polymer chain immersed in it. This assumption is consistent with the description of the hydrodynamic interaction among subbodies of the chain by the use of the Oseen tensor, i.e., the Green's function of the time-independent Stokes equation. Thus, the velocity $\mathbf{V}(\mathbf{R};t)$ of the fluid at a point $\mathbf{R}$ satisfies

$$\nabla \cdot \sigma(\mathbf{R};\, t) + \mathbf{F}(\mathbf{R};\, t) = \mathbf{0}\ , \tag{5A.1}$$

where σ is the stress tensor defined by

$$\sigma(\mathbf{R};\, t) = -\, p(\mathbf{R};\, t)\mathbf{I} + \eta_0\{\nabla\, \mathbf{V}(\mathbf{R};\, t) + [\nabla\, \mathbf{V}(\mathbf{R};\, t)]^T\} \tag{5A.2}$$

with p the pressure and $\mathbf{I}$ the 3×3 unit tensor, and $\mathbf{F}$ is the force density due to the frictional force exerted by one HW chain on the fluid and is given by

$$\mathbf{F}(\mathbf{R};\, t) = \sum_{p=1}^{N} \int_{S_p} \mathrm{d}\mathbf{r}_p \delta(\mathbf{R} - \mathbf{R}_p - \mathbf{r}_p)\mathbf{F}_p^{(S)}(\mathbf{r}_p;\, t) + \delta(\mathbf{R} - \mathbf{R}_{N+1})\mathbf{F}_{N+1}(t) \tag{5A.3}$$

with $\delta(\mathbf{R})$ the Dirac delta function. The last term on the right-hand side of Eq. (5A.3) represents the contribution from the $(N+1)$th bead. As defined in Sec. 2-2, this bead has vanishing rotatory friction coefficient, and therefore we may regard it as the point force which exerts the frictional force $\mathbf{F}_{N+1}$ on the fluid at a point $\mathbf{R}_{N+1}$. The dependence of $\mathbf{V}$, σ, and p on t comes from the dependence of $\mathbf{F}$ on t, and is immaterial in the present treatment. Thus, in what follows, we suppress t.

The stress tensor σ may be written as a sum of the stress tensor σ_0 of the pure fluid and the excess stress tensor σ' due to the force density $\mathbf{F}$, i. e., $\sigma = \sigma_0 + \sigma'$. Therefore, Eq. (5A.1) may be rewritten as

$$\nabla \cdot \sigma_0 = \mathbf{0} , \tag{5A.4}$$

$$\nabla \cdot \sigma' + \mathbf{F} = \mathbf{0} . \tag{5A.5}$$

In order to express σ' in terms of $\mathbf{F}_p^{(S)}(\mathbf{r}_p)$ $(p = 1, 2, \cdots, N)$ and $\mathbf{F}_{N+1}$, we take the Fourier transform of Eq. (5A.5),

$$i\mathbf{k} \cdot \tilde{\sigma}'(\mathbf{k}) + \tilde{\mathbf{F}}(\mathbf{K}) = \mathbf{0} , \tag{5A.6}$$

where

$$\tilde{\sigma}'(\mathbf{k}) = \int \sigma'(\mathbf{R}) e^{i\mathbf{k}\cdot\mathbf{R}} d\mathbf{R} , \tag{5A.7}$$

$$\begin{aligned} \tilde{\mathbf{F}}(\mathbf{K}) &= \int \mathbf{F}(\mathbf{R}) e^{i\mathbf{k}\cdot\mathbf{R}} \mathrm{d}\mathbf{R} \\ &= \sum_{p=1}^{N} \int_{S_p} d\mathbf{r}_p e^{i\mathbf{k}\cdot(\mathbf{R}_p+\mathbf{r}_p)} \mathbf{F}_p^{(S)}(\mathbf{r}_p) + e^{i\mathbf{k}\cdot\mathbf{R}_{N+1}} \mathbf{F}_{N+1} . \end{aligned} \tag{5A.8}$$

Let $\mathbf{R}_c$ be the vector position of a point properly chosen to represent the position of the HW chain in the external coordinate system, and let $\hat{\mathbf{R}}_p$ (p=1,2,$\cdots$, N+1) be the vector distance from the point $\mathbf{R}_c$ to the pth subbody, i.e., $\mathbf{R}_p=\mathbf{R}_c+\hat{\mathbf{R}}_p$. Equation (5A.8) may be rewritten as

$$\tilde{\mathbf{F}}(\mathbf{k}) = e^{i\mathbf{k}\cdot\mathbf{R}_c}\sum_{p=1}^{N+1}\mathbf{F}_p$$

$$+ i\mathbf{k}\cdot e^{i\mathbf{k}\cdot\mathbf{R}_c}\left\{\sum_{p=1}^{N}\int_{S_p}d\mathbf{r}_p\left[\int_0^1 e^{i\xi\mathbf{k}\cdot(\hat{\mathbf{R}}_p+\mathbf{r}_p)}d\xi\right](\hat{\mathbf{R}}_p+\mathbf{r}_p)\mathbf{F}_p^{(S)}(\mathbf{r}_p)\right.$$

$$\left.+\int_0^1 e^{i\xi\mathbf{k}\cdot\hat{\mathbf{R}}_{N+1}}d\xi\,\hat{\mathbf{R}}_{N+1}\mathbf{F}_{N+1}\right\}, \tag{5A.9}$$

where $\mathbf{F}_p$ (p=1, 2, $\cdots$, N) is the total frictional force exerted on the fluid by the pth subbody and is given by

$$\mathbf{F}_p = \int_{S_p}\mathbf{F}_p^{(S)}(\mathbf{r}_p)d\mathbf{r}_p\,. \tag{5A.10}$$

Under the condition for which viscosity measurements are carried out, there is not any external force other than shear flow field, and therefore the total frictional force $\sum_{p=1}^{N+1}\mathbf{F}_p$ must vanish. Then, from Eqs. (5A.6) and (5A.9), we obtain

$$\tilde{\sigma}'(\mathbf{k}) = -\,e^{i\mathbf{k}\cdot\mathbf{R}_c}\left\{\sum_{p=1}^{N}\int_{S_p}d\mathbf{r}_p\left[\int_0^1 e^{i\xi\mathbf{k}\cdot(\hat{\mathbf{R}}_p+\mathbf{r}_p)}d\xi\right](\hat{\mathbf{R}}_p+\mathbf{r}_p)\mathbf{F}_p^{(S)}(\mathbf{r}_p)\right.$$

$$\left.+\int_0^1 e^{i\xi\mathbf{k}\cdot\hat{\mathbf{R}}_{N+1}}d\xi\,\hat{\mathbf{R}}_{N+1}\mathbf{F}_{N+1}\right\}. \tag{5A.11}$$

Now we take the average of Eq. (5A.11) over the configuration with the time-dependent distribution function. In order to obtain a general expression, we do not need its explicit form, but only its two properties: (1) $\mathbf{R}_c$ distributes uniformly in the fluid of unit volume, and (2) the average over $\mathbf{R}_c$ may be taken independently of the other variables. With these properties, we obtain

$$<\tilde{\sigma}'(\mathbf{k})> = -(2\pi)^3\delta(\mathbf{k})\Big[\sum_{p=1}^{N+1}<\hat{\mathbf{R}}_p\mathbf{F}_p> + \sum_{p=1}^{N}<\int_{S_p}\mathbf{r}_p\mathbf{F}_p^{(S)}(\mathbf{r}_p)d\mathbf{r}_p>\Big], \tag{5A.12}$$

where $<\cdots>$ denotes an average with Ψ. Replacing $\hat{\mathbf{R}}_p$ by $\mathbf{R}_p$ and taking the inverse Fourier transform, we obtain Eq. (5.4).

Appendix 5-B. Evaluation of the Function X

In this Appendix, we derive an expression for the function X suitable for constructing a formal solution for the time-dependent distribution function . This does not require explicit forms of the matrix representations of operators such as E and L given in Chap. 3. Thus, the preaveraging approximation in the constraining matrix $\mathbf{C}^{-1}$ (see Chap. 2) is not necessary, and all results in this Appendix are derived without this approximation.

First, we derive a relation among the $3N\times3N$ matrices $\mathbf{M}$, $\mathbf{N}$, $\mathbf{B}$, and $\mathbf{E}$ defined by Eqs. (2.92), (2.93), (2.95), and (2.96),

respectively. From the definition given by Eq. (2.94), the constraining matrix $\mathbf{C}^{-1}$ may be written as a series,

$$\mathbf{C}^{-1} = \left[\sum_{n=0}^{\infty}(-1)^n(\zeta_r{}^{-1}\mathbf{B}^{-1}\cdot\mathbf{E}\cdot\mathbf{E}^T)^n\right]\cdot\zeta_r{}^{-1}\mathbf{B}^{-1} . \tag{5B.1}$$

Substitution of Eq. (5B.1) into Eq. (2.92) leads to

$$\mathbf{M} = \sum_{n=0}^{\infty}(-1)^n(\mathbf{E}^T\cdot\zeta_r{}^{-1}\mathbf{B}^{-1}\cdot\mathbf{E})^n . \tag{5B.2}$$

From Eq. (2.93) and Eqs. (5B.1) and (5B.2), we obtain the relation,

$$\mathbf{N} = \zeta_r{}^{-1}\mathbf{M}\cdot\mathbf{E}^T\cdot\mathbf{B}^{-1} . \tag{5B.3}$$

Then, we derive an expression for X. Substitution of Eqs. (5.5), (5.6), and (5B.3) into Eq. (2.100) with $U_e = 0$ leads to

$$\begin{aligned} X = \tfrac{1}{2}\varepsilon\Bigg[& \tfrac{1}{2}\mathscr{L}\sum_{p_1,\,p_2=1}^{N}(B^{-1})_{p_1p_2}\mathbf{a}_{p_1}\mathbf{a}_{p_2}:(\mathbf{e}_x\mathbf{e}_y + \mathbf{e}_y\mathbf{e}_x) \\ & - \sum_{p_1,\,p_2,\,p_3=1}^{N}\zeta_r{}^{-1}\Psi_{eq}{}^{-1}\mathbf{L}_{p_1}\Psi_{eq}\cdot\mathbf{M}_{p_1p_2}\cdot(B^{-1})_{p_2p_3}(\mathbf{L}_{p_2}\mathbf{a}_{p_2})\mathbf{a}_{p_3}:(\mathbf{e}_x\mathbf{e}_y - \mathbf{e}_y\mathbf{e}_x) \\ & + \sum_{p_1,\,p_2=1}^{N}\Psi_{eq}{}^{-1}\mathbf{L}_{p_1}\Psi_{eq}\cdot\mathbf{M}_{p_1p_2}\cdot\mathbf{A}_{p_2}\cdot\mathbf{e}_z\Bigg] . \end{aligned} \tag{5B.4}$$

where $\mathbf{a}_p$ is the pth bond vector whose components are expressed in the external coordinate system and is explicitly given by $\mathbf{a}_p = (a\sin\theta_p\cos\varphi_p,\ a\sin\theta_p\sin\varphi_p,\ a\cos\theta_p)$, and we have used the formal dyadic notation $\mathbf{L}_p\mathbf{a}_p$. In obtaining Eq. (5B.4), we have also used the following relations,

$$\mathbf{E}_p^T = \mathbf{L}_p\mathbf{a}_p , \tag{5B.5}$$

$$\mathbf{L}_{p_1}\Big[\sum_{p_2,\,p_3=1}^{N}(B^{-1})_{p_2p_3}\mathbf{a}_{p_2}\mathbf{a}_{p_3}:\mathbf{e}_x\mathbf{e}_y\Big]$$

$$=\sum_{p_2=1}^{N}(B^{-1})_{p_1p_2}(\mathbf{L}_{p_1}\mathbf{a}_{p_1})\mathbf{a}_{p_2}:(\mathbf{e}_x\mathbf{e}_y+\mathbf{e}_y\mathbf{e}_x)\ , \tag{5B.6}$$

where $\mathbf{E}_p$ in Eq. (5B.5) is the 3×3 matrix given by Eq. (2.78).

By the use of Eq. (2.93), Eq. (5B.3), and the relation,

$$\mathbf{E}_p\cdot\mathbf{A}_p\cdot\mathbf{e}_z=-(\mathbf{e}_x\mathbf{e}_y-\mathbf{e}_y\mathbf{e}_x)\cdot\mathbf{a}_p\ , \tag{5B.7}$$

the third term on the right-hand side of Eq. (5B.4) may be rewritten as

$$\sum_{p_1,\,p_2=1}^{N}\Psi_{\mathrm{eq}}^{-1}\mathbf{L}_{p_1}\Psi_{\mathrm{eq}}\cdot\mathbf{M}_{p_1p_2}\cdot\mathbf{A}_{p_2}\cdot\mathbf{e}_z=\sum_{p=1}^{N}\Psi_{\mathrm{eq}}^{-1}\mathbf{L}_p\Psi_{\mathrm{eq}}\cdot\mathbf{A}_p\cdot\mathbf{e}_z$$

$$+\sum_{p_1,\,p_2,\,p_3=1}^{N}\zeta_r^{-1}\Psi_{\mathrm{eq}}^{-1}\mathbf{L}_{p_1}\Psi_{\mathrm{eq}}\cdot\mathbf{M}_{p_1p_2}\cdot(B^{-1})_{p_2p_3}(\mathbf{L}_{p_2}\mathbf{a}_{p_2})\mathbf{a}_{p_3}:(\mathbf{e}_x\mathbf{e}_y-\mathbf{e}_y\mathbf{e}_x)\ . \tag{5B.8}$$

Substitution of Eq. (5B.8) into Eq. (5B.4) leads to Eq. (5.9) with Eqs. (5.10) and (5.11).

Appendix 5-C. Intrinsic Viscosity of the Einstein Sphere

In this appendix, we evaluate the right-hand side of Eq. (5.32). In general, an integral whose integrand includes the inverse $\mathbf{K}_p^{-1}(\mathbf{r}_p,\,\mathbf{r}_p')$ may be evaluated by converting it into an integral of a certain function which includes the solution of an integral equation with the kernel $\mathbf{K}_p(\mathbf{r}_p,\,\mathbf{r}_p')$. A simple example is

the translational friction tensor $\boldsymbol{\Xi}_p$ of the pth subbody. It may be written as

$$\boldsymbol{\Xi}_p = 8\pi\eta_0 \int_{S_p} d\mathbf{r}_p \int_{S_p} d\mathbf{r}'_p \mathbf{K}_p^{-1}(\mathbf{r}_p, \mathbf{r}'_p) , \tag{5C.1}$$

since Eq. (5C.1) may be converted into

$$\boldsymbol{\Xi}_p = \int_{S_p} \boldsymbol{\Psi}_p(\mathbf{r}_p) d\mathbf{r}_p \tag{5C.2}$$

with $\boldsymbol{\Psi}_p$ the solution of the integral equation,

$$(8\pi\eta_0)^{-1} \int_{S_p} \mathbf{K}_p(\mathbf{r}_p, \mathbf{r}'_p) \cdot \boldsymbol{\Psi}_p(\mathbf{r}'_p) d\mathbf{r}'_p = \mathbf{I} . \tag{5C.3}$$

Equation (5C.2) with Eq. (5C.3) is equivalent to the first of Eqs. (29) with Eq. (33) of Ref. 24.

In the present case, the right-hand side of Eq. (5.32), which we designate by σ, may be written as

$$\sigma = -\tfrac{1}{2}(\mathbf{e}_x\mathbf{e}_y + \mathbf{e}_y\mathbf{e}_x) : \int_{S_p} \mathbf{r}_p \mathbf{F}_p^{(S)}(\mathbf{r}_p) d\mathbf{r}_p \tag{5C.4}$$

with $\mathbf{F}_p^{(S)}(\mathbf{r}_p)$ the solution of the integral equation

$$(8\pi\eta_0)^{-1} \int_{S_p} \mathbf{K}_p(\mathbf{r}_p, \mathbf{r}'_p) \cdot \mathbf{F}_p^{(S)}(\mathbf{r}'_p) d\mathbf{r}'_p = -\tfrac{\varepsilon}{2}(\mathbf{e}_x\mathbf{e}_y + \mathbf{e}_y\mathbf{e}_x) \cdot \mathbf{r}_p . \tag{5C.5}$$

It is seen from Eq. (5C.5) that $\mathbf{F}_p^{(S)}(\mathbf{r}_p)$ represents the frictional force distribution on the pth sphere under the non-slip boundary condition when it is immersed in the unperturbed oscillating shear flow given by Eq. (5.1) and rotates around its center with the angular velocity $-\varepsilon\mathbf{e}_z/2$. Therefore, σ represents the increment of

the xy component of the stress tensor due to the single sphere,[24] and is given by Eq. (5.33).

Appendix 5-D. Matrix Elements

In this Appendix, we give the (2, 2)-body matrix elements $\overline{E}^{(j_1j_2,j_1'j_2')}_{L,(l_1l_2,l_1'l_2')[k_1k_2,k_1'k_2']}$ and $\overline{L}^{(j_1j_2,j_1'j_2')}_{L,(l_1l_2,l_1'l_2')[k_1k_2,k_1'k_2']}$ in the Fourier basis set defined by

$$<F^{M,(j_1j_2)*}_{L,(l_1l_2)[k_1k_2]}F^{M',(j_1'j_2')}_{L',(l_1'l_2')[k_1'k_2']}>_{\mathrm{eq}} = \delta_{LL'}\delta_{MM'}\overline{E}^{(j_1j_2,j_1'j_2')}_{L,(l_1l_2,l_1'l_2')[k_1k_2,k_1'k_2']}\ , \tag{5D.1}$$

$$<F^{M,(j_1j_2)*}_{L,(l_1l_2)[k_1k_2]}\mathcal{L}F^{M',(j_1'j_2')}_{L',(l_1'l_2')[k_1'k_2']}>_{\mathrm{eq}} = \delta_{LL'}\delta_{MM'}\overline{L}^{(j_1j_2,j_1'j_2')}_{L,(l_1l_2,l_1'l_2')[k_1k_2,k_1'k_2']}\ , \tag{5D.2}$$

where $F^{M,(j_1j_2)}_{L,(l_1l_2)[k_1k_2]}$ is the two-body excitation Fourier basis function defined by

$$F^{M,(j_1j_2)}_{L,(l_1l_2)[k_1k_2]}(\{\Omega_N\}) = \sum_{\substack{p_1,p_2=1\\ p_1\neq p_2}}^{N}\sum_{m_1=-l_1}^{l_1}\sum_{m_2=-l_2}^{l_2}Q^0_{p_1k_1}Q^0_{p_2k_2}$$

$$\times\ \overline{\mathscr{D}}^{m_1j_1}_{l_1}(\Omega_a)\overline{\mathscr{D}}^{m_2j_2}_{l_2}(\Omega_a)D^{M,(m_1m_2)}_{L,(l_1l_2)[p_1p_2]}(\Omega_{p_1},\ \Omega_{p_2}). \tag{5D.3}$$

In Eq. (5D.3), we have used the two-body excitation basis function $D^{M,(j_1j_2)}_{L,(l_1l_2)[p_1p_2]}(\Omega_{p_1},\ \Omega_{p_2})$ for the case of $p_1>p_2$, which is defined by

$$D^{M,(j_1j_2)}_{L,(l_1l_2)[p_1p_2]}(\Omega_{p_1},\ \Omega_{p_2}) = (-1)^{L-l_1-l_2}(8\pi^2)^{-(N-2)/2}\sum_{m_1,m_2}<l_1m_1l_2m_2\,|\,l_1l_2LM>$$

$$\times\mathscr{D}^{m_1j_1}_{l_1}(\Omega_{p_1})\mathscr{D}^{m_2j_2}_{l_2}(\Omega_{p_2})\qquad(p_1\ >\ p_2)\ , \tag{5D.4}$$

Note that $D^{M,(j_1j_2)}_{L,(l_1l_2)[p_1p_2]}(\Omega_{p_1},\ \Omega_{p_2})$ for $p_1 < p_2$ has already been defined by Eq. (3.4).

We may write the (2, 2)−body elements in the form,

$$\overline{E}^{(j_1j_2,j_1'j_2')}_{L,(l_1l_2,l_1'l_2')[k_1k_2,k_1'k_2']} = \sum_{\substack{p_1,p_2,p_1',p_2'=1 \\ p_1\neq p_2,p_1'\neq p_2'}}^{N} \sum_{m_1=-l_1}^{l_1} \sum_{m_2=-l_2}^{l_2} \sum_{m_1'=-l_1'}^{l_1'} \sum_{m_2'=-l_2'}^{l_2'} Q^0_{p_1k_1} Q^0_{p_2k_2} Q^0_{p_1'k_1'} Q^0_{p_2'k_2'}$$

$$\times \overline{\mathscr{D}}^{m_1j_1*}_{l_1}(\Omega_a) \overline{\mathscr{D}}^{m_2j_2*}_{l_2}(\Omega_a) \overline{\mathscr{D}}^{m_1'j_1'}_{l_1'}(\Omega_a) \overline{\mathscr{D}}^{m_2'j_2'}_{l_2'}(\Omega_a) E^{(m_1m_2,m_1'm_2')}_{L,(l_1l_2,l_1'l_2')[p_1p_2,p_1'p_2']} , \tag{5D.5}$$

and the like. By the use of Eqs. (3.17)−(3.22), we take the sums to obtain

$$\overline{E}^{(j_1j_2,j_1'j_2')}_{L,(l_1l_2,l_1'l_2')[k_1k_2,k_1'k_2']} = \delta_{l_1l_1'}\delta_{l_2l_2'}\delta_{k_1k_1'}\delta_{k_2k_2'}\delta_{j_1j_1'}\delta_{j_2j_2'}(1 + \delta_{l_1l_2}\delta_{k_1k_2}\delta_{j_1j_2}) \times (8\pi^2)^{-N} g^{j_1}_{l_1,k_1} g^{j_2}_{l_2,k_2} , \tag{5D.6}$$

$$\begin{aligned} \overline{L}^{(j_1j_2,j_1'j_2')}_{L,(l_1l_2,l_1'l_2')[k_1k_2,k_1'k_2']} &= \delta_{l_1l_1'}\delta_{l_2l_2'}\delta_{k_1k_1'}\delta_{k_2k_2'}(8\pi^2)^{-N}\zeta_{\mathrm{r}}^{-1} \\ &\times \Big(\delta_{j_1j_1'}\delta_{j_2j_2'}(1 + \delta_{l_1l_2}\delta_{k_1k_2}\delta_{j_1j_2}) \big[l_1(l_1+1) g^{j_2}_{l_2,k_2} + l_2(l_2+1) g^{j_1}_{l_1,k_1} \big] \\ &- \delta_{j_2j_2'} g^{j_2}_{l_2,k_2} \Big\{ h^{j_1j_1'}_{l_1,k_1} + \tfrac{1}{3}\delta_{l_11}(2 - (-1)^{L+l_2}) T^{j_1j_1',0}_{1,-1} (\lambda^C_{k_1})^{-1} \Big\} \\ &- \delta_{l_1l_2}\delta_{k_1k_2}\delta_{j_2j_1'} g^{j_2}_{l_2,k_2} \Big\{ h^{j_1j_2'}_{l_1,k_1} + \tfrac{1}{3}\delta_{l_11}(2 + (-1)^{L}) T^{j_1j_2',0}_{1,-1} (\lambda^C_{k_1})^{-1} \Big\} \\ &- \delta_{j_1j_1'} g^{j_1}_{l_1,k_1} \Big\{ h^{j_2j_2'}_{l_2,k_2} + \tfrac{1}{3}\delta_{l_21}(2 - (-1)^{L+l_1}) T^{j_2j_2',0}_{1,-1} (\lambda^C_{k_2})^{-1} \Big\} \\ &- \delta_{l_1l_2}\delta_{k_1k_2}\delta_{j_1j_2'} g^{j_1}_{l_1,k_1} \Big\{ h^{j_2j_1'}_{l_2,k_2} + \tfrac{1}{3}\delta_{l_21}(2 + (-1)^{L}) T^{j_2j_1',0}_{1,-1} (\lambda^C_{k_2})^{-1} \Big\} \Big) \end{aligned} \tag{5D.7}$$

with

$$h^{j_1'}_{l,k} = \tfrac{1}{2} \sum_{\Delta l=-1}^{1} \sum_{j''=-l-\Delta l}^{l+\Delta l} T^{j_1''j''}_{l,\Delta l} \sum_{k'=1}^{N} (N\lambda^C_{k'})^{-1} (g^{j''}_{l+\Delta l,k+k'} + g^{j''}_{l+\Delta l,k-k'}) , \tag{5D.8}$$

where $g^j_{l,k}$ is defined by

$$\begin{aligned} g^j_{l,k} &= -1 , \quad \text{if } l = j = 0 \text{ and } k = 2n(N+1) \quad (\text{with } n\text{integer}) \\ &= \tfrac{1}{2}[1 - e^{-2l(l+1)\Delta s}] \sum_{m=-1}^{1} (1 - \delta_{m0}) \end{aligned} \tag{5D.9}$$

$$\times \left[1 - 2e^{-l(l+1)\Delta s}\cos(j\nu\Delta s - mk\theta) + e^{-2l(l+1)\Delta s}\right]^{-1}, \quad \text{otherwise},$$

with $\theta = \pi/(N+1)$ and $\nu = (\kappa_0{}^2 + \tau_0{}^2)^{1/2}$, and $T^{j'j''}_{l'l}$ is defined by Eq. (3.53). In deriving Eqs. (5D.6) and (5D.7), we have ignored terms involving $e^{-N\Delta s}$, and retained terms of $\mathcal{O}(1)$.

We note that the terms involving $h^{ll'}_{lk}$ and $(\lambda^C_k)^{-1}$ in Eq. (5D.7) arise from the constraining matrix appearing in the diffusion operator $\mathcal{L}$. If these terms are ignored in Eq. (5D.7), then $\overline{L}^{(j_1j_2;j_1'j_2')}_{L;(l_1l_2;l_1'l_2')[k_1k_2;k_1'k_2']}$ become diagonal.

Appendix 5-E. The Six-Dimensional Eigenvalue Problem

In this Appendix, we give the analytical solution of the six-dimensional eigenvalue problem given by Eq. (5.43) (with $\kappa_0{}^2 + \tau_0{}^2 \neq 0$).

From Eqs. (5D.7) and (5D.8), the 6×6 matrix $M_{[k]}$ defined by

$$M_{[k]} = (\overline{E}_{2(2),[k]})^{-1/2}\,\overline{L}_{2(2),[k]}\,(\overline{E}_{2(2),[k]})^{-1/2} \tag{5E.1}$$

is explicitly given by

$$M_{[k]} = \zeta_r^{-1}\begin{pmatrix} a & -\sqrt{2}ic & -\sqrt{2}d & 0 & 0 & 0 \\ \sqrt{2}ic & \frac{1}{2}(a+b) & ic & -\sqrt{2}ic & -d & 0 \\ -\sqrt{2}d & -ic & a & 0 & -ic & -\sqrt{2}d \\ 0 & \sqrt{2}ic & 0 & b & \sqrt{2}ic & 0 \\ 0 & -d & ic & -\sqrt{2}ic & \frac{1}{2}(a+b) & \sqrt{2}ic \\ 0 & 0 & -\sqrt{2}d & 0 & -\sqrt{2}ic & a \end{pmatrix} \tag{5E.2}$$

with

$$a = (g^{-1}_{1,k})^{-1}\{4 - \tfrac{1}{2}\kappa_0{}^2\nu^{-2}[\tfrac{8}{3}(1 - \tfrac{1}{2N})(\lambda^C_k)^{-1} + S^0_{1,k} + \tfrac{1}{3}S^0_{2,k} + 2S^2_{2,k}]$$

$$- \tau_0{}^2\nu^{-2}(S^1_{1,k} + S^1_{2,k})\}\ , \tag{5E.3}$$

$$b = (g^0_{1,k})^{-1}\{4 - \kappa_0{}^2\nu^{-2}(S^1_{1,k} + S^1_{2,k})$$

$$- \tau_0{}^2\nu^{-2}[\tfrac{8}{3}(1 - \tfrac{1}{2N})(\lambda^C_k)^{-1} + \tfrac{4}{3}S^0_{2,k}]\}\ , \tag{5E.4}$$

$$c = \tfrac{1}{2\sqrt{2}}\kappa_0\tau_0\nu^{-2}(g^0_{1,k}g^1_{1,k})^{-1/2}[\tfrac{8}{3}(1 - \tfrac{1}{2N})(\lambda^C_k)^{-1}$$

$$- S^1_{1,k} - \tfrac{2}{3}S^0_{2,k} + S^1_{2,k}]\ , \tag{5E.5}$$

$$d = \tfrac{1}{4}\kappa_0{}^2\nu^{-2}(g^1_{1,k})^{-1}[\tfrac{8}{3}(1 - \tfrac{1}{2N})(\lambda^C_k)^{-1} - S^0_{1,k} + \tfrac{1}{3}S^0_{2,k}]\ , \tag{5E.6}$$

where $g^j_{l,k}$ is defined by Eq. (5D.9), $\nu = (\kappa_0{}^2 + \tau_0{}^2)^{1/2})$, λ^C_k is the kth approximate eigenvalue of the matrix $a^{-2}C$ given by Eq. (3.46), and $S^j_{l,k}$ is defined by

$$S^j_{l,k} = (2N)^{-1}\sum_{k'=1}^{N}(\lambda^C_{k'})^{-1}(g^j_{l,k+k'} + g^j_{l,k-k'})\ . \tag{5E.7}$$

The unitary transformation matrix $Q^L_{2(2),[k]}$ which diagonalizes the matrix $M_{[k]}$ is found to be of the form

$$Q^L_{2(2),[k]} = P_{[k]}Q_{[k]} \tag{5E.8}$$

with $P_{[k]}$ and $Q_{[k]}$ the 6×6 unitary transformation matrices given by

$$P_{[k]} = \begin{pmatrix} -\alpha/2 & \sqrt{\alpha\beta/2} & \beta/2 & 0 & -1/\sqrt{2} & 1/2 \\ i\sqrt{\alpha\beta} & i(\alpha-\beta)/\sqrt{2} & i\sqrt{\alpha\beta} & -i/\sqrt{2} & 0 & 0 \\ -\alpha/\sqrt{2} & \sqrt{\alpha\beta} & \beta/\sqrt{2} & 0 & 0 & -1/\sqrt{2} \\ \beta & \sqrt{2\alpha\beta} & -\alpha & 0 & 0 & 0 \\ i\sqrt{\alpha\beta} & i(\alpha-\beta)/\sqrt{2} & i\sqrt{\alpha\beta} & i/\sqrt{2} & 0 & 0 \\ -\alpha/2 & \sqrt{\alpha\beta/2} & \beta/2 & 0 & 1/\sqrt{2} & 1/2 \end{pmatrix}, \tag{5E.9}$$

and

$$Q_{[k]} = \begin{pmatrix} Q^{(1)}_{[k]} & 0_{3\times2} & 0_{3\times1} \\ 0_{2\times3} & Q^{(2)}_{[k]} & 0_{2\times1} \\ 0_{1\times3} & 0_{1\times2} & 1 \end{pmatrix}, \tag{5E.10}$$

respectively, where

$$\alpha = \kappa_0^{\,2}\nu^{-2}g^1_{1,k}/(\kappa_0^{\,2}\nu^{-2}g^1_{1,k} + \tau_0^{\,2}\nu^{-2}g^0_{1,k}), \tag{5E.11}$$

$$\beta = \tau_0^{\,2}\nu^{-2}g^0_{1,yk}/(\kappa_0^{\,2}\nu^{-2}g^1_{1,k} + \tau_0^{\,2}\nu^{-2}g^0_{1,k}). \tag{5E.12}$$

In Eq. (5E.10), $0_{n\times m}$ is the $n\times m$ null matrix, and $Q^{(1)}_{[k]}$ and $Q^{(2)}_{[k]}$ are the 3×3 and 2×2 unitary transformation matrices given by

$$Q^{(1)}_{[k]} = \begin{pmatrix} (x+1)/2 & y & (x-1)/2 \\ y & -x & y \\ (x-1)/2 & y & (x+1)/2 \end{pmatrix}, \tag{5E.13}$$

$$Q^{(2)}_{[k]} = \begin{pmatrix} [(1-z)/2]^{1/2} & [(1+z)/2]^{1/2} \\ -[(1+z)/2]^{1/2} & [(1-z)/2]^{1/2} \end{pmatrix}, \tag{5E.14}$$

respectively, where

$$x = A(A^2 + 2B^2)^{-1/2}, \tag{5E.15}$$

$$y = B(A^2 + 2B^2)^{-1/2}, \tag{5E.16}$$

$$z = (-a + b + 2d)[(a - b - 2d)^2 + 32c^2]^{-1/2} \tag{5E.17}$$

with

$$A = \tfrac{1}{2}(\beta - \alpha)(a - b - 2d) + 4\sqrt{2\alpha\beta}\, c \ , \tag{5E.18}$$

$$B = \sqrt{\alpha\beta/2}(a - b - 2d) + 2(\alpha - \beta)c \ . \tag{5E.19}$$

The desired eigenvalue $\lambda^{J}_{2(2),k}$ ($J = 1$–6), which is the Jth diagonal element of the diagonal matrix $\Lambda_{2(2),[k]} = Q^{\dagger}_{2(2),[k]} M_{[k]} Q_{2(2),[k]}$, is given by

$$\begin{aligned}
\lambda^{J}_{2(2),k} &= \zeta_r^{-1}[\tfrac{1}{2}(a + b) - d + (J - 2)(A^2 + 2B^2)^{1/2}] \\
&\qquad\qquad \text{for } J = 1, 2, 3 \\
&= (4\zeta_r)^{-1}\{(3a + b + 2d) - (-1)^J[(a - b - 2d)^2 + 32c^2]^{1/2}\} \\
&\qquad\qquad \text{for } J = 4, 5 \\
&= \zeta_r^{-1}(a + 2d) \qquad\qquad \text{for } J = 6 \ .
\end{aligned} \tag{5E.20}$$

References

[1] J. D. Ferry, *Viscoelastic Properties of Polymers*, 3rd ed. (Wiley, New York, 1980), Chap. 9.

[2] P. E. Rouse, Jr., J. Chem. Phys., **21**, 1272 (1953).

[3] B. H. Zimm, J. Chem. Phys., **24**, 269 (1956).

[4] H. Yamakawa, *Modern Theory of Polymer Solutions* (Harper & Row, New York, 1971).

[5] R. Cerf, Adv. Polym. Sci., **1**, 382 (1959).

[6] A. Peterlin, J. Polym. Sci., A-2, **5**, 129 (1967).

[7] S. A. Adelman and K. F. Freed, J. Chem. Phys., **67**, 1380 (1977).

[8] M. Doi, H. Nakajima, and Y. Wada, Colloid Polymer Sci., **254**, 559

(1976).

[9]M. Fixman and G. T. Evans, J. Chem. Phys., **64**, 3474 (1976).

[10]M. Fixman and G. T. Evans, J. Chem. Phys., **68**, 195 (1978).

[11]R. S. Adler and K. F. Freed, J. Chem. Phys., **72**, 2032 (1980).

[12]H. Brenner, Chem. Eng. Sci., **19**, 631 (1964).

[13]W. H. Stockmayer and M. E. Baur, J. Am. Chem. Soc., **86**, 3485 (1964).

[14]H. Yamakawa, Annu. Rev. Phys. Chem., **35**, 23 (1984).

[15]B. G. Brueggeman, M. G. Minnick, and J. L. Schrag, Macromolecules, **11**, 119 (1978).

[16]R. S. Moore, H. J. McSkimin, C. Gieniewski, and P. Andreatch, Jr., J. Chem. Phys., **50**, 5088 (1969).

[17]O. Kratky and G. Porod, Rec. Trav. Chim., **68**, 1106 (1949).

[18]J. G. Kirkwood and P. L. Auer, J. Chem. Phys., **19**, 281 (1951).

[19]N. Ookubo, M. Komatsubara, H. Nakajima, and Y. Wada, Biopolymers, **15**, 929 (1976).

[20]D. B. Roitman and B. H. Zimm, J. Chem. Phys., **81**, 6333 (1984).

[21]K. Nagasaka and H. Yamakawa, J. Chem. Phys., **83**, 6480 (1985).

[22]K. Osaki and J. L. Schrag, Polym. J., **2**, 541 (1971).

[23]J. W. M. Noordermeer, J. D. Ferry, and N. Nemoto, Macromolecules, **8**, 672 (1975).

[24]T. Yoshizaki and H. Yamakawa, J. Chem. Phys., **72**, 57 (1980).

LIST OF PUBLICATIONS

CHAPTER 2

1. Dynamics of Helical Wormlike Chains. I. Dynamic Model and Diffusion Equation ; H. Yamakawa and T. Yoshizaki, J. Chem. Phys., **75**, 1016 (1981).

CHAPTER 3

2. Dynamics of Helical Wormlike Chains. II. Eigenvalue Problems ; H. Yamakawa, T. Yoshizaki, and J. Shimada, J. Chem. Phys., **78**, 560 (1983).
3. Dynamics of Helical Wormlike Chains. III. Eigenvalue Spectra and Time-Correlation Functions ; H. Yamakawa and T. Yoshizaki, J. Chem. Phys., **78**, 572 (1983).

CHAPTER 4

4. Dynamics of Helical Worm-like Chains. IV. Dielectric Relaxation ; T. Yoshizaki and H. Yamakawa, J. Chem. Phys., **81**, 982 (1984).

CHAPTER 5

5. Dynamics of Helical Worm-like Chains. IX. Dynamic Intrinsic Viscosity ; T. Yoshizaki and H. Yamakawa, J. Chem. Phys., **88**, 1313 (1988).

Other Publications

1. Viscosity Constant in the Zimm Version ; T. Yoshizaki and H. Yamakawa, Macromolecules, **10**, 359 (1977).
2. Transport Coefficients of Helical Wormlike Chains. 1. Characteristic Helices ; H. Yamakawa, T. Yoshizaki, and M. Fujii, Macromolecules, **10**, 934 (1977).
3. Transport Coefficients of Helical Wormlike Chains. 2. Translational Friction Coefficient ; H. Yamakawa and T. Yoshizaki, Macromolecules, **12**, 32 (1979).

4. Dynamics of Spheroid-Cylindrical Molecules in Dilute Solution ; T. Yoshizaki and H. Yamakawa, J. Chem. Phys., **72**, 57 (1980).
5. Transport Coefficients of Helical Wormlike Chains. 3. Intrinsic Viscosity ; H. Yamakawa and T. Yoshizaki, Macromolecules, **13**, 633 (1980).
6. Validity of the Superposition Approximation in an Application of the Modified Oseen Tensor to Rigid Polymers ; T. Yoshizaki and H. Yamakawa, J. Chem. Phys., **73**, 578 (1980).
7. Scattering Functions of Wormlike and Helical Wormlike Chains ; T. Yoshizaki and H. Yamakawa, Macromolecules, **13**, 1518 (1980).
8. Temperature Coefficients of Unperturbed Chain Dimensions. Helical Wormlike Chains ; H. Yamakawa and T. Yoshizaki, Macromolecules, **15**, 1444 (1982).
9. Transport Coefficients of Weakly Bending Rods. Effects of the Preaveraging Approximation ; G. Tanaka, T. Yoshizaki, and H. Yamakawa, Macromolecules, **17**, 767 (1984).
10. Dynamics Helical Worm-like Chains. VI. Fluorescence Depolarization ; T. Yoshizaki, M. Fujii, and H. Yamakawa, J. Chem. Phys., **82**, 1003 (1985).
11. Dynamics of Helical Worm-like Chains. VII. General Scheme of the Higher-Order Subspace Approximations ; T. Yoshizaki and H. Yamakawa, J. Chem. Phys., **84**, 4684 (1986).
12. Dynamics of Helical Worm-like Chains. VIII. Higher-Order Subspace Approximations to Dielectric and Magnetic Relaxation and Fluorescence Depolarization for Flexible Chains ; H. Yamakawa, T. Yoshizaki, and M. Fujii, J. Chem. Phys., **84**, 4693 (1986).

13. Correction of Collision-Induced Polarizabilities to the Depolarized Rayleigh Scattering by Dilute Solutions of Oligomers and Polymers ; T. Yoshizaki and H. Yamakawa, Chem. Lett., **1987**, 2351 (1987).
14. Determination of Stereochemical Compositions of Oligostyrenes by ^{13}C NMR, T. Konishi, T. Yoshizaki, and H. Yamakawa, Polym. J., **20**, 175 (1988).
15. Transport Coefficients of Helical Wormlike Chains. 4. Intrinsic Viscosity of the Touched-Bead Model ; T. Yoshizaki, I. Nitta, and H. Yamakawa, Macromolecules, **21**, 165 (1988).
16. Characterization and Optical Anisotropy of Oligo- and Polystyrenes in Dilute Solutions ; T. Konishi, T. Yoshizaki, J. Shimada, and H. Yamakawa, Macromolecules, **22**, 1921 (1989).
17. Dynamics of Helical Worm-like Chains. X. Oscillatory Flow Birefringence ; K. Nagasaka, T. Yoshizaki, and H. Yamakawa, J. Chem. Phys., **90**, 5167 (1989).
18. Mean-Square Radius of Gyration of Oligo- and Polystyrenes in Dilute Solutions ; T. Konishi, T. Yoshizaki, T. Saito, Y. Einaga, and H. Yamakawa, Macromolecules (in press).
19. Dynamics of Helical Worm-like Chains. XI. Translational Diffusion with Fluctuating Hydrodynamic Interaction ; H. Yamakawa and T. Yoshizaki, J. Chem. Phys. (in press).

ACKNOWLEDGMENT

The present study has been carried out at Department of Polymer Chemistry, Kyoto University, under the guidance of Professor Hiromi Yamakawa. The author would like to express his sincere gratitude to Professor Hiromi Yamakawa for his guidance, suggestions of the problems, numerous instructive comments, and endless encouragement, and his critical reading of the manuscript. The author has learned from him many things not only of polymer science but also of other branches of natural (and supernatural) science. The most important thing of all is what the scientific investigation is. This must also be acknowledged.

Thanks are also tendered to Dr. Motoharu Fujii, Dr. Jiro Shimada, and Mr. Kyosuke Nagasaka for their helpful discussions. The author also wishes to thank other members in Yamakawa laboratory for their kind help.